

University of Split
Faculty of Science
PhD Study of Biophysics



Doctoral thesis

**STRUCTURE, BIOLOGICAL ACTIVITY AND
MECHANISM OF ACTION OF NEWLY
SYNTHESIZED QUATERNARY AMMONIUM
COMPOUNDS**

Doris Crnčević

Split, 2025, January

Sveučilište u Splitu
Prirodoslovno-matematički fakultet
Poslijediplomski sveučilišni doktorski studij
Biofizika



Doktorski rad

**STRUKTURA, BIOLOŠKA AKTIVNOST I
MEHANIZAM DJELOVANJA
NOVOSINTETIZIRANIH KVATERNIH
AMONIJEVIH SPOJEVA**

Doris Crnčević

Split, 2025, siječanj

Sveučilište u Splitu, Prirodoslovno-matematički fakultet
Odjel za fiziku, Poslijediplomski sveučilišni doktorski studij Biofizika

**STRUKTURA, BIOLOŠKA AKTIVNOST I MEHANIZAM DJELOVANJA
NOVOSINTETIZIRANIH KVATERNIH AMONIJEVIH SPOJEVA**

Doktorski rad autorice Doris Crnčević kao dio obaveza potrebnih da se dobije doktorat znanosti, izrađen je pod vodstvom mentorice izv. prof. dr. sc. Matilde Šprung.

Dobiveni akademski naziv i stupanj: doktorica prirodnih znanosti iz polja kemija.

Povjerenstvo za ocjenu doktorskog rada u sastavu:

1. prof. dr. sc. Renata Odžak

(Prirodoslovno-matematički fakultet, Sveučilište u Splitu, predsjednica)

2. izv. prof. dr. sc. Stjepan Orhanović

(Prirodoslovno-matematički fakultet, Sveučilište u Splitu, član)

3. izv. prof. dr. sc. Rosana Ribić

(Odjel za sestrinstvo, Sveučilište Sjever, članica)

potvrđuje da je disertacija obranjena dana _____

Voditelj studija

izv. prof. dr. sc. Damir Kovačić

Dekan

prof. dr. sc. Mile Dželalija

**STRUCTURE, BIOLOGICAL ACTIVITY AND MECHANISM OF ACTION OF NEWLY
SYNTHESIZED QUATERNARY AMMONIUM COMPOUNDS**

2025

Doris Crnčević

Thesis performed at Faculty of Science, University of Split

Abstract

This thesis investigates the development of novel quaternary ammonium compounds (QACs) with the aim of addressing the growing concerns regarding bacterial resistance and environmental impacts associated with conventional QACs. The research focusses on two different QAC series: traditional derivatives based on pyridine-4-aldoxime and biodegradable "soft" variants derived from 3-substituted quinuclidine. While the structural modifications of the traditional QACs resulted in potent antiviral properties, their antibacterial efficacy was impaired, possibly due to an increased polarity of the backbone that hinders electrostatic interactions with the bacterial membrane. Consequently, the polarity of the amide bond in the "soft" QAC variants was diminished by the addition of long hydrocarbon chains in its extension, resulting in compounds with a dual mechanism of action, lower toxicity and an improved biodegradability profile. In addition, the research emphasizes the importance of fine-tuning the hydrophobic/hydrophilic ratio, as demonstrated by the example of 3-aminoquinuclidine derived QACs in which the amino functional group mimics bis-QAC by protonation under physiological conditions. These derivatives showed potent bactericidal activity against a variety of bacterial strains, including the ability to disrupt biofilm formation and induce bacterial cell death by destabilization of the membrane and generation of the reactive oxygen species. Taken together, the obtained results and the established structure-activity relationships provide valuable insights for the rational design and synthesis of next-generation QACs with improved efficacy, biosafety profile and potential therapeutic applications.

108 pages, 70 figures, 7 tables, 120 references, 2 supplements, original in English

Thesis deposited in National and University Library in Zagreb, University Library in Split, and Library of the Faculty of Science, University of Split

Keywords: antibacterial activity, bacterial resistance, mechanism of action, membranolytic potential, structure-activity relationship, quaternary ammonium compounds

Supervisor: Assoc. Prof. Matilda Šprung, PhD

Reviewers: 1. Prof. Renata Odžak, PhD
2. Assoc. Prof. Stjepan Orhanović, PhD
3. Assoc. Prof. Rosana Ribić, PhD

Thesis accepted:

**STRUKTURA, BIOLOŠKA AKTIVNOST I MEHANIZAM DJELOVANJA
NOVOVISNTETIZIRANIH KVATERNIH AMONIJEVIH SPOJEVA**

2025

Doris Crnčević

Rad je izrađen na Prirodoslovno-matematičkom fakultetu, Sveučilišta u Splitu

Sažetak

Ova doktorska disertacija rezultirala je razvojem novih kvaternih amonijevih spojeva (QAC) s ciljem rješavanja rastućeg problema razvoja bakterijske rezistencije te negativnog ekološkog učinka uzrokovanog konvencionalnim QAC derivatima. Istraživanje se fokusira na dvije različite QAC serije: tradicionalne derivate temeljene na piridinijevom-4-aldoksimu i biorazgradive "meke" varijante 3-supstituiranog kinuklidina. Dok su strukturne modifikacije tradicionalnih QAC rezultirale snažnim antivirusnim svojstvima, isti su pokazali smanjenu antibakterijsku učinkovitost, koju je moguće pripisati povećanoj polarnosti okosnice što može ometati povoljne elektrostatske interakcije s bakterijskom membranom. Posljedično, polarnost amidne veze u "mekim" QAC varijantama smanjena je dodatkom dugih alkilnih lanaca u njenom produžetku, što je rezultiralo spojevima s dvostrukim mehanizmom djelovanja, nižom toksičnošću i poboljšanim profilom biorazgradivosti. Osim toga, istraživanje naglašava važnost optimalnog podešavanja omjera hidrofobno/hidrofilno, a isto je pokazano na primjeru QAC deriviranih na okosnici 3-aminokinuklidina u kojima protonirana amino skupina pruža mogućnost oponašanja bis-QAC. Ovi derivati su pokazali snažnu baktericidnu aktivnost, uključujući sposobnost inhibicije stvaranja biofilma i induciranja smrti bakterijske stanice destabilizacijom membrane i generiranjem reaktivnih vrsta kisika. Rezultati ovog istraživanja, zajedno sa zaključcima utjecaja strukture na aktivnost, omogućuju daljnji racionalan dizajn i sintezu novih QAC varijanti s poboljšanom učinkovitošću, biosigurnosnim profilom i potencijalnom terapijskom primjenom.

108 stranica, 70 slika, 7 tablica, 120 literaturnih navoda, 2 priloga, jezik izvornika engleski

Rad je pohranjen u Nacionalnoj sveučilišnoj knjižnici u Zagrebu, Sveučilišnoj knjižnici u Splitu i Knjižnici Prirodoslovno-matematičkog fakulteta Sveučilišta u Splitu

Ključne riječi: antibakterijska aktivnost, bakterijska rezistencija, kvaterni amonijevi spojevi, mehanizam djelovanja, membranolitički potencijal, odnos strukture i aktivnosti

Mentor: izv. prof. dr. sc. Matilda Šprung

Ocjenjivači: 1. Prof. dr. sc. Renata Odžak
2. Izv. prof. dr. sc. Stjepan Orhanović
3. Izv. prof. dr. sc. Rosana Ribić

Rad prihvaćen:

ACKNOWLEDGMENTS

PUBLICATIONS

The following list of publications constitutes the main part of the thesis:

1. Crnčević, Doris; Krce, Lucija; Cvitković, Mislav; Brkljača, Zlatko; Sabljčić, Antonio; Vuko, Elma; Primožič, Ines; Odžak, Renata; Šprung, Matilda. *New Membrane Active Antibacterial and Antiviral Amphiphiles Derived from Heterocyclic Backbone of Pyridinium-4-Aldoxime*. *Pharmaceuticals*, 15 (2022), DOI: 10.3390/ph15070775
2. Crnčević, Doris; Krce, Lucija; Brkljača, Zlatko; Cvitković, Mislav; Babić Brčić, Sanja; Čož-Rakovac, Rozelindra; Odžak, Renata; Šprung, Matilda. *A dual antibacterial action of soft quaternary ammonium compounds: Bacteriostatic effects, membrane integrity, and reduced in vitro and in vivo toxicity*. *RSC Advances*, 15 (2025), DOI: 10.1039/D4RA07975B
3. Crnčević, Doris; Ramić, Alma; Radman Kastelic, Andreja; Odžak, Renata; Krce, Lucija; Weber, Ivana; Primožič, Ines; Šprung, Matilda. *Naturally derived 3-aminoquinuclidine salts as new promising therapeutic agents*. *Scientific reports*, 14 (2024), DOI: 10.1038/s41598-024-77647-5

ABBREVIATIONS

ADBAC	alkyldimethylbenzylammonium chloride
AMP	antimicrobial peptide
ATMAC	alkyltrimethyl ammonium compound
BAC	benzyltrimethylammonium chloride / benzalkonium chloride
CPC	cetylpyridinium chloride
CTAB	cetyltrimethylammonium bromide
CWTA	cell wall teichoic acid
DABCO	1,4-diazabicyclo[2.2.2]octane
DADMAC	dialkyldimethyl ammonium compound
DDAC	didecyldimethylammonium chloride
DTDMAC	di-tallow dimethyl ammonium chloride
EC ₅₀	half-maximal effective concentration
EPA	Environmental Protection Agency
HMTA	hexamethylenetetramine
HPV	high-production volume
IR ₁	inverted repeat 1
LPS	lipopolysaccharide
LTA	lipoteichoic acid
MFS	major facilitator superfamily
MIC	minimum inhibitory concentration
NAG	N-acetyl glucosamine
NAM	N-acetyl muramic
OM	outer membrane
QAC	quaternary ammonium compound
QAS	quaternary ammonium salt
S _N 2	nucleophilic substitution
TA	teichoic acid
WWTP	waste water treatment plants

CONTENTS

1. INTRODUCTION	1
1.1. Structure, properties and application of quaternary ammonium compounds ...	1
1.2. Antibacterial potential of quaternary ammonium compounds	2
1.3. Mechanism of antibacterial action	3
1.4. Challenges in application of quaternary ammonium compounds.....	6
1.4.1. Bacterial resistance development	6
1.4.2. Ecotoxicological and toxicological concerns	9
1.5. Strategies for the development of next generation quaternary ammonium compounds.....	10
1.5.1. Natural scaffolds as new synthetic precursors	12
1.5.2. Environmentally friendly “ <i>soft</i> ” quaternary ammonium compounds.....	13
2. AIMS AND SCOPE OF THE RESEARCH.....	16
3. SCIENTIFIC PAPERS.....	17
3.1. New membrane active antibacterial and antiviral amphiphiles derived from heterocyclic backbone of pyridinium-4-aldoxime.....	18
3.2. A dual antibacterial action of soft quaternary ammonium compounds: bacteriostatic effects, membrane integrity, and reduced <i>in vitro</i> and <i>in vivo</i> toxicity	40
3.3. Naturally derived 3-aminoquinuclidine salts as new promising therapeutic agents	58
4. CONCLUSIONS AND FUTURE PERSPECTIVE.....	77
5. APPENDIX	80
5.1. Supplementary material to chapter 3.2.....	80
5.2. Supplementary material to chapter 3.3.....	83
6. REFERENCES.....	99
7. CURRICULUM VITAE	107
8. LIST OF PUBLICATIONS.....	108

1. INTRODUCTION

1.1. Structure, properties and application of quaternary ammonium compounds

Quaternary ammonium compounds (QACs), also known as *quats*, are a class of organic compounds synthesized from tertiary amines through the Menshutkin reaction. Synthetic mechanism involves a nucleophilic substitution (S_N2) reaction, where the nitrogen atom of the tertiary amine attacks a partially positive carbon atom in a quaternization reagent, typically an alkyl or aryl halide. As a result, the nitrogen becomes permanently positively charged, generating a quaternized ammonium ion. Depending on the number of quaternized nitrogen atoms, QACs can be classified into mono-, bis-, and poly-QACs, exhibiting distinct properties and effectiveness. The choice of quaternization reagent determines the counterion, most commonly including chloride, bromide and iodide due to their favorable leaving group characteristics. Since QACs consist of a positively charged cation and a corresponding anion, they are often referred to as quaternary ammonium salts (QASs), represented by the general formula $[NR_4]^+X^-$. Accordingly, QACs behave as ionic compounds in terms of physicochemical properties [1].

A defining feature of QACs is their amphiphilic cationic backbone, which allows them to aggregate into micelles in solution while simultaneously reducing surface tension [2], [3]. This property classifies QACs as cationic surfactants, making them valuable components of detergents and anti-static agents [4], as exemplified by the di-tallow dimethyl ammonium chloride (DTDMAC) – a widely used QAC in fabric softeners until the late 1990s [5].

Beyond their amphiphilic properties, the cationic backbone also enables strong adsorption to negatively charged surfaces, a characteristic that underpins the herbicidal activity of certain QACs. This was first observed with cetyltrimethylammonium bromide (CTAB), leading to the development of QAC-based herbicides like diquat and paraquat [1], [6], [7]. These compounds, characterized by two positively charged nitrogen atoms and pyridine rings, are highly effective due to their ability to generate reactive oxygen species, such as superoxide and hydroxyl radicals. Their strong adsorption to negatively charged soil particles helps localize their activity and minimize toxic effects on humans, although their rate of self-degradation or induced degradation in the environment remains notably low [1], [6], [7].

In addition to their role in household and agricultural applications, QACs are indispensable in healthcare and hygiene products due to their potent antimicrobial activity [8], [9], [10]. Their ability to target and inhibit microbial growth, combined with the flexibility to fine-tune their structural features for optimal efficacy, has made QACs essential in combating pathogenic microorganisms. However, their widespread use raises concerns about environmental persistence, bacterial resistance, and long-term safety [10–14].

1.2. Antibacterial potential of quaternary ammonium compounds

Quaternary ammonium compounds (QACs) are widely recognized for their ability to eradicate a broad spectrum of microorganisms, including planktonic and sessile bacterial species, fungi, viruses, and protozoa [2], [15–18]. However, despite their diverse antimicrobial properties, QACs are particularly valued for their profound activity against bacterial strains.

The effectiveness of QACs in suppressing bacterial pathogens was first demonstrated in early 1916 by Jacobs and Heidelberg who described the bactericidal effect of QACs derived from hexamethylenetetramine, HMTA [19]. In 1930s, German bacteriologist Gerhard Domagk reported benzyltrimethylammonium chloride, BAC (Figure 1), suggesting that the addition of an aliphatic chain to the core structure improves antibacterial activity [20]. Soon after his discovery, variants of BAC that differed in the length of the alkyl chain on the quaternary nitrogen atom were marketed under the common name “Zephirol”, which was mainly used as hospital disinfectant for both surfaces and hands [21]. In less than fifteen years after its discovery, BAC was an active ingredient incorporated in antiseptics for skin disinfection in 48% of hospitals across the United States of America [22], [23]. Nevertheless, the discovery of the potent antimicrobial activity of BAC paved the way for the development of new QAC variants. One of the first to reach the market was cetylpyridinium chloride, CPC, (Figure 1) introduced in 1939, just a few years after BAC [24]. Recognized as a powerful antibacterial agent, CPC was primarily incorporated into dental hygiene products, such as mouthwashes, where it remains in use today due to its targeted effect on the causative agent of caries, the bacterium *Streptococcus mutans* [25–27].

The broad-spectrum antibacterial properties of QACs soon led to the investigation of the structural features that enable their efficacy. In 1986, Jono *et al.* described the effects of structural modifications of BAC in terms of chain length on antibacterial activity [28].

They found that the bactericidal effect of BAC increases with increasing chain length, with the C₁₂ BAC analogue being the most effective. The same structural influence was further explored using quaternized cithosan derivatives as a starting point. In 1996 Ho Kim *et al.* synthesized cithosan QACs substituted with alkyl chains of varying length [29]. Having also recognized the superior effect of the C₁₂ analogue towards the representative Gram-positive strain, *Staphylococcus aureus*, they suggested that an increase in hydrophobicity of the core scaffold could serve as another important factor reflecting to antibacterial potency of QACs. This hypothesis was further supported by the development of didecyltrimethylammonium chloride, DDAC. The increased hydrophobicity, resulting from two aliphatic side chains, each with a length of ten carbon atoms attached to the quaternary nitrogen atom, established DDAC as an exceptionally potent antimicrobial agent (Figure 1). It soon became used in numerous disinfectant formulations effectively eradicating a wide range of bacterial pathogens, at the same time outperforming its analogue, BAC [27], [30], [31].

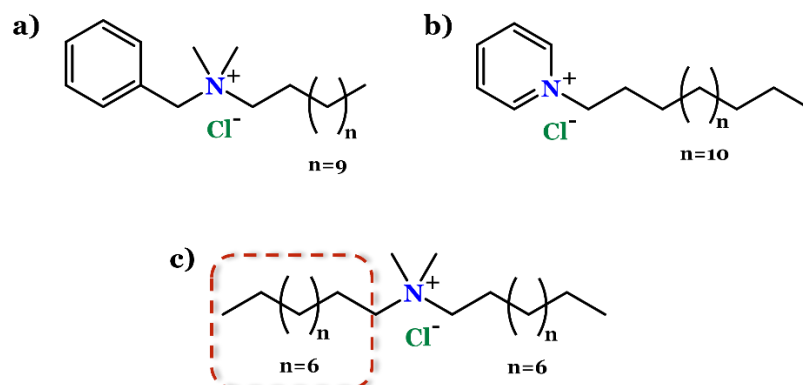


Figure 1. Chemical structures of common marketed monoquaternary ammonium compounds (QACs): **a)** benzyltrimethylammonium chloride (BAC), **b)** cetylpyridinium chloride (CPC) and **c)** didecyltrimethylammonium chloride (DDAC) with dashed red rectangle indicating increased hydrophobicity of the core scaffold.

These early investigations of structure-activity relationships led to speculations about their possible mode of action, with plausible indications of their membrane-targeting properties. Specific structural features of QACs point out the possibility of their incorporation into the lipid bilayers of the bacterial membrane, paving the way for more in-depth research into the mode of action.

1.3. Mechanism of antibacterial action

Despite the potent antibacterial properties of quaternary ammonium compounds (QACs) across a wide range of bacterial species, Gram-positive bacteria have been observed to be generally more susceptible to these agents [2], [13], [32]. This trend is

primarily attributed to the structural differences in bacterial cell envelopes, supporting the hypothesis that the mode of action of QACs primarily involves membranolytic approach [33].

Gram-negative bacteria have an inner membrane, followed by thin peptidoglycan layer surrounded by an additional outer membrane (OM) hindering the membranolytic properties of QACs (Figure 2). As a distinguishing feature of Gram-negative species, the OM contains the inner leaflet composed of the lipid bilayers and the differing outer leaflet comprised of glycolipids, namely lipopolysaccharide (LPS) [34], [35]. In contrast, the Gram-positive species lack the OM, but their intracellular contents are preserved with the cell envelope coated with 30 to 100 nanometer thick layer of peptidoglycan – complex network of N-acetyl glucosamine (NAG) and N-acetyl muramic (NAM) acids cross-linked with peptide chains (Figure 2) [34], [36], [37]. Although such thickness ensures mechanical protection, distinctive polymers anchored in the peptidoglycan matrix, known as teichoic acids (TA), enable strong membranolytic activity of QACs against Gram-positive strains. The backbone of TA includes repeats of negatively charged residues of glycerol, glucosyl or ribitol phosphate [34]. Depending on the type of attachment of TA to peptidoglycan, those polymers are generally divided into two large groups – covalently linked cell wall teichoic acid (CWTA) and lipoteichoic acid (LTA) attached to the head groups of the membrane lipids [34], [38], [39].

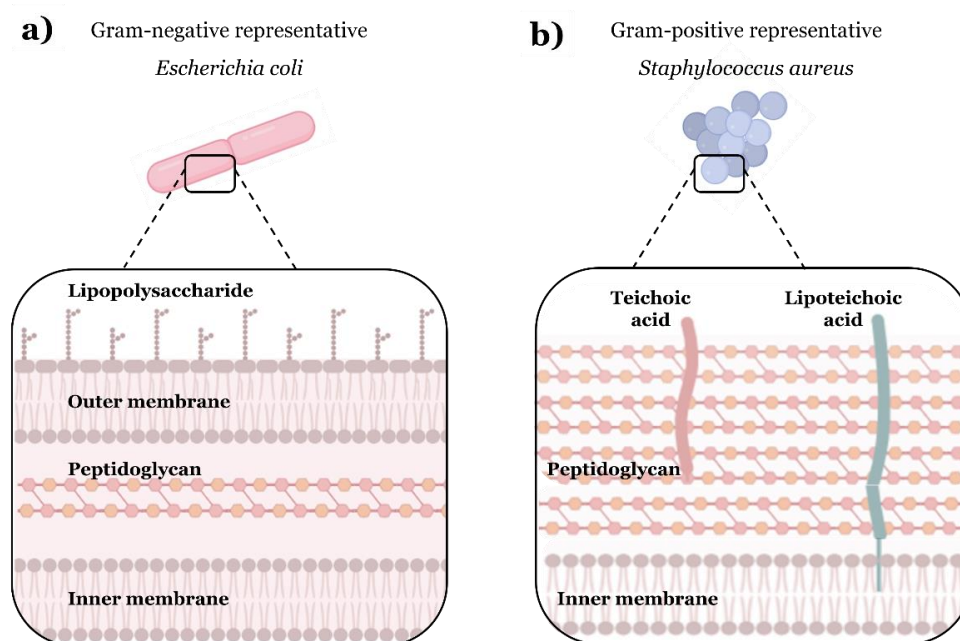


Figure 2. Schematic representation of cell envelope: **a)** representative Gram-negative bacterium *Escherichia coli* and **b)** representative Gram-positive bacterium *Staphylococcus aureus*.

Considering the structural nature of cationic surfactants, in 1968 Salton was the first to suggest the potential membranolytic activity of QACs, describing it as a sequence of events. The first step involves the adsorption of the compound onto the membrane surface facilitated by the electrostatic interaction of the positively charged QAC backbone with the negatively charged residues of CWTA and LTA. This is further followed by the insertion of hydrophobic substituents of QAC into the membrane matrix causing the efflux of cytoplasmic contents due to membrane disorganization. Ultimately, complete degradation of cell envelope is achieved through the activation of autolytic enzymes [33].

The proposed membranolytic approach was further supported through numerous literature data employing different experimental techniques. Lambert and Hammond described the membrane disorganization upon exposure to low concentrations of QACs through the disruption of cell osmoregulation processes by measuring the leakage of potassium ions and disbalance of proton gradient during the incubation time [40]. Additional studies demonstrated the depolarization of bacterial membrane caused by the increase of net positive charge on the membrane surface upon the initial electrostatic interaction [41–44]. Alkhalifa *et al.* combined computational modeling coupled with experimental approach to further inspect the potential of QACs to lyse the Gram-positive bacterial cell envelope [45]. Their computational model revealed that both mono- and poly- cationic QAC variants follow the same order of events in terms of initial electrostatic interaction and further insertion of hydrocarbon chains into the membrane matrix, with insertion of one tail at the time in case of poly- QACs. Furthermore, advanced microscopy techniques were also used to visualize the QAC-induced alterations in bacterial morphology, specifically showing cellular irregularities and surface indentations in treated bacterial cells [46–49].

Although QACs are generally considered to act as membrane targeting antimicrobials, their complete mode of action is yet not fully elucidated. Recent investigations demonstrated that QACs may employ multiple antibacterial mechanisms including the inhibition of protein synthesis pathways, DNA intercalation or down-regulation of proteins responsible for key metabolic processes and stress response pathways [50–54]. These findings underscore the need for further investigation, particularly into structure-activity relationships, which could lay the groundwork for the development of next-generation antimicrobials.

1.4. Challenges in application of quaternary ammonium compounds

The extensive use of quaternary ammonium compounds (QACs) across a wide range of industrial sectors has resulted in their classification as high-production volume (HPV) chemicals, with an estimated 500,000 tons released into the environment in 2004 [55]. Besides industrial runoffs, the introduction of QACs in environmental settings is also achieved through a variety of anthropogenic activities, most commonly implying the overuse of products containing QACs, e.g. hygiene and household products or antiseptic and disinfectant agents. Such overuse particularly raised great concern upon the recent pandemic outbreak caused by SARS-CoV-2 virus, with over 50% of disinfectants containing QACs as active ingredients, as evidenced by the United States Environmental Protection Agency (EPA) [56].

Due to their physicochemical properties, which confer long-term stability, it is crucial to consider the consequences of environmental accumulation of QACs. Most commercially available QACs eventually reach wastewater treatment plants (WWTPs), with dialkyldimethyl ammonium (DADMAC), alkyltrimethyl ammonium (ATMAC), and benzylalkyldimethyl ammonium compounds (BAC) being the most prevalent analogues [57]. Although QACs are considered biodegradable under aerobic conditions, their strong adsorption often limits the opportunity for complete decomposition. This adsorption is achieved through electrostatic interaction of cationic backbone with negatively charged surfaces, such as soil particles, sewage sludge, or sediments [57–59]. WWTPs, which are primarily designed to remove easily degradable organic contaminants, are generally ineffective at fully removing QACs. As a result, significant quantities of these compounds persist in treated effluents and are ultimately released into aquatic ecosystems, such as rivers or seas [57], [60], [61].

The persistence of sub-inhibitory concentrations of QACs in the environment not only promotes the development of bacterial resistance among environmental isolates but also exerts toxic effects on a wide range of aquatic organisms. Addressing this pressing issue implies the development of the next-generation QAC derivatives with improved environmental profiles and the implementation of more efficient wastewater treatment strategies to mitigate their ecological impact.

1.4.1. Bacterial resistance development

Selective pressure achieved through the constant presence of sub-lethal concentrations of commercially available quaternary ammonium compounds (QACs)

enabling bacterial adaptation, serves as a trigger for the activation of bacterial resistance mechanisms.

One of the most well-known bacterium resistant to a broad spectrum of antibacterial drugs is *Staphylococcus aureus*, categorized among the six most virulent and resistant pathogens under the acronym ESKAPE (*Enterococcus faecium*, *Staphylococcus aureus*, *Klebsiella pneumoniae*, *Acinetobacter baumannii*, *Pseudomonas aeruginosa*, and *Enterobacter* spp.). Nearly fifty years ago, Johnson and Dyke described the resistance of *S. aureus* to the ethidium bromide, QAC which is well-known as DNA-intercalating biological dye, attributing this phenomenon to a specific plasmid-encoded genetic elements [62]. Following their discovery, a series of plasmid-borne *qac* genes were identified, encoding the expression of specific transmembrane proteins commonly referred to as efflux pumps, which play a key role in mediating bacterial resistance to QAC [63].

One of the most studied *qac* genes is *qacA*, which encodes the expression of QacA efflux pump, a protein with 14 transmembrane segments. This efflux pump belongs to the major facilitator superfamily (MFS) and facilitates the active transport of various substances across the cell membrane [64], [65], [66]. The expression of QacA is tightly regulated by the transcriptional repressor QacR, a dimeric protein consisting of 188 amino acids (23 kDa) [67–70]. QacR functions as a negative regulator by binding to the inverted repeat 1 (IR1) sequence, the transcription initiation site of the *qacA* gene, in the form of a dimer pair [71]. QacR is activated by binding a wide range of structurally diverse compounds, which further serve as substrates for the QacA membrane transporter. Ligand binding induces a conformational change in QacR, causing its dissociation from the operator IR1 site. Consequently, this dissociation allows the transcription of *qacA* gene and subsequent expression of QacA efflux pump. These pumps utilize the energy originating from hydrolysis of adenosine triphosphate (ATP) to expel toxic compounds across the cell membrane, therefore diminishing their toxicity [72], [73].

Although it is not yet fully understood which ligands are structurally most favorable for the QacR binding site, it is known that conformational changes in QacR are triggered by the binding of lipophilic, cationic compounds. The binding site of the repressor contains four glutamic acid residues, along with various aromatic and polar amino acids, providing its suitability for recognition of a wide variety of structurally diverse ligands [74]. Negatively charged glutamic acid residues electrostatically interact with the positively charged nitrogen atom in the structure of QACs, thereby facilitating their

binding to the active site of the repressor leading to its conformational change that mediates the efflux of QACs. Schumacher *et al.* have published six distinct crystallized structures of QacR, each complexed with different QAC representatives within its highly adaptable binding site (Figure 3) [74], [75]. Interestingly, despite structural similarities of ligands in terms of aromatic rings, they have shown that the binding site of the QacR repressor accommodates both mono- and bis-QACs which underscores its multi-drug recognition potential.

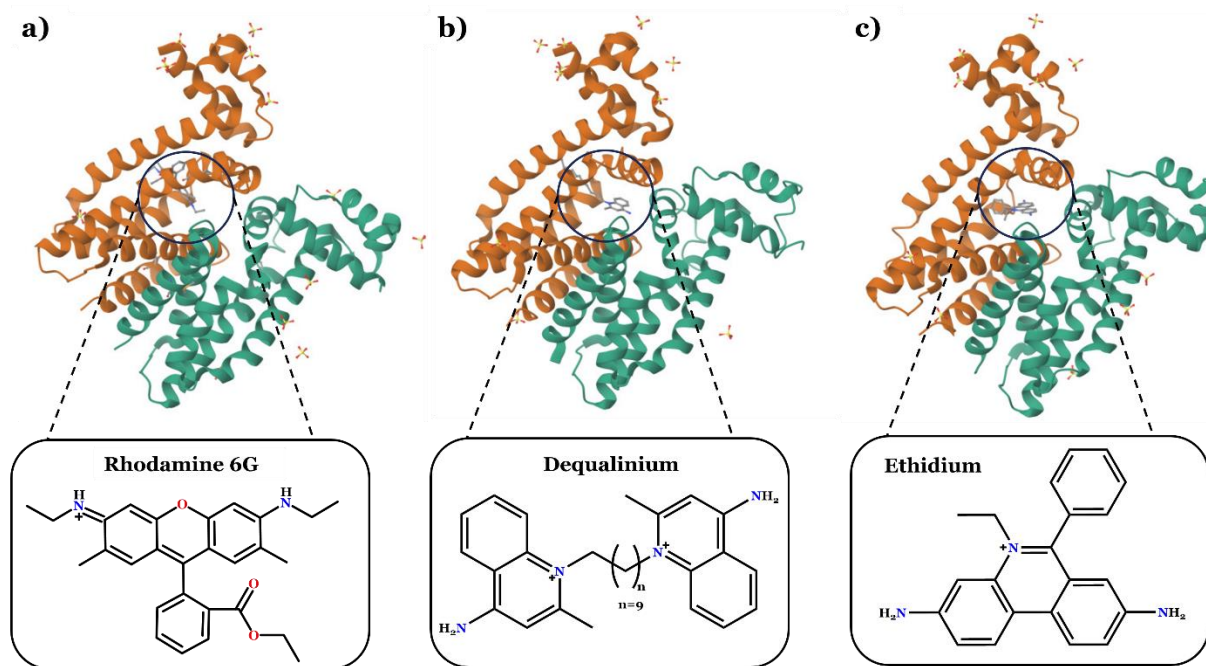


Figure 3. Crystal structures of QacR dimer complexed with different quaternary ammonium compounds (QACs): **a)** QacR complexed with rhodamine (PDB file 1JUS) [75], **b)** QacR complexed with dequalinium (PDB file 3BT9) [74] and **c)** QacR complexed with ethidium (PDB file 1JTY) [75].

Although resistance mechanisms mediated by the expression of Qac efflux pumps have been the most extensively studied, growing data suggest that changes in cell membrane composition serve as an alternative resistance pathway. These changes include modifications in fatty acid and protein composition, as observed in populations of *Pseudomonas aeruginosa* and *Listeria monocytogenes* exposed to commercially available QAC analogues [76–79]. Beyond these compositional changes, resistance can also involve alterations to the cell surface charge. Specifically, Nagai *et al.* demonstrated that *Pseudomonas fluorescens* reduces its net surface charge to disrupt electrostatic interactions with cationic agents, thereby diminishing their membranolytic activity [76], [80].

Addressing the challenge of bacterial resistance requires not only the synthesis of novel QACs unfamiliar to bacterial intrinsic resistance pathways, but also a deeper

investigation into how structural features influence biological activity and resistance development. Such efforts will be pivotal in mitigating the spread of resistance and ensuring the long-term efficacy of QAC-based disinfectants and antiseptics.

1.4.2. Ecotoxicological and toxicological concerns

The presence of quaternary ammonium compounds (QACs) in aquatic systems, due to their inefficient removal by wastewater treatment plants (WWTPs), has raised questions about the ecotoxicity of this class of antimicrobials. The chemical stability of commercially available QAC analogues can be exemplified by the nearly nine-month half-life of benzalkonium chloride (BAC), emphasizing the urgency of addressing the issue of environmental saturation with this class of cationic surfactants [73], [81].

Although QACs retain their biocidal properties upon introduction to environmental setting, this class of compounds have not been reported to cause an acute toxicity towards aquatic organisms, possibly due to their physicochemical properties including strong surface adsorption [82–84]. However, experimental studies suggest a more complex picture, with varying toxicity rates depending on species and QAC structure, particularly as their usage continues to grow. As early as 1997, Utsunomiya *et al.* reported that the half-maximal effective concentration (EC₅₀) of common QACs against the unicellular green algae *Dunaliella* sp. was 18 µg/mL – approximately five times higher than that of representative anionic surfactants [85], [86]. Similarly, *Chlorella pyrenoidosa* was shown to be sensitive to thirteen QACs in a comprehensive study by Jing *et al.*, where the length of alkyl chains was identified as key toxicity determinant [87]. Moreover, studies by Garcia *et al.* highlighted the superior toxicity of alkyl QACs compared to their benzylated analogues against planktonic crustaceans (*Daphnia magna*) and the symbiotic bacterium *Photobacterium phosphoreum* [88]. Not only do QACs affect algae and various planktonic species, but their toxicity extends to higher organisms, predominantly fishes, differing in toxicity profiles depending on the species [89–91].

Beyond ecotoxicological hazards, increasing evidence highlights the negative effects of QAC exposure on human health. While acute toxicity caused by high concentration levels of QACs is rare, chronic exposure through everyday household and hygiene products poses a more significant risk [91–93]. For many commercially available QACs, existing literature data emphasized the possibility of inducing respiratory side effects, such as asthma, especially among the healthcare sector employees [94–96]. The excessive use of QAC-based products has brought significant attention to the consequences of

chronic exposure, which were thoroughly investigated following the recent SARS-CoV-2 pandemic outbreak [97]. In their pilot study, Hrubec *et al.* detected QAC traces in the blood samples of 80% of participants, linking these findings to certain biochemical pathways in a statistically significant manner [98]. Similarly, Zheng *et al.* reported the presence of QACs in breast milk, identifying breastfeeding as a potential exposure route for newborns [99]. Furthermore, a recent study by Kirkpatrick *et al.* demonstrated that long-term exposure to a mixture of common QACs, including alkyltrimethylbenzylammonium chloride (ADBAC) and didecyltrimethylammonium chloride (DDAC), adversely affects the reproductive system. Their findings, based on both *in vitro* and *in vivo* mouse models, showed that the severity of these effects correlates with the duration of exposure [100].

In light of these findings, it is clear that the widespread use and environmental persistence of QACs necessitate urgent action. Stricter regulatory frameworks, alongside the optimization of existing formulations, are crucial to mitigate their ecotoxicological and human health risks. Furthermore, the development of safer and environmentally compatible QAC alternatives must be prioritized to address the pressing challenges posed by their accumulation and long-term exposure.

1.5. Strategies for the development of next generation quaternary ammonium compounds

Limitations of traditional commercially available quaternary ammonium compounds (QACs), particularly their tendency to accumulate in the environment and concerns about their safety, have driven the development of next-generation QACs. The primary goal in designing these new analogues is to retain potent antimicrobial activity while enhancing their environmental degradability and improving their safety profiles for broader and more responsible use.

The development of next-generation QACs often begins with the structural optimization of traditional compounds to create variants unable to activate intrinsic bacterial resistance mechanisms. Benzalkonium chloride (BAC), one of the most widely used QAC, has been of a major focus in such studies. Pernak *et al.* synthesized and evaluated a series of forty BAC analogues for their antimicrobial activity against bacteria and fungi. Their findings revealed that the minimum inhibitory concentration (MIC) values of these analogues were comparable to those of standard BAC. They further suggested that these derivatives could serve as potential antimicrobial agents in food

processing, with a reduced tendency to trigger bacterial resistance mechanisms [101]. Building on this approach, recent studies have also concentrated on modifying BAC derivatives. Brycki *et al.* introduced a pyridine moiety into the BAC scaffold, varying the alkyl chain lengths attached to the quaternary nitrogen atom. However, introducing nitrogen into the aromatic ring did not enhance the antibacterial activity, as the newly synthesized analogues exhibited slightly higher MIC values compared to standard BAC [102]. The same research group later explored multicationic modifications of the BAC core structure. These derivatives, particularly C₁₀ and C₁₂ analogues, demonstrated significantly improved antibacterial potency [103]. Similarly, Toles *et al.* synthesized twenty seven structurally diverse multicationic BAC analogues. Their findings revealed not only greater antibacterial activity but also reduced susceptibility of hospital-acquired methicillin-resistant *Staphylococcus aureus* (HA-MRSA), underlining multicationic derivatives as promising candidates in next-generation synthesis [104].

In addition to structural modifications of existing QAC scaffolds, establishing a clear correlation between structure and antibacterial activity can facilitate the rational design of new compounds with targeted effects. This can be achieved by synthesizing QAC derivatives with diverse structural motifs, such as alkyl chain modifications, incorporation of heterocyclic moieties, and functionalization of the QAC backbone. These approaches aim to enhance antimicrobial efficacy, selectivity, and environmental safety [105]. Recent advancements in this field include the development of antimicrobial peptide (AMP)-mimetic QACs, which exhibit favorable therapeutic indices and minimal toxicity toward mammalian cells [105–108]. Furthermore, alternative quaternary compounds, such as quaternary phosphonium or sulfonium derivatives, are emerging as promising non-nitrogen-based scaffolds, offering unique chemical and biological properties to expand the spectrum of antimicrobial agents [109].

While these approaches primarily emphasize synthetic modifications, natural product-guided synthesis remains an underexplored strategy for developing new antimicrobial agents. By leveraging natural scaffolds and bioactive molecules, the principles of natural product synthesis can be applied to the design of next-generation QACs, enabling the development of novel, highly effective, and structurally diverse antimicrobial compounds.

1.5.1. Natural scaffolds as new synthetic precursors

An early example of the broad-spectrum biological activity of naturally occurring substances is berberine, plant-derived alkaloid with inherent quaternary ammonium compound (QAC) structure (Figure 4). Recognized for its potent antibacterial and antitumor properties, berberine underscores the therapeutic potential of naturally occurring scaffolds as promising precursors for the development of new antibacterial agents [110–113].

The use of natural substances as scaffolds for QAC synthesis represents a cost-effective and sustainable approach, despite the limited number of studies reported to date. Building on prior findings, Joyce *et al.* synthesized mono- and bis-QAC derivatives using alkaloid cores such as quinine and nicotine (Figure 4) as starting materials [114]. In both cases, quaternization significantly enhanced antimicrobial activity compared to the precursor structures, demonstrating the benefits of structural modification. Similarly, Burilova *et al.* employed 1-azabicyclo[2.2.2]octane, known as quinuclidine (Figure 4), a bicyclic alkaloid found in *Cinchona* bark, to create long-chained QAC derivatives. Their results revealed that analogues with longer alkyl chains exhibit superior antibacterial potency, exceeding the efficacy of norfloxacin. Importantly, the most active compound demonstrated minimal cytotoxicity against a healthy human epidermal cell line, highlighting its potential for practical applications [115]. Bazina *et al.* further explored this precursor by utilizing 1-azabicyclo[2.2.2]octan-3-ol, 3-hydroxyquinuclidine, (Figure 4) to synthesize QACs with alkyl chains ranging from three to fourteen carbon atoms. They identified a chain length of at least ten carbons as critical for activity, with the most potent derivative bearing the longest chain [116]. Upon the treatment with their candidate compound at concentrations above the minimal inhibitory, they observed significant morphological changes of *Staphylococcus aureus* cells, suggesting its potency to disrupt bacterial membrane. Building on the precursor structure also analogous to quinuclidine, Kontos and coworkers reported the synthesis of new QACs derived from 1,4-diazabicyclo[2.2.2]octane, DABCO, (Figure 4). By fine-tuning the lipophilicity of mono- and bis-cationic derivatives, they developed compounds with sub-micromolar antibacterial activity, further outlining the versatility of quaternary ammonium scaffolds depending on the structural features [117].

Demonstrating the diversity of potential natural precursors, Allen *et al.* quaternized ianthelliformisamine C, a compound isolated from a sea sponge. The resulting derivatives

exhibited a wide range of pharmacological activities, including antibacterial effects, membrane-perforation potential, and cytotoxicity [118].

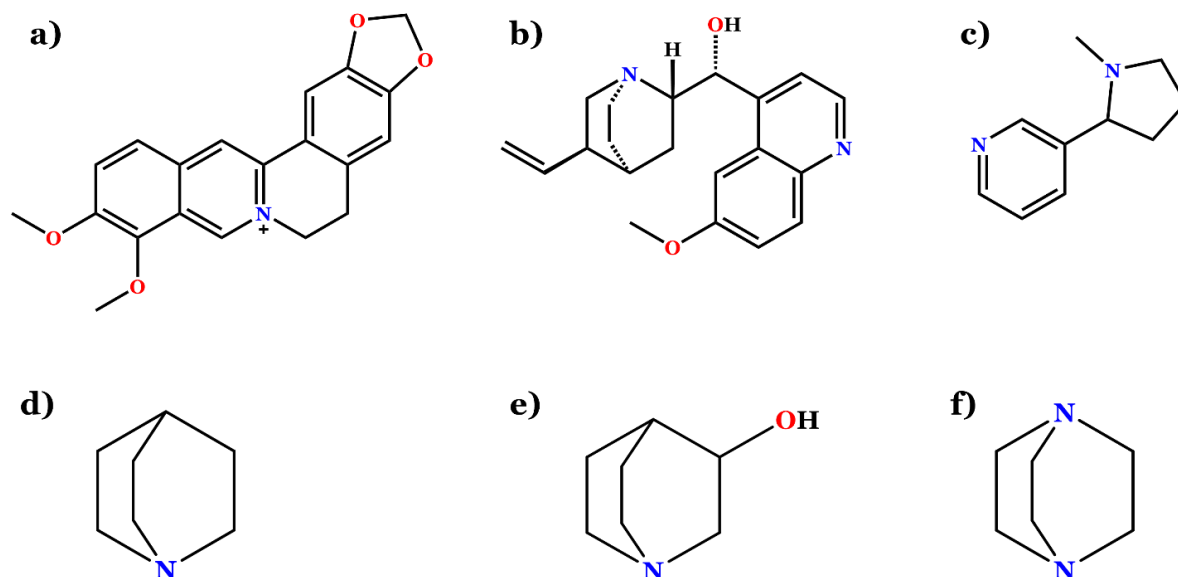


Figure 4. Chemical structures of **a)** berberine – naturally occurring quaternary ammonium compound and precursors used as quaternization backbones of natural-guided synthesis of novel QACs: **b)** quinine, **c)** nicotine, **d)** 1-azabicyclo[2.2.2]octane (quinuclidine), **e)** 1-azabicyclo[2.2.2]octan-3-ol (3-hydroxyquinuclidine) and **f)** 1,4-diazabicyclo[2.2.2]octane (DABCO).

These examples shed light to the immense potential of natural scaffolds for designing next-generation QACs. Exploring underutilized natural products and deeper investigation of structure-activity relationship could accelerate the design of effective, sustainable antimicrobial agents tailored for specific applications.

1.5.2. Environmentally friendly “soft” quaternary ammonium compounds

To mitigate the environmental accumulation of conventional quaternary ammonium compounds (QACs) and the subsequent development of bacterial resistance, novel synthetic strategies focus on integrating hydrolysable functional groups into the compound's core. Such quaternized products are often referred to as “soft” QACs. The key hypothesis behind this synthetic approach is that controlled decomposition of the initial structure into biologically inactive compounds reduces the likelihood of activating intrinsic resistance mechanisms.

The most common functionalities enabling the production of “soft” QAC variants are ester and amide groups, which are prone to hydrolysis under specific conditions. An early example of “soft” QACs-driven synthesis was reported by Lindstedt *et al.*, who synthesized a series of betaine ester-based quaternary derivatives [119]. Although these

compounds demonstrated antibacterial activity comparable to that of traditional QAC cetyltrimethylammonium bromide (CTAB), the ester analogues exhibited a pronounced tendency for hydrolysis. This high hydrolysis rate could potentially threaten the opportunity of antibacterial action.

In their study, Alkhalifa *et al.* demonstrated differences in the membranolytic activity of alkyl and “soft” ester QAC variants with identical hydrocarbon chain lengths [45]. While all series exhibited membranolytic activity, both computational simulations and experimental data pointed out superior antibacterial activity of alkyl derivatives. Based on these findings, the authors hypothesized that the chemical instability of the ester functionality, along with its susceptibility to uncontrolled decomposition, is likely to explain the lower antibacterial potential of these analogues.

On the other hand, further exploration of hydrolysis-prone groups revealed the substantial potential of the more robust amide functionality. Due to the lower electronegativity of nitrogen compared to oxygen, the amide bond is chemically more stable than the ester bond. This was confirmed by Allen *et al.*, who investigated the degradation rates of amide- and ester-based QAC variants in solutions with varying pH values [73]. They observed that ester-containing QACs had a half-life of approximately 3 hours at pH 7, with almost immediate decomposition at both lower and higher pH levels, highlighting the instability of these QACs and their inability to reach full antibacterial potential. In contrast, amide analogues remained stable for over 16 hours across a wide range of pH values, at the same time exhibiting greater activity towards selected bacterial panels. Similarly, Kontos *et al.* found amide-based QACs derived from piperazine and 2,2-diazabicyclo[2.2.2]octane (DABCO) to be potent bacterial agents, with the low micromolar range of minimum inhibitory concentrations [117].

In addition to the possibility of chemical degradation under low-pH conditions, the structural nature of the amide bond allows for potential enzymatic breakdown by proteases upon cell uptake. Given both the antibacterial potential and the controlled degradation of amide-based QACs, the synthesis and investigation of the biological activity and mechanisms of action of these variants is an essential future perspective.

Moreover, considering the enhanced polarity introduced by the electron density distribution of the amide bond, understanding how this property correlates with antibacterial potential and mode of action is crucial. To date, studies on QAC structure-activity relationships have primarily focused on the impact of precursor rigidity on

antimicrobial potential leaving the influence of backbone functionalization as an unexplored field [117], [120].

However, with recent synthetic strategies focusing on functionalizing the core scaffold with polar, hydrolysis-prone groups, further research is needed to elucidate how increased polarity influences the biological activity of new QAC derivatives. Since the antimicrobial potential of this class of compounds is largely attributed to their structural characteristics as cationic surfactants, a more detailed investigation into the optimal balance between hydrophilic and hydrophobic properties of the scaffold will provide valuable insight into structure-activity relationships. This knowledge could ultimately lead to the specific fine-tuning of structural elements, enabling the design and development of biologically potent yet environmentally friendly QAC variants.

2. AIMS AND SCOPE OF THE RESEARCH

This dissertation addresses the critical public health challenge of bacterial resistance by focusing on the development of novel antimicrobial agents, quaternary ammonium compounds (QACs), and examining their biological activity and mechanisms of action.

The main objectives of this doctoral dissertation are:

(O1) Synthesis of new quaternary ammonium compounds (QACs) from different heterocyclic precursors. Quaternized products derived from pyridine-4-aldoxime scaffold will represent traditional QACs analogues of commercially available cetylpyridinium chloride, CPC. On the other hand, QACs derived from 3-amidoquinuclidine will result in “soft” environmentally compatible variants.

(O2) Evaluation of the biological activity of the newly synthesized “traditional” and “soft” QAC derivatives, with emphasis on their antibacterial potential and prediction of toxicity towards mammalian cell lines of epidermal origin.

(O3) Structure-activity relationship investigation of the QAC’s backbone polarity to antibacterial properties in comparison with commercial mono- quaternary ammonium compounds.

The doctoral dissertation is based on the following hypotheses:

(H1) Newly synthesized QAC derivatives will exhibit better antibacterial activity compared to their non-quaternary precursors.

(H2) Increasing the polarity of the functional group on the heterocyclic backbone of the new QAC derivatives will have a varying impact on their antibacterial activity.

(H3) Selected newly synthesized “soft” QAC derivatives will be susceptible to degradation, making them less likely to trigger bacterial resistance mechanisms.

3. SCIENTIFIC PAPERS






**3.1. NEW MEMBRANE ACTIVE ANTIBACTERIAL AND ANTIVIRAL
AMPHIPHILES DERIVED FROM HETEROCYCLIC BACKBONE OF
PYRIDINIUM-4-ALDOXIME**

Reproduced from

Crnčević, D; Kree, L; Cvitković, M; Brkljača, Z; Sabljic, A; Vuko, E; Primožič, I; Odžak, R; Šprung, M. New Membrane Active Antibacterial and Antiviral Amphiphiles Derived from Heterocyclic Backbone of Pyridinium-4-Aldoxime // *Pharmaceuticals*, 15 (2022),
doi: 10.3390/ph15070775

Article

New Membrane Active Antibacterial and Antiviral Amphiphiles Derived from Heterocyclic Backbone of Pyridinium-4-Aldoxime

Doris Crnčević^{1,2}, Lucija Krce³ , Mislav Cvitković³ , Zlatko Brkljača^{4,5}, Antonio Sabljic^{1,2}, Elma Vuko⁶ , Ines Primožič⁷, Renata Odžak^{1,*}  and Matilda Šprung^{1,*} 

- ¹ Department of Chemistry, Faculty of Science, University of Split, R. Bošković 33, 21 000 Split, Croatia; dcrncevic@pmfst.hr (D.C.); asablji1@pmfst.hr (A.S.)
- ² Doctoral Study of Biophysics, Faculty of Science, University of Split, R. Bošković 33, 21 000 Split, Croatia
- ³ Department of Physics, Faculty of Science, University of Split, R. Bošković 33, 21 000 Split, Croatia; lucija.krce@pmfst.hr (L.K.); mcvitkovi@pmfst.hr (M.C.)
- ⁴ Division of Organic Chemistry and Biochemistry, Ruđer Bošković Institute, Bijenička c. 54, 10 000 Zagreb, Croatia; zlatko.brkljaca@irb.hr
- ⁵ Selvita Ltd., Prilaz Baruna Filipovića 29, 10 000 Zagreb, Croatia
- ⁶ Department of Biology, Faculty of Science, University of Split, R. Bošković 33, 21 000 Split, Croatia; elma@pmfst.hr
- ⁷ Department of Chemistry, Faculty of Science, University of Zagreb, Horvatovac 102a, 10 000 Zagreb, Croatia; ines.primozic@chem.pmf.hr
- * Correspondence: rodzak@pmfst.hr (R.O.); msprung@pmfst.hr (M.Š.)



Citation: Crnčević, D.; Krce, L.; Cvitković, M.; Brkljača, Z.; Sabljic, A.; Vuko, E.; Primožič, I.; Odžak, R.; Šprung, M. New Membrane Active Antibacterial and Antiviral Amphiphiles Derived from Heterocyclic Backbone of Pyridinium-4-Aldoxime. *Pharmaceuticals* **2022**, *15*, 775. <https://doi.org/10.3390/ph15070775>

Academic Editor: Serena Massari

Received: 31 May 2022

Accepted: 20 June 2022

Published: 22 June 2022

Publisher's Note: MDPI stays neutral with regard to jurisdictional claims in published maps and institutional affiliations.



Copyright: © 2022 by the authors. Licensee MDPI, Basel, Switzerland. This article is an open access article distributed under the terms and conditions of the Creative Commons Attribution (CC BY) license (<https://creativecommons.org/licenses/by/4.0/>).

Abstract: Quaternary ammonium salts (QAS) are irreplaceable membrane-active antimicrobial agents that have been widely used for nearly a century. Cetylpyridinium chloride (CPC) is one of the most potent QAS. However, recent data from the literature indicate that CPC activity against resistant bacterial strains is decreasing. The major QAS resistance pathway involves the QacR dimer, which regulates efflux pump expression. A plausible approach to address this issue is to structurally modify the CPC structure by adding other biologically active functional groups. Here, a series of QAS based on pyridine-4-aldoxime were synthesized, characterized, and tested for antimicrobial activity in vitro. Although we obtained several potent antiviral candidates, these candidates had lower antibacterial activity than CPC and were not toxic to human cell lines. We found that the addition of an oxime group to the pyridine backbone resulted in derivatives with large topological polar surfaces and with unfavorable cLog *P* values. Investigation of the antibacterial mode of action, involving the cell membrane, revealed altered cell morphologies in terms of corrugated and/or disrupted surface, while 87% of the cells studied exhibited a permeabilized membrane after 3 h of treatment at 4 × minimum inhibitory concentration (MIC). Molecular dynamic (MD) simulations of the interaction of QacR with a representative candidate showed rapid dimer disruption, whereas this was not observed for QacR and QacR bound to the structural analog CPC. This might explain the lower bioactivity of our compounds, as they are likely to cause premature expression of efflux pumps and thus activation of resistance.

Keywords: quaternary ammonium salts; pyridinium-4-aldoxime; antimicrobial activity; cytotoxicity; mode of action mechanism

1. Introduction

Antimicrobial membrane-active amphiphiles, such as quaternary ammonium salts (QAS), are important antiseptic and disinfectant agents in many different commercial products. QAS with permanent positive charge can occur naturally as a product of microbial secondary metabolism or can be synthesized from alkyl halides, alcohols, or amides [1,2].

The first QAS introduced to the disinfectant market in the 1930s and 1940s was benzalkonium chloride (BAC), and today there are other common QAS besides this, namely bromine and chlorine salts such as benzalkonium bromide (BAB), cetylpyridinium chloride (CPC), and didecyldimethylammonium chloride (DDAC) [3]. Due to the amphiphilic nature of QAS, they exhibit a detergent-like mode of action that targets the cell membrane. This involves electrostatic interaction between the negatively charged bacterial membrane and the positive charge of the QAS, whereupon the alkyl chain penetrates the lipid bilayer, leading to the release of the intracellular contents and cell death [3–5].

Although these agents are already widely used, some projections indicate that their consumption will increase in the coming years as public health is threatened by the current and future spread of infectious diseases [6]. Due to their increased chemical stability and longer retention time in the environment, there are legitimate concerns about the emergence of bacterial resistance to QAS. In 1999, 63% of methicillin-resistant *Staphylococcus aureus* (MRSA) isolates in Europe were already resistant to this class of compounds [7] and in 2012, 83% were resistant in the United States [8]. Commercial QAS can have 2- to 4-fold lower efficacy against resistant bacteria, particularly CPC, one of the most effective commercial disinfectants, which has 4-fold lower efficacy against MRSA in the biofilm state [1]. It was found that the major acquired resistance pathway in Gram-positive bacteria is the *qacA/qacR* system [3]. This system consists of the negative transcriptional regulator QacR, which binds to the IR1 site of DNA, thereby inactivating transcription of the QacA efflux pump [9]. QacR ligands are various aryl-substituted mono- and bicationic QAS that, when bound to QacR, induce a conformational change leading to its dissociation from DNA and production of the QacA efflux pump [10,11]. Therefore, solving the problem of bacterial resistance by developing new or structurally modified QAS is the focus of further scientific investigation.

Several research groups have made considerable efforts to develop new QAS with structural modifications of CPC [1,2,12–15]. In this sense, environmentally friendly CPC derivatives (“soft QAS”) have been synthesized [1]. Although these pyridinium derivatives have the potential to decompose more rapidly, which could halt the development of bacterial resistance, they have been less effective because antimicrobial activity has been shown to be closely related to the structural stability of these compounds. On the other hand, pyridinium derivatives with more than one positive center and different alkyl chain lengths have shown potent antimicrobial activity at low micromolar concentrations, most likely due to a multicationic-specific interaction with the negatively charged bacterial surface [12–14,16]. In addition, the authors speculate that QAS bearing more than two positive centers may be poor substrates for QacR, thus repressing the expression of specific efflux pumps.

QSAR studies have shown that various properties such as substituents on the pyridine moiety, alkyl side chain length, hydrophobicity, pKa value, and cell surface absorptivity are crucial aspects for antimicrobial activity [17]. In this sense, Marek et al. synthesized derivatives of pyridinium-4-aldoxime with alkyl chains of different lengths (C8 to C20) [18]. They found that the C14 and C16 derivatives were the most effective and less toxic than commercial QAS and proposed them as new potential antimicrobial candidates. In addition to their potent antibacterial potential, derivatives of pyridine oximes have also shown strong antiviral activity against *influenza B-Mass* and HIV-1 viruses [19], and some of them have been discovered as potential antidotes for organophosphate poisoning [20–22] because the oxime group upon deprotonation leads to a strong nucleophile that acts as a cleaver of esters and amides [23].

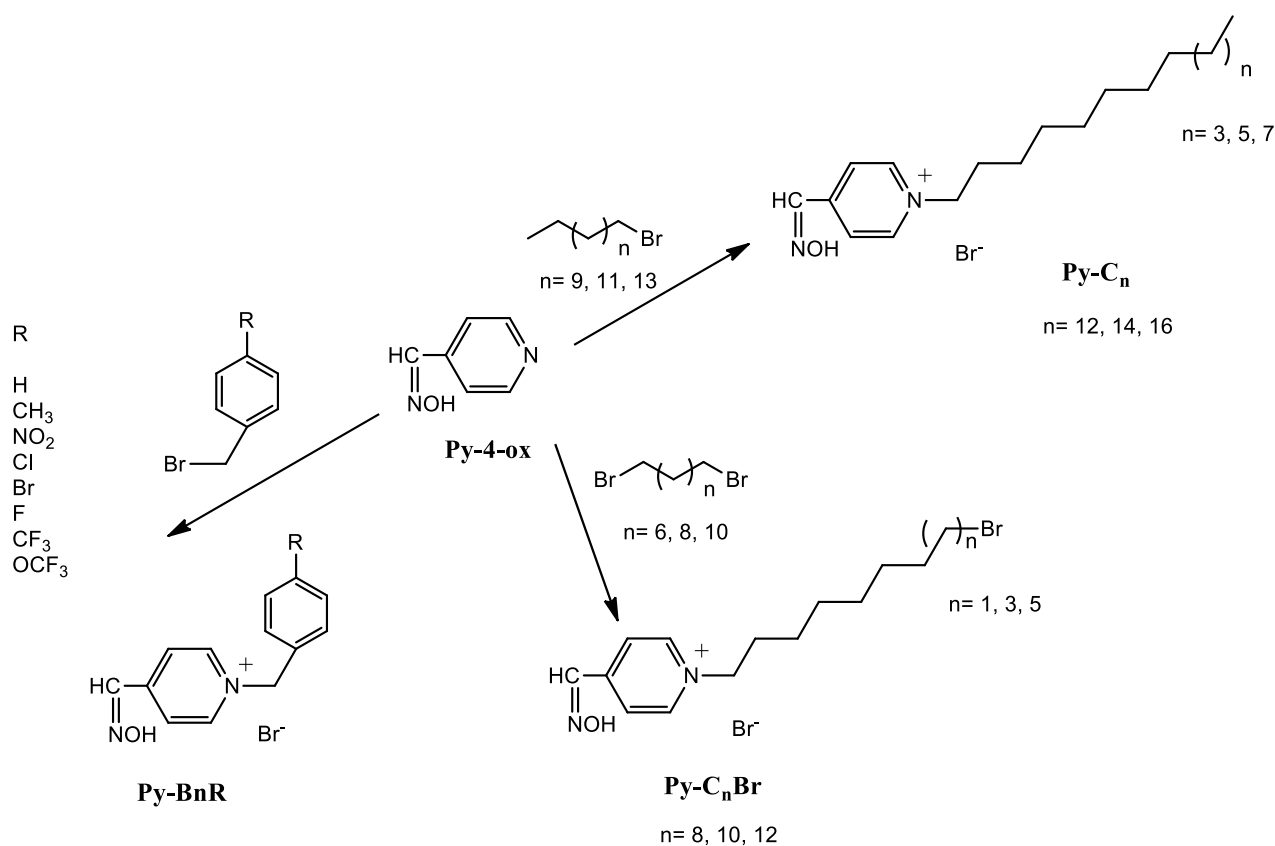
Inspired by previous studies [18,24], in this work we extended the structure-activity investigation by studying the effect of different aryl and alkyl substituents on the biological and physical properties of pyridinium-4-aldoxime. The biological potential of the synthesized compounds was determined by measuring the minimum inhibitory concentrations (MIC) against representative Gram-positive and Gram-negative bacteria and by determining the number of local lesions in plants infected with *Tobacco mosaic virus*. Due to

the potential application of the identified candidates as antibacterial and antiviral agents, cytotoxicity was determined on healthy human cell lines, namely HaCaT and RPE1. For all compounds, the topological polar surface area and *cLogP* values were calculated to estimate the effects of the oxime group and other substituents on the physical properties of the pyridine backbone. In addition, the membranolytic mechanism of action was investigated using atomic force and inverted optical fluorescence microscopies. Using molecular dynamics (MD) simulations, we were able to predict the stability of the QacR dimer in complex with the candidate compound, which provides an explanation for the decreased antibacterial activity of the quaternary pyridinium-4-aldoxime salts.

2. Results and Discussion

2.1. Chemistry

The preparation of monoquaternary oxime salts is a simple one-step reaction of pyridine-4-aldoxime with aryl or alkyl bromides/dibromides (Scheme 1). Nevertheless, repeated crystallization was necessary to obtain the required purity of the compounds. We must point out that some of the compounds have been previously synthesized [18,22,24]. All quaternization reactions were carried out at room temperature in acetone and the reaction products were obtained in very good yields. Alkylated QAS, more specifically, **Py-C₁₂**, **Py-C₁₄** and **Py-C₁₆**, were obtained in better yields ($\eta = 79\text{--}82\%$) than reported by Marek et al. who used reflux with two different solvents, acetonitrile and ethanol ($\eta = 55\text{--}87\%$ and $\eta = 70\text{--}75\%$) [18]. Our reaction conditions using a less polar solvent at room temperature are also supported by the fact that we obtained alkylated QAS with terminal bromine atom in high yields ($\eta = 60\text{--}73\%$).



Scheme 1. Preparation of aryl/alkyl quaternary pyridinium-4-aldoxime salts.

2.2. In Vitro Evaluation of Biological Activity

2.2.1. Antibacterial Activity

The antibacterial activity of all compounds was evaluated by determining the minimum inhibitory concentration (MIC), which is defined as the lowest concentration of the compound at which no visible bacterial growth is detected. The compounds were tested against representatives of Gram-positive and Gram-negative strains, including the ESKAPE bacterium *Staphylococcus aureus* ATCC25923 and the clinical isolate of methicillin-resistant *S. aureus* (MRSA), which are known for their pathogenicity [3].

As can be seen in Tables 1 and 2, all pyridine-4-aldoxime QAS have much better antibacterial potential than the precursor pyridine-4-aldoxime, but higher MIC than the standard CPC. The MIC values of CPC against representative Gram-positive bacteria and *Escherichia coli* are in the μM range, in contrast to our QAS whose MICs are ranging from μM to mM values. In contrast to our previous experience with quaternization of other heterocycles [25,26], here we obtained poorly active QAS regardless of the type of substituent used for quaternization.

In this series, slightly better activities were observed for alkylated pyridinium-4-aldoxime QAS, although these activities were still in the mM range. In general, we can conclude that the alkylated QAS have better MIC for Gram-positive than for Gram-negative bacteria, which is in agreement with previous studies that also found better activity of QAS against Gram-positive strains [3]. This is mainly attributed to the different membrane structure and composition of these two types of bacteria, as Gram-negative bacteria have a double membrane that is more difficult to penetrate. We have also confirmed that chain length affects MIC, such that longer alkyl chain derivatives generally have a lower MIC [3]. Studies have shown that antibacterial activity depends mainly on the hydrophilic-hydrophobic balance of the amphiphilic compounds [27] and not solely on the length of the chain, since derivatives with longer chains have poor solubility [28]. Moreover, when investigating the antibacterial activity of pyridine-4-aldoxime QAS, Marek et al. reported the lowest MIC values for derivatives with C₁₂, C₁₄, and C₁₆ atoms in the chain, which is in agreement with our observation [18]. Therefore, these compounds were considered as antimicrobial candidates.

In our study, **Py-C₁₄** showed consistently better MIC for the series of Gram-positive strains (Table 2). Mereghetti et al. showed that of 97 isolates of *L. monocytogenes*, 17 exhibited resistance to QAS at high concentrations (MIC up to 18 mg/L) [29]. In our study, the alkylated pyridinium-4-aldoxime QAS showed promising antibacterial potential against *L. monocytogenes* ATCC7644 with the lowest MIC of 0.31 mg/mL for **Py-C₁₄**. The derivative with an alkyl chain of 16 carbon atoms, **Py-C₁₆**, showed the lowest MIC, but these values were limited to *S. aureus* ATCC25923 (0.09 mM), MRSA, and *Bacillus cereus* strains (0.37 mM). We must note that **Py-C₁₆** has the same MIC against Gram-negative *Escherichia coli* as for Gram-positive *B. cereus*, which is consistent with the observation that QAS containing C₁₄-C₁₆ have the best antibacterial activity against Gram-negative strains [30]. When antibacterial efficacy was compared with standards, **Py-C₁₆** was found to have 28-fold and 10-fold higher MIC for CPC and cefotaxime against *S. aureus* ATCC25923, respectively. However, MRSA had comparable MIC values for **Py-C₁₆** and cefotaxime (160 and >119.4 $\mu\text{g}/\text{mL}$, respectively), leading us to conclude that this bacterial strain may use the same efflux pump system to drive bactericidal agents out of the cell. Interestingly, it has been reported that there are examples of efflux pumps that export both QAS and other antimicrobial agents. It has been shown that *qacA/B* and a gene conferring resistance to β -lactams, such as cefotaxime, are both found on large plasmids in various *Staphylococcus* species [31].

Table 1. Antibacterial activities of benzylated derivatives of pyridinium-4-aldoxime. The minimal inhibitory concentrations (MIC) are expressed in mg mL⁻¹ and mM units. MIC is the highest concentration of the compound required to suppress bacterial growth in three replicate experiments.

Bacterial Strain	Strain Origin	MIC (mg mL ⁻¹ /mM)								
		Py-4-ox M _r = 122.1	Py-Bn M _r = 293.2	Py-BnCH ₃ M _r = 307.2	Py-BnNO ₂ M _r = 338.2	Py-BnCl M _r = 327.6	Py-BnF M _r = 311.2	Py-BnBr M _r = 372.1	Py-BnCF ₃ M _r = 361.2	Py-BnOCF ₃ M _r = 377.2
Gram-positive bacteria										
<i>Staphylococcus aureus</i>	ATCC25923	>5/>40.9	>5/>17.05	2.5/8.14	5/14.78	1.25/3.82	5/16.07	1.25/3.36	0.63/1.74	0.31/0.82
<i>Staphylococcus aureus</i>	Clinical/MRSA	>5/>40.9	>5/>17.05	5/16.28	>5/>14.78	2.5/7.63	>5/>16.07	1.25/3.36	1.25/3.46	1.25/3.31
<i>Bacillus cereus</i>	ATCC14579	>5/>40.9	>5/>17.05	5/16.28	>5/>14.78	5/15.26	>5/>16.07	2.5/6.72	1.25/3.46	2.5/6.63
<i>Enterococcus faecalis</i>	ATCC29212	5/40.9	>5/>17.05	2.5/8.14	>5/>14.78	5/15.26	>5/>16.07	2.5/6.72	2.5/6.92	2.5/6.63
<i>Listeria monocytogenes</i>	ATCC7644	>5/>40.9	>5/>17.05	1.25/4.07	>5/>14.78	2.5/7.63	>5/>16.07	2.5/6.72	2.5/6.92	2.5/6.63
Gram-negative bacteria										
<i>Escherichia coli</i>	ATCC25922	>5/>40.9	1.25/4.26	5/16.28	2.5/7.39	0.31/0.95	0.63/2.02	0.16/0.43	2.5/6.92	0.31/0.82
<i>Salmonella enterica</i>	Food isolate	5/40.9	>5/>17.05	0.63/2.05	5/14.78	2.5/7.63	>5/>16.07	0.63/1.69	1.25/3.46	2.5/6.63
<i>Pseudomonas aeruginosa</i>	ATCC27853	>5/>40.9	>5/>17.05	>5/>16.28	>5/>14.78	5/15.26	>5/>16.07	5/13.44	5/13.84	2.5/6.63

Table 2. Antibacterial activities of alkylated derivatives of pyridinium-4-aldoxime. The minimal inhibitory concentrations (MIC) are expressed in mg mL⁻¹/mM and µg mL⁻¹/µM. MIC is the highest concentration of the compound required to suppress bacterial growth in three replicate experiments.

Bacterial Strain	Strain Origin	MIC (mg mL ⁻¹ /mM)						MIC (µg mL ⁻¹ /µM)	
		Py-C ₈ Br M _r = 394.2	Py-C ₁₀ Br M _r = 422.2	Py-C ₁₂ Br M _r = 450.3	Py-C ₁₂ M _r = 371.4	Py-C ₁₄ M _r = 399.4	Py-C ₁₆ M _r = 427.5	CPC M _r = 339.9	Cefotaxime M _r = 477.5
Gram-positive bacteria									
<i>Staphylococcus aureus</i>	ATCC25923	5/12.68	0.63/1.49	0.16/0.36	0.08/0.22	0.08/0.20	0.04/0.09	1.4/4.1	3.7/10
<i>Staphylococcus aureus</i>	Clinical/MRSA	2.5/6.34	0.31/0.73	0.31/0.69	0.31/0.83	0.16/0.40	0.16/0.37	2.7/10	>119.4/>250
<i>Bacillus cereus</i>	ATCC14579	2.5/6.34	0.63/1.49	0.63/1.40	1.25/3.37	1.25/3.13	0.16/0.37	5.3/20	3.7/10
<i>Enterococcus faecalis</i>	ATCC29212	2.5/6.34	5/11.84	1.25/2.78	0.63/1.70	0.31/0.78	2.5/5.85	2.7/10	29.8/60
<i>Listeria monocytogenes</i>	ATCC7644	1.25/3.17	5/11.84	1.25/2.78	0.63/1.70	0.31/0.78	1.25/2.92	2.7/10	3.7/10
Gram-negative bacteria									
<i>Escherichia coli</i>	ATCC25922	1.25/3.17	0.63/1.49	0.63/1.40	0.63/1.70	0.63/1.58	0.16/0.37	5.3/20	0.2/0.4
<i>Salmonella enterica</i>	Food isolate	>5/>12.68	5/11.84	2.5/5.55	0.63/1.70	2.5/6.26	5/11.70	21.2/60	0.1/0.2
<i>Pseudomonas aeruginosa</i>	ATCC27853	>5/>12.68	>5/>11.84	2.5/5.55	2.5/6.73	2.5/6.26	2.5/5.85	850/250	59.7/130

Compounds containing a terminal bromine atom (**Py-C₈Br**, **Py-C₁₀Br** and **Py-C₁₂Br**) in an alkyl chain showed a gradual improvement in MIC values with the higher number of carbons in the chain. Nevertheless, these values were generally poor, suggesting that a large halogen atom at the end of the alkyl chain negatively affects the biological activity of QAS.

Interestingly, arylated QAS have better potential against Gram-negative strains, which may be due to the different mode of action. QAS with substituted benzyl ring showed better antibacterial potential than **Py-Bn** alone, which is probably due to the preferential substitution at *para* position. However, the best activity in this series was observed for **Py-BnCl**, **Py-BnF**, **Py-BnBr**, and **Py-BnOCF₃** against *E. coli* with MIC values ranging from 0.43 to 2.02 mM. Similarly, **Py-BnCH₃** and **Py-BnBr** showed MIC between 1.69 and 2.05 mM against *Salmonella enterica*. The observed potential against Gram-negative strains, especially *E. coli*, could be explained by the size of the *para* substituent or by the specific unknown mechanism of action.

2.2.2. Antiviral Activity

Recent data have shown that QAS have good antiviral potential, which is why these compounds were used extensively during the COVID-19 pandemic [32]. Coronaviruses have a lipophilic membrane that is easily destroyed by the application of topical antiseptics or disinfectants [6]. Numerous plant viruses are important pathogens for agricultural crops, and new antiviral agents are welcome for economic and environmental reasons. Therefore, one of our goals was to investigate whether our new QAS have antiphytoviral potential. Tobacco mosaic virus (TMV) occupies a unique place in the history of virology and remains one of the most important pathogens of agricultural crops infecting over 200 species of herbaceous and, to a lesser extent, woody plants. The viral disease has the greatest impact on vegetables, where it can reduce yield and significantly affect quality. Extensive research has been conducted to control TMV. The most common methods include biological and chemical control. Natural products such as essential oils, flavonoids, polyphenols, and organic, alcoholic, and aqueous extracts from plants and other organisms, such as fungal metabolites, have been tested against plant diseases caused by viruses and other phytopathogens [33–36]. It is undisputed that chemical control methods continue to play an important role in disease control because of their ease of use and economic advantages. As a result, the development of efficient, environmentally friendly antiviral agents by chemical synthesis has become the core area of research to eradicate TMV and/or prevent TMV attacks. All of this has encouraged us to conduct antiviral studies that will increase our knowledge of the biological effects and potential applications of QAS.

The results of the efficacy of selected alkylated pyridinium-4-aldoxime QAS, namely **Py-C₁₂ Br**, **Py-C₁₂**, **Py-C₁₄**, and BAB against TMV infection on local host plants are shown in Figure 1. The results show that simultaneous inoculation of the tested compounds and TMV significantly reduced the number of local lesions on host plant leaves (Figure 1a). Plants treated with BAB as a control substance developed almost no infection symptoms (Figure 1c), and the percentage of inhibition of local lesions was 98.7% (Figure 1b). Among the tested series of alkylated QAS, **Py-C₁₄** reduced the number of local lesions most efficiently with a percent inhibition of 93.7% (Figure 1b). This is a very promising antiviral activity that opens a new field of research for these compounds. In the same series, **Py-C₁₂Br** and **Py-C₁₂** had slightly lower activity, but the inhibition rate was still worth mentioning with a promising 57.7 and 78.1%, respectively. The results show that simultaneous inoculation of the tested compounds and TMV significantly reduced the number of local lesions on plant leaves (Figure 1a). The control BAB showed the highest potential to suppress the symptoms of virus infection with the lowest number of local lesions (LLN 0.2), i.e., a percentage inhibition of 98.7% compared to control plants. Among the tested series of alkylated QAS, **Py-C₁₄** had 5-fold higher LLN than the control and showed almost maximum inhibition of 93.7%. In the same series, **Py-C₁₂Br** and **Py-C₁₂** had lower antiviral activity but inhibition greater than 50% (57.7 and 78.1%, respectively).

Thus, we can conclude that **Py-C₁₄** is a new potent antiviral candidate in the series of alkylated QAS, which has similar activity to the commercial standard. Although the antibacterial and antiviral potentials are not comparable at first glance, an increasing trend in bioactivity can clearly be observed for the **Py-C₁₂Br**, **Py-C₁₂**, and **Py-C₁₄** sequence. Despite the lower antibacterial activity, we show here that the alkylated pyridine-4-aldoxime salts have strong antiviral activity comparable to standard. This was expected since viruses lack the *qacR/qacA* resistance pathway typical of bacteria.

2.2.3. Cytotoxic Activity

Py-C₁₆ has the best antibacterial potential and shows versatile activity against Gram-positive and Gram-negative strains, while **Py-C₁₄** has the best activity against *Tobacco mosaic virus* (TMV). Therefore, these two candidates were tested for their cytotoxicity. Keratinocytes are the primary cell type found in the outermost layer of the skin. Therefore, HaCaT cells were used as a model for human skin, and RPE1 are retinal pigment epithelial cells, thus a model for epithelial cell type. These healthy human cell lines were used to test the cytotoxicity of standard CPC, precursor, **Py-4-ox**, **Py-C₁₄**, and **Py-C₁₆**.

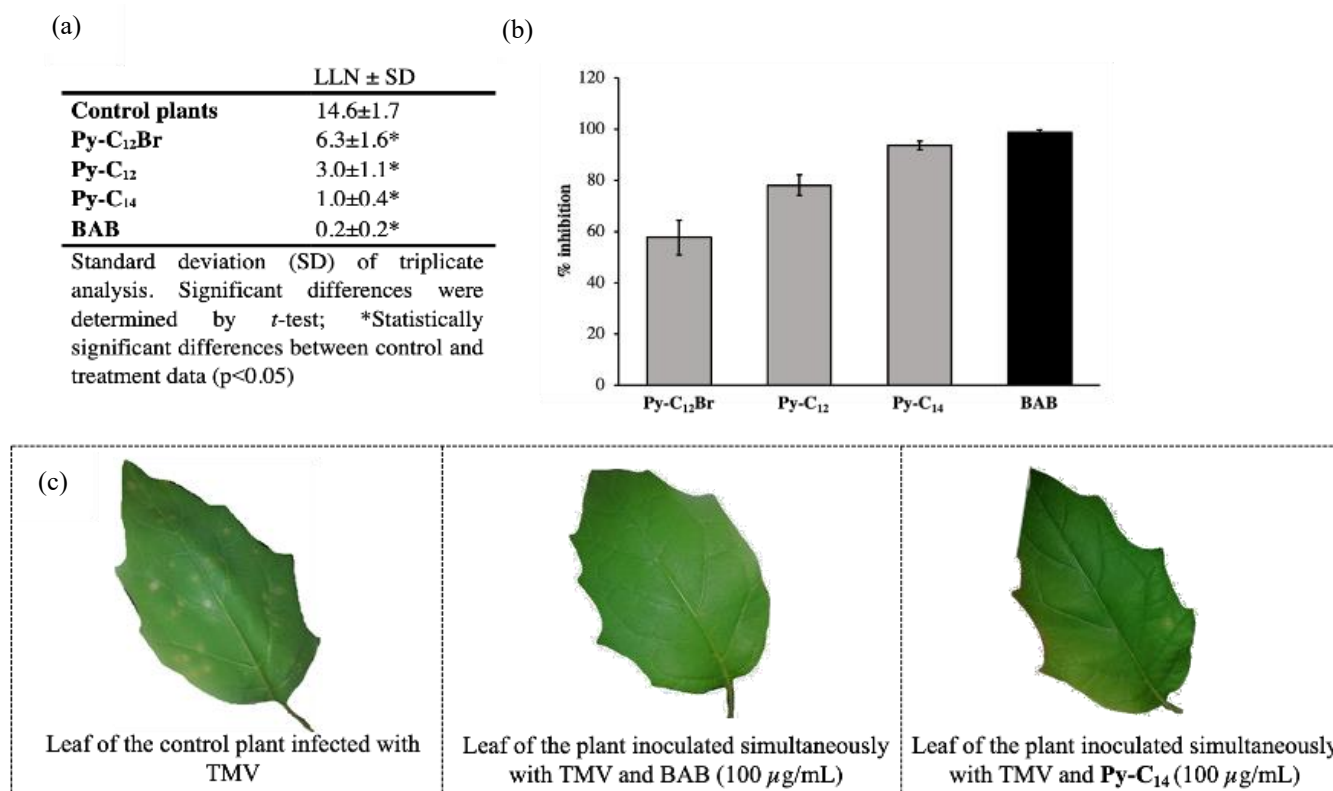


Figure 1. (a) Number of local lesions (LLN) on leaves of treated and control *Datura stramonium* plants. Treated plants were simultaneously inoculated with *Tobacco mosaic virus* (TMV) and tested compounds. (b) Percentage of inhibition of LLN for the tested QAS and BAB. Error bars show standard deviation of triplicate analyses. (c) Local symptoms of TMV infection on leaves of control plants and plants inoculated with TMV and BAB or TMV and **Py-C₁₄**.

Figure 2 shows the cytotoxicity results in the form of bars representing the concentration of the compound at which 50% inhibition of cell growth is observed. The standard CPC was the most toxic and inhibited cell growth at the lowest concentrations (below 0.5 mM). The precursor **Py-4-ox**, and the candidates **Py-C₁₄** and **Py-C₁₆** were moderately toxic to both cell lines, with **Py-C₁₆** being the least toxic. This is interesting considering that **Py-C₁₆** is a structural analogue of CPC, differing only in the presence of the oxime group. Most importantly, the IC_{50} values for the identified candidates were 10- to 50-fold higher than

the concentrations at which antimicrobial activity was observed. Therefore, results suggest that these new antimicrobial candidates could be considered as potentially non-toxic and safe QAS.

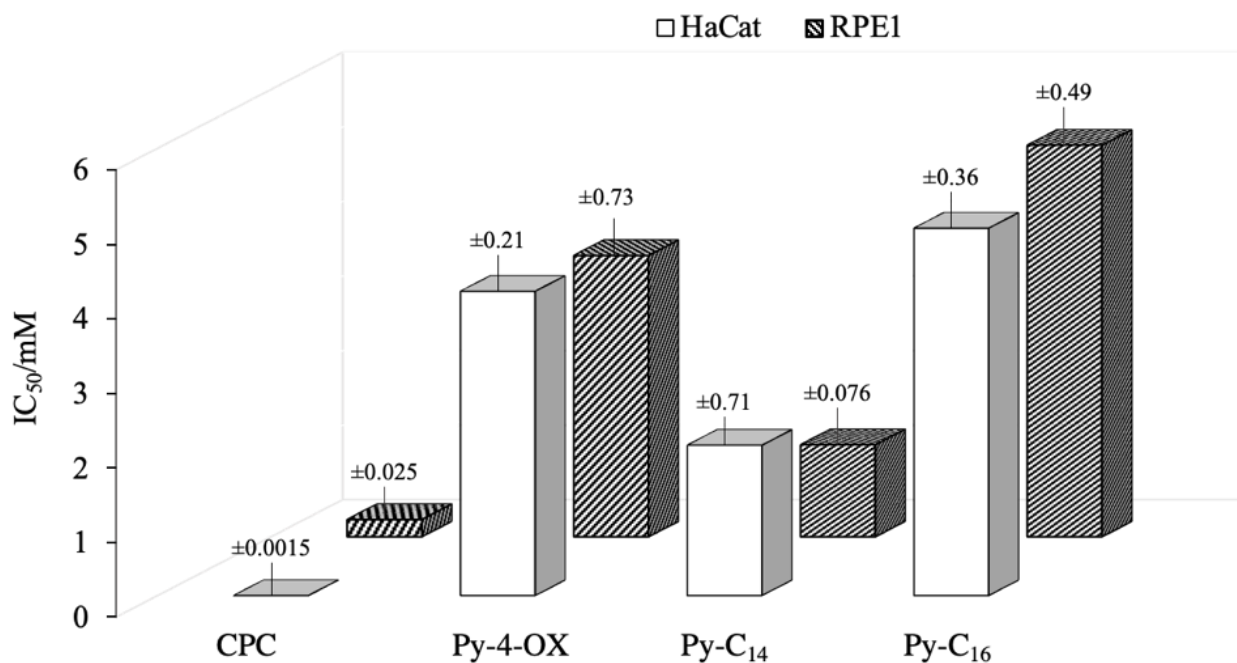


Figure 2. Cytotoxicity of CPC, Py-4-ox, Py-C₁₄, and Py-C₁₆ expressed as a concentration (IC₅₀/mM) of the compounds at which 50% inhibition of cell growth is observed. Experiments were performed in triplicate and results are given as means of three independent experiments, with standard deviations presented as error bars. The experiments were performed with HaCaT and RPE1 cells.

2.3. Hydrophobicity and Electron Density Distribution of Synthesized QAS

In this study, the prediction of hydrophobicity for all compounds was generated using the SwisADME online tool. This tool provides an average cLogP value from iLogP, xLogP, wLogP, mLogP, and silicos-it [37]. A higher cLogP value indicates a stronger distribution of the compound in the lipid phase, which could be a good indicator of how compounds behave in complex biological systems.

The calculated cLogP values are listed in Table 3. All benzylated salts of the pyridine-4-aldoxime backbone have very low cLogP values, indicating that these compounds are almost evenly distributed between the lipid and aqueous phases. Given their low cLogP values, it is reasonable to assume that they are less susceptible to membrane penetration. On the other hand, the cLogP values of the alkylated pyridine-4-aldoxime derivatives are much higher, suggesting that they are much more hydrophobic and, therefore, most likely to interact with the membrane. Our cLogP data for Py-C₁₂, Py-C₁₄, and Py-C₁₆ are consistent with those of Marek et al. although the values are different due to the effect of the bromide counterion [18]. It can be seen that these values are similar or close to those of CPC and BAB for alkylated derivatives. We must note that compounds with terminal bromine atom have high cLogP values like the standard CPC and BAB, but have low antimicrobial potential, possibly due to the strong steric hindrance caused by the large halogen atom at the end of the chain.

Table 3. Consensus partition coefficients (cLogP) and topological polar surface area (TPSA/Å²) of compounds.

	Compound	cLogP	TPSA/Å ²
Aryl substituent	Py-4-ox	0.73	45.48
	Py-Bn	0.95	36.47
	Py-BnCH ₃	0.69	36.47
	Py-BnNO ₂	-0.62	82.29
	Py-BnCl	0.86	36.47
	Py-BnF	0.63	36.47
	Py-BnBr	0.93	36.47
	Py-BnCF ₃	1.50	36.47
	Py-BnOCF ₃	0.90	45.70
Alkyl substituent	Py-C ₈ Br	1.76	36.47
	Py-C ₁₀ Br	2.40	36.47
	Py-C ₁₂ Br	3.12	36.47
	Py-C ₁₂	1.51	36.47
	Py-C ₁₄	2.07	36.47
	Py-C ₁₆	2.82	36.47
	CPC	3.24	3.88
	BAB	3.55	0.00

In addition, calculation of the topological polar surface area (TPSA) (Table 3) shows that all synthesized derivatives have higher polar surface area values than structurally similar CPC, suggesting that the addition of oxime group and/or strong electron withdrawing and polar groups, e.g., NO₂ or OCF₃, negatively affects the lipophilicity of the structures. This is clearly seen in the structure of the pyridine-4-aldoxime backbone (Figure 3), which has a polar surface over the oxime group and the nitrogen atom in the pyridine ring. Moreover, a comparison of **Py-C₁₆** and CPC, which are both structurally similar and have similar cLogP values, shows a large difference in TPSA, which can be explained by the influence of the polar oxime groups on the synthesized QAS. Nevertheless, this compound shows the best biological activity. For illustration, the TPSA of the representative structures is shown in Figure 3.

2.4. Atomic Force Microscopy (AFM)

Optical and atomic force microscopy of the immobilized untreated and treated cells was performed to visualize the effect of **Py-C₁₂** on the bacterial membrane. For these experiments we used *Escherichia coli* DH5α cells because these cells allowed solid immobilization with persevered cell viability.

Prior to the measurements, we determined the minimum inhibitory concentration of **Py-C₁₂** against *E. coli* DH5α and found it to be equivalent to that of *E. coli* ATTC 25922. The height AFM image in Figure 4a shows the untreated characteristically rod-shaped *E. coli* DH5α cells with smooth cell surface in an ongoing cell division process (white arrow). After making sure that the cells were properly immobilized and proliferating (a few new generations of cells were observed via optical microscopy), we started the treatment. To accelerate the process of time-dependent membrane damage, the cells were treated with the 4xMIC of **Py-C₁₂** for three hours after which the sample was rinsed with the fresh growth medium. Bright-field images in Figure 4b,c show an unchanged number of bacterial cells at the start and immediately after the treatment, demonstrating the bacteriostatic effect of **Py-C₁₂**. Interestingly, the unidentified spherical structures (red arrows) seen in these images

could be from the highly aggregated Py-C₁₂, which leads to the formation of vesicles at the concentration used (4xMIC).

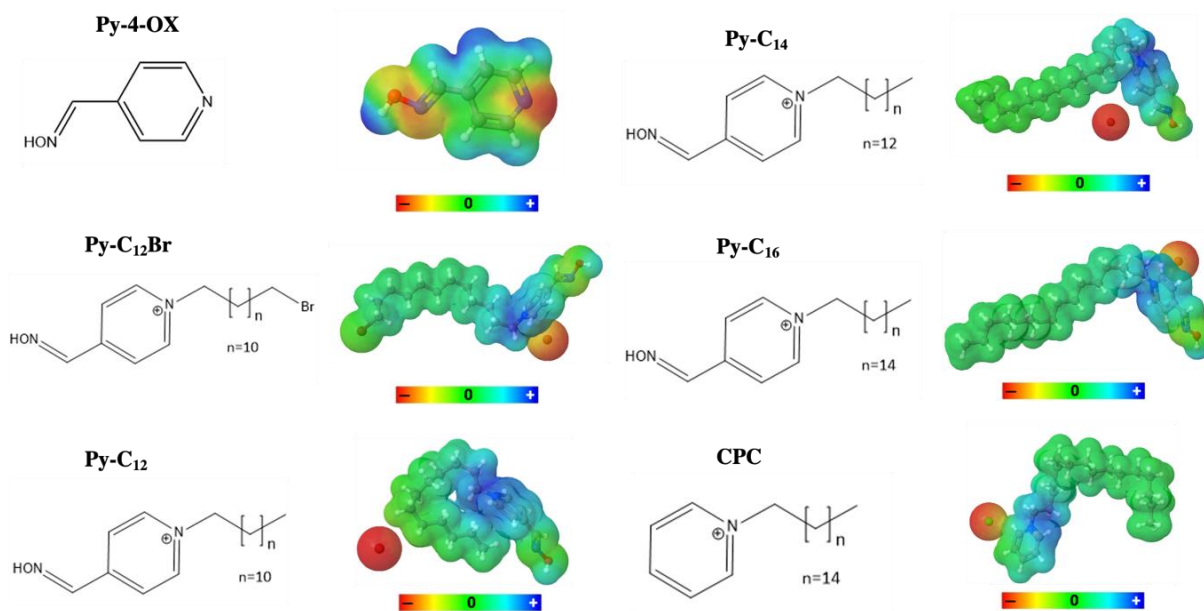


Figure 3. Representative structures of pyridinium-4-aldoxime and its quaternary salts with visualized topological polar surface areas (TPSA).

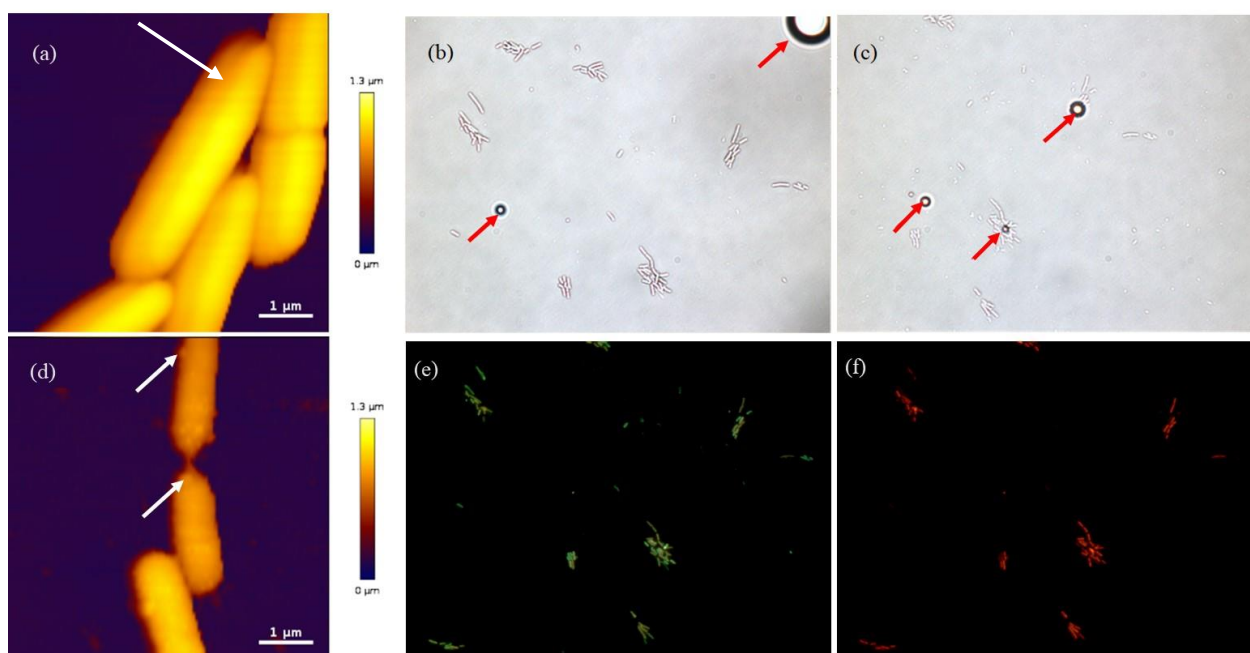


Figure 4. Atomic force and optical microscopy data of untreated and treated bacterial cells: (a) Height AFM image of untreated *Escherichia coli* DH5 α cells, (b) bright-field image of cell groups taken at the very beginning of treatment—the arrows indicate possible vesicles, (c) bright-field image of the exact same sample area as in (b) taken after 3 h of cell treatment and vigorous rinsing with the Muller-Hinton broth—the arrows indicate possible vesicles, (d) height AFM image of bacterial cells—the arrows indicate possible micelles attached at the cell surface or membrane blebbing, (e) SYTO 9 fluorescence image of the exact same sample area as in (b,c), acquired after 3 h of treatment, (f) Propidium iodide fluorescence image of the exact same area as in (e), acquired after 3 h of treatment.

These formations were stable during the 3-hour treatment and after rinsing of the cells with the growth medium (Figure 4c).

The height AFM image (Figure 4d) of the 3-hours treated cells at $4 \times \text{MIC}$ shows an altered cell morphology with a corrugated and/or disrupted cell surface, but without massive lysis since the cells have preserved their characteristic rod shape. A similar effect was previously observed when *E. coli* cells were treated with newly synthesized quaternary *N*-benzylimidazole salts [26]. Moreover, the false color ruler, which reveals the height of the structures in the image, indicates the reduction in height of treated cells when compared to the untreated cells. Furthermore, white arrows in Figure 4d point to bulges on the cell surface that could be signs of either membrane blebbing and/or micelle attachment.

To estimate the percentage of cells whose membrane had been permeabilized by the treatment, the same group of cells was stained simultaneously with two fluorescent nucleic dyes, SYTO9 and propidium iodide (PI). Figure 4e,f show the SYTO9 staining of all cells and the PI staining of the permeabilized cells. When applied together, PI tends to displace SYTO9 from nucleic acid and the cells fluorescence in red [38]. However, there is some overlap in the SYTO9 and the PI signal, which results with different shades of green as seen in Figure 4e (the permeabilized cells tend to be green-orange in the SYTO9 signal, while the preserved cells tend to florescent bright green). Images such as Figure 4e,f allowed us to calculate the percentage of permeabilized cells—87% of the 344 cells were identified as permeabilized.

2.5. The Effect of Py-C₁₄ Binding to the Transcriptional Factor QacR Dimer

To investigate the effect of the ligand binding on the conformation of QacR, we performed MD simulations of the three systems, namely QacR dimer, QacR:CPC complex and QacR:Py-C₁₄ complex. We thereby observe rather drastic differences in the three systems (Figure 5). More precisely, one can notice that the distance between the centers of mass of the two monomeric subunits of QacR behaves in a radically different fashion depending on the presence/lack of the ligand, and also on the very nature of the ligand at hand. The average distance between the two subunits in the last 450 ns of the simulation, denoted d_{m-m} , is significantly smaller in the case of both QacR ($d_{m-m} \approx 2.6$ nm) and QacR:CPC ($d_{m-m} \approx 3.1$ nm) systems compared to QacR:Py-C₁₄ ($d_{m-m} \approx 5.1$ nm) system, see Figure 5a.

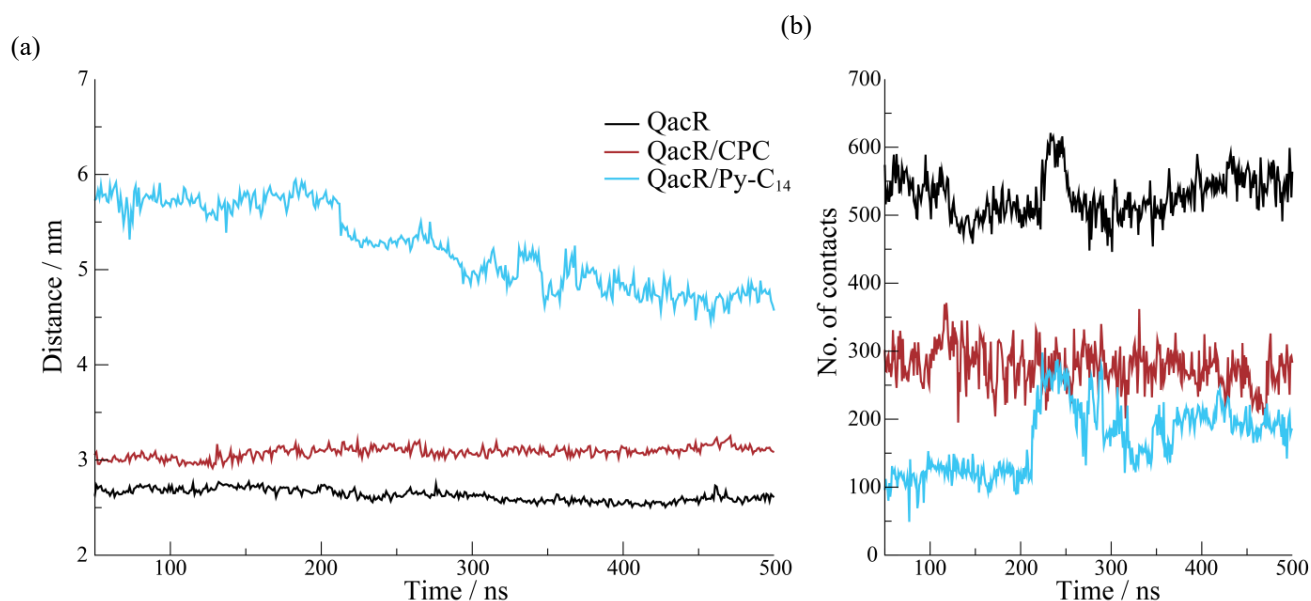


Figure 5. Time evolution of the distance between the centers of mass (a) and the number of contacts between the two monomers of the QacR protein (b), with the contact threshold set at 0.6 nm.

Taking only this finding into consideration, one could be prone to hypothesize the following—while the dimer remains stable in the cases of QacR and QacR:CPC systems, **Py-C₁₄** ligand has a disruptive effect on the protein, causing it to dissociate into individual subunits, i.e., into two monomers. Specifically, inspection of the contacts between the two monomeric subunits reveals that QacR dimer, lacking any ligand, possesses by far the largest number of contacts between its monomeric subunits on average (≈ 550 contacts), compared to either QacR:CPC (≈ 290 contacts) or QacR:**Py-C₁₄** (≈ 200 contacts). We thus observe the following relation: QacR:**Py-C₁₄** \gg QacR:CPC $>$ QacR (Figure 5a) regarding the distance between the centers of mass of the two monomeric subunits, while QacR \gg QacR:CPC $>$ QacR:**Py-C₁₄** (Figure 5b) regarding the number of contacts. It is to be noted that the inversely proportional behavior of the two trends is fully expected, as the smaller average distance indeed implies a larger number of contacts. However, such a similar number of contacts between the two monomers in the cases of QacR:CPC and QacR:**Py-C₁₄** is quantitatively rather unexpected.

In this respect, we further examined conformational behavior of the QacR protein in detail, finding that dimer reorganizes when either of the investigated ligands is present (compare right panel to the left panel of Figure 6). Evidently, binding of **Py-C₁₄** first induces the dimer disruption and then reintegration of only a portion of the interactions. While both ligands have a pronounced effect on QacR, the outcome with respect to dimer *organization* is qualitatively different in the case of CPC and **Py-C₁₄** (compare Figure 6b to Figure 6a,b). In this regard, if we imagine a monomer as a cylinder, the interactions between the monomers in the dimer could be perceived along their cylinder jackets (Figure 6, left panel). While this kind of interaction is preserved in the case of CPC ligand (Figure 6a, right), the dimer containing **Py-C₁₄** shows a different arrangement, with the base-to-base interactions between the monomers being predominant (Figure 6b, right).

We also analyzed the conformational behavior of the two ligands and the specific interactions the ligands form with QacR. We thus find that rather similar initial conformations of both ligands with the aliphatic tails approximately straight (“open” states of the ligands, Figure 6, left panel), become different in the post-equilibrium stage of MD simulations. More precisely, **Py-C₁₄** retains the “open” state conformation, while CPC adopts the “closed” conformation, as seen from insets of Figures 6b and 6a, respectively. Finally, we also analyzed the specific interactions between the two ligands and amino acid residues belonging to the QacR monomers to which they are anchored, focusing primarily on the hydrogen bond (HB) interactions. HB is considered to have formed if the X-H \cdots Y bond is shorter than 0.35 nm and if the angle closed with the three atoms defining HB is smaller than 30°. Due to the fact that CPC possesses only one HB acceptor (nitrogen atom of the pyridinium moiety), its ability to form HBs with the amino acids of QacR is significantly reduced compared to **Py-C₁₄**, which due to the presence of the oxime group, additionally forms HBs with six amino acid residues lining the ligand binding pocket (Table 4). In light of this, it is not surprising that CPC forms no HBs during the entire course of the simulation. However, it does readily form π - π -interactions via its pyridinium moiety with the aromatic sidechain of Trp60, as well as favorable electrostatic interactions with Gln95 and Thr87.

On the other hand, **Py-C₁₄** forms 0.3 ± 0.5 HBs on average during its respective MD simulation, with the HBs being most readily formed with the sidechains of Glu67 and Gln63 through -OH moiety of **Py-C₁₄**, accounting for 73% of all HBs this ligand forms with QacR (Table 4). However, it is worth noting that, regardless of the presence/lack of the HB interactions in the case of **Py-C₁₄** and CPC, respectively, both ligands remain bound to QacR for the entire 500 ns of the MD simulations.

Overall, one can conclude that binding of both ligands strongly affects the initial conformation of the QacR dimer. However, binding of **Py-C₁₄**, as compared to CPC, additionally initiates the dimer dissociation and subsequent reintegration of base-to-base contacts between the monomers.

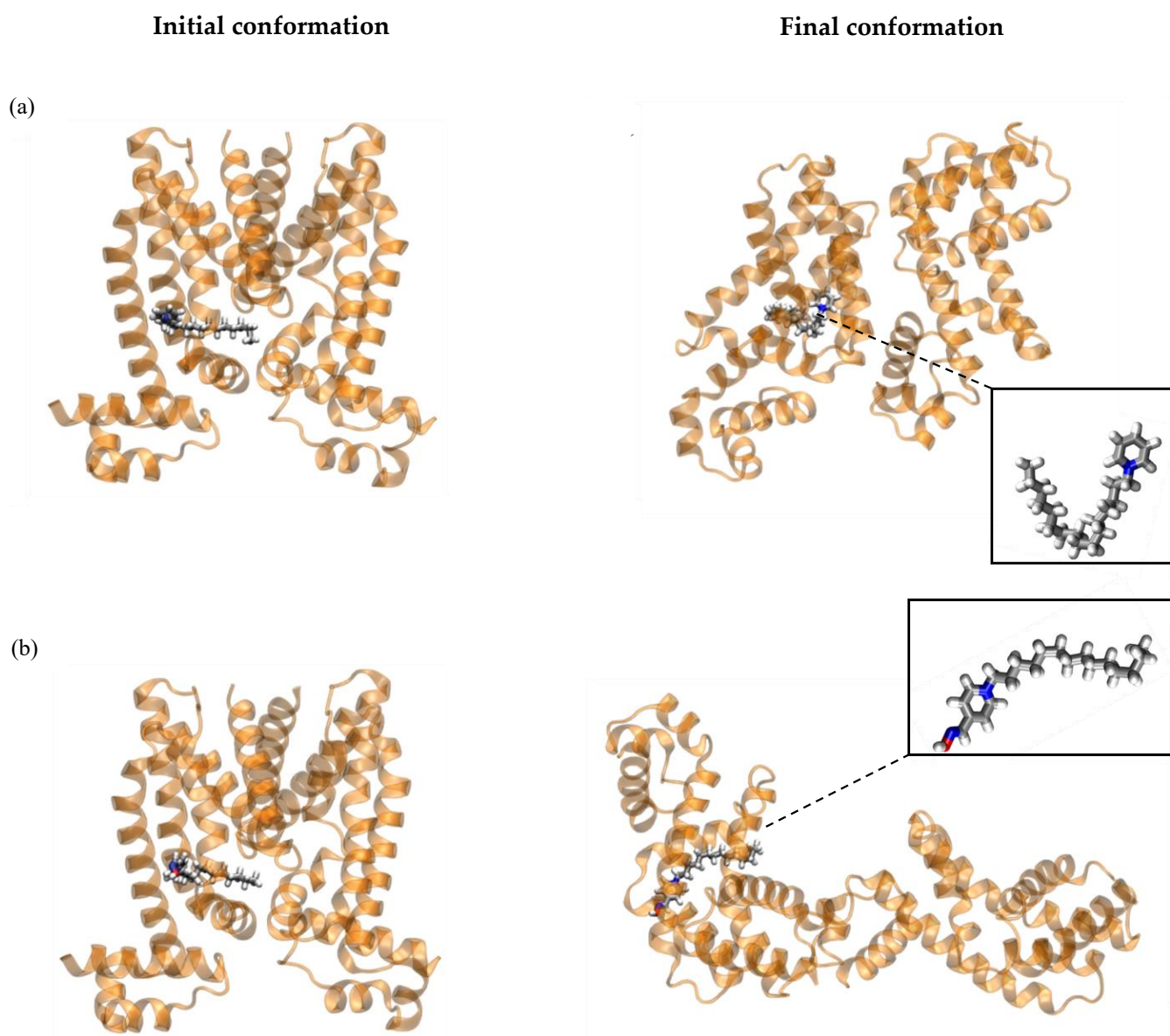


Figure 6. Dimer conformations representing the state of QacR during MD simulations for: (a) QacR:CPC at 200 ns (right; inset: the CPC ligand enlarged), (b) QacR:Py-C₁₄ at the beginning (starting snapshot, left) and during the last 200 ns (right; inset: Py-C₁₄ ligand enlarged). Protein is given in orange (new cartoon representation), with the ligands shown in the licorice.

Table 4. Contribution of all the amino acid residues forming hydrogen-bonds (HB) with Py-C₁₄ to the overall Py-C₁₄—protein HB count.

Amino Acid	Overall Hydrogen-Bond (HB) Count (%)
Glu67	50
Gln63	23
Leu94	12
Tyr91	9
Thr87	5
Leu80	1

3. Material and Methods

3.1. Synthesis

The synthesis of the compounds Py-Bn, Py-BnCH₃, Py-BnNO₂, Py-BnCl, Py-BnBr, Py-C₁₂, Py-C₁₄, and Py-C₁₆ with associated NMR spectra was described in [9–11]. However, for the purpose of this investigation, all these and new monoquaternary oximes were prepared by adding the appropriate reagents for quaternization: 4-benzyl bromide, 4-methylbenzyl bromide, 4-nitrobenzyl bromide, 4-chlorobenzyl bromide, 4-bromobenzyl bromide, 4-fluorobenzyl bromide, 4-(trifluoromethyl)benzyl bromide, 4-methoxybenzyl bromide, 1, 8-dibromooctane, 1, 10-dibromodecane, 1, 12-dibromododecane, 1-bromododecane, 1-bromotetradecane, and 1-bromohexadecane; in equimolar amounts to the solution of 4-hydroxyiminomethylpyridine in dry acetone at room temperature. The reaction mixture was kept in the dark without stirring for 2–3 days to obtain a solid product. The excess of the acetone was removed under reduced pressure and the white crystals were washed several times with dry diethyl ether. The quaternary compounds were obtained as white crystals in good yields. All synthesized compounds were identified by IR and NMR spectroscopies.

Pyridinium-4-aldoxime and all reagents for quaternization were commercially available (Alfa Aesar) and were used without further purification. The progress of quite simple one-step reaction was monitored by thin layer chromatography using DC-Alufohlen Aluminiumoxide 60 F₂₅₄ plates (Merck) with 5:1 and 9:1 chloroform/methanol as eluent. Spots were detected by UV light and by reversible absorption of iodine. Repeated crystallization was necessary to achieve the required purity of the compounds. Melting points were determined in open capillaries using a Büchi B-540 instrument and are uncorrected. Elemental analyses were performed using a PerkinElmer PE 2400 Series II CHNS/O Analyzer. FTIR spectra were recorded using a PerkinElmer FTIR 1725 X spectrometer. All samples were prepared by mixing FTIR-grade KBr (Sigma-Aldrich) with 1% (*w/w*) salt and grinding to a fine powder. Spectra were recorded over the range 400–4000 cm⁻¹ without baseline corrections. ¹H and ¹³C NMR spectra were recorded in DMSO-*d*₆ solutions using a Bruker Avance III HD 400 MHz/54 mm Ascend spectrometer (400 MHz) at room temperature. Chemical shifts are reported as δ values in ppm using TMS as the internal standard. Abbreviations for the data reported are: *s*, singlet; *d*, doublet; *t*, triplet; *m*, multiplet. The coupling constants (*J*) are given in Hz.

N-*p*-fluorobenzyl-4-hydroxyiminomethylpyridinium bromide (**Py-BnF**). Yield: 89%; mp: 181–183 °C; IR (KBr) $\tilde{\nu}$ /cm⁻¹: 3313, 3075, 2924, 1666, 1466, 1220, 1008, 775. ¹H-NMR (400 MHz, DMSO-*d*₆): δ /ppm 12.85 (*s*, 1H, OH); 9.21 (*d*, 2H, *J* = 6.9 Hz, H2 and H6 Py); 8.44 (*s*, 1H, CH=N); 8.26 (*d*, 2H, *J* = 6.9 Hz, H3 and H5 Py); 7.64–7.71 (*m*, 2H, ArH); 7.34–7.26 (*m*, 2H, ArH); 5.88 (*s*, 2H, NCH₂). ¹³C-NMR (100 MHz, DMSO-*d*₆): δ /ppm 163.5 (*q*, *J*_{C-F} = 246 Hz), 169.3, 145.4, 132.0, 131.0, 124.9, 116.6 (*d*, *J*_{C-F} = 22 Hz), 62.2. Anal. Calcd. for C₁₃H₁₂BrFN₂O: 50.18% C; 3.89% H; 9.00% N. Found: 50.14% C; 3.88% H; 8.97% N.

N-(*p*-trifluoromethyl)benzyl-4-hydroxyiminomethylpyridinium bromide (**Py-BnCF₃**). Yield: 97%; mp: 186–187 °C; IR (KBr) $\tilde{\nu}$ /cm⁻¹: 3423, 3108, 2990, 1655, 1428, 1288, 1001, 782. ¹H-NMR (400 MHz, DMSO-*d*₆): δ /ppm 12.89 (*s*, 1H, OH); 9.22 (*d*, 2H, *J* = 6.7 Hz, H2 and H6 Py); 8.45 (*s*, 1H, CH=N); 8.29 (*d*, 2H, *J* = 6.7 Hz, H3 and H5 Py); 7.83 (*d*, 2H, *J* = 8.5 Hz, ArH); 7.76 (*d*, 2H, *J* = 8.5 Hz, ArH); 6.00 (*s*, 2H, NCH₂). ¹³C-NMR (100 MHz, DMSO-*d*₆): δ /ppm 150.6, 149.5, 145.6, 139.2, 130.1, 124.9, 124.4 (*q*, *J*_{C-F} = 273 Hz), 62.3. Anal. Calcd. for C₁₄H₁₂BrF₃N₂O: 46.56% C; 3.35% H; 7.76% N. Found: 46.49% C; 3.35% H; 7.77% N.

N-(*p*-trifluoromethoxy)benzyl-4-hydroxyiminomethylpyridinium bromide (**Py-BnOCF₃**). Yield: 61%; mp: 175–176 °C; IR (KBr) $\tilde{\nu}$ /cm⁻¹: 3311, 3112, 2995, 1644, 1458, 1311, 1004, 765. ¹H-NMR (400 MHz, DMSO-*d*₆): δ /ppm 12.88 (*s*, 1H, OH); 9.22 (*d*, 2H, *J* = 6.7 Hz, H2 and H6 Py); 8.46 (*s*, 1H, CH=N); 8.28 (*d*, 2H, *J* = 6.7 Hz, H3 and H5 Py); 7.73 (*d*, 2H, *J* = 8.5 Hz, ArH); 7.47 (*d*, 2H, *J* = 8.5 Hz, ArH); 5.94 (*s*, 2H, NCH₂). ¹³C-NMR (75 MHz, DMSO-*d*₆): δ /ppm 149.4, 147.1, 145.6, 134.1, 124.9, 122.2, 121.3, 120.4 (*q*, *J*_{C-F} = 257 Hz), 62.1. Anal. Calcd. for C₁₄H₁₂BrF₃N₂O₂: 44.58% C; 3.21% H; 7.43% N. Found: 44.68% C; 3.20% H; 7.44% N.

N-(8-bromooctyl)-4-hydroxyiminomethylpyridinium bromide (**Py-C₈Br**). Yield: 60%; mp: 100–101 °C; IR (KBr) $\tilde{\nu}/\text{cm}^{-1}$: 3410, 3208, 2713, 1602, 1410, 999, 538. ¹H-NMR (400 MHz, DMSO-*d*₆): δ/ppm 12.82 (s, 1H, OH); 9.10 (d, 2H, *J* = 6.7 Hz, H2 and H6 Py); 8.61 (s, 1H, CH=N); 8.25 (d, 2H, *J* = 6.8 Hz, H3 and H5 Py); 4.59 (t, *J* = 7.4 Hz, 2H, NCH₂); 1.91–1.71 (m, 2H, CH₂); 1.38–1.24 (m, 12H, CH₂). ¹³C-NMR (100 MHz, DMSO-*d*₆): δ/ppm 149.3, 147.7, 145.9, 123.4, 59.6, 34.6, 31.5; 29.9, 27.6, 24.7. Anal. Calcd. for C₁₄H₂₂Br₂N₂O: 42.66% C; 5.63% H; 7.11% N. Found: 42.78% C; 5.61% H; 7.13% N.

N-(10-bromodecyl)-4-hydroxyiminomethylpyridinium bromide (**Py-C₁₀Br**). Yield: 71%; mp: 103–105 °C; IR (KBr) $\tilde{\nu}/\text{cm}^{-1}$: 3400, 3188, 2718, 1641, 1438, 999, 547. ¹H-NMR (400 MHz, DMSO-*d*₆): δ/ppm 12.82 (s, 1H, OH); 9.08 (d, 2H, *J* = 6.8 Hz, H2 and H6 Py); 8.60 (s, 1H, CH=N); 8.25 (d, 2H, *J* = 6.8 Hz, H3 and H5 Py); 4.61 (t, *J* = 7.3 Hz, 2H, NCH₂); 1.92–1.71 (m, 2H, CH₂); 1.38–1.23 (m, 16H, CH₂). ¹³C-NMR (100 MHz, DMSO-*d*₆): δ/ppm 150.6, 148.8, 145.6, 124.5, 60.67, 35.7, 32.7; 31.1, 29.2, 27.6, 25.8. Anal. Calcd. for C₁₆H₂₆Br₂N₂O: 45.52% C; 6.21% H; 6.64% N. Found: 45.34% C; 6.22% H; 6.63% N.

N-(12-bromododecyl)-4-hydroxyiminomethylpyridinium bromide (**Py-C₁₂Br**). Yield: 73%; mp: 109–110 °C; IR (KBr) $\tilde{\nu}/\text{cm}^{-1}$: 3388, 3200, 2719, 1622, 1440, 1003, 543. ¹H-NMR (400 MHz, DMSO-*d*₆): δ/ppm 12.83 (s, 1H, OH); 9.01 (d, 2H, *J* = 6.8 Hz, H2 and H6 Py); 8.62 (s, 1H, CH=N); 8.26 (d, 2H, *J* = 6.7 Hz, H3 and H5 Py); 4.62 (t, *J* = 7.4 Hz, 2H, NCH₂); 1.93–1.71 (m, 2H, CH₂); 1.39–1.23 (m, 20H, CH₂). ¹³C-NMR (100 MHz, DMSO-*d*₆): δ/ppm 150.1, 148.4, 145.6, 123.5, 59.8, 35.1, 32.7, 31.4; 31.14, 29.3, 27.4, 24.9. Anal. Calcd. for C₁₈H₃₀Br₂N₂O: 48.02% C; 6.72% H; 6.22% N. Found: 47.91% C; 6.73% H; 6.21% N.

3.2. In Vitro Evaluation of Biological Activity

3.2.1. Bacterial Strains

To evaluate antibacterial efficacy, the synthesized QAS were tested against representative Gram-positive and Gram-negative bacterial strains. All strains were acquired from Biognost (Zagreb, Croatia), except for the clinical isolate of methicillin-resistant *Staphylococcus aureus* (MRSA), which was kept as part of the culture collection in the Department of Chemistry, Faculty of Science, and the food isolate *Salmonella enterica*, which was kept in the culture collection of the University Department of Marine Studies in Split.

The collection included five Gram-positive strains, including *Staphylococcus aureus* (ATCC 25923 and a methicillin-resistant *Staphylococcus aureus* clinical strain MRSA), *Bacillus cereus* ATCC 14579, *Enterococcus faecalis* ATCC 29212, and *Listeria monocytogenes* ATCC 7644; and three Gram-negative strains: *Escherichia coli* ATCC 25922, *Pseudomonas aeruginosa* ATCC 27853 and the food isolate *Salmonella enterica*. All microbial strains were maintained at –80 °C for long-term storage and subcultured on Mueller-Hinton (MH) agar (Biolife, Italy) prior to broth microdilution experiments. The MH plates were stored at +4 °C for no longer than one month.

3.2.2. The Standard Curves for Bacterial Colony Forming Units per Milliliter (CFU/mL) versus A₆₀₀

The standard growth curve was determined for each bacterial strain by plotting the A₆₀₀ value with the number of colony-forming units in milliliter (CFU/mL).

The overnight bacterial culture was diluted (1:10, *v/v*) in Mueller-Hinton broth (MHB; Biolife) and incubated at 220 rpm at 37 °C until the mid-exponential growth phase was reached (A₆₀₀ = 0.34–0.65). Then, 10-fold serial dilutions of the bacterial culture were prepared and 50 μL of each dilution was plated on Mueller-Hinton agar plates after measuring A₆₀₀. The dilution plate on which 30–100 colonies grew was used to calculate CFU/mL. The optical density of a culture was measured using a spectrophotometer (Perkin Elmer Lambda Bio 40) and a densitometer (BioSan, DEN-1) relative to a blank sample of the medium. *Listeria monocytogenes* ATCC 7644 and *Enterococcus faecalis* ATCC 29212 were cultured on nutrient media containing 0.5% peptone, 0.3% yeast extract, 0.5% NaCl, and 1.5% agar. These two strains were cultured at 220 rpm and 35 °C.

3.2.3. Broth Microdilution Assays

Antibacterial activity was evaluated using the Broth Microdilution Assay according to the Clinical and Laboratory Standard Institute's Methods for Dilution Antimicrobial Susceptibility Test for Bacteria That Grow Aerobically; Approved Standard-Tenth Edition [39].

The stock solution of QAS (10 mg/mL) was prepared in 4% DMSO. Then, 100 µL of the tested QAS was added to the first well of the microtiter plate. Twofold serial dilutions in Muller-Hinton broth were performed over the entire plate at a concentration range of 5 mg/mL to 5 µg/mL. To each well, 50 µL of mid-exponentially grown inoculum containing 10^5 CFU/mL in Mueller-Hinton broth was added and incubated at 37 °C for 18 hours. The minimum inhibitory concentration (MIC) was determined as the lowest concentration at which no visually detectable bacterial growth occurred in the wells.

3.2.4. Virus and Plant Hosts

Leaves of *Nicotiana tabacum* L. cv. Samsun plants systemically infected with *Tobacco mosaic virus* (TMV) were ground in 0.06 mol/L phosphate buffer, pH 7.0 (1:1, *w/v*) to prepare virus inocula. Leaves were ground in 0.06 mol/L phosphate buffer, pH 7.0 (1:1, *w/v*), and centrifuged at low speed to prepare virus inoculum. Leaves of the local host *Datura stramonium* L. were dusted with silicon carbide (Sigma-Aldrich, St. Louis, MO, USA) before virus inoculation, and the inoculum was diluted with inoculation buffer to obtain 5–20 lesions per inoculated leaf. Experiments were performed when the experimental plants reached the 4–6 leaf stage.

3.2.5. Antiphytoviral Activity Assay

The tested QAS (10 mg/mL) were dissolved in 4% DMSO and added to the virus inocula at a final concentration of 100 µg/mL. DMSO was added to the control virus inocula at the same concentration. The control and treated plants were then rubbed with the prepared inocula and the antiviral activity of the tested compounds was evaluated by the percentage inhibition of the number of local lesions on the leaves of the treated and control plants as described in [40]. The obtained data were analyzed in Excel (Microsoft Office) and significant differences were determined by *t*-test.

3.2.6. Cytotoxicity

Cytotoxicity of selected QAS was performed using three different human cell lines (RPE1 and HaCaT) and compared with the standard cetylpyridinium chloride (CPC). Cells were grown in DMEM media in a humidified environment with 5% CO₂ and 37 °C. To determine cytotoxicity, a twofold serial dilution of a tested compound starting at 5 mg/mL was prepared in a 96-well plate. Five thousand cells were pipetted into each well, and the cells were grown for an additional 48 h. Then, the reagent MTS (20 µL) was added to the cells according to the manufacturer's instructions (CellTiter 96[®] Aqueous One Solution Cell Proliferation Assay, Promega). After 3 h of incubation, the absorbance was measured at 490 nm. IC₅₀ values were determined by plotting compound concentration against absorbance using GraFit6 software [41]. Measurements were performed in duplicates and results are reported as means of at least three independent experiments with standard deviation (±SD) indicated.

3.3. SwissADME Calculations and Visualization of Electron Density Distribution

CLogP values and topological polar surface area (TPSA) were calculated using the online tool SwissADME available at <http://www.swissadme.ch> (accessed on 4 March 2022). The chemical structures of the compounds were drawn using Chem Draw [42] and the generated list of SMILES (Table 5) was used to perform the corresponding calculations. The topological polar surface area (TPSA) was visualized using Jmol [43].

Table 5. Compound abbreviations and list of generated smiles used for ADME calculations.

Compound	SMILES
Py-4-ox	<chem>ON=CC1=CC=NC=C1</chem>
Py-Bn	<chem>ON=CC1=CC=[N+](CC2=CC=CC=C2)C=C1.[Br-]</chem>
Py-BnCH ₃	<chem>CC(C=C1)=CC=C1C[N+](C)2=CC=C(C=NO)C=C2.[Br-]</chem>
Py-BnNO ₂	<chem>ON=CC1=CC=[N+](CC2=CC=C([N+](O)=O)C=C2)C=C1.[Br-]</chem>
Py-BnCl	<chem>ClC(C=C1)=CC=C1C[N+](C)2=CC=C(C=NO)C=C2.[Br-]</chem>
Py-BnF	<chem>FC(C=C1)=CC=C1C[N+](C)2=CC=C(C=NO)C=C2.[Br-]</chem>
Py-BnBr	<chem>BrC(C=C1)=CC=C1C[N+](C)2=CC=C(C=NO)C=C2.[Br-]</chem>
Py-BnCF ₃	<chem>ON=CC1=CC=[N+](CC2=CC=C(C(F)(F)F)C=C2)C=C1.[Br-]</chem>
Py-BnOCF ₃	<chem>ON=CC1=CC=[N+](CC2=CC=C(OC(F)(F)F)C=C2)C=C1.[Br-]</chem>
Py-C ₈ Br	<chem>ON=CC1=CC=[N+](CCCCCCCCBr)C=C1.[Br-]</chem>
Py-C ₁₀ Br	<chem>ON=CC1=CC=[N+](CCCCCCCCCBr)C=C1.[Br-]</chem>
Py-C ₁₂ Br	<chem>ON=CC1=CC=[N+](CCCCCCCCCCCCBr)C=C1.[Br-]</chem>
Py-C ₁₂	<chem>ON=CC1=CC=[N+](CCCCCCCCCCCC)C=C1.[Br-]</chem>
Py-C ₁₄	<chem>ON=CC1=CC=[N+](CCCCCCCCCCCCC)C=C1.[Br-]</chem>
Py-C ₁₆	<chem>ON=CC1=CC=[N+](CCCCCCCCCCCCCCCC)C=C1.[Br-]</chem>
CPC	<chem>CCCCCCCCCCCCCCCC[N+](C)1=CC=CC=C1.[Cl-]</chem>
BAB	<chem>C[N+](CC1=CC=CC=C1)(C)CCCCCCCCCCCC.[Br-]</chem>

3.4. Atomic Force Microscopy

AFM measurements of immobilized cells, both untreated and treated, were performed using the Nano-wizard IV system (JPK/Bruker, Berlin, Germany) operating in quantitative imaging (QI) mode with SNL-B probes (Bruker, Billerica, MA, USA). The AFM system was integrated with an IX73 inverted fluorescence optical microscope (Olympus, Tokyo, Japan). *Escherichia coli* DH5 α cells and FluoroDish Petri dishes (WPI, Sarasota, FL, USA) coated with Cell-Tak (Corning, NY, USA) solution were prepared as previously reported [44]. After preparing the coated dish, a 30 μ L aliquot of the exponentially grown bacterial cells was applied and rinsed vigorously with MHB after 10 min. The final volume of the medium in the dish was 1 mL, while the temperature was always kept at 37 °C. The immobilized bacterial cells were examined with the bright-field microscope to select the AFM imaging region of choice. The cells were then grown for 2 hours under constant conditions to confirm intact cell division and elongation processes. After incubation, the cell culture was once again washed vigorously with fresh MHB, and AFM images of untreated cells were acquired. Cell treatment was initiated by adding a **Py-C₁₂** stock solution to reach the final concentration equivalent to 4 \times MIC. After 3 h of treatment, cells were washed again with fresh MHB and AFM images of treated cells were acquired. During the imaging of the treated and untreated cells, the set point was maintained at 0.9 nN, the extend/retract speed was between 100 and 150 μ m s⁻¹ while the Z length was up to 6000 nm. The resolution of each measurement was 128 \times 128 pixels. Finally, the collected AFM data were processed using JPK data processing software.

To confirm cell membrane permeation, **Py-C₁₂** treatment was replaced with physiological saline (1 mL) containing 1.5 μ L of each fluorescent dye—the green fluorescent SYTO 9, and the red fluorescent propidium iodide (PI), which are components of the LIVE/DEAD BacLight Bacterial Viability Kit L7012 (Invitrogen, Carlsbad, USA). Fluorescence images were taken 30 min after addition of the dyes.

3.5. Docking Analysis

We performed all-atom molecular dynamics (MD) simulations of QacR protein in the presence of CPC (QacR:CPC system) and **Py-C₁₄** (QacR:**Py-C₁₄** system) ligands, as well as in their absence (QacR system). In this respect, the starting protein structure was obtained from crystal structure with PDB code 3BTJ (dimer). The dimer (crystal water, ions, and the ligand present in the 3BTJ pdb file removed) was solvated using 40,000 water molecules (rectangular periodic boundary conditions), while chloride anions were added to each simulated system to neutralize the overall charge of the prepared simulation

boxes (four chloride ions in the case of the “pure” protein, five in the cases of QacR:ligand systems). A common and consistent set of parameters was used to describe the protein and its surrounding, namely AMBER ff14SB force field [45] was used to describe the protein, with chloride anions and water molecules were represented using TIP3P water model and parameters developed by Cheatham III et al. [46], respectively. The two ligands investigated in this study were parameterized according to general AMBER force field (GAFF) [47], whereby the only missing parameters, namely partial charges of the two ligands, were calculated employing a restrained single-conformer fit to the electrostatic potential (RESP) [48]. The electrostatic potential via which partial charges were estimated was obtained using quantum mechanical calculations (HF/6-31G(d)//B3LYP/6-31G(d) level of theory). The ligands were positioned in QacR dimer on the basis of the position of the ligand (dequalinium, DEQ) found in the aforementioned crystal structure, which was performed utilizing the program Maestro from Schrödinger software suite [49].

All three prepared systems (QacR, QacR:CPC, QacR:Py-C₁₄) were subjected to the equivalent minimization/equilibration procedure, consisting of the following steps: (a) minimization of the systems employing steepest descent algorithm (5000 steps), (b) relaxation of the systems in the duration of 10 ns at $T = 310$ K (NVT ensemble, 2 fs time step, Berendsen thermostat with time constant for temperature coupling equal to 1 ps, position restraints applied on all heavy atoms of the ligands (if present) and the protein ($500 \text{ kJ mol}^{-1} \text{ nm}^{-2}$)), (c) equilibration at $T = 310$ K in the duration of 10 ns (NPT ensemble, 2 fs time step, Berendsen thermostat with time constant for temperature coupling equal to 1 ps, Berendsen barostat with $p = 1$ bar and time constant for pressure coupling equal to 5.0 ps), position restraints on all heavy atoms of the protein and ligands ($200 \text{ kJ mol}^{-1} \text{ nm}^{-2}$). Upon equilibration, all three prepared system were propagated at $T = 310$ K with no applied positional restraints (free MD) in the duration of 500 ns (MD parameters of the production simulations: NPT ensemble, 2 fs time step, Nosé-Hoover thermostat with time constant for temperature coupling set to 1 ps, Parrinello-Rahman barostat with $p = 1$ bar and time constant for pressure coupling equal to 5.0 ps). All aforementioned simulations were performed taking into account periodic boundary conditions, where the particle mesh Ewald method was employed to properly account for the long-range electrostatic interactions beyond a 1.2 nm cutoff [50]. In the subsequent analysis, the first 50 ns of each individual simulation were ignored, corresponding to the equilibration period of the simulations. All MD simulations and subsequent analyses were produced using GROMACS 2020 software package [51]. The systems are visualized via VMD visualization software [52].

4. Conclusions

In this paper we describe synthesis and biological evaluation of quaternary ammonium salts (QAS) with aryl and alkyl substituents on pyridine-4-aldoxime. We noticed that alkyl, as opposed to aryl substituted quaternary oximes, generally show much better antibacterial potential with lowest MIC values ranging from 0.04 to 0.31 mg/mL. Moreover, the same compounds exhibit potent antiphytoviral activity against *Tobacco mosaic virus* (TMV) with Py-C₁₄ inhibiting up to 93.7% of viral load comparable to the standard compound BAB. More importantly, the identified candidates did not show toxicity toward healthy human cell lines, namely RPE1 and HaCaT, implicating that these compounds might be new potent antimicrobial agents. Furthermore, the compounds have a membranolytic mode of action, inducing an alteration of bacterial morphologies displaying corrugated and/or disrupted cell surfaces. While the presence of the oxime group unfavorably increases the topological polar surface area as compared to structurally similar CPC, the candidate compounds still exhibit potent membranolytic activity with 87% of the cells with permeabilized membrane after 3 h of treatment at $4 \times \text{MIC}$. The effect of new compounds on the most studied QAS resistance system involving QacR transcriptional regulator was investigated by MD simulations. We observed strikingly different QacR conformations in the presence of either ligand, CPC or Py-C₁₄. However, the detrimental effect of Py-C₁₄ binding was most pronounced as this ligand induced QacR dimer dissociation and its re-assembly during

the respective MD simulation suggesting that this class of compounds could induce a premature activation of QAS resistance system.

Author Contributions: R.O. designed the new compounds; D.C. and R.O. were responsible for the preparation and purity analysis of the compounds; I.P. recorded the NMR spectra and performed the spectral analysis; A.S. and D.C. determined the antibacterial activity, E.V. determined the antiviral activity; A.S. and D.C. calculated cLogP and TPSA; D.C. determined cytotoxicity; L.K. and D.C. collected and analyzed AFM data; M.C. and Z.B. were responsible for computational simulations and analysis and interpretation of data; M.Š. and R.O. designed and directed the study, secured funding, wrote the manuscript, and were responsible for correspondence. All authors have read and agreed to the published version of the manuscript.

Funding: This work was financially supported by the Croatian Ministry of Science and Education as part of the multi-annual financing intended for institution, the Croatian Science Foundation grant no. UIP-2020-02-2356 awarded to M.Š. and STIM-REI, Contract Number: KK.01.1.1.01.0003, a project funded by the European Union through the European Regional Development Fund—the Operational Programme Competitiveness and Cohesion 2014–2020 (KK.01.1.1.01).

Institutional Review Board Statement: Not applicable.

Informed Consent Statement: Not applicable.

Data Availability Statement: Data is contained within the article.

Acknowledgments: The Authors would like to thank I. Tolić lab from the Ruđer Bošković Institute for the generous gift of RPE1 cells.

Conflicts of Interest: The authors declare no conflict of interest. The founding sponsors had no role in the design of the study; in the collection, analyses, or interpretation of data; in the writing of the manuscript, and in the decision to publish the results.

References

- Loftsson, T.; Thorsteinsson, T.; Hilmarsson, H.; Hjálmarisdóttir, M.A.; Kristinsson, K.G.; Másson, M. Soft Antimicrobial Agents: Synthesis and Activity of Labile Environmentally Friendly Long Chain Quaternary Ammonium Compounds. *J. Med. Chem.* **2003**, *46*, 4173–4181. [[CrossRef](#)]
- Minbiole, K.P.C.; Jennings, M.C.; Ator, L.E.; Black, J.W.; Grenier, M.C.; LaDow, J.E.; Caran, K.L.; Seifert, K.; Wuest, W.M. From antimicrobial activity to mechanism of resistance: The multifaceted role of simple quaternary ammonium compounds in bacterial eradication. *Tetrahedron* **2016**, *72*, 3559–3566. [[CrossRef](#)]
- Jennings, M.C.; Minbiole, K.P.C.; Wuest, W.M. Quaternary ammonium compounds: An antimicrobial mainstay and platform for innovation to address bacterial resistance. *ACS Infect. Dis.* **2016**, *1*, 288–303. [[CrossRef](#)] [[PubMed](#)]
- Alkhalifa, S.; Jennings, M.C.; Granata, D.; Klein, M.; Wuest, W.M.; Minbiole, K.P.C.; Carnevale, V. Analysis of the Destabilization of Bacterial Membranes by Quaternary Ammonium Compounds: A Combined Experimental and Computational Study. *ChemBioChem* **2020**, *21*, 1510–1516. [[CrossRef](#)]
- Tischer, M.; Pradel, G.; Ohlsen, K.; Holzgrabe, U. Quaternary ammonium salts and their antimicrobial potential: Targets or nonspecific interactions? *ChemMedChem* **2012**, *7*, 22–31. [[CrossRef](#)] [[PubMed](#)]
- Xiling, G.; Yin, C.; Ling, W.; Xiaosong, W.; Jingjing, F.; Fang, L.; Xiaoyan, Z.; Yiyue, G.; Ying, C.; Lunbiao, C.; et al. In vitro inactivation of SARS-CoV-2 by commonly used disinfection products and methods. *Sci. Rep.* **2021**, *11*, 2418. [[CrossRef](#)] [[PubMed](#)]
- Buffet-Bataillon, S.; Tattevin, P.; Bonnaure-Mallet, M.; Jolivet-Gougeon, A. Emergence of resistance to antibacterial agents: The role of quaternary ammonium compounds—A critical review. *Int. J. Antimicrob. Agents* **2012**, *39*, 381–389. [[CrossRef](#)]
- Jennings, M.C.; Buttaró, B.A.; Minbiole, K.P.C.; Wuest, W.M. Bioorganic Investigation of Multicationic Antimicrobials to Combat QAC-Resistant *Staphylococcus aureus*. *ACS Infect. Dis.* **2016**, *1*, 304–309. [[CrossRef](#)]
- Schumacher, M.A.; Miller, M.C.; Grkovic, S.; Brown, M.H.; Skurray, R.A.; Brennan, R.G. Structural basis for cooperative DNA binding by two dimers of the multidrug-binding protein QacR. *EMBO J.* **2002**, *21*, 1210–1218. [[CrossRef](#)]
- Forman, M.E.; Fletcher, M.H.; Jennings, M.C.; Duggan, S.M.; Minbiole, K.P.C.; Wuest, W.M. Structure-Resistance Relationships: Interrogating Antiseptic Resistance in Bacteria with Multicationic Quaternary Ammonium Dyes. *ChemMedChem* **2016**, *11*, 958–962. [[CrossRef](#)]
- Jennings, M.C.; Forman, M.E.; Duggan, S.M.; Minbiole, K.P.C.; Wuest, W.M. Efflux Pumps Might Not Be the Major Drivers of QAC Resistance in Methicillin-Resistant *Staphylococcus aureus*. *ChemBioChem* **2017**, *18*, 1573–1577. [[CrossRef](#)] [[PubMed](#)]
- Al-Khalifa, S.E.; Jennings, M.C.; Wuest, W.M.; Minbiole, K.P.C. The Development of Next-Generation Pyridinium-Based multiQAC Antiseptics. *ChemMedChem* **2017**, *12*, 280–283. [[CrossRef](#)] [[PubMed](#)]

13. Ator, L.E.; Jennings, M.C.; McGettigan, A.R.; Paul, J.J.; Wuest, W.M.; Minbiole, K.P.C. Beyond paraquats: Dialkyl 3,3'- and 3,4'-bipyridinium amphiphiles as antibacterial agents. *Bioorganic Med. Chem. Lett.* **2014**, *24*, 3706–3709. [CrossRef]
14. Garrison, M.A.; Mahoney, A.R.; Wuest, W.M. Tricepyridinium-inspired QACs yield potent antimicrobials and provide insight into QAC resistance. *ChemMedChem* **2021**, *16*, 463–466. [CrossRef] [PubMed]
15. Haldar, J.; Kondaiah, P.; Bhattacharya, S. Synthesis and Antibacterial Properties of Novel Hydrolyzable Cationic Amphiphiles. Incorporation of Multiple Head Groups Leads to Impressive Antibacterial Activity. *J. Med. Chem.* **2005**, *48*, 3823–3831. [CrossRef]
16. Grenier, M.C.; Davis, R.W.; Wilson-Henjum, K.L.; Ladow, J.E.; Black, J.W.; Caran, K.L.; Seifert, K.; Minbiole, K.P.C. The antibacterial activity of 4,4'-bipyridinium amphiphiles with conventional, bicephalic and gemini architectures. *Bioorganic Med. Chem. Lett.* **2012**, *22*, 4055–4058. [CrossRef]
17. Rodríguez-Morales, S.; Compadre, R.L.; Castillo, R.; Breen, P.J.; Compadre, C.M. 3D-QSAR, synthesis, and antimicrobial activity of 1-alkylpyridinium compounds as potential agents to improve food safety. *Eur. J. Med. Chem.* **2005**, *40*, 840–849. [CrossRef]
18. Marek, J.; Malinak, D.; Dolezal, R.; Soukup, O.; Pasdiorova, M.; Dolezal, M.; Kuca, K. Synthesis and disinfection effect of the pyridine-4-aldoxime based salts. *Molecules* **2015**, *20*, 3681–3696. [CrossRef]
19. Abele, E.; Abele, R.; Lukevics, E. Pyridine Oximes: Synthesis, Reactions, and Biological Activity. *Chem. Heterocycl. Compd.* **2003**, *39*, 825–865. [CrossRef]
20. Gašo-Sokač, D.; Katalinić, M.; Kovarik, Z.; Bušić, V.; Kovač, S. Synthesis and evaluation of novel analogues of vitamin B6 as reactivators of tabun and paraoxon inhibited acetylcholinesterase. *Chem.-Biol. Interact.* **2010**, *187*, 234–237. [CrossRef]
21. Čalić, M.; Vrdoljak, A.L.; Radić, B.; Jelić, D.; Jun, D.; Kuča, K.; Kovarik, Z. In vitro and in vivo evaluation of pyridinium oximes: Mode of interaction with acetylcholinesterase, effect on tabun- and soman-poisoned mice and their cytotoxicity. *Toxicology* **2006**, *219*, 85–96. [CrossRef] [PubMed]
22. Odžak, R.; Čalić, M.; Hrenar, T.; Primožič, I.; Kovarik, Z. Evaluation of monoquaternary pyridinium oximes potency to reactivate tabun-inhibited human acetylcholinesterase. *Toxicology* **2007**, *233*, 85–96. [CrossRef] [PubMed]
23. Foretić, B.; Damjanović, V.; Vianello, R.; Picek, I. Novel insights into the thioesterolytic activity of N-substituted pyridinium-4-oximes. *Molecules* **2020**, *25*, 2385. [CrossRef] [PubMed]
24. Crnčević, D.; Odžak, R. Synthesis of quaternary ammonium salts based on quinuclidin-3-ol and pyridine-4-aldoxime with alkyl chains. *ST-OPEN* **2020**, *1*, 1–8. [CrossRef]
25. Bazina, L.; Maravić, A.; Krce, L.; Soldo, B.; Odžak, R.; Popović, V.B.; Aviani, I.; Primožič, I.; Šprung, M. Discovery of novel quaternary ammonium compounds based on quinuclidine-3-ol as new potential antimicrobial candidates. *Eur. J. Med. Chem.* **2019**, *163*, 626–635. [CrossRef]
26. Crnčević, D.; Krce, L.; Mastelić, L.; Maravić, A.; Soldo, B.; Aviani, I.; Primožič, I.; Odžak, R.; Šprung, M. The mode of antibacterial action of quaternary N-benzylimidazole salts against emerging opportunistic pathogens. *Bioorganic Chem.* **2021**, *112*, 104938. [CrossRef]
27. Zhang, N.; Ma, S. Recent development of membrane-active molecules as antibacterial agents. *Eur. J. Med. Chem.* **2019**, *184*, 111743. [CrossRef]
28. Kontos, R.C.; Schallenger, S.A.; Bentley, B.S.; Morrison, K.R.; Feliciano, J.A.; Tasca, J.A.; Kaplan, A.R.; Bezpalko, M.W.; Kassel, W.S.; Wuest, W.M.; et al. An Investigation into Rigidity–Activity Relationships in BisQAC Amphiphilic Antiseptics. *ChemMedChem* **2019**, *14*, 83–87. [CrossRef]
29. Mereghetti, L.; Quentin, R.; der Mee, N.M.-V.; Audurier, A. Low sensitivity of *Listeria monocytogenes* to quaternary ammonium compounds. *Appl. Environ. Microbiol.* **2000**, *66*, 5083–5086. [CrossRef]
30. Kwaśniewska, D.; Chen, Y.L.; Wiczorek, D. Biological activity of quaternary ammonium salts and their derivatives. *Pathogens* **2020**, *9*, 459. [CrossRef]
31. Sunde, M.; Langsrud, S.; Yazdankhah, S.P.; Hegstad, K.; Lunestad, B.T.; Scheie, A.A. Does the wide use of Quaternary Ammonium Compounds enhance the selection and spread of antimicrobial resistance and thus threaten our health? *Microb. Drug Resist.* **2010**, *16*, 91–104. [CrossRef]
32. Ogilvie, B.H.; Solis-Leal, A.; Lopez, J.B.; Poole, B.D.; Robison, R.A.; Berges, B.K. Alcohol-free hand sanitizer and other quaternary ammonium disinfectants quickly and effectively inactivate SARS-CoV-2. *J. Hosp. Infect.* **2021**, *108*, 142–145. [CrossRef]
33. Rusak, G.; Kraja, M.; Krsnik-Rasol, M.; Gutzeit, H.O. Quercetin influences response in *Nicotiana megalosiphon* infected by satellite-associated cucumber mosaic virus. *J. Plant Dis. Prot.* **2007**, *114*, 145–150. [CrossRef]
34. Othman, B. Antiphytoviral Activity of the *Plectranthus Tenuiflorus* on Some Important Viruses. 2016. Available online: <https://www.researchgate.net/publication/228906668> (accessed on 2 February 2022).
35. Kratović, E.; Rusak, G.; Bezić, N.; Krajačić, M. Inhibition of tobacco mosaic virus infection by quercetin and vitexin. *Acta Virol.* **2008**, *52*, 119–124. [PubMed]
36. Vuko, E.; Dunkić, V.; Maravić, A.; Ruščić, M.; Nazlić, M.; Radan, M.; Ljubenković, I.; Soldo, B.; Fredotović, Ž. Not only a weed plant—biological activities of essential oil and hydrosol of *Dittrichia viscosa* (L.) greuter. *Plants* **2021**, *10*, 1837. [CrossRef]
37. Daina, A.; Michielin, O.; Zoete, V. SwissADME: A free web tool to evaluate pharmacokinetics, drug-likeness and medicinal chemistry friendliness of small molecules. *Sci. Rep.* **2017**, *7*, 42717. [CrossRef] [PubMed]
38. Stocks, S.M. Mechanism and use of the commercially available viability stain, BacLight. *Cytom. Part A* **2004**, *61*, 189–195. [CrossRef]

39. Clsi, M07-A9: Methods for Dilution Antimicrobial Susceptibility Tests for Bacteria That Grow Aerobically; Approved Standard—Ninth Edition, n.d. Available online: www.clsi.org (accessed on 11 November 2021).
40. Vuko, E.; Dunkić, V.; Ruščić, M.; Nazlić, M.; Mandić, N.; Soldo, B.; Šprung, M.; Fredotović, Ž. Chemical composition and new biological activities of essential oil and hydrosol of *Hypericum perforatum* l. Ssp. veronense (schrank) h. lindb. *Plants* **2021**, *10*, 1014. [[CrossRef](#)]
41. Leatherbarrow, R.J. *GraFit Version 7*; Erithacus Software Ltd.: Horley, UK, 2009.
42. PerkinElmer, Chemdraw, (RRID:SCR_016768), (n.d.). Available online: <https://perkinelmerinformatics.com/> (accessed on 6 October 2021).
43. Jmol Development Team, Jmol. 2016. Available online: <http://jmol.sourceforge.net> (accessed on 6 October 2021).
44. Krce, L.; Šprung, M.; Maravić, A.; Umek, P.; Salamon, K.; Krstulović, N.; Aviani, I. Bacteria exposed to silver nanoparticles synthesized by laser ablation in water: Modelling *E. coli* growth and inactivation. *Materials* **2020**, *13*, 653. [[CrossRef](#)]
45. Maier, J.A.; Martinez, C.; Kasavajhala, K.; Wickstrom, L.; Hauser, K.E.; Simmerling, C. ff14SB: Improving the Accuracy of Protein Side Chain and Backbone Parameters from ff99SB. *J. Chem. Theory Comput.* **2015**, *11*, 3696–3713. [[CrossRef](#)]
46. Joung, S.; Cheatham, T.E., III. Determination of alkali and halide monovalent ion parameters for use in explicitly solvated biomolecular simulations. *J. Phys. Chem. B* **2008**, *112*, 9020–9041. [[CrossRef](#)] [[PubMed](#)]
47. Wang, J.; Wolf, R.M.; Caldwell, J.W.; Kollman, P.A.; Case, D.A. Development and testing of a general AMBER force field. *J. Comput. Chem.* **2004**, *25*, 1157–1174. [[CrossRef](#)] [[PubMed](#)]
48. Cieplak, P.; Cornell, W.D.; Bayly, C.I.; Kollman, P.A. Application of the multimolecule and multiconformational RESP methodology to biopolymers: Charge derivation for DNA, RNA, and proteins. *J. Comput. Chem.* **1995**, *16*, 1357–1377. [[CrossRef](#)]
49. Schrödinger, LLC. *Schrödinger Release 2022-1: Maestro*; Schrödinger, LLC: New York, NY, USA, 2021.
50. Darden, T.; York, D.; Pedersen, L. Particle mesh Ewald: An N·log(N) method for Ewald sums in large systems. *J. Chem. Phys.* **1993**, *98*, 10089–10092. [[CrossRef](#)]
51. Abraham, M.J.; Murtola, T.; Schulz, R.; Páll, S.; Smith, J.C.; Hess, B.; Lindahl, E. GROMACS: High performance molecular simulations through multi-level parallelism from laptops to supercomputers. *SoftwareX* **2015**, *1*, 19–25. [[CrossRef](#)]
52. Humphrey, W.; Dalke, A.; Schulten, K. VMD—Visual Molecular Dynamics. *J. Mol. Graph.* **1996**, *14*, 33–38. [[CrossRef](#)]

**3.2. A DUAL ANTIBACTERIAL ACTION OF SOFT QUATERNARY
AMMONIUM COMPOUNDS: BACTERIOSTATIC EFFECTS,
MEMBRANE INTEGRITY, AND REDUCED *IN VITRO* AND *IN VIVO*
TOXICITY**

Reproduced from

Crnčević D, Krce L, Brkljača Z, Cvitković M, Babić Brčić S, Čož-Rakovac R, Odžak R, Šprung M. A dual antibacterial action of soft quaternary ammonium compounds: bacteriostatic effects, membrane integrity, and reduced *in vitro* and *in vivo* toxicity // RSC Advances, 15 (2025), doi: 10.1039/D4RA07975B


 Cite this: *RSC Adv.*, 2025, 15, 1490

A dual antibacterial action of soft quaternary ammonium compounds: bacteriostatic effects, membrane integrity, and reduced *in vitro* and *in vivo* toxicity†

 Doris Crnčević,^{ab} Lucija Krce,^c Zlatko Brkljača,^d Mislav Cvitković,^{id c} Sanja Babić Brčić,^{ef} Rozelindra Čož-Rakovac,^{ef} Renata Odžak^a and Matilda Šprung^{id *a}

Quaternary ammonium compounds (QACs) have served as essential antimicrobial agents for nearly a century due to their rapid membrane-disrupting action. However, the emergence of bacterial resistance and environmental concerns have driven interest in alternative designs, such as “soft QACs”, which are designed for enhanced biodegradability and reduced resistance potential. In this study, we explored the antibacterial properties and mechanisms of action of our newly synthesized soft QACs containing a labile amide bond within a quinuclidine scaffold. Our findings revealed that these compounds primarily exhibit a bacteriostatic mode of action, effectively suppressing bacterial growth even at concentrations exceeding their minimum inhibitory concentrations (MICs). Unlike traditional QACs, fluorescence spectroscopy and microscopy demonstrated membrane preservation during treatment, with reduced membrane integration compared to cetylpyridinium chloride (CPC), as corroborated by parallel artificial membrane permeability assays. Additionally, molecular dynamics simulations revealed “hook-like” conformations that limit lipid bilayer penetration and promote the formation of larger aggregates, reducing their effective concentration and minimizing cytotoxic effects. Interestingly, secondary antibacterial mechanisms, including inhibition of protein synthesis, were observed, further enhancing their activity. Zebrafish embryotoxicity and *in vitro* cytotoxicity studies confirmed significantly lower toxicity compared to CPC. By addressing limitations associated with conventional QACs, including toxicity, resistance, and environmental persistence, these soft QACs provide a promising foundation for next-generation antimicrobials. This work advances the understanding of QAC mechanisms while paving the way for safer, eco-friendly applications in healthcare, agriculture, and industrial settings.

 Received 9th November 2024
 Accepted 28th December 2024

DOI: 10.1039/d4ra07975b

rsc.li/rsc-advances

1 Introduction

Quaternary ammonium compounds (QACs) are a class of cationic surfactants that have been employed for nearly

a century across a wide range of industries, including healthcare, agriculture, and the production of household cleaning supplies.^{1–3} Their most prominent characteristic is antibacterial efficacy, first identified in the early 1930s with benzalkonium chloride (BAC), which quickly became a key active ingredient in disinfectants and surface sanitizers commonly used in hospital settings.^{4–6} The antibacterial activity of QACs is primarily attributed to their distinct structural elements, which facilitate interactions with bacterial cell membrane components. Although the precise mechanism of action is not fully understood, it is proposed that QACs act as membranolytic agents in a few steps. The electrostatic interaction of QAC’s positively charged nitrogen atom and negatively charged residues of teichoic and lipoteichoic acids within the peptidoglycan matrix and lipid bilayer causes initial membrane destabilization.⁷ This is further followed by the insertion of hydrophobic substituents into the membrane matrix causing the leakage of cytoplasmic contents and ultimately leading to cell lysis.^{8–10} In addition to

^aUniversity of Split, Faculty of Science, Department of Chemistry, R. Bošković 33, Split, Croatia. E-mail: dcrncevic@pmfst.hr; rodzak@pmfst.hr; msprung@pmfst.hr

^bUniversity of Split, Faculty of Science, Doctoral Study in Biophysics, R. Bošković 33, Split, Croatia

^cUniversity of Split, Faculty of Science, Department of Physics, R. Bošković 33, Split, Croatia. E-mail: lucija.krce@pmfst.hr; mcvitkovi@pmfst.hr

^dSelvita Ltd., Prilaz Baruna Filipovića 29, Zagreb, Croatia. E-mail: zlatko.brkljaca@selvita.com

^eRuder Bošković Institute, Laboratory for Biotechnology in Aquaculture, Division of Materials Chemistry, Bijenička 54, Zagreb, Croatia. E-mail: sanja.babic@irb.hr; rrvakovac@irb.hr

^fCenter of Excellence for Marine Bioprospecting (BioProCro), Ruder Bošković Institute, Bijenička 54, Zagreb, Croatia

† Electronic supplementary information (ESI) available. See DOI: <https://doi.org/10.1039/d4ra07975b>

their role as “biological detergents” that act on biological membranes, some QACs have also demonstrated antibacterial activity by targeting intracellular components, such as DNA or pyridoxal-dependent enzymes targeting.^{11–13}

Due to their strong antibacterial activity, the demand for these compounds has surged, particularly during the SARS-CoV-2 pandemic which was followed by an urgent need for effective topical antiseptic formulations.¹⁴ At the same time, the inherent chemical stability of commercially available QACs has become a subject of considerable concern within the scientific community, as these compounds have the potential to simultaneously activate bacterial resistance mechanisms and pose significant risks to human health.^{15–17} These findings underscore the need for further new-generation QACs development, exploration of their antibacterial mechanism of action, as well as a comprehensive investigation of their structure–activity relationship.

In pursuit of environmentally friendly yet biologically effective QAC variants, contemporary synthetic strategies involve the functionalization of the compound backbone with hydrolysable groups, such as ester or amide, enabling the controlled degradation of so-called “soft QACs”. Among these, QACs with amide groups are considered promising new derivatives, as ester-containing QACs tend to self-degrade, diminishing the reliability of their antibacterial effectiveness.^{18–20} We have previously reported the new soft amido-QACs prone to protease degradation derived from heterocyclic backbone of naturally occurring quinuclidine (Scheme 1).²¹ The assessment of their biological activity, ranging from non-active to moderately active structures (Scheme 1) led us to hypothesize that the polar amide functional group at the C-3 atom of the quinuclidine scaffold significantly impacts the antibacterial efficacy of the new QAC derivatives potentially hindering the electrostatic interactions with the bacterial membrane.

In this study, we provide a comprehensive investigation of the antibacterial mechanisms and structure–activity relationships of four newly synthesized soft QACs, incorporating a polar

amide group within a quinuclidine scaffold. Unlike conventional QACs, these compounds exhibit a dual mode of action, combining membrane interaction with protein synthesis inhibition, which may help address bacterial resistance. Time-kill assays revealed a bacteriostatic effect, while microscopy and fluorescence spectroscopy confirmed preserved membrane integrity at their respective minimum inhibitory concentrations (MICs).

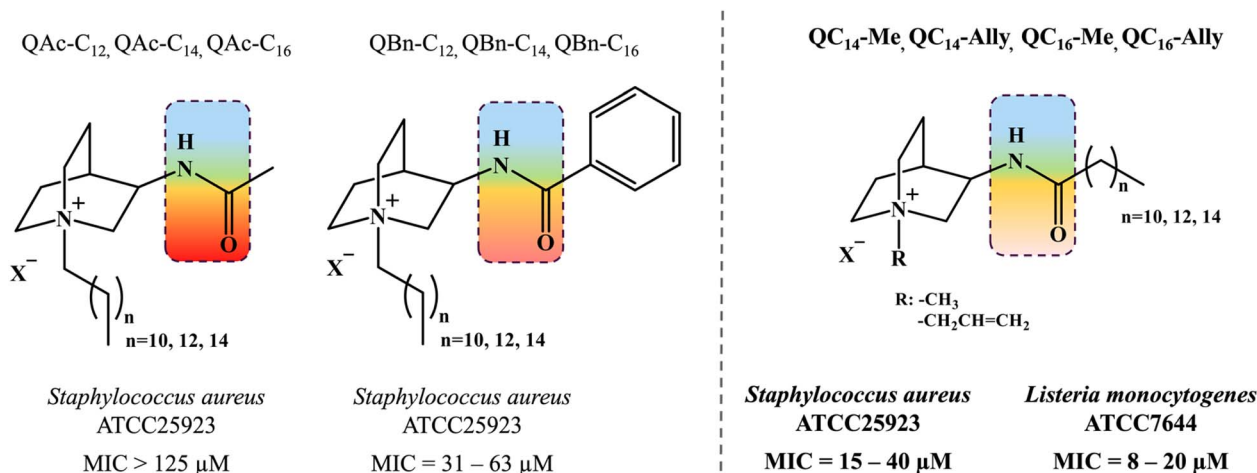
Molecular dynamics (MD) simulations revealed that these compounds adopt unique “hook-like” conformations that limit membrane penetration compared to the commercial standard, CPC, a finding supported by parallel artificial membrane permeability assays (PAMPA). This reduced interaction correlates with significantly lower cytotoxicity and embryotoxicity, as demonstrated through *in vitro* and *in vivo* testing.

By linking structure to activity, this study advances the understanding of QAC mechanisms and highlights the potential of these soft QACs as safer, environmentally friendly antimicrobials for applications in healthcare and beyond.

2 Results and discussion

2.1. Bacteriostatic activity

Examination of bacterial viability during the treatment over a certain incubation time provides initial insight into the mode of action of the tested agent. Namely, antibacterial agents can generally exhibit bactericidal or bacteriostatic effect.^{22,23} While bactericidal agents kill 99.99% of cells during a 24 hours treatment, the bacteriostatic mode of action implies keeping the population in the stationary growth phase without directly causing cell death. Due to their membranolytic potency, quaternary ammonium compounds (QACs) are most known as bactericidal agents causing almost immediate membrane damage and cell death. Although some QACs are also prone to cellular uptake followed by DNA or proteins targeting, such antibacterial activity requires further exploration.^{12,13,24,25}



Scheme 1 Previous investigations on soft quaternary ammonium compounds (QACs) derived from heterocyclic backbone of quinuclidine taken from ref. 21. Amide functional group is located at third carbon atom of quinuclidine scaffold depicted in the colored squares reflecting the polar character. Different substituents in extension of amide functionality (QAc – acetamide, QB_n – benzamide and QC_n – alkylamide) were found to exhibit differential antimicrobial activity.

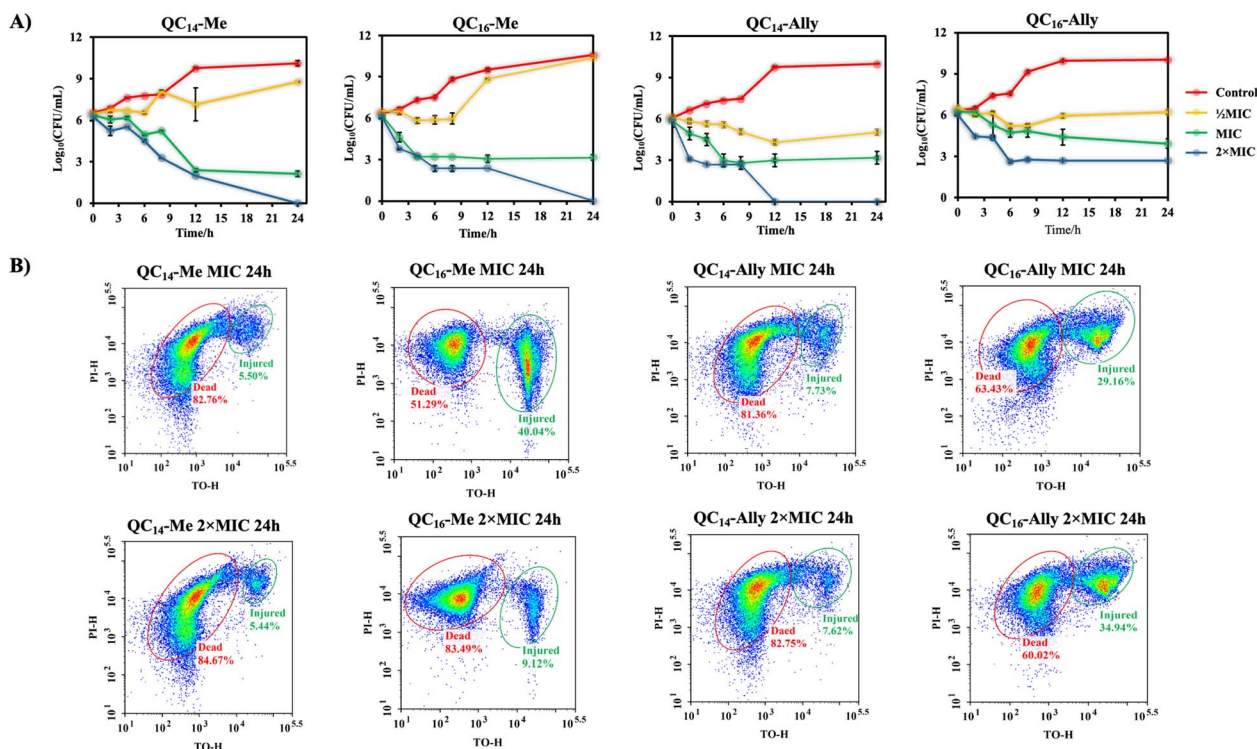


Fig. 1 (A) Time-resolved \log_{10} of colony forming units per milliliter (CFU mL^{-1}) curves obtained by plate count method during the 24 hours long treatment of *Staphylococcus aureus* ATCC25923 with, $\frac{1}{2}$ MIC, MIC and $2 \times$ MIC of QC₁₄-Me, QC₁₄-Ally, QC₁₆-Me and QC₁₆-Ally. (B) Flow cytometry dot plot of injured and dead thiazole orange (TO) and propidium iodide (PI) fluorescently stained *Staphylococcus aureus* ATCC25923 cells after 24 hours long treatment at MIC and $2 \times$ MIC concentration of QC₁₄-Me, QC₁₄-Ally, QC₁₆-Me and QC₁₆-Ally.

The cell viability of *Staphylococcus aureus* ATCC25923 during the 24 hours treatment at $\frac{1}{2}$ MIC, MIC and $2 \times$ MIC is shown in Fig. 1. Time-resolved curves of \log_{10} of colony forming units per milliliter (CFU mL^{-1}) point out subtle differences between methyl and allyl analogues of QAC candidates at $\frac{1}{2}$ MIC treatment. The results show that methylated QACs (QC₁₄-Me and QC₁₆-Me) keep cells in stationary phase for six hours, in contrast to more effective allyl analogues (QC₁₄-Ally and QC₁₆-Ally) that manage to stop cells from dividing during the entire incubation time. Treatment with concentrations of candidate compounds corresponding to MIC, despite resulting in diminished \log_{10} (CFU mL^{-1}) over time, surprisingly revealed the same effect of each compound on bacterial population. Namely, after six hours of MIC treatment with candidate compounds, *S. aureus* ATCC25923 population was kept in the stationary phase with no indicative cell division. Furthermore, the drop in the number of bacterial cells of $\leq 3 \log_{10}$ (CFU mL^{-1}) after 24 hours of exposure further supported that these compounds are indeed bacteriostatic agents that rather inhibit bacterial growth without damaging bacteria to the extent of cell death. On the contrary, treatment with $2 \times$ MIC resulted in almost complete bacterial eradication upon 12 or 24 hours of treatment with only QC₁₆-Ally displaying reduced potential to annihilate bacteria as further confirmed by flow cytometry (Fig. 1B).

These results clearly show that even at prolonged MICs exposure (24 h) at least half of the population is dead with a similar fraction of injured cells that can potentially recover in

favorable conditions. It seems those candidates bearing C₁₄ alkyl chains are better than candidates with longer chains which can be due to several reasons. Firstly, QACs with longer chains tend to be less soluble, or secondly, they tend to form larger aggregates that diminish their antibacterial potential. This trend is visible at $2 \times$ MIC, which also did not result in complete bacterial eradication even at 24 h of exposure to the antibacterial agent. However, as opposed to MIC treatment, treatment with $2 \times$ MIC clearly shows a larger fraction of dead cells, leaving just about 5–10% of injured cells that can potentially recover. Together, these results confirm our initial observation about a bacteriostatic mode of action which provides a new insight into the different mechanism that has not been documented for these compounds up until now.

2.2. Membranolytic activity

2.2.1. Morphological examination of bacterial cells.

To investigate morphological changes of bacterial cells during the treatment, atomic force microscopy (AFM) was employed. Since the newly synthesized compounds showed more pronounced antimicrobial activity against Gram-positive bacteria, *Listeria monocytogenes* ATCC7644 was selected for the AFM measurements. Apart from the low micromolar minimum inhibitory concentrations of candidate compounds (Scheme 1), the rod-shaped form of *L. monocytogenes* and high proportion of proteins in the cell wall enable better adhesion and immobilization required for the AFM measurements.²⁶ Furthermore, as

AFM usually detects morphological changes upon treatment, cells were treated with $2 \times \text{MIC}$ concentration of each candidate compound in the total duration of three hours.

The untreated *L. monocytogenes* cells, shown in Fig. 2, exhibit the characteristic densely packed rod-shaped morphology, even post-fixation.

Treatment with $2 \times \text{MIC}$ concentrations of **QC₁₄-Me**, **QC₁₄-Ally**, **QC₁₆-Me**, and **QC₁₆-Ally** resulted in no detectable loss of distinct cell morphology, although a consistent increase in cell height was observed across all treated cells. Furthermore, a 3 hours long exposure to $2 \times \text{MIC}$ of these compounds did not induce significant membrane damage, which aligns with prior findings in *Staphylococcus aureus*, another Gram-positive representative. Instead, the cell membranes in treated *L. monocytogenes* cells appeared preserved, with only minor irregularities along the cell edges. To further investigate membrane integrity, both bacterial strains were subjected to optical fluorescence microscopy and fluorescence spectroscopy analysis.

2.2.2. Membrane perforation potential. Optical fluorescence microscopy was employed to examine the membrane integrity of *Listeria monocytogenes* ATCC7644 upon the atomic force microscopy (AFM) measurements utilizing two common fluorophores, SYTO9 and propidium iodide (PI).²⁷ While SYTO9 can passively diffuse through intact cellular membranes, PI can only pass through compromised membranes indicating their damage. Fig. 3A shows the same optical field of *L. monocytogenes* ATCC7644 cells treated with $2 \times \text{MIC}$ concentration of candidate compounds for three hours. The observed intensity of the red fluorescent signal originating from the PI dye bound to DNA molecule indicates compromised cell membranes of

almost all cells, which is further confirmed by the images of SYTO9 stained cells. In this case, the orange color originating from the spectral overlap of the green and red fluorescent signals upon the exposure to the $2 \times \text{MIC}$ concentration of candidate compounds indicates membrane damage despite the preserved membrane appearance observed in AFM measurements, suggesting a membranolytic effect at higher concentrations of our soft QACs.

Furthermore, the uptake of PI by *Staphylococcus aureus* ATCC25923 cells in treatment was measured spectrofluorimetrically at different time intervals over six hours of treatment with $4 \times \text{MIC}$, $2 \times \text{MIC}$ and MIC concentrations of the selected compounds (Fig. 3B). The treatment with $4 \times \text{MIC}$ and $2 \times \text{MIC}$ concentrations showed the same effect for all tested QACs. An almost immediate steep increase of the relative fluorescent units (RFUs) of PI suggested pronounced membrane disruption. On the other hand, at concentrations corresponding to MIC, RFUs were slightly higher for all compounds when compared to the untreated control cells indicating an absence of pronounced membrane damage over six-hours long period of treatment.

Obtained results underlined the previously observed implication of the bacteriostatic activity of **QC₁₄-Me**, **QC₁₄-Ally**, **QC₁₆-Me** and **QC₁₆-Ally** suggesting the need for further investigation of their mode of action through alternative pathways, primarily including the inactivation of the protein synthesis pathways.

2.3. Inhibition of protein synthesis

Antibacterial agents are generally classified in two large groups regarding their mechanism of combating pathogens.

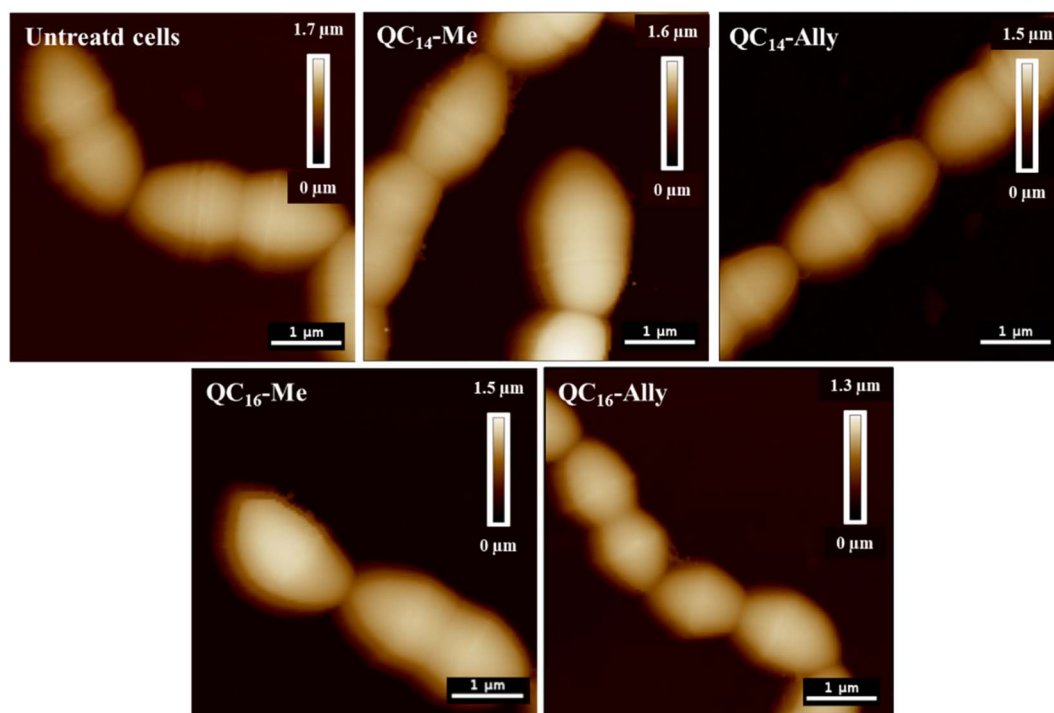


Fig. 2 Height atomic force microscopy (AFM) data of untreated *Listeria monocytogenes* ATCC7644 control cells in contrast to the cells of the same bacteria treated with $2 \times \text{MIC}$ concentration of candidate compounds **QC₁₄-Me**, **QC₁₄-Ally**, **QC₁₆-Me** and **QC₁₆-Ally** in total of three hours.

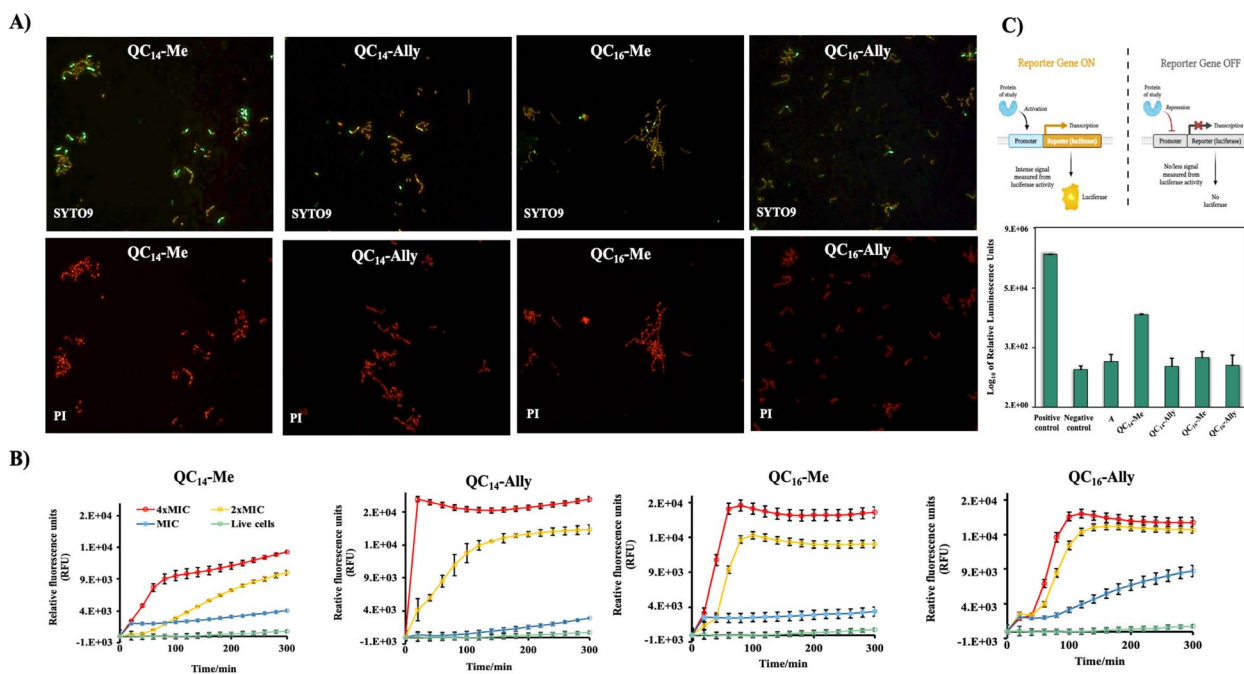


Fig. 3 (A) Fluorescent images of the *Listeria monocytogenes* ATCC7644 cells treated with 2 × MIC concentration of candidate compounds **QC₁₄-Me**, **QC₁₄-Ally**, **QC₁₆-Me** and **QC₁₆-Ally** for three hours and stained with SYTO9 and propidium iodide (PI). Fluorescent images were taken in the same field of view. (B) Spectrofluorimetric analysis of propidium iodide (PI) uptake during *Staphylococcus aureus* ATCC25923 treatment with 4 × MIC, 2 × MIC and MIC concentration of **QC₁₄-Me**, **QC₁₄-Ally**, **QC₁₆-Me** and **QC₁₆-Ally** candidate compounds in contrast to untreated control cells. Results were recorded in time intervals during six hours of treatment. (C) Log₁₀ of relative luminescence units (RLUs) upon inhibition of master mix with **QC₁₄-Me**, **QC₁₄-Ally**, **QC₁₆-Me** and **QC₁₆-Ally** and kanamycin for one hour. Positive control with plasmid DNA containing luciferase gene and negative control with no plasmid DNA.

Bactericidal agents, such as carbapenems and polymyxins, are known for their membrane and cell wall targeting effect.²⁸ Besides membrane disorganization, bactericidal agents can also act as blockers of DNA replication or inhibitors of cell wall synthesis.^{29,30} In both cases the result is extermination of the entire population during 24 hours long incubation time. On the other hand, bacteriostatic activity implies prevention of bacterial division resulting in the stationary growth phase of the population in treatment which is attributed to the potency of protein synthesis inhibition.^{23,31} In most cases, this effect is caused by irreversible binding to the 30S ribosomal subunit which is a common pattern for aminoglycosides, such as kanamycin and spectinomycin³².

Quaternary ammonium compounds (QACs) are categorized as potent membranolytic agents, especially when it comes to Gram-positive pathogens given the simplicity of membrane composition in contrast to Gram-negative bacterial isolates.^{8,10} The unique structure of QAC's scaffold comprised of permanently positively charged nitrogen plays a pivotal role in their proposed mechanism of antibacterial action, exploiting electrostatic interaction with components of bacterial cell membrane. Further membrane disorganization is achieved by incorporating hydrophobic substituents into the membrane matrix resulting in membrane perforation and ultimately cell lysis. Although QACs are known for their membrane-targeting antibacterial approach, some QACs employ different antibacterial potency acting on intracellular components such as DNA and/or proteins.^{12,33,34}

Previously observed bacteriostatic effect prompted us to examine the potential of **QC₁₄-Me**, **QC₁₄-Ally**, **QC₁₆-Me** and **QC₁₆-Ally** to inhibit the protein synthesis pathways. For this purpose, we employed an assay based on *in vitro* synthesis of luciferase protein – expression product of a reporter sequence under the control of T7 promoter. If the expression is successful, luciferase protein degrades its natural substrate luciferin to the product coelenteramide followed by the emission of an intense luminescent signal expressed in relative luminescence units (RLUs). In contrast, if the addition of the tested compound prevents the transcription of protein of interest, a luminescent signal is absent.

The reaction mixture that served as a positive control for luciferase protein expression, apart from T7 extract and S30 ribosomal mixture, contained nuclease-free water and a DNA template that contained luciferase reporter gene downstream of the T7 promoter site. On the other hand, the composition of the negative control differed in absence of the DNA template, preventing the expression of luciferase and therefore emission of luminescent signal. The effect of tested compounds **QC₁₄-Me**, **QC₁₄-Ally**, **QC₁₆-Me** and **QC₁₆-Ally** on *in vitro* luciferase protein expression was compared with the effect of kanamycin which is known to act as the protein synthesis inhibitor employing a bacteriostatic mode of action.³⁵ Fig. 3C shows RLUs detected in each reaction mixture upon one hour of incubation. As expected, the highest RLUs were observed in positive control, indicating a successful expression of luciferase protein. When compared to positive control, all the tested candidate

compounds showed 100–10 000-fold decrease in RLUs, pointing out the absence of expressed luciferase. This is further confirmed in comparison with the RLUs detected in negative control and kanamycin respectively. Furthermore, **QC₁₄-Ally** and **QC₁₆-Ally** exhibited greater inhibitory effects in regard to methylated QACs, which is consistent with previously observed trend in biological activity of selected candidate compounds. The evaluation of their ability to inhibit protein synthesis pathways indicates a potential new antibacterial mechanism for selected QACs, simultaneously highlighting a promising direction for future research into the mode of action of this class of compounds.

2.4. Membrane interaction analysis

2.4.1. Molecular dynamics (MD) simulations and membrane integration. In order to further inspect membranolytic potency we conducted a set of molecular dynamics (MD) simulations of commercial representative cetylpyridinium chloride, CPC, and our candidate compound **QC₁₆-Ally** interacting with realistic *Staphylococcus aureus* membrane. Specifically, we analyzed penetration of CPC and **QC₁₆-Ally** within the model *S. aureus* membrane over time. To assess this, we monitored the average distance of each compound's head and tail groups from the membrane center (Fig. 4A). This distance was measured in the z-direction, perpendicular to the plane of the membrane. For both CPC and **QC₁₆-Ally**, the head group is defined as the protonated nitrogen atom, while the tail group corresponds to the terminal carbon atom of their 16-C aliphatic chain.

Fig. 4A reveals that both compounds incorporate into the membrane rather swiftly, likely due to their long hydrophobic

tails. CPC integrates into the membrane fully by approximately 40 ns (and partially as early as 20 ns, data not shown), whereas **QC₁₆-Ally** requires about 60 ns to achieve full integration, suggesting that CPC may penetrate the membrane more readily than **QC₁₆-Ally**. Additionally, we compared the average positions of the head and tail groups of each compound, focusing on the behavior after 60 ns – when both compounds are fully incorporated (highlighted in Fig. 4A) to the right of the green dashed line. While the distance of the tail groups of CPC and **QC₁₆-Ally** from the membrane center is rather similar, a notable difference can be observed in the positioning of their head groups. Specifically, the head group of CPC is located 16.0 Å from the membrane center, whereas this distance for **QC₁₆-Ally** is 17.8 Å. This indicates that the head group of CPC penetrates deeply into the membrane compared to **QC₁₆-Ally** which seems to protrude more prominently toward the membrane: water interface. This might be explained by the favorable interactions of the polar amide group with the water molecules at the membrane surface.

Next, we examined the conformational behavior of CPC and **QC₁₆-Ally** within the model membrane. **QC₁₆-Ally** occupies a significantly broader conformational phase space than CPC, adopting both “hook” or “L-shaped” and elongated conformations (Fig. 4B). In contrast, CPC shows a much more restricted phase space, predominantly existing in the elongated form (Fig. 4B). To quantify these observations, we monitored the distance (d_{AC}) between the terminal carbon atom and the C-2 atom of the aliphatic chain over the last 40 ns (see Fig. S1†). In **QC₁₆-Ally**, 40% of the conformations had a d_{AC} of less than 14.5 Å whereas $d_{AC} < 14.5$ Å is regarded as approximate cut-off distance indicating the “L-shaped” form. On the contrary, only about 13% of CPC conformations met this criterion with

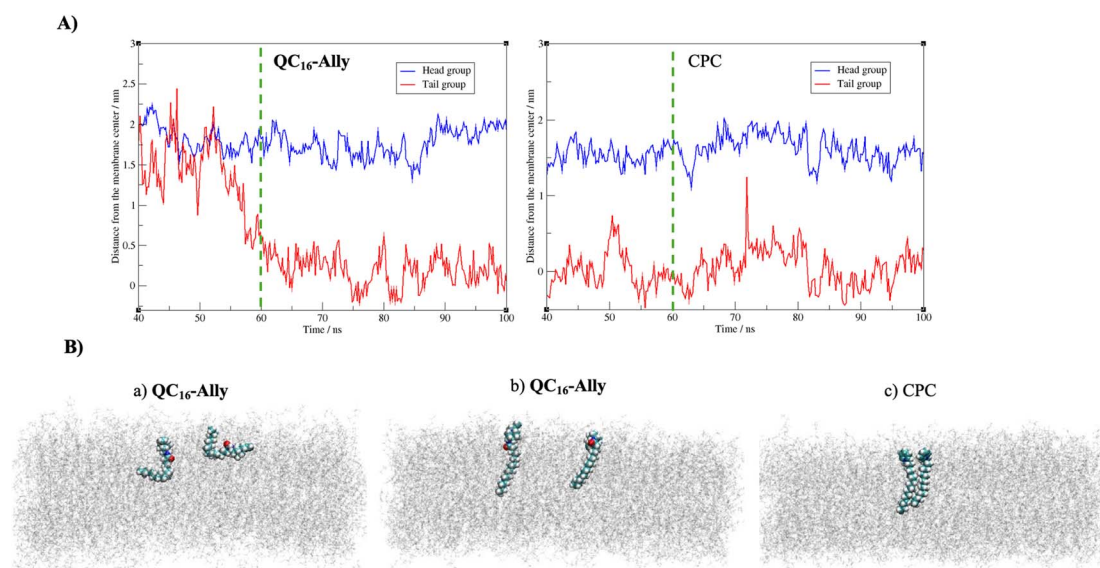


Fig. 4 (A) Average distance in the z-direction (averaged over two molecules present in each of the two systems), i.e., in the direction perpendicular to membrane, between the head group, denoted via the protonated nitrogen atom, and the center of the membrane, as well as between the tail group (terminal carbon atom in the aliphatic chain) and the center of the membrane, for cetylpyridinium chloride, CPC (right) and **QC₁₆-Ally** (left). (B) Conformations of **QC₁₆-Ally** (a and b) and cetylpyridinium chloride, CPC (c) upon incorporation into the model *Staphylococcus aureus* membrane.

majority of conformers displaying $d_{AC} \geq 14.5 \text{ \AA}$ indicating elongated conformations. These results clearly show that both CPC and QC₁₆-Ally exist in two conformations namely elongated and “L-shaped”, with significantly higher percentage of “L-shaped” conformers in QC₁₆-Ally (40%) compared to CPC (13%).

2.4.2. Molecular dynamics (MD) simulations of aggregation in water environment. Given the amphiphilic nature of quaternary ammonium compounds (QACs), we aimed to examine how selected compounds aggregate in water. For each system (cetylpyridinium chloride, CPC/water and QC₁₆-Ally/water), three simulations with different initial conditions were monitored (see Molecular dynamics simulation methodology and Fig. 10). Each simulation box contained approximately 35 000 water molecules and chloride counterions, with the molecules randomly placed

using Packmol³⁶ (Fig. 10, bottom panel). To monitor the potential aggregation, several aggregation-related metrics were calculated, namely the number of clusters and the average cluster size as the functions of time, and a histogram of cluster sizes. These indicators allow us to observe both how the systems approach equilibrium and the typical size of aggregates formed.³⁷ Molecules were considered part of the same cluster if the minimum distance between them was less than 3.5 Å. The average cluster size, \bar{N}_c , was calculated as

$$\bar{N}_c = \frac{\sum_k k \cdot N_k}{\sum_k N_k},$$

where N_k is the number of clusters containing k molecules. The average cluster size is calculated from $k = 2$, *i.e.*, the monomers

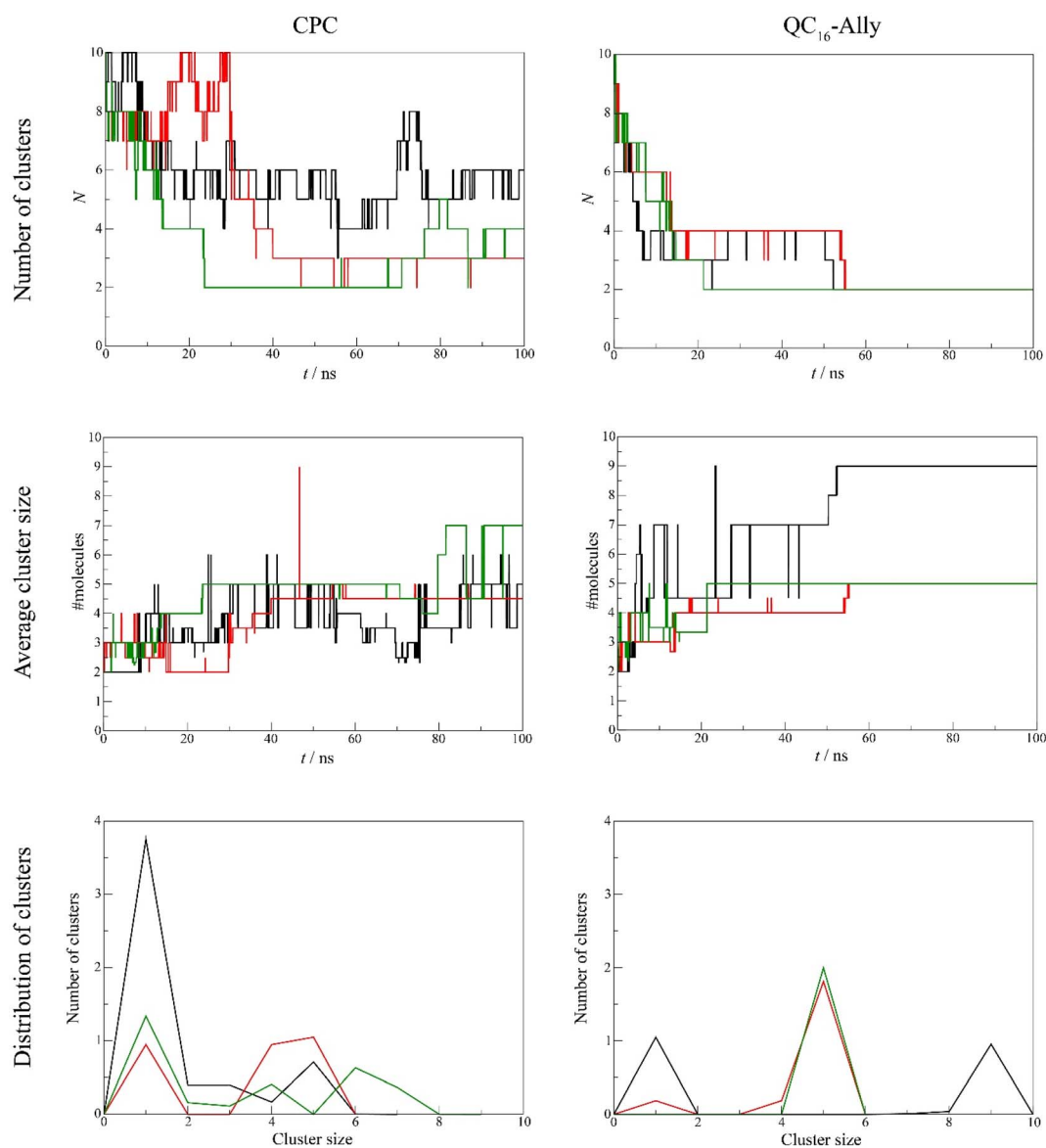


Fig. 5 Number of clusters (top panel), average cluster size (middle panel) and distribution of clusters (bottom panel) for cetylpyridinium chloride, CPC (left column) and QC₁₆-Ally (right column). Black, red and green lines denote results of the three distinct simulations that were propagated per each system.

are purposely not accounted for.³⁷ On the other hand, the histogram of cluster sizes was obtained by averaging the number of clusters of k molecules over the last 50 ns of respective simulation.

Our analysis revealed clear differences in aggregation tendencies between commercial standard CPC, and **QC₁₆-Ally**, with our candidate compound exhibiting greater tendency to form clusters. The number of **QC₁₆-Ally** clusters dropped to ≤ 4 within 20 ns and stabilized at 2 clusters by 50 ns across all three simulations. In contrast, CPC does not reach such convergence, with cluster numbers ranging from 3 to 6 throughout the simulations. Similarly, **QC₁₆-Ally** forms larger and more stable clusters reaching up to 9 molecules, in contrast to CPC with approximately 7 molecules in aggregate (Fig. 5).

Regarding cluster morphology, **QC₁₆-Ally** exhibited more spherical and thus more stable clusters, whereas CPC predominantly formed elongated, less defined clusters (Fig. 6).

2.4.3. Parallel artificial membrane permeability assay (PAMPA). Membrane permeability was further investigated using an *in vitro* model of passive transcellular permeation. The model membrane was constructed from lecithin, which contains both saturated and unsaturated fatty acids,

phosphoric acid, and choline, thereby mimicking mammalian cell membranes.³⁸ The parallel artificial membrane permeability assay, PAMPA, due to its methodological design, is commonly employed to assess the ability of potential drug compounds to passively diffuse across mammalian membranes.³⁹ Given that quaternary ammonium compounds (QACs) are frequently used in topical antiseptics aimed at skin disinfection, it is crucial to evaluate their effects on phospholipid-based membranes to predict potential toxicity. Fig. 7 illustrates the percentage concentrations of the examined QACs in the donor and acceptor wells of the multiplate, as well as the percentage of each compound integrated into the artificial membrane. We observed that the commercial standards, cetylpyridinium chloride, CPC and dimethyldodecylbenzylammonium bromide, BAB, almost completely integrate into the membrane layer ($\approx 97\%$). In contrast, our methylated candidate compounds, **QC₁₄-Me** and **QC₁₆-Me**, exhibited a high percentage in the donor wells but showed low rates of passive diffusion across the artificial membrane, likely due to their reduced solubility attributed to the iodine counterion. Conversely, candidates with an allyl group on the quaternary nitrogen center, **QC₁₄-Ally** and **QC₁₆-Ally**, demonstrated

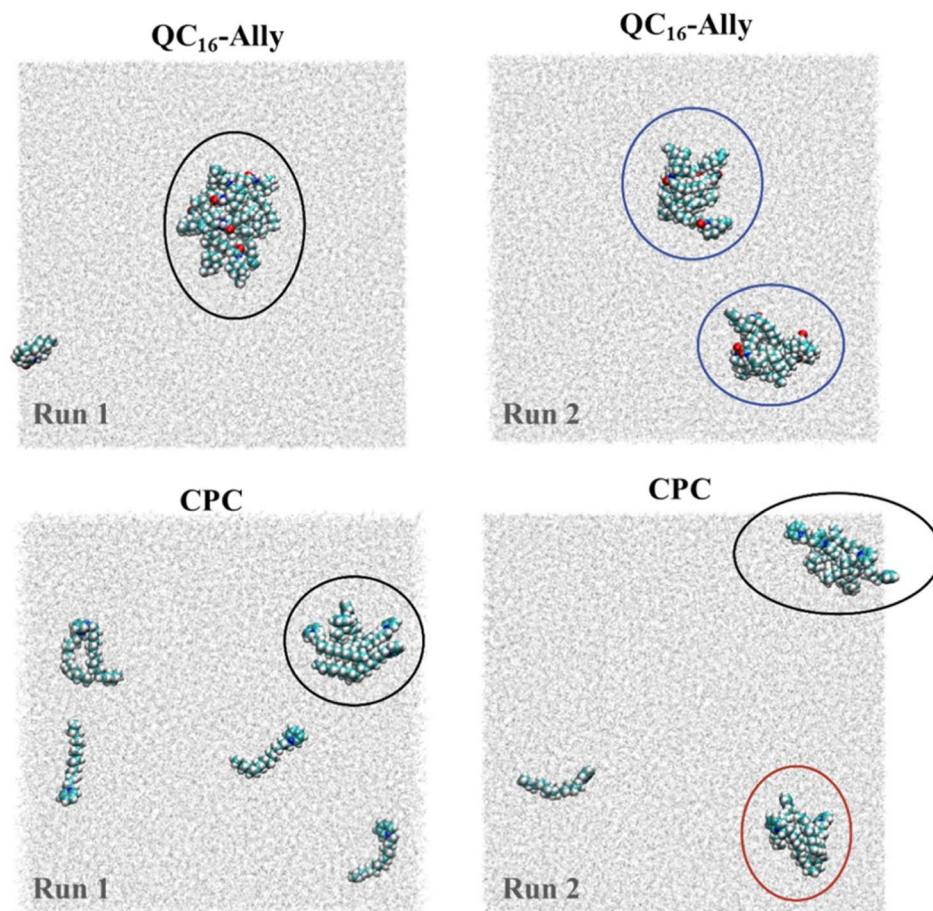


Fig. 6 Clusters/aggregates formed at $t = 100$ ns, for **QC₁₆-Ally**/water (top panel) and cetylpyridinium chloride/water, CPC/water (bottom panel) systems. Results of the two propagations shown (left and right columns), with the third simulation of each system omitted. Observed clusters/aggregates are denoted with ellipses (black – dominant cluster/aggregate, blue – two equally sized clusters/aggregates, red – smaller cluster/aggregate).

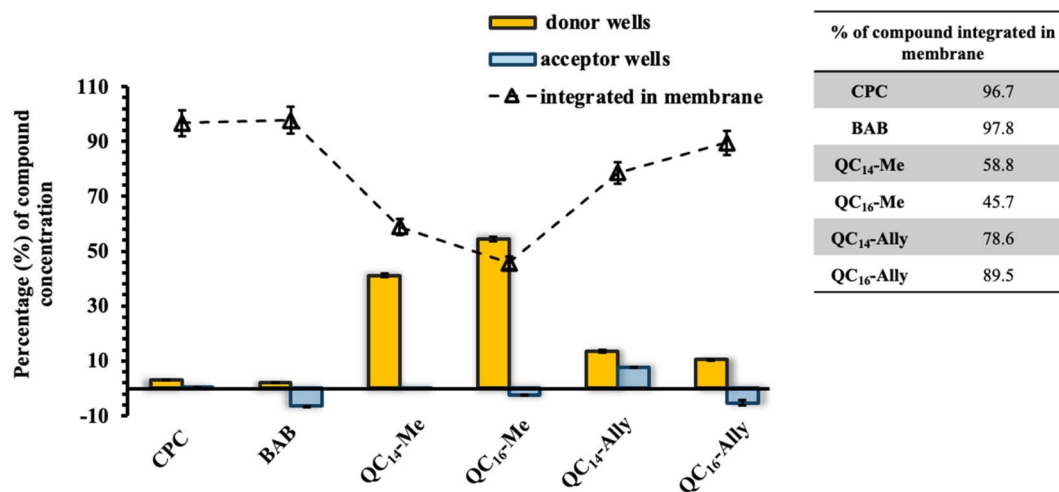


Fig. 7 The percentage of corresponding compound concentration in donor and acceptor wells after 24 h incubation at 37 °C. The percentage of compound integrated in membrane was calculated subtracting the final concentration in donor and accept wells from the initial concentration expressed as percentage.

a greater potential for membrane integration compared to the methylated QACs, though they still integrated less effectively than the commercial standards. These findings suggest that our compounds may have lower toxicity toward mammalian cells, which was further examined through *in vitro* and *in vivo* toxicity tests.

2.5. *In vitro* and *in vivo* toxicity

2.5.1. *In vitro* toxicity. Owing to their antimicrobial potency, quaternary ammonium compounds (QACs) are widely

utilized as the active ingredients in household cleaning and hygiene products. Although generally considered safe, recent studies have raised concerns regarding their potential hazardous effects, especially since traces of QACs have been detected in breast milk and blood samples.^{40–42} Prolonged exposure to high concentrations of QACs may pose risks, including dermal irritation, respiratory side effects, and potential development of allergic conditions.⁴⁰

Given the potential applications of our synthesized soft QAC derivatives, we aimed to further evaluate their toxicity on two

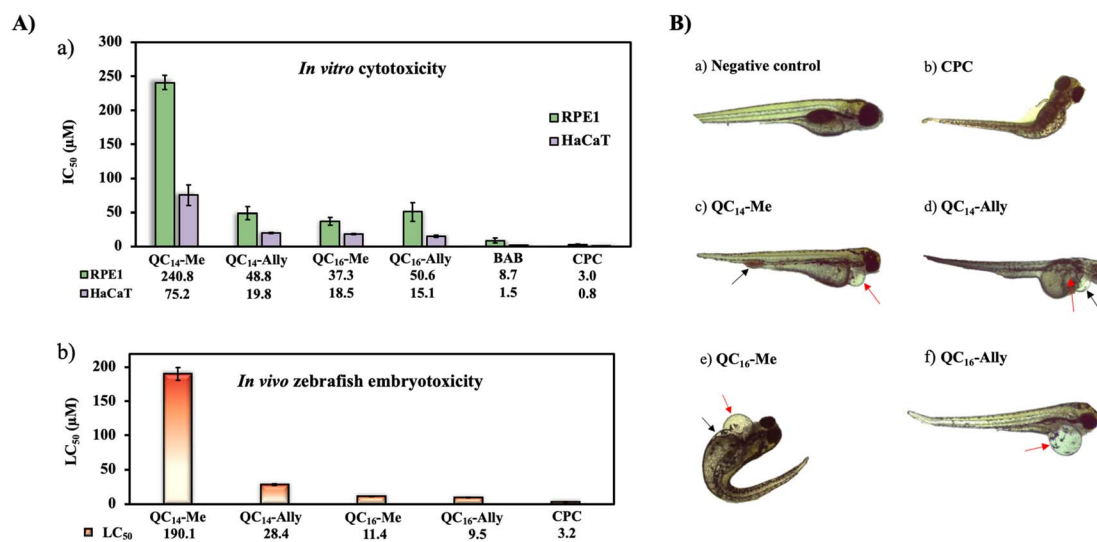


Fig. 8 (A) (a) Cytotoxicity of candidate compounds QC₁₄-Me, QC₁₄-Ally, QC₁₆-Me and QC₁₆-Ally towards healthy human cell lines retinal pigment epithelial (RPE1) and keratinocytes (HaCaT). Obtained values of half maximal inhibitory concentration, IC₅₀, (μM) were compared to the commercially available standards dimethyldodecylbenzylammonium bromide (BAB) and cetylpyridinium chloride (CPC) respectively. (b) Graphical representation of lethal concentration of 50% (LC₅₀) *Danio rerio* embryos with table containing corresponding LC₅₀ values. Determined LC₅₀ values are within 95% confidence interval (Fig. S2†). (B) Representation of morphological abnormalities upon treatment with concentration higher than LC₅₀ for each tested compound: (a) negative control – a normally developed individual without morphological abnormalities, (b) CPC – scoliosis, (c) QC₁₄-Me – pericardial edema (red arrow), blood accumulation in the tail area (black arrow); (d) QC₁₄-Ally – pericardial edema (black arrow), yolk sac edema (red arrow); (e) QC₁₆-Me – pericardial edema (red arrow), yolk sac edema (black arrow), scoliosis; (f) QC₁₆-Ally – pericardial edema (red arrow), scoliosis.

healthy human cell lines, retinal pigment epithelial (RPE1) and keratinocytes (HaCaT). The *in vitro* half maximal inhibitory concentration, IC_{50} , values obtained were compared to the toxicity profiles of commercially available QACs, cetylpyridinium chloride (CPC) and dimethyldodecylbenzylammonium bromide (BAB) respectively. As depicted in Fig. 8A, the commercial QACs, CPC and BAB, exhibit cytotoxic activity towards both RPE1 and HaCaT cell lines at low, single digit micromolar concentrations, corresponding to their MIC values. In contrast, the synthesized derivatives, **QC₁₄-Me**, **QC₁₄-Ally**, **QC₁₆-Me** and **QC₁₆-Ally**, demonstrated reduced toxicity compared to CPC and BAB, with **QC₁₄-Me** exhibiting the lowest cytotoxicity against both cell lines. Coupled with their low minimal inhibitory concentration (MIC) and the potential for degradation into non-toxic products, these findings suggest that our soft QACs could be considered as promising candidates for the development of new QACs that are safe for both human health and the environment.

2.5.2. *In vivo* zebrafish embryotoxicity test. In addition to *in vitro* cytotoxicity studies, we further aimed to assess the toxicity

of selected compounds towards zebrafish *Danio rerio*. Other than rational aspects such as its size, external fertilization and transparency, zebrafish contains 84% of genes known to be associated with human disease, which is the main reason of its use as a toxicity model organism.^{43–46} After exposure of zebrafish *Danio rerio* embryo samples to **QC₁₄-Me**, **QC₁₄-Ally**, **QC₁₆-Me**, **QC₁₆-Ally** and cetylpyridinium chloride (CPC) an increased embryotoxicity in a concentration-dependent manner was observed. The lethal concentration of 50% *Danio rerio* embryos, LC_{50} , values obtained are presented in the table in Fig. 8A and are consistent with the previously determined half maximal inhibitory concentration, IC_{50} , values in the *in vitro* cytotoxicity experiment, with the commercially available CPC exhibiting the highest toxicity. Morphological abnormalities Fig. 8B were observed in treatment with the selected compounds at concentrations above the obtained LC_{50} values.

2.5.3. Quantification of locomotor activity in larval zebrafish. Other than gene and morphological homology, zebrafish behavioral studies serve as foundation for modeling neurological disorders as those organisms exhibit complex behaviors

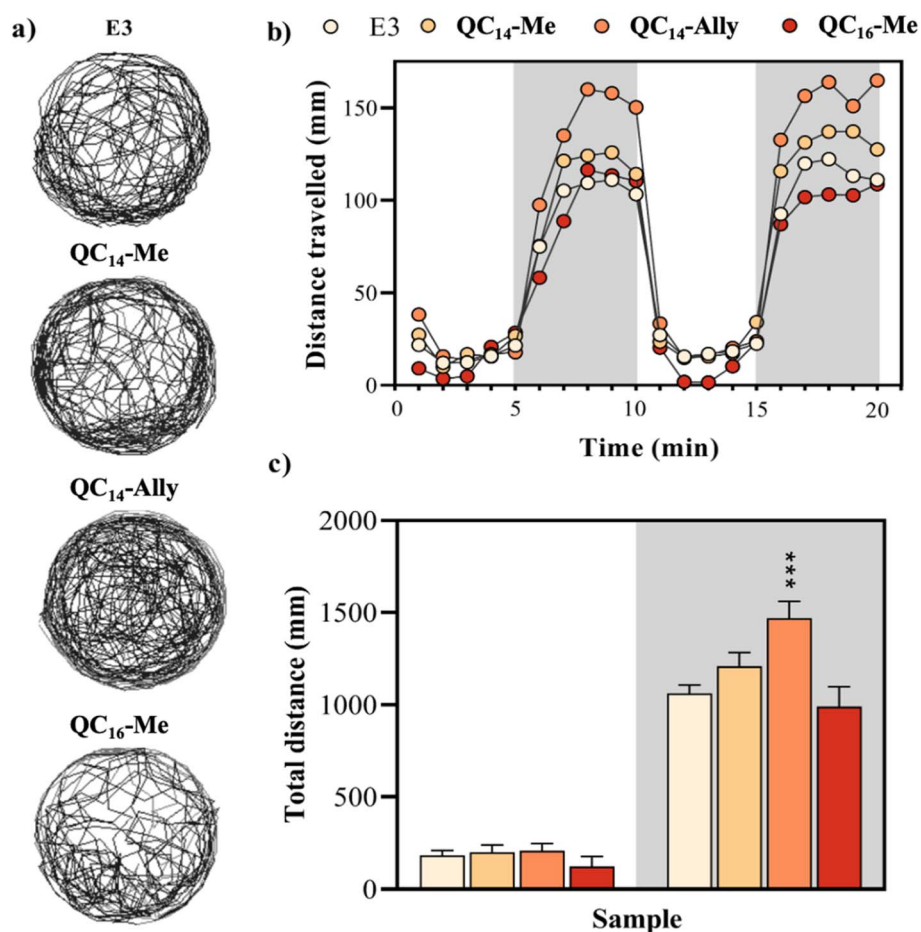


Fig. 9 Locomotor activity assessment of zebrafish larvae ($N = 48$) following 120 hours of exposure to **QC₁₄-Me** (20 μ M), **QC₁₄-Ally** (8 μ M), and **QC₁₆-Me** (8 μ M). Control larvae were treated with E3 medium. (a) Representative swimming trajectories of individual larvae recorded over a 20 minutes observation period. (b) Mean distance traveled by each experimental group, presented in 1 minute time bins. The horizontal bars represent the lighting conditions during the experiment, with white boxes indicating light, and gray boxes indicating dark phases. (c) Total distance traveled within light and dark conditions. Data are represented as mean \pm SE. Asterisks denote statistically significant differences compared to the control group (***) ($p < 0.001$).

close to mammals.^{46–48} Three compounds, **QC₁₄-Me**, **QC₁₄-Ally**, and **QC₁₆-Me**, were selected for further analysis based on the concordance between their lethal concentration 50% (LC_{50}) values obtained from *in vivo* assay (see Section 2.5.2), half maximal inhibitory concentration (IC_{50}) values determined using *in vitro* assay (see Section 2.5.1), and previously determined minimal inhibitory concentration (MIC). Concentrations chosen for locomotor assessment corresponded to their respective MIC values. To investigate whether tested samples are associated with a locomotor deficit, swimming behavior was monitored at 120 h of exposure to tested samples. **QC₁₄-Ally** exhibited a significant increase of locomotor activity during dark phases (38% increase compared to the control group on E3). This effect was not observed during light periods. No significant changes in locomotor activity were detected following exposure to **QC₁₄-Me** and **QC₁₆-Me** (Fig. 9).

3 Conclusions

This study provides new insights into the bacteriostatic properties and dual mechanisms of action of soft quaternary ammonium compounds (QACs) designed with a labile amide bond in the quinuclidine scaffold. In contrast to traditional QACs, which rapidly kill bacteria by disrupting membranes, our findings indicate that these soft QACs primarily inhibit bacterial growth through a combination of membrane interaction and protein synthesis interference. This dual mode of action positions them as promising alternatives for addressing challenges associated with bacterial resistance.

Key experiments, including time-kill assays and membrane integrity analyses, demonstrated that our soft QACs primarily maintain bacterial populations in a stationary phase without immediate cell death. Molecular dynamics (MD) simulations further revealed their unique “hook-like” conformations that restrict deep membrane penetration and facilitate aggregate formation, reducing their effective concentration at the membrane surface. This reduced permeability aligns with their lower cytotoxicity, as validated by zebrafish embryotoxicity assays and human cell line studies, highlighting their safety advantages over conventional QACs. Furthermore, evidence of protein synthesis inhibition underscores their ability to target intracellular bacterial processes, providing a secondary antibacterial mechanism.

These findings emphasize the potential of soft QACs as safer, environmentally friendly alternatives for antimicrobial applications. While the current study establishes their antibacterial properties and safety profile, further investigations could focus on optimizing their chemical scaffolds to enhance antibacterial potency while retaining biodegradability and low toxicity. Expanding efficacy testing against a broader range of bacterial strains, including antibiotic-resistant pathogens, would strengthen their relevance as next-generation antimicrobials. Additionally, exploring their potential for synergistic combinations with existing antimicrobials could help improve overall treatment efficacy while mitigating resistance development.

Beyond their antimicrobial properties, future research should address the environmental degradation pathways of soft

QACs to confirm their eco-friendly nature under real-world conditions. Moreover, efforts to incorporate these compounds into practical formulations, such as surface disinfectants, medical device coatings, and personal care products, will be essential to bridge the gap between laboratory findings and industrial applications.

The reduced toxicity, biodegradability, and dual antibacterial activity demonstrated by these soft QACs underscore their promise as innovative, sustainable solutions to the challenges posed by bacterial resistance and environmental concerns. These insights provide a strong foundation for further development and highlight the potential for soft QACs to play a pivotal role in advancing safer, more effective antimicrobials across healthcare, agriculture, and industry.

4 Materials and methods

4.1. Viability of bacterial cells in treatment over time (time-kill assay)

The time kill assay was performed with a representative Gram-positive bacterium, *Staphylococcus aureus* ATCC25923. The overnight culture was diluted in fresh temperature-controlled Mueller–Hinton broth (MHB) and propagated in a shaking incubator at the temperature of 37 °C with the constant rotation at 220 rpm. The pre-exponentially grown culture was diluted to a final concentration of 5×10^5 CFU mL⁻¹ and an aliquot of 50 μL of the prepared cell culture suspension was added to the 96-well microtiter plate containing 50 μL of the compounds to be tested at final concentrations corresponding to the minimum inhibitory concentration (MIC) and 2 × MIC. The untreated *S. aureus* ATCC25923 cells served as growth control. At the start of the experiment, after the addition of the cell culture suspension, a 10 μL aliquot was pipetted from each well, diluted in 990 μL MHB and further serially diluted up to 10⁶-fold. A 20 μL aliquot of each cell suspension dilution was plated on MHB agar using a sterile loop. The 96-well plate containing the treated cells was incubated at 37 °C and the previously described dilution and plating of the treated culture was repeated at the desired time intervals (2, 4, 6, 8, 12 and 24 hours). The Petri dishes were incubated for 24 hours. The bacterial colonies formed were then counted and the number of viable cells after treatment was calculated at each time interval. The results were plotted graphically as log₁₀ of colony forming units per milliliter (CFU mL⁻¹) versus time.

4.2. Flow cytometry measurement of the cells in treatment

The cell viability of the representative Gram-positive bacterium *Staphylococcus aureus* ATCC25923 during treatment with candidate compounds was further tested by flow cytometry (NovoCyte Advanteon). Two overnight cultures were diluted 10 times and incubated in a shaking incubator at 220 rpm and the temperature of 37 °C. Pre-exponentially grown cells were centrifuged at 4500 g for 10 minutes at room temperature. After discarding the supernatant of the culture medium, one cell pellet was resuspended in an equal volume of the staining buffer (phosphate buffer, pH = 7.4, 1 mM EDTA, 0.1% Tween-

20) and the other in an equal volume of the absolute ethanol. The cell pellet to which absolute ethanol has been added was incubated for 30 minutes and then centrifuged again under the same conditions. After centrifugation, the supernatant of absolute ethanol was discarded, and the cell pellet was resuspended in the staining buffer. Both prepared cultures were diluted in the desired volume of staining buffer to the final cell concentration of 1×10^6 colony forming units per milliliter (CFU mL^{-1}) and served as fluorescently labeled compensation specimens along with the same concentration of unstained cells. BD Biosciences (BD™ Cell Viability) kit containing two fluorescent dyes (thiazole orange, TO and propidium iodide, PI) was used for cell labelling and detection according to the manufacturer's instructions. 50 μL cell suspension in staining buffer was added to the wells of 96-well plate containing tested compounds in staining buffer in MIC and $2 \times$ MIC final concentrations and incubated at 37 °C. At the desired time intervals, the treated cells were stained with a mixture of TO and PI dyes followed by flow cytometric detection of cell viability.

4.3. Atomic force microscopy (AFM)

29.5 μL of the Cell-Tak solution in 0.1 M NaHCO_3 , pH = 8.00 was pipetted into the center of a sterile Petri dish and incubated in the laminar flow hood for 30 minutes. Petri dishes were further washed with at least ten portions of mQ water. After thorough rinsing, the Petri dishes were air dried in a sterile laminar flow hood for about 40 minutes, or longer if necessary. The overnight culture of *Listeria monocytogenes* ATCC7644 was diluted 10-fold and propagated in culture medium in a shaking incubator at 35 °C and 180 rpm. After thirty minutes, an aliquot of the culture was added to the previously coated surface of the Petri dish and incubated at 35 °C for 30 minutes. After incubation, the Petri dish was thoroughly rinsed with fresh culture medium and then with the sterile phosphate buffer (PBS). The cells were fixed with a 2.5% solution of glutaraldehyde (GT) in PBS for a total of four hours at 4 °C. After fixation and rinsing in sterile PBS, the untreated cells were measured using the atomic force microscope (AFM). To image bacterial cells treated with candidate compounds using the AFM, a solution of the corresponding compound was added to the cells in the culture medium before the fixation, so that the final concentration of the compound in the treatment is $2 \times$ MIC. After the treated cells have been exposed to the treatment for three hours, they were fixed in GT in the same manner as described above. The AFM measurements of treated and untreated *L. monocytogenes* ATCC7644 cells were performed using a Nano-wizard IV system (JPK/Bruker, Berlin, Germany) in quantitative imaging mode with a ScanAsyst Fluid probe (Bruker, Billerica, MA, USA). During the measurements, the set point was maintained at 0.7 nN, the length along the Z-axis was 1200 nm, and the images were acquired at a resolution of 256×256 pixels. The collected data was analyzed using the JPK software for data processing.

4.4. Optical fluorescence microscopy

A Petri dish (FluoroDish) with adhesive (Cell-Tak in 0.1 M NaHCO_3 , pH = 8.00) was prepared in the same way as for the AFM

measurements. The overnight culture of *Listeria monocytogenes* ATCC7644 was diluted 10-fold in tempered nutrient culture medium and propagated in an incubator shaker at 35 °C and 170 rpm. After incubation, 30 μL of the bacterial cell suspension was pipetted onto the surface of the coated Petri dish and incubated for 10 minutes at appropriate temperature to ensure the highest possible number of immobilized bacterial cells. The contents of the Petri dish was washed with tempered culture medium and the immobilized cells were further incubated at 35 °C on the stand of an optical microscope. At the beginning and after incubation, optical images of the immobilized cells were taken to confirm their initial viability. At the end of the incubation, the contents of the Petri dish were washed again, and the culture medium was replaced with a solution of the selected compounds in culture medium at a final concentration of $2 \times$ MIC. The cells were exposed to the treatment for a total of three hours. At the end of the treatment, the Petri dish was washed with sterile physiological solution. The immobilized treated cells were stained with a mixture of fluorescent SYTO9 and propidium iodide (PI) dyes (1.5 μL dye per mL), which are components of the LIVE/DEAD BacLight Bacterial Viability Kit L7012. The images of the fluorescently labelled treated bacterial cells were taken after 30 minutes of incubation in the dark.

4.5. Propidium iodide (PI) uptake assay

An overnight culture of *Staphylococcus aureus* ATCC25923 was diluted 20-fold in tempered Mueller-Hinton broth (MHB) and propagated for one hour in a shaking incubator at 37 °C and 220 rpm. The compounds were diluted in sterile filtered phosphate buffer (PBS), pH = 7.4, to a final concentration of $8 \times$ MIC. The prepared solutions were serially diluted to concentrations of $4 \times$ MIC, $2 \times$ MIC and MIC. The optical density of the bacterial suspension was measured at 600 nm and the cell pellet was precipitated by centrifugation at 4500g for ten minutes. The supernatant was discarded, and the cell pellet was resuspended in sterile filtered PBS buffer. The resuspended bacterial cells were further diluted in PBS buffer to a final concentration of 1×10^6 colony forming units per milliliter (CFU mL^{-1}). An aliquot of 500 μL of the diluted suspension of bacterial cells was added to microtubes containing previously prepared solutions of the tested compounds in PBS buffer. 1 μL of propidium iodide solution (3 mg mL^{-1}) was added to each microtube so that the final concentration of fluorescent dye was 5 μM . Fluorescence intensity (ex: 536 nm; em: 617 nm) was measured over six hours of treatment at 37 °C using Tecan Infinite 200 Pro plate reader.

4.6. *In vitro* inhibition of protein synthesis

The potential of tested candidate compounds to inhibit protein synthesis was evaluated using a commercially available S30 T7 High Yield Protein Expression System kit (Promega) based on *Escherichia coli* cell lysate containing T7 polymerase for transcription of the gene of interest. In addition to the T7 extract, the expression was additionally ensured by the S30 mixture containing amino acids, ribonucleoside triphosphates (rNTPs), transfer RNA (tRNA), ATP-regenerating enzymes and isopropyl- β -D-1-thiogalactopyranoside (IPTG). The expression vector was pFN6A

plasmid DNA which contains the *hRluc* reporter gene downstream of the T7 promoter site. After preparation of mastermix, reaction tubes were incubated in a thermomixer for one hour at a temperature of 37 °C with rotation of 1200 rpm. The commercially available Renilla Luciferase Assay System kit (Promega) was used to evaluate the results after incubation. An aliquot of each mastermix reaction was diluted 40 times in Renilla Luciferase Lysis Assay buffer. A total of 50 μ L of the samples prepared in this way was added to the wells of the white microtiter plate. Renilla Luciferase Assay substrate was diluted 5-fold in Renilla Luciferase Assay Buffer and 50 μ L was added to each well of 96-well plate. After the addition of the substrate solution, the relative luminescence intensity units, RLUs, were measured using Tecan Infinite 200 Pro plate reader with a signal integration time of ten seconds.

4.7. Molecular dynamics (MD) simulation studies

4.7.1. Interactions with realistic *Staphylococcus aureus* model membrane. Force field converter module available at

CHARMM-GUI (<http://www.charmm-gui.org/>)^{49–51} was used to convert the force field and starting geometry of a realistic *Staphylococcus aureus* model membrane (SA-membrane)⁵² to the ones appropriate for simulating *via* GROMACS,⁵³ with the force field utilized for the membrane constituents (Tables S1 and S2†) being CHARMM36m.⁵⁴ The overall simulation box contained approximately 35 000 water molecules (TIP3P water model), 360 sodium ions and 52 chloride ions. CHARMM-GUI membrane builder minimization and equilibration procedure was used to obtain equilibrated simulation box of the *S. aureus* model membrane at $T = 30$ °C. Upon initial equilibration, the membrane was simulated for 100 ns using unbiased all-atom molecular dynamics (MD). The snapshot corresponding to $t = 100$ ns was extracted and then employed in preparation of the cetylpyridinium chloride (CPC) + *S. aureus* (CPC/SA-membrane) and QC₁₆-Ally + *S. aureus* (QC₁₆-Ally/SA-membrane) membrane systems. Both CPC and QC₁₆-Ally were parameterized consistently with the lipid forcefield, namely using CHARMM36m force field.

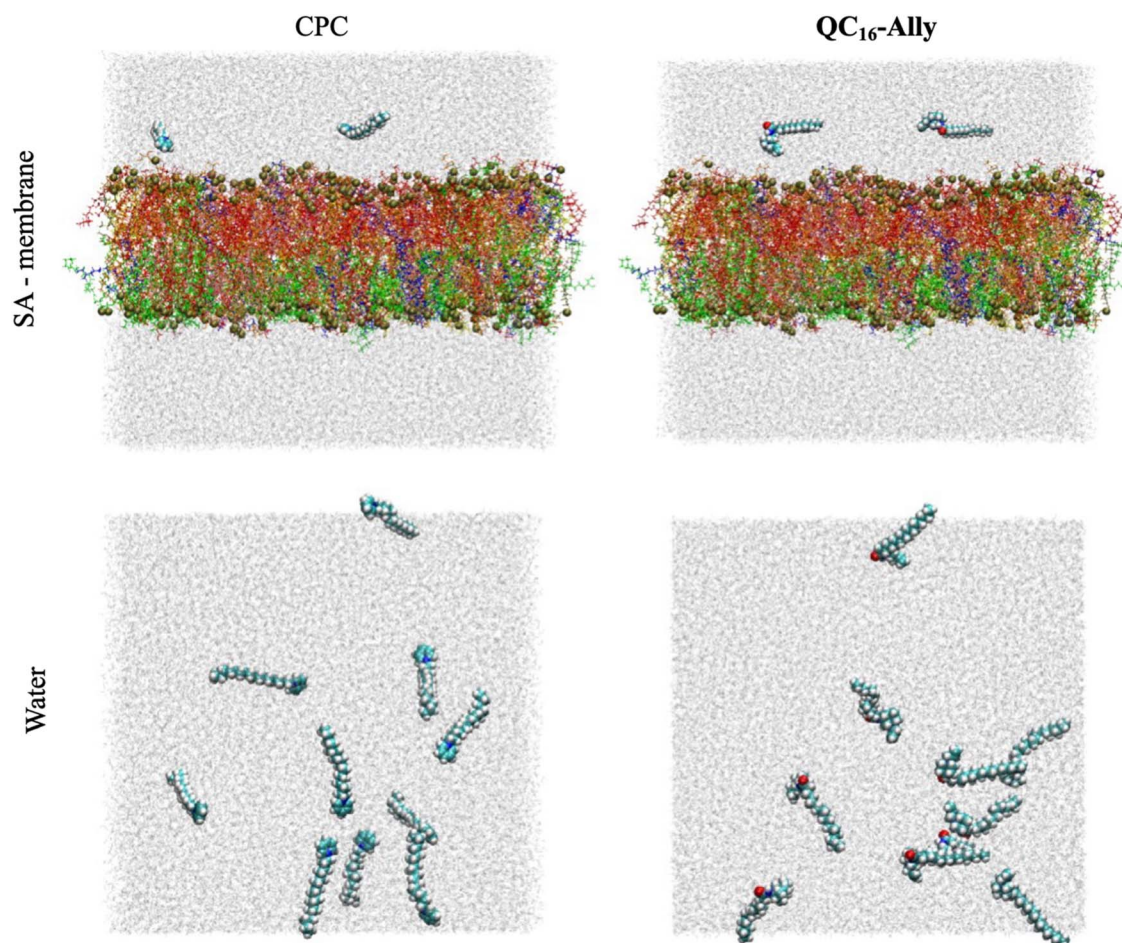


Fig. 10 Starting configurations of cetylpyridinium chloride (CPC)/SA-membrane (left) and QC₁₆-Ally/SA-membrane (right) systems are shown in the top panel, with the initial configurations of the CPC/water (left) and QC₁₆-Ally/water (right) systems shown in the bottom panel. Water molecules are shown in light gray, CPC and QC₁₆-Ally using van der Waals sphere representation, with the different lipids constituting the model *Staphylococcus aureus* membrane shown using licorice representation, and in different colors. More precisely, FPPG and IFPG are shown in blue, PFPG, JFPG, ZFPG, JIPG and ZIPG are shown in red, SFPG, VFPG, TFPG and TIPG are colored orange, XFPG is colored yellow, OIPG and OFPG are shown in tan, JFPG, ZFPG, SFGK and TFGK are colored green, and ZFCL is colored pink (consult Tables S1 and S2† for further clarification of the lipid codenames). Phosphorous atoms belonging to the lipid headgroups are shown in van der Waals sphere representation and colored yellow.

To prepare the initial simulation boxes containing both the lipid bilayer and the chosen molecules, exactly two molecules of each compound were placed in the previously equilibrated simulation box of the model membrane. Tested compounds were placed inside the water layer, above the outer leaflet of the *Staphylococcus aureus* model membrane. Upon the initial placement, the simulation boxes were firstly minimized and equilibrated for 5 ns in the NPT ensemble, using Nosé–Hoover thermostat⁵⁵ with Berendsen barostat⁵⁶ ($p = 1$ bar, semiisotropic pressure coupling). The duration of each production run was 100 ns.

4.7.2. Behavior of compounds in water environment. Additionally, three sets of molecular dynamics simulations of CPC and QC₁₆-Ally molecules in water environment with no membrane present were propagated. The simulated system consisted of approximately 35 000 water molecules and cetylpyridinium chloride, CPC and QC₁₆-Ally in final concentration of approximately 15 mM (10 molecules per simulation box). All the MD simulations were performed using GROMACS 2021.5 simulation package,⁵³ with a time step of 2 fs, short-range Coulomb and van der Waals cut-offs set at 10 Å, three-dimensional periodic boundary conditions, and incorporating the PME procedure.⁵⁷ All MD simulations were propagated using Nosé–Hoover thermostat⁵⁵ with the pressure being monitored *via* Parrinello–Rahman barostat⁵⁸ ($p = 1$ bar, isotropic pressure coupling) in the duration of $t = 100$ ns. The starting snapshots of the propagated systems containing CPC and QC₁₆-Ally, respectively, are shown in Fig. 10.

4.8. Parallel artificial membrane permeability assay (PAMPA assay)

The simulated membrane was prepared by dissolving lecithin in dodecane while heating in an ultrasonic bath to a final mass fraction of 1%. An aliquot of 5 μ L of the prepared solution was pipetted onto the surface of the donor wells (Multiscreen-IP Filter Plate, 0.45 μ m, Clear, Hydrophobic PVDF membrane, Millipore). Before the lecithin solution was dried out, 150 μ L of the tested compound solution was added to the donor wells. A “sandwich” composed of donor/acceptor wells was assembled so that the simulated membrane is constantly immersed in the solvent in the acceptor wells during incubation. The plate was incubated at 37 °C for 24 hours. After incubation, the absorption spectrum of donor and acceptor wells was recorded in the wavelength range from 190 to 400 nm. The concentration of the tested compound in each well, both donor and acceptor, was calculated from the maximum absorbance. The integrity of the simulated membrane was tested using two different dyes, brilliant cresyl blue and lucifer yellow.

4.9. *In vitro* cytotoxicity

The cytotoxicity of selected compounds was tested on two healthy human cell lines – human retinal pigment epithelial (RPE-1) and human keratinocytes (HaCaT) cells. The results were compared with the results of the commercially available quaternary ammonium salts, cetylpyridinium chloride (CPC) and benzidodecyltrimethylammonium bromide (BAB). Human cells were grown in Dulbecco's Modified Eagle medium

(DMEM) at 37 °C in a humidified atmosphere with 5% CO₂. The tested compounds were dissolved in DMEM medium and serially diluted in a microtiter plate in the concentration range from 250 to 0.25 μ M. 5000 human cells were pipetted into each well of the plate and the prepared plate was incubated for 48 hours. At the end of the incubation, 20 μ L of the CellTiter 96[®] Aqueous MTS reagent (Promega) was added to the wells of the microtiter plate according to the manufacturer's instructions. After three hours of incubation with the reagent, the absorbance was measured at a wavelength of 490 nm. The half maximal inhibitory concentration, IC₅₀, value for each compound was calculated by plotting the percentage of viable cells *versus* concentration of compound using the GraFit 6.0 software.

4.10. *In vivo* zebrafish embryotoxicity test

Zebrafish *Danio rerio* (WIK type) were obtained from the European Zebrafish Resource Center of the Karlsruhe Institute of Technology. Zebrafish maintenance and embryo production are described in detail in our previous study.⁵⁹ A zebrafish embryotoxicity test (ZET) was performed in accordance with OECD 236.⁶⁰ In dose range-finding experiments, embryos ($N = 10$) were exposed to a wide range of concentrations in serial dilutions: QC₁₄-Me (500–31 μ M), QC₁₄-Ally (500–15.6 μ M), QC₁₆-Me (500–3.9 μ M), QC₁₆-Ally (500–1.56 μ M), and cetylpyridinium chloride, CPC (0.5–0.0078 μ M). Once a relevant range of concentrations was identified, a refined concentration range was tested using 48 embryos per concentration. E3 medium was used as a negative control. Plates were kept at 27.5 \pm 0.5 °C (Innova 42 incubator, New Brunswick). Mortalities and abnormalities were recorded 120 hours post fertilization (hpf) using an inverted microscope (Olympus CKX41), equipped with a Leica EC3 digital camera and LAS EZ 3.2.0 digitizing software statistical program.

4.11. The zebrafish locomotor assessment

The swimming behavior of zebrafish larvae ($N = 48$) was assessed following 120 h of exposure to tested samples in a 96-well plate using the DanioVision system (Noldus Information Technology, Netherlands). Concentrations chosen for locomotor assessment were as follows: QC₁₄-Me (20 μ M), QC₁₄-Ally (8 μ M), and QC₁₆-Me (8 μ M). Zebrafish activity was recorded using the EthoVision XT software (Noldus Information Technology, Netherlands) over a 20 min period, including three periods of light and darkness (5 min in the darkness and 10 min in the light). To minimize the background noise, a smoothing profile with a minimum distance moved threshold of 0.2 cm was applied. The temperature during the measurement was maintained at 27.5 °C. After tracking, larvae were examined under inverted microscope to identify malformed or dead specimens, which were excluded from statistical analysis.

4.12. Statistical analysis

Statistical analysis and graphical representations were conducted using GraphPad Prism 6.01 software. Results are expressed as means \pm SD, with a significance threshold set at $p \leq 0.05$ for all data. Prior to determination of the median lethal

concentration (LC50), data were subjected to logarithmic transformation. One-way analysis of variance (ANOVA) and Tukey's post hoc test were employed to assess the significance of differences between treatments. In cases where the assumption of normality was violated, the Kruskal–Wallis one-way analysis of variance on ranks was utilized.

Ethical statement

Animal housing and spawning were performed in aquaria units approved by the Croatian Ministry of Agriculture and in compliance with Directive 2010/63/EU. All experiments in this study were conducted on the non-protected embryonal stages (up to 96 hpf), which do not require approval from the animal welfare commissions.^{6†}

Data availability

The data supporting this article have been included as part of the ESI.†

Author contributions

D. C. performed experiments providing results about bacteriostatic activity and cytotoxicity; L. K. and D. C. collected and analyzed AFM and fluorescence microscopy data; Z. B. and M. C. collected and analysed MD simulation data, S. B. B. and R. Č.-R. conducted *in vivo* studies, R. O. designed compounds, M. Š. directed the study, D. C. and M. Š. analyzed all data and wrote the manuscript. All authors contributed to and approved the final version of the manuscript.

Conflicts of interest

The authors declare no conflict of interest.

Acknowledgements

This research was supported by the the Croatian Science Foundation grant number UIP-2020-02-2356 (M. Š.) and institutional projects 641-01/23-02/0008 (M. Š.), 641-01/23-02/0010 (R. O.) funded by the Faculty of Science, University of Split.

References

- 1 W. A. Arnold, et al., Quaternary Ammonium Compounds: A Chemical Class of Emerging Concern, *Environ. Sci. Technol.*, 2023, 7645–7665, DOI: [10.1021/acs.est.2c08244](https://doi.org/10.1021/acs.est.2c08244).
- 2 F. Bureš, Quaternary Ammonium Compounds: Simple in Structure, Complex in Application, *Top. Curr. Chem.*, 2019, 14, DOI: [10.1007/s41061-019-0239-2](https://doi.org/10.1007/s41061-019-0239-2).
- 3 C. P. Gerba, Quaternary ammonium biocides: Efficacy in application, *Appl. Environ. Microbiol.*, 2015, 464–469, DOI: [10.1128/AEM.02633-14](https://doi.org/10.1128/AEM.02633-14).
- 4 G. Domagk, Eine neue Klasse von Desinfektionsmitteln, *Dtsch. Med. Wochenschr.*, 1935, 61, 829–832.
- 5 P. B. Price, BENZALKONIUM CHLORIDE (ZEPHIRAN CHLORIDE®) AS A SKIN DISINFECTANT, *Arch. Surg.*, 1950, 61(1), 23, DOI: [10.1001/archsurg.1950.01250020026004](https://doi.org/10.1001/archsurg.1950.01250020026004). [Online]. Available: <http://archsurg.jamanetwork.com/>.
- 6 B. M. P. Pereira and I. Tagkopoulos, Benzalkonium chlorides: Uses, regulatory status, and microbial resistance, *Appl. Environ. Microbiol.*, 2019, e00377, DOI: [10.1128/AEM.00377-19](https://doi.org/10.1128/AEM.00377-19).
- 7 S. Brown, J. P. Santa Maria and S. Walker, Wall teichoic acids of gram-positive bacteria, *Annu. Rev. Microbiol.*, 2013, 67, 313–336, DOI: [10.1146/annurev-micro-092412-155620](https://doi.org/10.1146/annurev-micro-092412-155620).
- 8 M. R. J. Salton, Lytic Agents, Cell Permeability, and Monolayer Penetrability, *J. Gen. Physiol.*, 1968, 227–252.
- 9 P. Gilbert and L. E. Moore, Cationic antiseptics: Diversity of action under a common epithet, *J. Appl. Microbiol.*, 2005, 703–715, DOI: [10.1111/j.1365-2672.2005.02664.x](https://doi.org/10.1111/j.1365-2672.2005.02664.x).
- 10 S. Alkhalifa, et al., Analysis of the Destabilization of Bacterial Membranes by Quaternary Ammonium Compounds: A Combined Experimental and Computational Study, *ChemBioChem*, 2020, 21(10), 1510–1516, DOI: [10.1002/cbic.201900698](https://doi.org/10.1002/cbic.201900698).
- 11 M. R. Garipov, et al., Targeting pathogenic fungi, bacteria and fungal-bacterial biofilms by newly synthesized quaternary ammonium derivative of pyridoxine and terbinafine with dual action profile, *Bioorg. Chem.*, 2020, 104, 104306, DOI: [10.1016/j.bioorg.2020.104306](https://doi.org/10.1016/j.bioorg.2020.104306).
- 12 W. B. Hugo and M. Frier, Mode of action of the antibacterial compound dequalinium acetate, *Appl. Microbiol.*, 1969, 17(1), 118–127, DOI: [10.1128/am.17.1.118-127.1969](https://doi.org/10.1128/am.17.1.118-127.1969).
- 13 M. Tischer, G. Pradel, K. Ohlsen and U. Holzgrabe, Quaternary ammonium salts and their antimicrobial potential: Targets or nonspecific interactions?, *ChemMedChem*, 2012, 22–31, DOI: [10.1002/cmdc.201100404](https://doi.org/10.1002/cmdc.201100404).
- 14 A. L. Frantz, Chronic quaternary ammonium compound exposure during the COVID-19 pandemic and the impact on human health, *J. Toxicol. Environ. Health Sci.*, 2023, 199–206, DOI: [10.1007/s13530-023-00173-w](https://doi.org/10.1007/s13530-023-00173-w).
- 15 A. R. Mahoney, M. M. Safaee, W. M. Wuest and A. L. Furst, iScience The silent pandemic: Emergent antibiotic resistances following the global response to SARS-CoV-2, *iScience*, 2021, 24, 102304, DOI: [10.1016/j.isci](https://doi.org/10.1016/j.isci).
- 16 J. M. Boyce, Quaternary ammonium disinfectants and antiseptics: tolerance, resistance and potential impact on antibiotic resistance, *Antimicrob. Resist. Infect. Control*, 2023, 32, DOI: [10.1186/s13756-023-01241-z](https://doi.org/10.1186/s13756-023-01241-z).
- 17 T. G. Osimitz and W. Droege, Quaternary ammonium compounds: perspectives on benefits, hazards, and risk, *Toxicol. Res. Appl.*, 2021, 5, 239784732110490, DOI: [10.1177/23978473211049085](https://doi.org/10.1177/23978473211049085).
- 18 S. V. Sapozhnikov, et al., Design, synthesis, antibacterial activity and toxicity of novel quaternary ammonium compounds based on pyridoxine and fatty acids, *Eur. J. Med. Chem.*, 2021, 211, 113100, DOI: [10.1016/j.ejmech.2020.113100](https://doi.org/10.1016/j.ejmech.2020.113100).
- 19 R. A. Allen, M. C. Jennings, M. A. Mitchell, S. E. Al-Khalifa, W. M. Wuest and K. P. C. Minbiole, Ester-and Amide-containing MultiQACs: Exploring Multicationic Soft

- Antimicrobial Agents, 2017, [Online]. Available: <http://www.elsevier.com/open-access/userlicense/1.0/>.
- 20 D. S. S. M. Uppu, et al., Side Chain Degradable Cationic-Amphiphilic Polymers with Tunable Hydrophobicity Show *in Vivo* Activity, *Biomacromolecules*, 2016, 17(9), 3094–3102, DOI: [10.1021/acs.biomac.6b01057](https://doi.org/10.1021/acs.biomac.6b01057).
- 21 R. Odžak, D. Crnčević, A. Sabljic, I. Primožič and M. Šprung, Synthesis and Biological Evaluation of 3-Amidoquinuclidine Quaternary Ammonium Compounds as New Soft Antibacterial Agents, *Pharmaceuticals*, 2023, 16(2), 187, DOI: [10.3390/ph16020187](https://doi.org/10.3390/ph16020187).
- 22 P. F. McDermott, R. D. Walker and D. G. White, Antimicrobials: modes of action and mechanisms of resistance, *Int. J. Toxicol.*, 2003, 22(2), 135–143, DOI: [10.1080/10915810305089](https://doi.org/10.1080/10915810305089).
- 23 G. A. Pankey and L. D. Sabath, Clinical Relevance of Bacteriostatic *versus* Bactericidal Mechanisms of Action in the Treatment of Gram-Positive Bacterial Infections, [Online]. Available: <https://academic.oup.com/cid/article/38/6/864/320723>.
- 24 S. V. Sapozhnikov, et al., Design, synthesis, antibacterial activity and toxicity of novel quaternary ammonium compounds based on pyridoxine and fatty acids, *Eur. J. Med. Chem.*, 2021, 211, 113100, DOI: [10.1016/j.ejmech.2020.113100](https://doi.org/10.1016/j.ejmech.2020.113100).
- 25 J. Fedorowicz, et al., Synthesis and biological evaluation of hybrid quinolone-based quaternary ammonium antibacterial agents, *Eur. J. Med. Chem.*, 2019, 179, 576–590, DOI: [10.1016/j.ejmech.2019.06.071](https://doi.org/10.1016/j.ejmech.2019.06.071).
- 26 H. Bierne and P. Cossart, *Listeria monocytogenes* Surface Proteins: from Genome Predictions to Function, *Microbiol. Mol. Biol. Rev.*, 2007, 71(2), 377–397, DOI: [10.1128/mmr.00039-06](https://doi.org/10.1128/mmr.00039-06).
- 27 L. Boulos, M. Prevost, B. Barbeau, J. Coallier, R. Desjardins and D. Desjardins, LIVE/DEAD BacLightE: application of a new rapid staining method for direct enumeration of viable and total bacteria in drinking water, *J. Microbiol. Methods*, 1999, 77–86.
- 28 C. A. Moubareck, Polymyxins and bacterial membranes: A review of antibacterial activity and mechanisms of resistance, *Membranes*, 2020, 181, DOI: [10.3390/membranes10080181](https://doi.org/10.3390/membranes10080181).
- 29 P. Sarkar, V. Yarlagadda, C. Ghosh and J. Haldar, A review on cell wall synthesis inhibitors with an emphasis on glycopeptide antibiotics, *Medchemcomm*, 2017, 516–533, DOI: [10.1039/c6md00585c](https://doi.org/10.1039/c6md00585c).
- 30 D. C. Hooper, Mechanisms of Action and Resistance of Older and Newer Fluoroquinolones, [Online]. Available: <http://cid.oxfordjournals.org/>.
- 31 R. I. Aminov, A brief history of the antibiotic era: Lessons learned and challenges for the future, *Front. Microbiol.*, 2010, 1, 134, DOI: [10.3389/fmicb.2010.00134](https://doi.org/10.3389/fmicb.2010.00134).
- 32 M. E. O'Sullivan, et al., Aminoglycoside ribosome interactions reveal novel conformational states at ambient temperature, *Nucleic Acids Res.*, 2018, 46(18), 9793–9804, DOI: [10.1093/nar/gky693](https://doi.org/10.1093/nar/gky693).
- 33 J. Fedorowicz, et al., Synthesis and biological evaluation of hybrid quinolone-based quaternary ammonium antibacterial agents, *Eur. J. Med. Chem.*, 2019, 179, 576–590, DOI: [10.1016/j.ejmech.2019.06.071](https://doi.org/10.1016/j.ejmech.2019.06.071).
- 34 S. V. Sapozhnikov, et al., Design, synthesis, antibacterial activity and toxicity of novel quaternary ammonium compounds based on pyridoxine and fatty acids, *Eur. J. Med. Chem.*, 2021, 211, 113100, DOI: [10.1016/j.ejmech.2020.113100](https://doi.org/10.1016/j.ejmech.2020.113100).
- 35 R. Chulluncuy, C. Espiche, J. A. Nakamoto, A. Fabbretti and P. Milón, Conformational response of 30S-bound IF3 to A-site binders streptomycin and kanamycin, *Antibiotics*, 2016, 5(4), 38, DOI: [10.3390/antibiotics5040038](https://doi.org/10.3390/antibiotics5040038).
- 36 L. Martinez, R. Andrade, E. G. Birgin and J. M. Martínez, PACKMOL: A package for building initial configurations for molecular dynamics simulations, *J. Comput. Chem.*, 2009, 30(13), 2157–2164, DOI: [10.1002/jcc.21224](https://doi.org/10.1002/jcc.21224).
- 37 T. F. Headen, E. S. Boek, G. Jackson, T. S. Totton and E. A. Müller, Simulation of Asphaltene Aggregation through Molecular Dynamics: Insights and Limitations, *Energy Fuel.*, 2017, 31(2), 1108–1125, DOI: [10.1021/acs.energyfuels.6b02161](https://doi.org/10.1021/acs.energyfuels.6b02161).
- 38 S. Otasevic and T. Vojinovic, Lecithin and anionic lipids as an imitation of the lipid membrane in Parallel Artificial Membrane Permeation Assay (PAMPA) blood-brain barrier Models, *Prog. Nutr.*, 2020, 22(3), e2020035, DOI: [10.23751/pn.v22i3.9720](https://doi.org/10.23751/pn.v22i3.9720).
- 39 M. Kansy, F. Senner and K. Gubernator, Physicochemical high throughput screening: parallel artificial membrane permeation assay in the description of passive absorption processes, *J. Med. Chem.*, 1998, 41(7), 1007–1010, DOI: [10.1021/jm970530e](https://doi.org/10.1021/jm970530e).
- 40 W. A. Arnold, et al., Quaternary Ammonium Compounds: A Chemical Class of Emerging Concern, *Environ. Sci. Technol.*, 2023, 7645–7665, DOI: [10.1021/acs.est.2c08244](https://doi.org/10.1021/acs.est.2c08244).
- 41 G. Zheng, E. Schreder, S. Sathyanarayana and A. Salamova, The first detection of quaternary ammonium compounds in breast milk: Implications for early-life exposure, *J. Expo. Sci. Environ. Epidemiol.*, 2022, 32(5), 682–688, DOI: [10.1038/s41370-022-00439-4](https://doi.org/10.1038/s41370-022-00439-4).
- 42 A. Salamova, G. Zheng and T. F. Webster, Quaternary ammonium compounds: Bioaccumulation potentials in humans and levels in blood before and during the covid-19 pandemic, *Environ. Sci. Technol.*, 2021, 55(21), 14689–14698, DOI: [10.1021/acs.est.1c01654](https://doi.org/10.1021/acs.est.1c01654).
- 43 R. M. Basnet, D. Zizioli, M. Guarienti, D. Finazzi and M. Memo, Methylxanthines induce structural and functional alterations of the cardiac system in zebrafish embryos, *BMC Pharmacol. Toxicol.*, 2017, 18(1), 72, DOI: [10.1186/s40360-017-0179-9](https://doi.org/10.1186/s40360-017-0179-9).
- 44 A. V. Kalueff, D. J. Echevarria and A. M. Stewart, Gaining translational momentum: More zebrafish models for neuroscience research, *Prog. Neuro-Psychopharmacol. Biol. Psychiatry*, 2014, 1–6, DOI: [10.1016/j.pnpbp.2014.01.022](https://doi.org/10.1016/j.pnpbp.2014.01.022).
- 45 K. Howe, et al., The zebrafish reference genome sequence and its relationship to the human genome, *Nature*, 2013, 496(7446), 498–503, DOI: [10.1038/nature12111](https://doi.org/10.1038/nature12111).

- 46 R. M. Basnet, D. Zizioli, S. Taweedet, D. Finazzi and M. Memo, Zebrafish larvae as a behavioral model in neuropharmacology, *Biomedicines*, 2019, 23, DOI: [10.3390/biomedicines7010023](https://doi.org/10.3390/biomedicines7010023).
- 47 W. Norton, Towards developmental models of psychiatric disorders in zebrafish, *Front. Neural Circuits*, 2013, 79, DOI: [10.3389/fncir.2013.00079](https://doi.org/10.3389/fncir.2013.00079).
- 48 J. A. Morris, Zebrafish: A model system to examine the neurodevelopmental basis of schizophrenia, *Prog. Brain Res.*, 2009, 179(C), 97–106, DOI: [10.1016/S0079-6123\(09\)17911-6](https://doi.org/10.1016/S0079-6123(09)17911-6).
- 49 S. Jo, T. Kim and W. Im, Automated builder and database of protein/membrane complexes for molecular dynamics simulations, *PLoS One*, 2007, 2(9), e880, DOI: [10.1371/journal.pone.0000880](https://doi.org/10.1371/journal.pone.0000880).
- 50 E. L. Wu, et al., CHARMM-GUI membrane builder toward realistic biological membrane simulations, *J. Comput. Chem.*, 2014, 1997–2004, DOI: [10.1002/jcc.23702](https://doi.org/10.1002/jcc.23702).
- 51 J. Lee, et al., CHARMM-GUI Input Generator for NAMD, GROMACS, AMBER, OpenMM, and CHARMM/OpenMM Simulations Using the CHARMM36 Additive Force Field, *J. Chem. Theory Comput.*, 2016, 12(1), 405–413, DOI: [10.1021/acs.jctc.5b00935](https://doi.org/10.1021/acs.jctc.5b00935).
- 52 F. Joodaki, L. M. Martin and M. L. Greenfield, Supporting Information: Generation and computational characterization of a complex *Staphylococcus aureus* lipid bilayer, *Langmuir*, 2022, 38(31), 9481–9499.
- 53 M. J. Abraham, et al., Gromacs: High performance molecular simulations through multi-level parallelism from laptops to supercomputers, *SoftwareX*, 2015, 1–2, 19–25, DOI: [10.1016/j.softx.2015.06.001](https://doi.org/10.1016/j.softx.2015.06.001).
- 54 J. Huang, et al., CHARMM36m: An improved force field for folded and intrinsically disordered proteins, *Nat. Methods*, 2016, 14(1), 71–73, DOI: [10.1038/nmeth.4067](https://doi.org/10.1038/nmeth.4067).
- 55 S. Nosé, A molecular dynamics method for simulations in the canonical ensemble, *Mol. Phys.*, 1984, 52(2), 255–268, DOI: [10.1080/00268978400101201](https://doi.org/10.1080/00268978400101201).
- 56 H. J. C. Berendsen, J. P. M. Postma, W. F. Van Gunsteren, A. Dinola and J. R. Haak, Molecular dynamics with coupling to an external bath, *J. Chem. Phys.*, 1984, 81(8), 3684–3690, DOI: [10.1063/1.448118](https://doi.org/10.1063/1.448118).
- 57 U. Essmann, L. Perera, M. L. Berkowitz, T. Darden, H. Lee and L. G. Pedersen, A smooth particle mesh Ewald method, *J. Chem. Phys.*, 1995, 103(19), 8577–8593, DOI: [10.1063/1.470117](https://doi.org/10.1063/1.470117).
- 58 M. Parrinello and A. Rahman, Polymorphic transitions in single crystals: A new molecular dynamics method, *J. Appl. Phys.*, 1981, 52(12), 7182–7190, DOI: [10.1063/1.328693](https://doi.org/10.1063/1.328693).
- 59 S. Babić, et al., Utilization of the zebrafish model to unravel the harmful effects of biomass burning during Amazonian wildfires, *Sci. Rep.*, 2021, 11(1), 2527, DOI: [10.1038/s41598-021-81789-1](https://doi.org/10.1038/s41598-021-81789-1).
- 60 S. 2, 1–22. OECD 236 (2013). Fish embryo acute toxicity (FET) test. OECD Guidelines for the Testing of Chemicals, “OECD/OCDE 2”.
- 61 “DIRECTIVE 2010/63/EU OF THE EUROPEAN PARLIAMENT AND OF THE COUNCIL of 22 September 2010 on the protection of animals used for scientific purposes (Text with EEA relevance)”.

3.3. NATURALLY DERIVED 3-AMINOQUINUCLIDINE SALTS AS NEW PROMISING THERAPEUTIC AGENTS

Reproduced from

Crnčević, D; Ramić, A; Radman Kastelic, A; Odžak, R; Krce, L; Weber, I; Primožič, I; Šprung, M. Naturally derived 3-aminoquinuclidine salts as new promising therapeutic agents // *Scientific reports*, 14 (2024), doi: 10.1038/s41598-024-77647-5



OPEN Naturally derived 3-aminoquinuclidine salts as new promising therapeutic agents

Doris Crnčević^{1,2}, Alma Ramić³, Andreja Radman Kastelic³, Renata Odžak¹, Lucija Krce⁴, Ivana Weber⁴, Ines Primožič³✉ & Matilda Šprung¹✉

Quaternary ammonium compounds (QACs) are a biologically active group of chemicals with a wide range of different applications. Due to their strong antibacterial properties and broad spectrum of activity, they are commonly used as ingredients in antiseptics and disinfectants. In recent years, the spread of bacterial resistance to QACs, exacerbated by the spread of infectious diseases, has seriously threatened public health and endangered human lives. Recent trends in this field have suggested the development of a new generation of QACs, in parallel with the study of bacterial resistance mechanisms. In this work, we present a new series of quaternary 3-substituted quinuclidine compounds that exhibit potent activity across clinically relevant bacterial strains. Most of the derivatives had minimal inhibitory concentrations (MICs) in the low single-digit micromolar range. Notably, QApCl and QApBr were selected for further investigation due to their strong antibacterial activity and low toxicity to human cells along with their minimal potential to induce bacterial resistance. These compounds were also able to inhibit the formation of bacterial biofilms more effectively than commercial standard, eradicating the bacterial population within just 15 min of treatment. The candidates employ a membranolytic mode of action, which, in combination with the generation of reactive oxygen species (ROS), destabilizes the bacterial membrane. This treatment results in a loss of cell volume and alterations in surface morphology, ultimately leading to bacterial cell death. The prominent antibacterial potential of quaternary 3-aminoquinuclidines, as exemplified by QApCl and QApBr, paves the way for new trends in the development of novel generation of QACs.

Keywords Quaternary ammonium salts, 3-substituted quinuclidine, Biological activity, Mode of antibacterial action

The unique biological potential and physicochemical properties of quaternary ammonium compounds (QACs) play a central role in modern healthcare making them indispensable components in the fight against microbial pathogens and in maintaining public health¹. Since their initial introduction as highly effective agents for disinfecting surgical surfaces, QACs have quickly become ingredients in numerous commercial products covering a wide range of applications and industries². Due to their extensive use, QACs are produced in high volumes generating approximately \$1.8 billion in sales which is expected to grow at a compound annual growth rate (CAGR) of 4.2–4.7% over the next several years^{3,4}.

Since QACs are ionic compounds, two distinct parts of the structure can be differentiated: the positively charged cationic amphiphile and the corresponding counterion. While the counterion primarily influences solubility, numerous studies have consistently shown its minimal impact on bioactivity⁴. In contrast, the cationic amphiphile constitutes the bioactive core, with its chemical composition and physicochemical attributes significantly influencing bioactivity⁵. The hydrophilic moiety of the cationic amphiphile comprises a polar head characterized by a positively charged nitrogen as a part of the quaternary ammonium cation. Conversely, the hydrophobic components consist of alkyl and/or aryl substituents, which play pivotal roles in determining optimal biological activity. Typically, elongated alkyl chains function as dynamic extensions forming integral elements within the structure⁶.

One of the most important features of QACs is their ability to disrupt the cell membranes of microorganisms, leading to their inactivation and eventual death. The proposed mechanism of action involves adsorption to the

¹Faculty of Science, Department of Chemistry, University of Split, R. Bošković 33, Split, Croatia. ²Faculty of Science, Doctoral Study in Biophysics, University of Split, R. Bošković 33, Split, Croatia. ³Faculty of Science, Department of Chemistry, University of Zagreb, Horvatovac 102a, Zagreb, Croatia. ⁴Faculty of Science, Department of Physics, University of Split, R. Bošković 33, Split, Croatia. ✉email: ines.primozic@chem.pmf.hr; msprung@pmfst.hr

membrane, which is triggered by an electrostatic interaction between the positively charged nitrogen of the QACs and the negatively charged groups on the membrane surface^{7–9}. Consequently, concentration-dependent adsorption, followed by subsequent penetration of alkyl chains, disrupts the membrane's structural integrity, resulting in heightened permeability and leakage of intracellular components. With increasing concentrations of QACs, this disruption impairs vital cellular processes like osmoregulation and nutrient uptake, ultimately leading to cellular dysfunction^{10–12}. In addition, QACs can inhibit the bacterial respiratory chain, which further impairs energy production¹³. The cumulative effect of membrane damage and cellular dysfunction eventually leads to bacterial cell death. This mechanism underlines the strong antimicrobial effect of quaternary ammonium compounds and their crucial role in fighting the spread of microbial infections¹.

However, despite their potent antimicrobial effects, their widespread use has led to the emergence of bacterial resistance, presenting a significant challenge in infection control and public health¹⁴. Additionally, studies have shown that these compounds can be toxic to various organisms, including aquatic and terrestrial species, raising concerns about their safety and ecological impact¹⁵.

The development of resistance to QACs primarily stems from prolonged exposure to these compounds at subMIC concentrations, allowing bacteria to adapt and evolve mechanisms to circumvent their antimicrobial effects¹⁶. One of the key mechanisms of resistance involves the upregulation of Qac efflux pumps, which actively remove QACs from bacterial cells, thereby reducing their intracellular concentration and rendering them less effective. Additionally, alterations in membrane composition and charge can hinder the binding of QACs to bacterial cell membranes, diminishing their ability to disrupt membrane integrity and exert antimicrobial activity¹⁷.

To address the growing concern of QACs resistance, several innovative strategies aimed at circumventing or overcoming resistance mechanisms have been proposed. One such strategy involves structural modifications which can be used to develop analogs with enhanced antimicrobial potency or altered modes of action that bypass resistance mechanisms^{4,18}. Such modifications may include altering the length or branching of alkyl or aryl groups⁵, addition of more positive nitrogen centers^{19–21}, introducing novel functional groups, or designing molecules that degrade rapidly^{2,22}. These design choices promote faster degradation, reducing bacteria's exposure time to the active agents and thus effectively combating resistance²³.

In our recent research on 3-substituted quinuclidine QACs, we have proposed promising solutions to overcome some challenges in the field. We focused on using the natural bioactive scaffold quinuclidine as a base for quaternization, resulting in a class of compounds bearing polar substituents at the C-3 position and lipophilic substituent at the quaternary center^{24–27}. This approach confirmed that quaternizing natural scaffolds is a viable strategy for crafting new broad-spectrum antimicrobials (Fig. 1). Concerned with their high toxicity and ecological impact, we subsequently explored a second class of derivatives. These derivatives feature a quinuclidine backbone substituted at the C-3 atom with an amide group, extended by long alkyl chains of varying lengths and methyl or allyl substituent at the quaternary center²⁸.

Introducing amide functionality at the targeted site within the structure results in compounds that can undergo spontaneous or enzyme mediated degradation, consequently mitigating their adverse environmental impact and reducing the likelihood of resistance development. Despite demonstrating their potential susceptibility to protease cleavage, the antimicrobial activity of these candidates proved to be lower than initially anticipated. Thus, our findings suggested that careful consideration of substituents at this position of quinuclidine backbone might yield derivatives that hold promise in overcoming antimicrobial resistance, improving biodegradability, and reducing toxicity relative to traditional QACs²⁸.

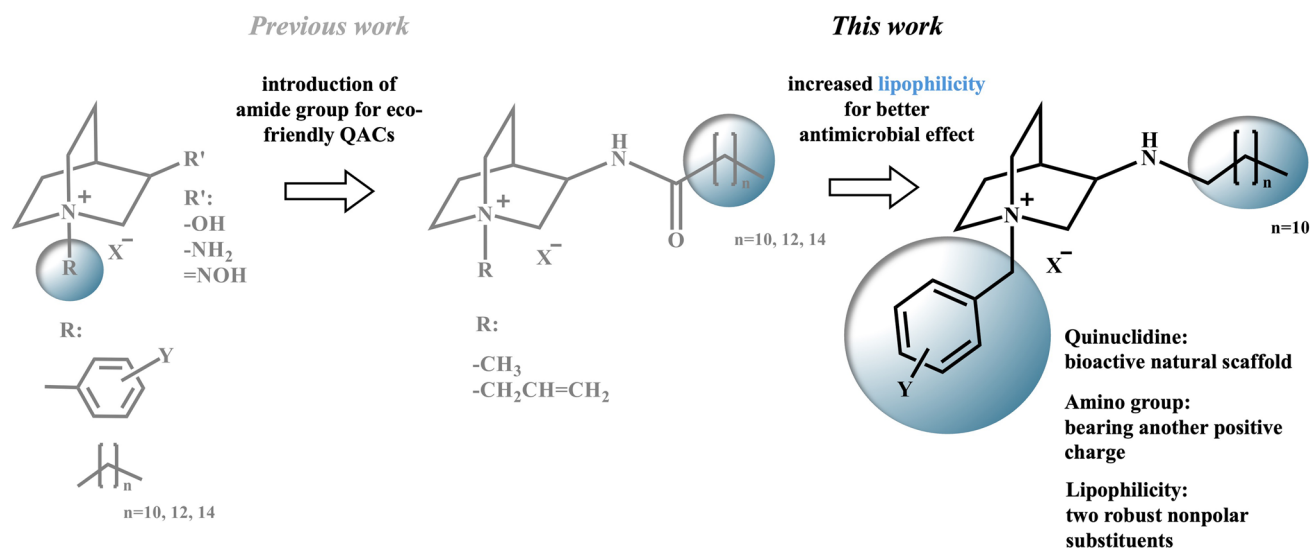


Figure 1. Overview of 3-substituted quinuclidine QACs structures from our previous and current work where X = Br/I, and Y = Cl/Br/NO₂/CH₃.

Inspired by results of these studies and driven by the further pursuit for biologically potent 3-substituted quinuclidine QACs, here we synthesized quaternary salts of 3-dodecylaminoquinuclidine with benzyl substituents at the quaternary center to acquire further insights that can aid the development of novel antimicrobial agents with enhanced efficacy and safety profiles.

Results and discussion

Synthesis

Previous investigations have shown that introducing an amide group into the structure of QACs can provide new functionalities, such as biodegradability, but can also negatively impact antibacterial activity. These compounds, while gaining desired properties, often exhibit reduced effectiveness as antimicrobial agents^{28,29}. Wuest and coworkers have explored the role of multiple positive charges in QACs, finding that compounds with more than one positive nitrogen atom exhibit better antimicrobial activities and are less prone to intrinsic resistance mechanisms^{2,30,31}. This enhanced activity is likely due to the additional positive charge, which strengthens electrostatic interactions with the negatively charged groups on bacterial membranes. The increased positive charge may reduce the likelihood of these compounds being recognized and neutralized by bacterial resistance elements, thereby enhancing their effectiveness as antimicrobial agents.

To mitigate the negative effects of the amide group, we synthesized 3-aminoquinuclidine (QA) with a dodecyl chain attached to the nitrogen atom of the amino group at the C-3 position of the quinuclidine ring. These compounds contain amine functionality, which under physiological conditions can bear an additional positive charge, similar to QACs with multiple positive nitrogen centers. QA was prepared through the reductive amination of commercially available quinuclidine-3-one with dodecyl amine, as shown in Fig. 2.

Understanding that the choice of the quaternizing agent is crucial for determining the bioactivity of QACs⁵, it is also essential to consider other factors that contribute to their effectiveness. One such factor is maintaining an optimal hydrophilic-hydrophobic balance³², which has been consistently observed as vital for the bioactivity of these compounds. Increased hydrophobicity, for instance, can significantly enhance the interaction between QACs and lipid membranes during the later stages of membrane penetration, thereby improving the antibacterial effect³³ but can also diminish water solubility.

The approach that implements these findings, e.g. more positive centers and an optimal hydrophilic-hydrophobic balance, has the potential to yield compounds with potent antimicrobial efficacy and less susceptibility to resistance mechanisms, providing a promising path for the development of new antimicrobials. For this reason, quaternary products of QA were synthesized using methyl iodide, benzyl bromide or differently *para*- and *meta*- substituted benzyl bromides. The reactions were carried out in dry acetone under inert atmosphere as shown in Fig. 3.

The prepared QA and its eight quaternary derivatives are compounds which have not been described in the literature so far. They were synthesized in moderate to good yields and their structures were determined by 1D and 2D NMR and HRMS analyses (Supporting information).

Antibacterial activity

Minimal inhibitory concentrations (MICs)

The antibacterial activity of 3-substituted aminoquinuclidine salts was investigated by determining the minimum inhibitory concentrations (MICs) on representative Gram-positive and Gram-negative bacteria. These values were compared with the MICs of commercially available standard QACs, cetylpyridinium chloride (CPC) and benzododecinium bromide (BAB), as well as the precursor QA, which served as a non-quaternized control.

As shown in Table 1, the non-quaternized control showed no relevant antibacterial activity compared to the QACs, demonstrating that rational quaternization is indeed a powerful tool to obtain potent antibacterial agents³⁴. However, the choice of quaternizing agent significantly impacts bioactivity. For example, the QAMe compound, which features simple methylation, did not reach the full antibacterial potential observed with QABn. This indicates that more robust and hydrophobic quaternizing agents may be required to achieve optimal antibacterial efficacy.

Nevertheless, we must consider QAMe (MICs $\geq 16 \mu\text{M}$) alongside two structurally similar QACs, which showed minimal activity against *Staphylococcus aureus* with MICs $\geq 100 \mu\text{M}$ ^{26,28}. One of these analogues carries amino group in the C-3 position and long alkyl chains in the quaternary center, the other is functionalized with a non-polar dodecyl chain in continuation of the amide group at the C-3 position and methyl or allyl substituent at the quaternary center (Fig. 1). It seems that a sole amino group at C-3 position is insufficient to

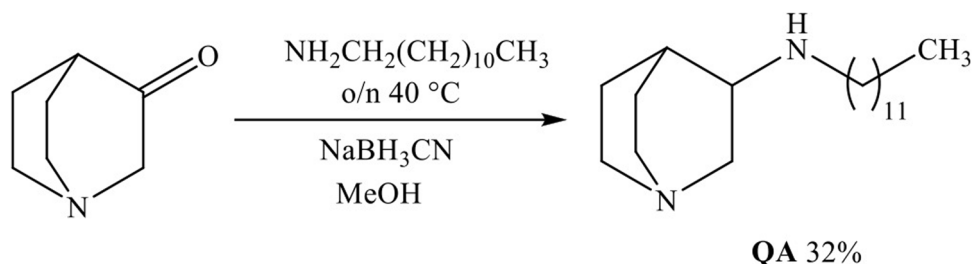


Figure 2. Preparation of QA.

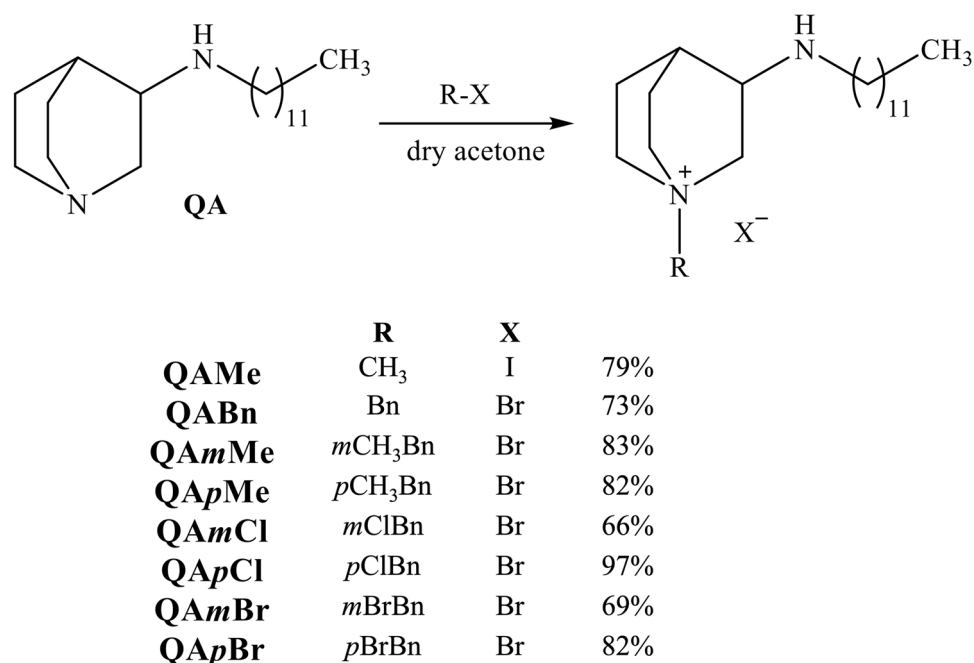


Figure 3. Preparation and structures of *N*-substituted quaternary QA derivatives.

Minimal inhibitory concentrations (μ M)									
Compound	Gram-positive bacteria						Gram-negative bacteria		
	<i>Staphylococcus aureus</i> ATCC25923	<i>Staphylococcus aureus</i> ATCC33591	MRSA Clinical isolate	<i>Bacillus cereus</i> ATCC14579	<i>Listeria monocytogenes</i> ATCC7644	<i>Enterococcus faecalis</i> ATCC29212	<i>Escherichia coli</i> ATCC25922	<i>Salmonella enterica</i> Food isolate	<i>Pseudomonas aeruginosa</i> ATCC27853
QA	63	63	31	31	31	31	63	31	> 125
QAMe	16	31	63	31	63	125	63	63	> 125
QABn	8	8	8	31	8	4	16	16	125
QAmMe	2	4	4	16	4	2	8	8	63
QApMe	4	4	4	8	4	2	8	8	63
QAmCl	2	4	4	16	4	2	8	8	63
QApCl	4	2	4	16	2	2	4	8	31
QAmBr	8	4	4	16	4	2	8	8	31
QApBr	2	2	4	8	2	2	4	8	31
Commercial QACs									
CPC	4	6	8	16	8	8	16	63	250
BAB	10	25	25	13	10	15	63	50	> 125

Table 1. Minimal inhibitory concentrations (MICs/ μ M) of antimicrobial agents against the panel of selected bacteria.

obtain fully bioactive structure instead a non-polar functionality in the continuation of the amino group seems to be required. Taken together, these structure-activity insights indicate the importance of the functional group and the correct hydrophilic-hydrophobic balance at the C-3 position for efficacy. Besides having the optimal hydrophilic-hydrophobic balance, the amino functional group in QAMe can further enhance the antibacterial properties due to its ionization state, which is similar to the double positive charge of bisQACs under measurement conditions. Therefore, it can be hypothesized that, among other known structural determinants, the functionality at the C-3 atom of the quinuclidine backbone is indeed an important point that requires special attention in the development of future QACs.

On the contrary, benzylated derivatives, featuring a highly hydrophobic benzyl ring at the quaternary center, displayed robust antibacterial activity, often achieving single-digit micromolar values (Table 1). These broad-spectrum activities were either much better or equivalent to conventional BAB or CPC, thus underlining the antibacterial potential of the new candidates. Notably, QABn exhibited higher MICs compared to derivatives with a halogen atom or a methyl group in the *para*- or *meta*- position on the benzyl ring, suggesting that the substituents on the benzyl ring and their position also play a role in enhancing antibacterial activity. For example, QApCl

and QApBr demonstrated particularly potent activities against Gram-negative *Escherichia coli* and *Salmonella enterica*, with MICs of 4 and 8 μM , respectively. Similar results were observed with 3-hydroxyiminoquinuclidine QACs bearing a benzyl ring at the quaternary center and chloride or bromide substituents at the *meta* and *para* positions²⁴. These derivatives, despite lacking long alkyl chains, exhibited potent activity against *S. aureus* and *E. coli*, also achieving single-digit MIC values. The role of electron-donating elements on the benzyl ring might be responsible for increased activities. This is supported by earlier reports from Ali et al., where derivatives with 2,6-dichloro and 2-methoxy substituents on the phenyl ring showed excellent antimicrobial and wound healing properties³⁵.

To explore their antimicrobial potential against methicillin-resistant *Staphylococcus aureus* (MRSA), which is known to harbor *qac* resistance genes, this collection of QACs was tested against clinically isolated and hospital-acquired HA-MRSA strains (ATTC33591) (Table 1). Based on the determined MICs, QApCl and QApBr once again exhibited compelling activity, underscoring the importance of *para*-position substitution. These findings suggest that *para*-substituted derivatives could be particularly effective in overcoming resistance mechanisms in MRSA, making them promising candidates for further development in the fight against antibiotic-resistant bacterial infections.

Given the potent activities of QApCl and QApBr against both Gram-positive and Gram-negative bacteria, they were selected for a more comprehensive investigation of their antibacterial potential and mechanism of action.

Potential for resistance development

The possibility of developing resistance, especially to quaternary ammonium compounds (QACs), is a major challenge in microbiology and public health¹⁶. Resistance to these compounds primarily arises from the plasma efflux system encoded by *qac* genes, which relies on the cellular ATP pool's availability. Consequently, reduced minimum inhibitory concentrations (MICs) under conditions of limited ATP supply suggest that the tested QACs may act as substrates for the efflux system³⁶.

To further evaluate the potential of QApCl and QApBr to induce bacterial resistance, we assessed their MICs against *Staphylococcus aureus* ATCC33591, a known carrier of *qac* resistance genes, in the presence of the protonophore carbonyl cyanide-3-chlorophenylhydrazone (CCCP). Previous research has demonstrated that CCCP, at concentrations below the MIC, can indeed diminish the efflux activity of *S. aureus* ATCC33591 by reducing the cellular ATP level³⁷. Therefore, evaluating MICs in the presence of CCCP may offer valuable insights into whether synthesized QACs act as substrates for Qac efflux pumps and the extent to which they contribute to bacterial resistance.

Table 2 illustrates the determined minimum inhibitory concentrations (MICs) for QApCl and QApBr in the presence and absence of CCCP. Interestingly, the MICs remained unchanged regardless of the presence of CCCP, indicating that these compounds did not exhibit a reduction in MICs. This observation suggests that QApCl and QApBr may not trigger known resistance mechanisms associated with efflux system.

Furthermore, the lack of change in MIC values in the presence of CCCP implies that these compounds are not substrates for the efflux pumps affected by ATP depletion induced by CCCP. This finding is significant as it suggests that QApCl and QApBr may exert their antibacterial activity through mechanisms independent of QAC efflux pumps and different from commercial BAB or CPC which both exhibit 32 and 16 \times MICs reduction during the CCCP treatment²⁸. Additionally, this finding highlights the potential of these compounds as promising antimicrobial agents that are less susceptible to resistance development through known efflux mechanisms.

Minimal biofilm inhibition concentrations (MBICs)

Bacterial biofilms consist of individual bacteria embedded in extracellular polymeric substances (EPS). Due to the genetic diversity within biofilm populations and the protective role of EPS, bacteria in biofilms exhibit heightened resistance to antibacterial agents³⁸. Notably, many human pathogens responsible for healthcare-associated infections, posing severe threats to human health through colonization of wounds and medical devices, are known for their ability to form biofilms³⁹. Consequently, there is considerable interest among scientists in developing novel antibacterial agents with potent antibiofilm activities.

The antibiofilm activity of QACs has been extensively documented, expanding their application to long-term antimicrobial materials and coatings⁴⁰. Two mechanisms have been proposed: firstly, QACs inhibit bacterial

Minimum inhibitory concentrations (μM)		
<i>Staphylococcus aureus</i> ATCC33591		
Compound	-CCCP	+CCCP
QApCl	2	2
QApBr	2	2
CPC ²⁸	6.25	0.39
BAB ²⁸	25	0.78

Table 2. Minimal inhibitory concentrations (MICs/ μM) of candidate compounds QApCl and QApBr against *Staphylococcus aureus* ATCC33591 in Mueller Hinton broth without (black) and in the presence (red) of carbonyl cyanide-3-chlorophenylhydrazone (CCCP).

adhesion to surfaces, thus suppressing biofilm formation; secondly, QACs actively eradicate bacteria within biofilms.

The minimal inhibitory concentrations (MICs) demonstrated the potent antibacterial activity of two candidates, QApCl and QApBr. Consequently, we investigated their antibiofilm activity against *Staphylococcus aureus* ATCC25923 in comparison to conventional CPC. The *S. aureus* was chosen due to documented cases of persistent *S. aureus* biofilm infections associated with high mortality rates⁴¹. Figure 4 clearly demonstrates the greater ability of QApCl and QApBr to suppress the formation of bacterial biofilms compared to commercial QAC.

These candidates effectively inhibited biofilm formation across all tested concentrations, ranging from 3.13 to 100 $\mu\text{g mL}^{-1}$, with inhibition percentages exceeding 70%. Remarkably, they exhibited pronounced inhibition at the two lowest concentrations, where CPC showed no activity. This finding is particularly noteworthy considering that CPC is typically recognized as a potent antibacterial agent, often used in mouthwash solutions to eradicate and inhibit *Streptococcus mutans*, the primary bacteria responsible for cavities^{41,42}. *Streptococcus mutans* forms intricate and multidimensional structures on oral mucosa and tooth enamel, contributing to cavity development⁴³. Taken together, these findings underscore the potential of new compounds as potent alternatives to existing antibacterial agents, particularly in applications requiring effective biofilm inhibition.

Bacterial growth kinetic analysis

Bacterial growth kinetic analysis elucidates how bacterial populations evolve over time under specific conditions, influenced by factors such as temperature, pH, oxygen levels, nutrient availability, and the presence of inhibitory substances like antibiotics or toxins⁴⁴. When subjected to an antibacterial agent, the growth curve deviates from the standard pattern, notably in comparison to the untreated control. Typically, the discrepancy between the curves is observed during the lag phase, wherein bacterial growth may be delayed or halted as bacteria adapt to the antibacterial agent⁴⁵. Subsequently, during the exponential phase, the antibacterial agent often induces a reduction in the rate of bacterial growth compared to the untreated control. Instead of the anticipated rapid and exponential growth, the bacterial population may exhibit slower growth or even remain relatively constant as the antibacterial agent continues to exert its inhibitory effects.

Considering the role of the bacterial growth curves in evaluating the effectiveness of antibacterial agents within defined measurement conditions, our study aimed to explore potential variations in bacterial growth curves when treated with QApCl and QApBr. The findings depicted in Fig. 5 distinctly illustrate the contrasting growth curves observed in the presence of the antibacterial agents. Notably, as the growth curves span a 24-hour incubation period, it becomes apparent that both agents effectively suppress bacterial growth at their respective MICs. However, intriguingly, at half the MIC concentration, QApBr demonstrates a notable reduction in bacterial growth compared to QApCl. This observation suggests a differential impact of the two agents on bacterial proliferation, emphasizing the importance of further investigation into their antibacterial mechanisms and potency.

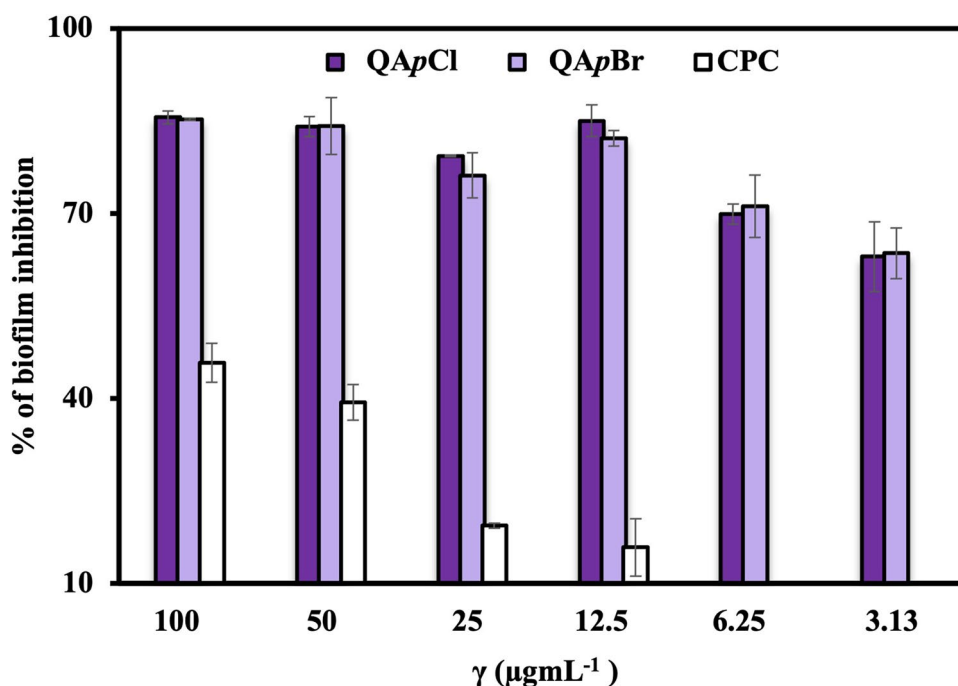


Figure 4. The percentage (%) of *Staphylococcus aureus* ATCC25923 biofilm inhibition in relation to mass concentration ($\mu\text{g mL}^{-1}$) of the antibacterial agents: QApCl, QApBr and CPC.

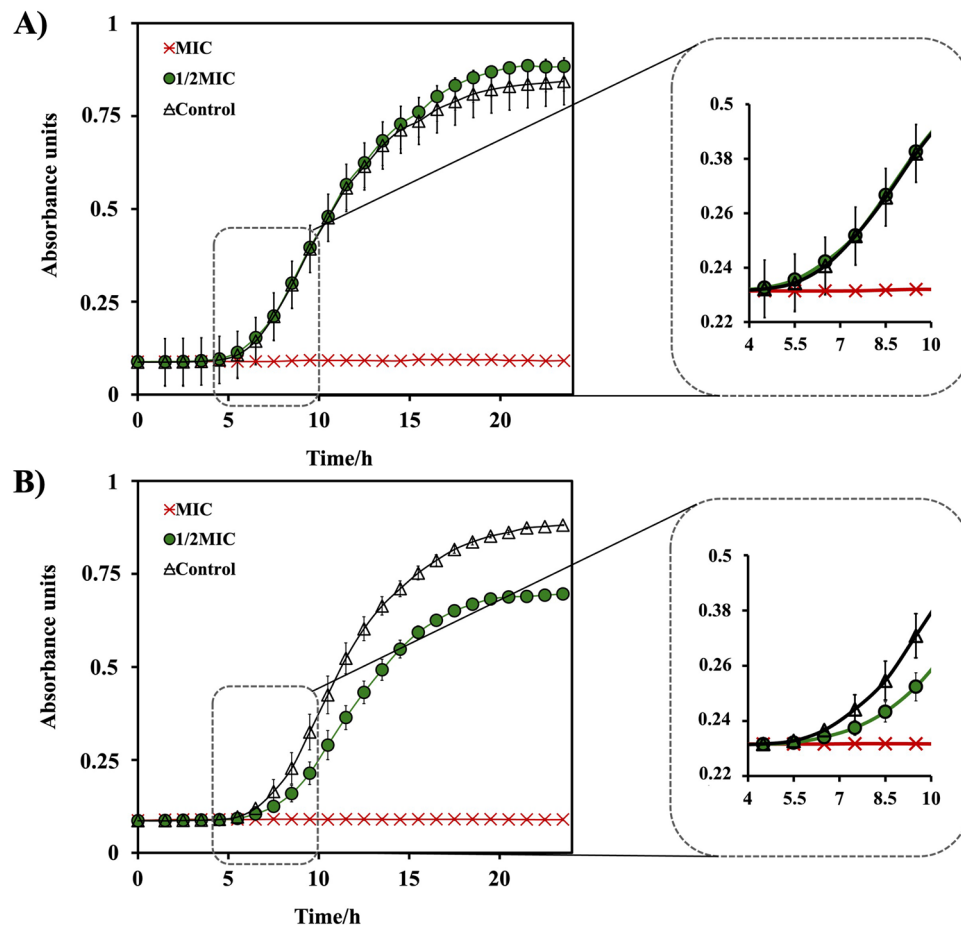


Figure 5. Time-resolved growth curves of *Escherichia coli* ATCC25922 during a 24-hour exposure to (A) QApCl and (B) QApBr, respectively. The inserts in the graphs provide enhanced resolution of the growth curves at MIC and $\frac{1}{2}$ MIC, clearly depicting a halt in bacterial growth at $\frac{1}{2}$ MIC for QApBr.

Cytotoxicity

The drawback of quaternary ammonium compounds (QACs) lies in their toxicity, which restricts their widespread use and application. Consequently, recent attention in the scientific community has shifted towards the development of environmentally friendly variants that exhibit easy degradation and lower toxicity towards both terrestrial and aquatic organisms^{2,28,46,47}. Given the common utilization of QACs as disinfectants and antiseptics, ensuring their safety for potential use in humans and animals is paramount.

Hence, we determined the cytotoxicity of all newly synthesized QACs using healthy cell lines, human embryonic kidney (HEK293) and retinal pigment epithelial cells (RPE1), respectively. We further compared obtained IC_{50} with MICs for Gram-positive representative, namely *Staphylococcus aureus* ATCC25923 to obtain therapeutic index which provides insight into the safety of our compounds as potential therapeutic agents. The candidates expressing IC_{50} higher than the corresponding MIC were declared to be the least toxic for healthy cells and potentially safe for selected application. The resultant IC_{50} values, illustrated in Fig. 6, reveal distinct toxicity profiles for all QACs.

We can also observe different selectivity of QACs against two human cell lines. Specifically, HEK293 cells are generally more sensitive to all QACs evidenced by low IC_{50} values. On the other side, RPE1 cells display higher resistance to QACs, and given their epithelial origin and resemblance to keratinocytes, RPE1 could be taken as a reference cell line. Higher therapeutic indices of selected QACs in contrast to commercial standard, CPC, suggest their higher safety, with QApBr recognized as more prominent candidate compound.

Taken together, these findings are reassuring and support the potential application of QApCl and QApBr as ingredients in topical solutions, disinfectants, and antiseptics, given their selective toxicity profiles and efficacy. We have to note the strong therapeutic index of QAmCl which was expected given its higher IC_{50} value compared to MIC. However, QAmCl was not considered as candidate due to its diminished antibacterial potential.

Mode of antibacterial action

Atomic force and scanning electron microscopies

The antibacterial mechanism of QACs is primarily based on their membranolytic properties leading to the disruption of the bacterial cell envelope and subsequent cell lysis^{7,48}. Gram-positive bacteria protect their cell

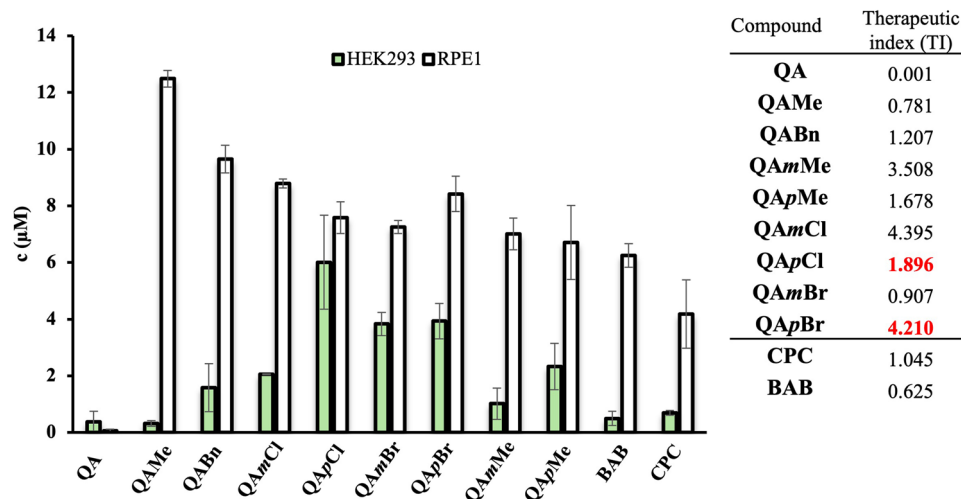


Figure 6. The toxicity of quaternary 3-aminoquinuclidine salts expressed as concentration (μM) at which 50% of HEK293 and RPE1 cells are dead (IC_{50}). The obtained therapeutic indices (TI) are presented in corresponding table and were calculated as ratio of IC_{50} value towards RPE1 reference cell line and MIC determined for *Staphylococcus aureus* ATCC25923.

contents with a membrane covered by a thick layer of peptidoglycan, whereas Gram-negative bacteria have an additional outer membrane that restricts the access of QACs to their target site. This difference explains the increased efficacy of QACs against Gram-positive bacterial strains.

Motivated by the previously demonstrated antibacterial efficacy of the QAC candidates, QApCl and QApBr, against a panel of both Gram-positive and Gram-negative bacteria, we wanted to further investigate their mode of action against most common representative bacterial pathogens. Atomic force microscopy (AFM) and scanning electron microscopy (SEM) were used to evaluate the morphological changes of *Escherichia coli* after the treatment with selected QACs in comparison to untreated cells (Fig. 7).

The strain selected for measurements was *E. coli* DH5 α , due to its ability to be immobilized without compromising the cell viability. The minimum inhibitory concentration (MIC) for both compounds was determined prior to microscopy measurements and was found to be consistent with the values observed for *E. coli* ATCC25922, namely 8 μM for QApCl and 4 μM for QApBr. Height AFM image of untreated, viable *E. coli* DH5 α in their characteristic rod shape with smooth, intact surfaces indicative of division (white arrow) is shown on panel A (Fig. 7).

Once the viability of the immobilized bacteria was confirmed, the cells were exposed to a 4 \times MIC concentration of the candidate compounds for three hours to accelerate the time-dependent membrane disruption. Interestingly, height AFM images of treated cells pointed out different extent of damage depending on candidate compound (panel A, Fig. 7). Cells treated with 4 \times MIC concentration of QApCl were unable to proliferate as evidenced by cellular elongation, while the cell surface seemed preserved. In contrast, treatment with QApBr resulted in pronounced damage manifested by a roughened cell surface and loss of characteristic rod shape which led to increased adhesion between the sample and the AFM probe tip significantly aggravating the measurement.

In contrast to AFM measurements, the inspection of both untreated and treated cells using scanning electron microscopy (SEM) necessitates fixation and air drying^{49,50}. Although these procedures can alter cell morphology, panel B in Fig. 7 illustrates significant differences between untreated *E. coli* DH5 α cells and those treated with candidate QACs. Despite the potential morphological alterations due to sample preparation, the untreated cells exhibit their characteristic morphology. Conversely, the presence of membrane bulges in the treated cells confirms the membranolytic activity of both selected compounds. Although both compounds act as membranolytic agents, QApBr demonstrates potent efficacy, causing more extensive cellular damage and complete membrane disruption, as evidenced by the leakage of intracellular contents observed on the sample surface.

Uptake of propidium iodide (PI)

Bacterial membrane damage upon treatment can also be evidenced by fluorescent labeling, most commonly using red fluorescent nuclear dye propidium iodide (PI). Due to its molecular size, PI cannot penetrate the intact cell membranes of viable cells. It therefore serves as a marker to distinguish cells with damaged membranes⁵¹.

To further investigate membranolytic potency of candidate QACs, treated *Escherichia coli* DH5 α cells were fluorescently labelled with a mixture of two fluorophores, SYTO9 and PI. When treated culture is simultaneously stained, SYTO9, unlike PI, penetrates all cells, regardless of their membrane integrity, and emits green fluorescent signal upon binding to the nucleic acid. Comparison of the optical fluorescence microscopy images provides information on the quantity of the bacterial cell population with the compromised cell membranes⁵².

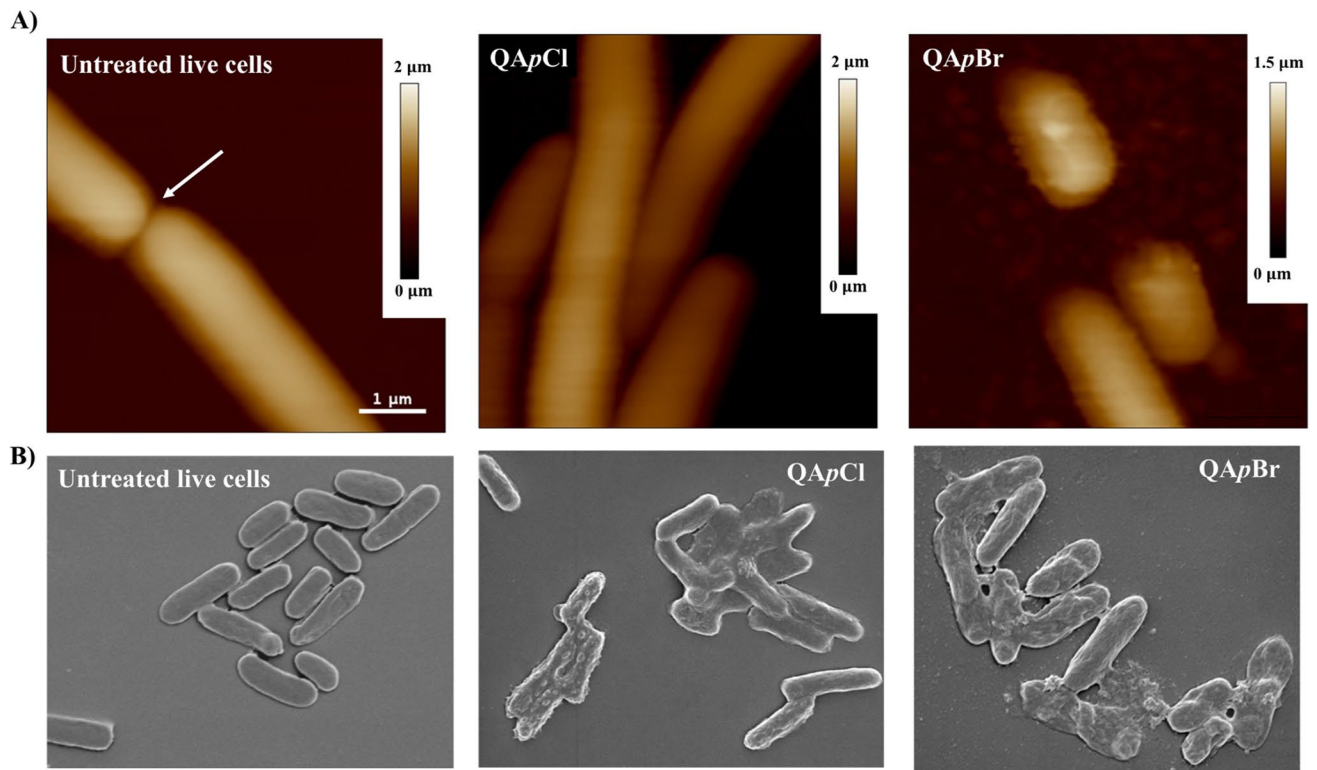


Figure 7. Panel A: Height atomic force microscopy images before and after three-hour long treatment of *Escherichia coli* DH5α cells - untreated viable *E. coli* DH5α cells upon division (white arrow), *E. coli* DH5α cells after treatment with a $4 \times$ MIC concentration of QApCl and *E. coli* DH5α cells after treatment with a $4 \times$ MIC concentration of QApBr. Scale bar for all AFM data is given in the first image. Panel B: Scanning electron microscopy data - untreated *E. coli* DH5α cells, cells treated with $16 \times$ MIC concentration of QApCl and $8 \times$ MIC concentration of QApBr. Scalebar corresponding to $1 \mu\text{m}$ is given below each image.

Figure 8, panel A, shows the population of fluorescently labelled *E. coli* DH5α cells after exposure to $4 \times$ MIC concentration of QApCl and QApBr. While atomic force microscopy did not indicate severe membrane damage subsequent to QApCl treatment, the distribution of fluorescently PI and SYTO9 labelled cells was nearly identical for both candidates, suggesting their membranolytic mechanism of action. Given the low single-digit micromolar values exhibited by the candidate compounds against a representative Gram-negative bacterium, it is noteworthy that these compounds exhibit strong antibacterial activity. This is particularly interesting considering the composition of the cell envelope in Gram-negative strains.

The observed membranolytic activity of the QAC candidates against *E. coli* DH5α prompted us to investigate their efficacy against *Staphylococcus aureus* ATCC25923, a representative Gram-positive strain characterized by the absence of an outer membrane. Moreover, negatively charged teichoic acid anchored in the peptidoglycan matrix can interact electrostatically with the QAC backbone, facilitating their membranolytic effect.

To determine how selected QACs affect the *S. aureus* ATCC25923 membrane, we used different fluorescence-based techniques, namely spectrofluorimetric determination of propidium iodide (PI) uptake and temporal monitoring of treated culture by flow cytometry. Figure 8, panel B, depicts relative fluorescence units (RFU) of PI over six-hour long treatment of *S. aureus* ATCC25923 with different concentrations of QApCl and QApBr. The evaluation of PI fluorescence intensity for both the treated cells and the untreated control points out almost immediate membrane damage. In addition, QApBr was found to be more effective, as indicated by a continuously high PI fluorescence intensity for each concentration tested.

The treatment of *S. aureus* ATCC25923 with MIC and $2 \times$ MIC concentrations of QApCl and QApBr was further analyzed by flow cytometry. Given the previously indicated prompt membrane damage, these measurements were performed at shorter time intervals. Flow cytometric analysis showed that after only 15 min of treatment with MIC concentration of both candidates, no viable cells were present, while half of the bacterial population was dead (Fig. 9) which was consistent with spectrofluorimetric analysis.

The investigation of the antibacterial mode of action of QApCl and QApBr highlights their potential to combat both Gram-positive and Gram-negative pathogenic bacteria. At the same time, their lower toxicity to human cells and reduced potential to trigger bacterial resistance mechanisms points out these compounds as promising new antibacterial agents.

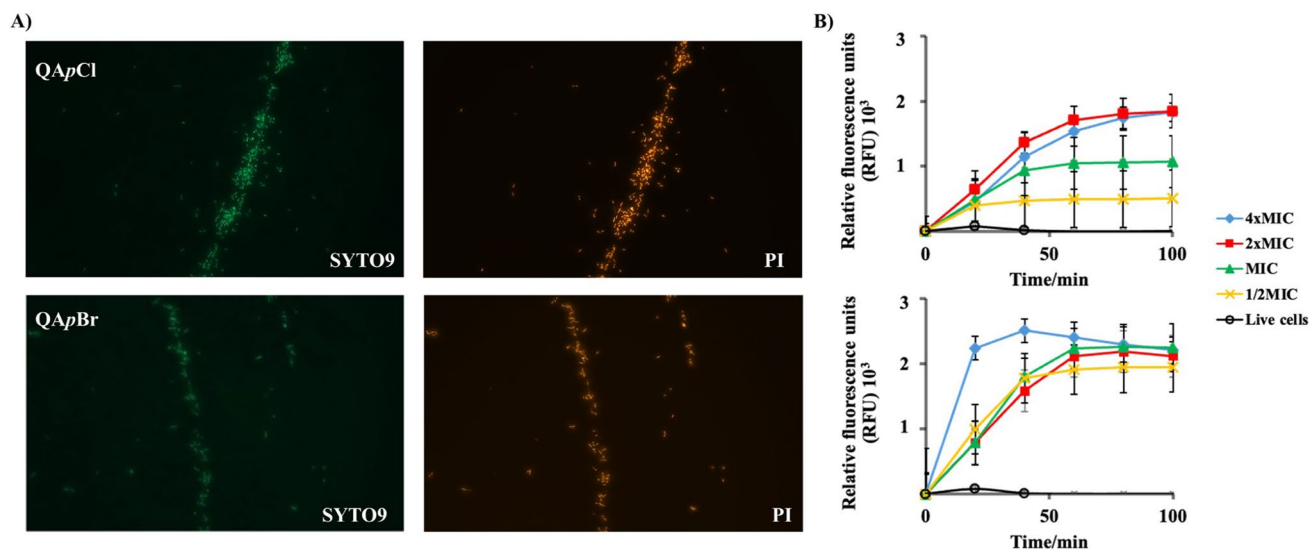


Figure 8. Panel A: *Escherichia coli* DH5 α cells stained with the mixture of SYTO9 and propidium iodide (PI) nucleic fluorophores subsequent to exposure of 4 \times MIC concentration of QApCl and QApBr. Panel B: Spectrofluorimetric determination of propidium iodide (PI) uptake during the time of *Staphylococcus aureus* ATCC25923 treatment with different concentrations of selected candidate compounds QApCl (upper graph) and QApBr (lower graph).

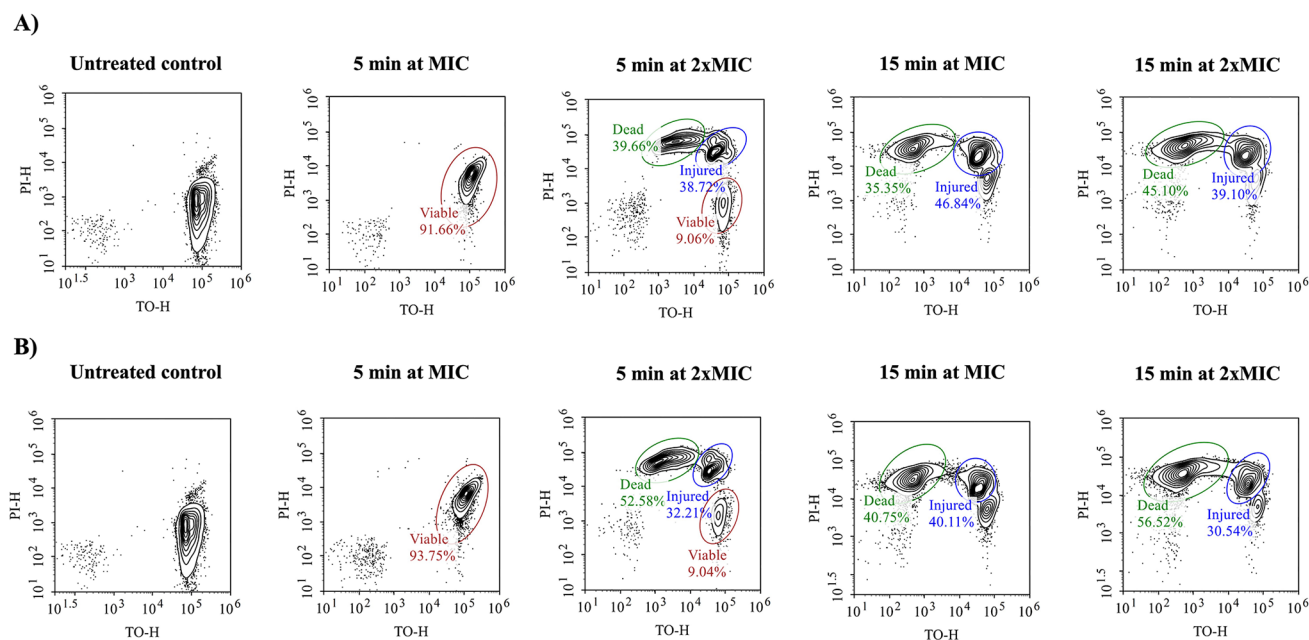


Figure 9. Time-dependent flow cytometry detection of live and dead *Staphylococcus aureus* ATCC25923 bacterial cells upon the treatment with the antibacterial agents (A) QApCl and (B) QApBr at MIC and 2 \times MIC concentrations.

Generation of reactive oxygen species (ROS)

A promising strategy to eradicate bacteria while simultaneously targeting multiple crucial bacterial pathways involves the generation of reactive oxygen species (ROS)⁵³. Previous studies have demonstrated that exposure to quaternary ammonium compounds (QACs) can induce ROS production by inhibiting key bacterial enzymes. Notably, enzymes such as superoxide dismutase (SOD) and catalase (CAT), which play vital roles in scavenging ROS, are inhibited by QACs during treatment. This inhibition is more pronounced with longer alkyl chains in QACs, resulting in increased ROS generation⁵⁴. The ROS accumulation triggered by QACs can cause extensive damage to cellular components, potentially leading to apoptosis and cell death⁵⁵.

Led by these investigations, we aimed to assess ROS generation resulting from QApCl and QApBr treatments, comparing these results to the background ROS levels produced by untreated live cells and hydrogen peroxide as a positive control (Fig. 10). Notably, all treatments led to high ROS production, eventually saturating the instrument's detector. However, differences between the candidates are apparent and consistently demonstrate distinct profiles. Although both compounds induce ROS generation, the extent of ROS production varies between them. Specifically, QApCl treatment results in lower ROS generation compared to QApBr and the hydrogen peroxide control. For example, ROS production from QApCl continues beyond the 80-minute exposure time, while ROS production from hydrogen peroxide and QApBr ceases around 70 min due to detector saturation.

These findings may explain the stronger antibacterial activity of QApBr, suggesting an additional mechanism of action that induces faster bacterial death due to higher toxicity. This indicates that QApBr could be more effective in situations requiring stronger oxidative stress to eliminate resilient bacterial strains.

In conclusion, the comparative analysis of ROS generation by QApCl and QApBr enhances our understanding of their bioactive profiles, guiding their appropriate application in antimicrobial strategies. Further research is warranted to explore the underlying mechanisms driving these differences and to optimize the use of these compounds in various clinical and environmental settings.

Materials and methods

Synthesis

General notes

Reagents and solvents for the preparation of compounds were purchased from Sigma-Aldrich (St. Louis, MO, USA), Fluka. The reactions were monitored by thin-layer chromatography plates coated with aluminum oxide (Sigma-Aldrich, St. Louis, MO, USA). TLC plates were visualized by UV irradiation (254 nm) or by iodine fumes. 1D and 2D ^1H and ^{13}C NMR spectra were recorded on a Bruker Avance Neo 600 MHz/54 mm Ascend spectrometer equipped with a 5 mm inverse TCI Prodigy cryoprobe (Bruker Optics Inc, Billerica, MA, USA). Chemical shifts are given in ppm downfield from tetramethyl silane (TMS) as an internal standard and coupling constants (J) in Hz. Splitting patterns are designated as s (singlet), d (doublet), ddd (doublet of doublet of doublets), t (triplet), dt (doublet of triplets) or m (multiplet). Dodecyl hydrogen and carbon atoms are marked with an apostrophe. Benzyl hydrogen and carbon atoms are marked with an asterisk. Melting points were determined on a Melting Point B-540 apparatus (Büchi, Essen, Germany) and are uncorrected. HPLC analyses were performed on Agilent 1260 series instrument equipped with a quaternary pump, autosampler, column compartment and diode array detector (DAD). HPLC conditions: Zorbax Eclipse C18 column, 4.6×250 mm, 5 μm pore size; column temperature 25 $^\circ\text{C}$; flow rate 1.0 mL/min; mobile phase A: 0.1% phosphoric acid, mobile phase B: CH_3CN ; 10/90/90/10/10% B in time intervals 0/10/15/20/25; the volume of injection 10 μL ; UV detection at 220 nm. All prepared compounds have purity > 95%. HRMS analyses were carried out on Q Exactive™ Plus Hybrid Quadrupole-Orbitrap™ Mass Spectrometer.

Synthesis of 3-aminododecylquinuclidine QA

Quinuclidin-3-one (1 mmol), sodium cyanoborohydride (1.4 mmol) and dodecyl amine (1 mmol) were mixed in methanol overnight at 40 $^\circ\text{C}$. Solvent was evaporated, residue made alkaline with 1 M NaOH and transferred in separation funnel. After extraction with chloroform, organic extracts were dried over anhydrous sodium sulphate, filtered and evaporated. Residue was purified with column chromatography (aluminum oxide, $\text{CHCl}_3:\text{MeOH} = 9:1$) to acquire oily product.

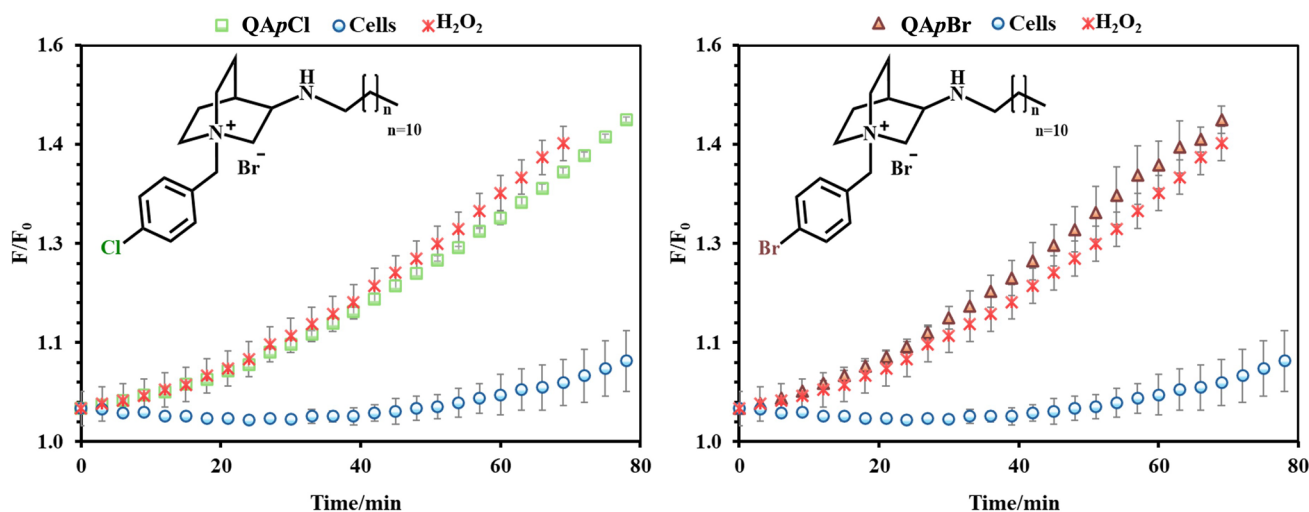


Figure 10. The generation of reactive oxygen species (ROS) upon treatment with QApCl and QApBr. The results are compared with untreated live cells and cells treated with hydrogen peroxide control.

3-aminododecylquinuclidine, QA, Yield: 32%. (Supporting information, S1-2, S19) ^1H NMR (600 MHz, CDCl_3) δ /ppm: 0.88 (t, $J=6.9$ Hz, 3 H, H12') 1.21–1.37 (m, 19 H, H3'-H11', H5b) 1.43–1.51 (m, 3 H, H2', H7b) 1.63–1.71 (m, 1 H, H7a) 1.78–1.84 (m, 2 H, H5a, H4) 2.39 (ddd, $J=13.6, 4.8, 2.3$ Hz, 1 H, H2b) 2.48–2.61 (m, 2 H, H6b, H8a) 2.68–2.92 (m, 5 H, H1', H3, H6a, H8b) 3.13 (ddd, $J=13.2, 8.8, 2.2$ Hz, 1 H, H2a); ^{13}C NMR (151 MHz, CDCl_3) δ /ppm: 14.12 (C12') 20.01 (C5) 22.65; 25.15 (C4); 26.37 (C7); 27.46; 29.32; 29.55; 29.59; 29.64; 30.46 (C2'); 31.90; 47.10 (C1') 47.68 (C8) 47.72 (C6) 55.22 (C3) 57.07 (C2); HRMS (Electrospray ionisation (ESI) m/z calcd for $\text{C}_{19}\text{H}_{39}\text{N}_2^+$ = 295.3108, found 295.3106.

General procedure for synthesis of quaternary compounds

N-dodecyl-3-amino-quinuclidine (1 mmol) was mixed with methyl iodide (1 mmol) or appropriate benzyl bromide (1 mmol) in dry acetone under nitrogen atmosphere. Reaction was monitored with thin-layer chromatography. Crude product was filtered off and washed extensively with diethyl ether.

3-dodecylamino-1-methylquinuclidinium iodide, QAMe, Yield: 79%, mp 110.8–111.5 °C. (Supporting information, S3-4, S20, S28) ^1H NMR (600 MHz, CDCl_3) δ /ppm: 0.88 (t, $J=6.9$ Hz, 3 H, H12') 1.22–1.35 (m, 18 H, H3'-H11') 1.43–1.50 (m, 2 H, H2') 1.86–1.95 (m, 1 H, H5b) 1.98–2.07 (m, 1 H, H7a) 2.09–2.18 (m, 1 H, H7b) 2.24–2.26 (m, 1 H, H4) 2.27–2.36 (m, 1 H, H5a) 2.47–2.57 (m, 2 H, H1') 3.11 (dt, $J=12.5, 2.9$ Hz, 1 H, H2b) 3.26–3.29 (m, 1 H, H3) 3.32 (s, 3 H, N-CH₃) 3.52–3.59 (m, 1 H, H6b) 3.75–3.93 (m, 3 H, H8a, H6b, H8b) 4.15 (ddd, $J=12.3, 8.9, 2.9$ Hz, 1 H, H3); ^{13}C NMR (151 MHz, CDCl_3) δ /ppm: 14.03 (C12') 18.50 (C5) 22.61, 22.85 (C7) 23.82 (C4) 27.30, 29.28, 29.48, 29.55, 29.57, 29.60, 30.13 (C2') 31.86, 47.40 (C1') 52.60 (C3) 52.80 (CH₃) 56.47 (C8) 57.82 (C6) 64.73 (C2); HRMS (Electrospray ionisation (ESI) m/z calcd for $\text{C}_{20}\text{H}_{41}\text{N}_2^+$ = 309.3264, found 309.3261.

3-dodecylamino-1-benzylquinuclidinium bromide, QABn, Yield: 73%, mp 70.2–70.4 °C. (Supporting information, S5-6, S21, S29) ^1H NMR (600 MHz, CDCl_3) δ /ppm: 0.88 (t, $J=6.7$ Hz, 3 H, H12') 1.20–1.33 (m, 18 H, H3'-H11') 1.39–1.48 (m, 2 H, H2') 1.74–1.83 (m, 1 H, H5b) 1.91–2.02 (m, 1 H, H7a) 2.02–2.09 (m, 1 H, H7b) 2.19–2.21 (m, 1 H, H4) 2.22–2.28 (m, 1 H, H5a) 2.43–2.54 (m, 2 H, H1') 3.14–3.18 (m, 1 H, H2b) 3.22–3.28 (m, 1 H, H3) 3.51–3.58 (m, 1 H, H6b) 3.70–3.79 (m, 2 H, H8a, H6b) 3.93–4.00 (m, 1 H, H8b) 4.21 (ddd, $J=12.29, 8.99, 2.93$ Hz, 1 H, H2a) 4.92 (d, $J=13.21$ Hz, 1 H, CH₂a) 4.99 (d, $J=13.20$ Hz, 1 H, CH₂b) 7.38–7.46 (m, 3 H, H2*, H4*, H6*) 7.63 (d, $J=6.60$ Hz, 2 H, H3*, H5*); ^{13}C NMR (151 MHz, CDCl_3) δ /ppm: 14.03 (C12') 18.45 (C5) 22.62, 22.91 (C7) 24.64 (C4) 27.24, 29.28, 29.41, 29.52, 29.55, 29.57, 29.59, 29.59 (C2') 31.86, 47.41 (C1') 52.95 (C3) 53.86 (C8) 54.14 (C6) 61.11 (C2) 67.04 (CH₂) 126.95 (C1*) 129.13 (C3*; C5*) 130.46 (C4*) 133.31 (C2*; C6*); HRMS (Electrospray ionisation (ESI) m/z calcd for $\text{C}_{26}\text{H}_{45}\text{N}_2^+$ = 385.3577, found 385.3572.

3-dodecylamino-1-(3-methylbenzyl)quinuclidinium bromide, QAmMe, Yield: 83%, mp 145.6–146.2 °C. (Supporting information, S7-8, S22, S30) ^1H NMR (600 MHz, CDCl_3) δ /ppm: 0.88 (t, $J=6.9$ Hz, 3 H, H12') 1.16–1.34 (m, 18 H, H3'-H11') 1.37–1.45 (m, 2 H, H2') 1.72–1.86 (m, 1 H, H5a) 1.89–2.12 (m, 2 H, H7) 2.12–2.30 (m, 2 H, H4, H5b) 2.31–2.40 (m, 3 H, CH₃) 2.40–2.54 (m, 2 H, H1') 3.09 (dt, $J=12.3, 3.1$ Hz, 1 H, H2a) 3.16–3.26 (m, 1 H, H3) 3.44–3.57 (m, 1 H, H6a) 3.67–3.84 (m, 2 H, H6b, H8a) 3.92–4.06 (m, 1 H, H8b) 4.15–4.29 (m, 1 H, H2b) 4.80–4.98 (m, 2 H, CH₂) 7.21–7.32 (m, 2 H, H4*, H6*) 7.36–7.43 (m, 2 H, H2*, H5*); ^{13}C NMR (151 MHz, CDCl_3) δ /ppm: 14.07 (C12') 18.40 (C5) 21.27 (CH₃) 22.63, 22.87 (C7) 24.65 (C4) 27.26, 29.30, 29.43, 29.53, 29.57, 29.58, 29.61, 30.05 (C2') 31.86 47.40 (C1') 52.89 (C3) 53.83 (C6) 54.09 (C8) 61.33 (C2) 67.15 (CH₂) 126.78 (C1*) 128.97 (C4*) 130.38 (C6*) 131.22 (C5*) 133.69 (C2*) 139.03 (C3*); HRMS (Electrospray ionisation (ESI) m/z calcd for $\text{C}_{27}\text{H}_{47}\text{N}_2\text{Br}^+$ = 399.3734, found 399.3732.

3-dodecylamino-1-(4-methylbenzyl)quinuclidinium bromide, QApMe, Yield: 82%, mp 128.6–129.1 °C. (Supporting information, S9-10, S23, S31) ^1H NMR (600 MHz, CDCl_3) δ /ppm: 0.83–0.95 (m, 3 H, H12') 1.13–1.28 (m, 18 H, H3'-H11') 1.36–1.39 (m, 1 H, H2') 1.70–1.79 (m, 1 H, H5a) 1.87–2.11 (m, 2 H, H7) 2.12–2.30 (m, 2 H, H4, H5b) 2.37 (s, 3 H, CH₃) 2.40–2.58 (m, 2 H, H1') 3.01–3.06 (m, 1 H, H2a) 3.15–3.25 (m, 1 H, H3) 3.41–3.50 (m, 1 H, H8a) 3.65–3.82 (m, 2 H, H6a, H8b) 3.89–4.02 (m, 1 H, H8a) 4.11–4.28 (m, 1 H, H2b) 4.82–4.99 (m, 2 H, CH₂) 7.21 (d, $J=7.9$ Hz, 2 H, H3*, H5*) 7.50 (d, $J=7.9$ Hz, 2 H, H2*, H6*); ^{13}C NMR (151 MHz, CDCl_3) δ /ppm: 14.07 (C12') 18.38 (C5) 21.25 (CH₃) 22.63, 22.87 (C7) 24.70 (C4) 27.25, 29.29, 29.43, 29.52, 29.56, 29.57, 29.60, 30.05 (C2') 31.86, 47.38 (C1') 52.87 (C3) 53.71 (C6) 53.93 (C8) 61.20 (C2) 66.83 (CH₂) 123.85 (C1*) 129.75 (C3*, C5*) 133.15 (C2*, C6*) 140.64 (C4*), HRMS (Electrospray ionisation (ESI) m/z calcd for $\text{C}_{27}\text{H}_{47}\text{N}_2\text{Br}^+$ = 399.3734, found 399.3731.

3-dodecylamino-1-(3-chlorobenzyl)quinuclidinium bromide, QAmCl, Yield: 66%, mp 129.2–130.1 °C. (Supporting information, S11-12, S24, S32) ^1H NMR (600 MHz, CDCl_3) δ /ppm: 0.88 (t, $J=6.9$ Hz, 3 H, H12') 1.24–1.31 (m, 18 H, H3'-H11') 1.39–1.41 (m, 2 H, H2') 1.75–1.84 (m, 1 H, H5b) 1.91–2.00 (m, 1 H, H7a) 2.03–2.11 (m, 1 H, H7b) 2.15–2.20 (m, 1 H, H4) 2.21–2.27 (m, 1 H, H5a) 2.39–2.53 (m, 2 H, H1') 3.08–3.12 (m, 1 H, H2b) 3.17–3.24 (m, 1 H, H3) 3.48–3.56 (m, 1 H, H6b) 3.74–3.84 (m, 2 H, H8b, H6a) 3.94–4.02 (m, 1 H, H8b) 4.21 (ddd, $J=12.1, 9.2, 2.2$ Hz, 1 H, H2a) 5.04 (d, $J=12.5$ Hz, 1 H, CH₂a) 5.10 (d, $J=13.2$ Hz, 1 H, CH₂b) 7.36 (t, $J=7.7$ Hz, 1 H, H6*) 7.41 (d, $J=8.1$ Hz, 1 H, H4*) 7.60 (s, 1 H, H2*) 7.66 (d, $J=7.3$ Hz, 1 H, H5*); ^{13}C NMR (151 MHz, CDCl_3) δ /ppm: 14.05 (C12') 18.37 (C5) 22.63, 22.86 (C7) 24.59 (C4) 27.25, 29.28, 29.43, 29.52, 29.57, 29.60, 30.03 (C2') 31.86, 47.39 (C1') 52.86 (C3) 54.01 (C6) 54.15 (C8) 61.28 (C2) 65.72 (CH₂) 129.03 (C1*) 130.45 (C4*) 130.68 (C6*) 131.79 (C2*) 132.81 (C5*) 134.95 (C3*); HRMS (Electrospray ionisation (ESI) m/z calcd for $\text{C}_{26}\text{H}_{44}\text{N}_2\text{Cl}^+$ = 419.3188, found 419.3184.

3-dodecylamino-1-(4-chlorobenzyl)quinuclidinium bromide, QApCl, Yield: 97%, mp 154.2–155.2 °C. (Supporting information, S13–14, S25, S33) $^1\text{H NMR}$ (600 MHz, CDCl_3) δ /ppm: 0.88 (t, $J=6.9$ Hz, 3 H, H12') 1.21–1.33 (m, 18 H, H3'-H11') 1.37–1.42 (m, 2 H, H2') 1.72–1.81 (m, 1 H, H5b) 1.90–1.98 (m, 1 H, H7a) 2.01–2.08 (m, 1 H, H7b) 2.15–2.17 (m, 1 H, H4) 2.20–2.24 (m, 1 H, H5a) 2.38–2.51 (m, 2 H, H1') 3.06 (dt, $J=12.5$, 2.9 Hz, 1 H, H2a) 3.16–3.21 (m, 1 H, H3) 3.43–3.51 (m, 1 H, H6b) 3.70–3.80 (m, 2 H, H8b, H6a) 3.90–4.00 (m, 1 H, H8a) 4.12–4.23 (m, 1 H, H2b) 5.03 (d, $J=13.2$ Hz, 1 H, CH_2a) 5.11 (d, $J=12.5$ Hz, 1 H, CH_2b) 7.37 (d, $J=8.1$ Hz, 2 H, H2*, H6*) 7.63 (d, $J=8.8$ Hz, 2 H, H3*, H5*); $^{13}\text{C NMR}$ (151 MHz, CDCl_3) δ /ppm: 14.06 (C12') 18.38 (C5) 22.64, 22.85 (C7) 24.67, 27.25, 29.30, 29.44, 29.53, 29.57, 29.59, 29.61, 30.02 (C2') 31.86, 47.40 (C1') 52.84 (C3) 53.89 (C6) 54.02 (C8) 61.22 (C2) 65.65 (CH_2) 125.52 (C1*) 129.37 (C3*, C5*) 134.68 (C2*, C6*) 136.95 (C4*); HRMS (Electrospray ionisation (ESI) m/z calcd for $\text{C}_{26}\text{H}_{44}\text{N}_2\text{Cl}^+$ = 419.3188, found 419.3186.

3-dodecylamino-1-(3-bromobenzyl)quinuclidinium bromide, QAmBr, Yield: 69%, mp 142.8–143.4 °C. (Supporting information, S15–16, S26, S34) $^1\text{H NMR}$ (600 MHz, CDCl_3) δ /ppm: 0.88 (t, $J=6.9$ Hz, 3 H, H12') 1.14–1.34 (m, 18 H, H3'-H11') 1.37–1.42 (m, 2 H, H2') 1.74–1.86 (m, 1 H, H5b) 1.86–2.14 (m, 2 H, H7) 2.15–2.32 (m, 2 H, H4, H5a) 2.38–2.57 (m, 2 H, H1') 3.07–3.13 (m, 1 H, H2a) 3.17–3.26 (m, 1 H, H3) 3.45–3.59 (m, 1 H, H6b) 3.70–3.88 (m, 2 H, H6a, H8b) 3.95–4.08 (m, 1 H, H8a) 4.17–4.32 (m, 1 H, H2b) 5.00–5.17 (m, 2 H, CH_2) 7.28–7.32 (m, 1 H, H6*) 7.56–7.59 (m, 1 H, H5*) 7.70–7.79 (m, 2 H, H2*, H4*); $^{13}\text{C NMR}$ (151 MHz, CDCl_3) δ /ppm: 14.07 (C12') 18.36 (C5) 22.63, 22.85 (C7) 24.56, 27.25, 29.29, 29.43, 29.52, 29.57, 29.60, 30.02 (C2') 31.86, 47.39 (C1') 52.84 (C3) 53.97 (C6) 54.10 (C8) 61.24 (C2) 65.63 (CH_2) 122.97 (C3*) 129.28 (C1*) 130.70 (C6*) 132.28 (C4*) 133.62 (C5*) 135.60 (C2*); HRMS (Electrospray ionisation (ESI) m/z calcd for $\text{C}_{26}\text{H}_{44}\text{N}_2\text{Br}^+$ = 463.2682, found 463.2680.

3-dodecylamino-1-(4-bromobenzyl)quinuclidinium bromide, QApBr, Yield: 82%, mp 133.8–134.7 °C. (Supporting information, S17–18, S27, S35) $^1\text{H NMR}$ (600 MHz, CDCl_3) δ /ppm: 0.88 (t, $J=6.9$ Hz, 3 H, H12') 1.14–1.34 (m, 18 H, H3'-H11') 1.39–1.43 (m, 2 H, H2') 1.72–1.82 (m, 1 H, H5b) 1.87–1.97 (m, 1 H, H7a) 1.99–2.08 (m, 1 H, H7b) 2.13–2.31 (m, 2 H, H4, H5a) 2.38–2.56 (m, 2 H, H1') 3.07 (dt, $J=12.5$, 3.0 Hz, 1 H, H2b) 3.15–3.22 (m, 1 H, H3) 3.43–3.53 (m, 1 H, H6b) 3.68–3.81 (m, 2 H, H6a; H8b) 3.86–4.00 (m, 1 H, H8a) 4.16 (ddd, $J=12.2$, 8.9, 2.6 Hz, 1 H, H2b) 4.98–5.14 (m, 2 H, CH_2) 7.50–7.54 (m, 2 H, H2*; H6*) 7.54–7.58 (m, 2 H, H3*; H5*); $^{13}\text{C NMR}$ (101 MHz, CDCl_3) δ /ppm: 14.07 (C12') 18.35 (C5) 22.64, 22.83 (C7) 24.62 (C4) 27.24, 29.29, 29.43, 29.53, 29.57, 29.58, 29.61, 30.00 (C2') 31.86, 47.38 (C1') 52.82 (C3) 53.89 (C6) 53.98 (C8) 61.14 (C2) 65.62 (CH_2) 125.24 (C4*) 125.99 (C1*) 132.32 (C2*; C6*) 134.90 (C3*; C5*); HRMS (Electrospray ionisation (ESI) m/z calcd for $\text{C}_{26}\text{H}_{44}\text{N}_2\text{Br}^+$ = 463.2682, found 463.2684.

Broth microdilution assay

The minimum inhibitory concentration (MIC) of the newly synthesized quaternary 3-aminoquinuclidine compounds and the precursor of quaternization was tested on a panel of Gram-positive (*Staphylococcus aureus* ATCC25923, *Staphylococcus aureus* MRSA (clinical isolate), *Staphylococcus aureus* ATCC33591, *Bacillus cereus* ATCC14579, *Listeria monocytogenes* ATCC7644, *Enterococcus faecalis* ATCC29212) and Gram-negative (*Escherichia coli* ATCC25922, *Salmonella enterica* (food isolate), *Pseudomonas aeruginosa* ATCC27853) bacteria. The bacterial strains used for this study were obtained from BioGnost. The method for determining the MIC was performed according to the standardized protocol of the Clinical and Laboratory Standard Institute ref. The selected bacteria were grown overnight in Mueller-Hinton broth (MHB) at the desired optimal temperature for the tested strain. The next day, the culture was inoculated into fresh MHB and propagated further until the exponential growth phase was reached. The culture was then diluted again in MHB to a final concentration of 5×10^5 CFU/mL. An aliquot of 50 μL of the prepared bacterial cell culture was added to the wells of the 96-well plate containing twofold dilutions of the tested compounds in MHB (250 μM to 0.25 μM). After overnight incubation of the cells, the MIC values were visually determined as the lowest concentration that inhibited bacterial growth. Visual inspection of the MIC was verified with 2-(4-iodophenyl)-3-(4-nitrophenyl)-5-phenyltetrazolium chloride reagent (INT) (6 mg/mL), which turns purple in the presence of viable bacterial cells.

Biofilm inhibition assay

The efficacy of the selected QAC candidates in inhibiting bacterial biofilm formation was investigated using the representative Gram-positive bacterium *Staphylococcus aureus* ATCC25923. The overnight culture of the selected strain was diluted 10 times and further propagated in MHB. Once the culture reached the exponential growth phase, it was diluted to a final concentration of 5×10^6 CFU/mL and added to the wells of the previously prepared duplicates of 2-fold serial dilutions of the tested compounds (100 $\mu\text{g}/\text{mL}$ to 3.25 $\mu\text{g}/\text{mL}$) in the wells of the 96-well plate. The minimum biofilm inhibitory concentrations (MBICs) were determined the following day using the crystal violet staining method. Briefly, MHB supernatant was aspirated from each analysed well and plates were dried in an incubator at 60 °C for 1 h. After the formed biofilm was immobilized, it was further incubated with 100 μL of 1% crystal violet (CV) solution at room temperature. After the stain was removed, wells were rinsed twice with sterile Milli-Q water. Residues of CV-stained biofilms were treated with 100 μL of 70% ethanol for 1 h at room temperature. If necessary, the contents of the wells were resuspended using the multichannel pipette prior to absorbance measurement. The absorbance of samples was measured using the ELx808 optical plate reader (Bio-Tek) at 595 nm. The results were expressed as a percentage of biofilm inhibition formation compared to the formed biofilm of the untreated control.

Time-resolved growth analysis

The effect of treatment with MIC and sub-MIC concentrations of the QAC candidates on the growth curve of the *Escherichia coli* ATCC25922 cell population was evaluated by in-time absorbance measurements for 24 h. Exponentially grown *E. coli* ATCC25922 population was diluted in MHB to the final concentration of 5×10^4 CFU/mL, upon which a 50 μ L aliquot of prepared culture was added to the wells of the 96-well plate containing $\frac{1}{2}$ MIC and MIC concentrations of the candidate compounds. Plates were incubated at 37 °C with constant shaking in the ELx808 optical reader (Bio-Tek). Optical density of tested samples was measured at intervals of 10 min for 24 h. Obtained growth curves of the cells in treatment were compared to the growth curve of untreated cells and represent the mean values of two independent experiments performed in triplicates.

Potential of bacterial resistance development

The potential of QAC candidates to activate bacterial resistance mechanisms was investigated by determining the MIC of selected compounds in the presence of carbonyl cyanide-3-chlorophenylhydrazone (CCCP) (Sigma Aldrich). CCCP acts as an inhibitor of ATP synthesis pathways and prevents the elimination of toxic compounds from the cell mediated by the efflux pump. The bacterial strain used for this purpose was *Staphylococcus aureus* ATCC33591 (MRSA), which contains genes coding for the expression of efflux pumps. The optimal CCCP concentration used in this experiment was determined based on the previously determined MIC of CCCP against the selected bacteria. An exponentially grown culture of *S. aureus* ATCC33591 was diluted in MHB to a final concentration of 5×10^5 CFU/mL and added to the wells of the 96-well plate containing two-fold dilutions of the tested compounds (250 μ M to 0.25 μ M) and a final concentration of CCCP of 10 μ M. The MICs of the candidate compounds in the presence of CCCP were recorded visually after overnight incubation and confirmed with the INT reagent.

Time-kill kinetics assay

Two independent exponentially grown *Staphylococcus aureus* ATCC25923 cultures were centrifuged at 4500 g for a total of 10 min at room temperature. The supernatant of MHB was discarded and the cell pellet from one tube was resuspended in sterile staining buffer (phosphate buffer, pH = 7.4, 1 mM EDTA, 0.1% Tween-20). The cell pellet from another tube was treated with absolute ethanol for ten minutes and centrifuged again under the same conditions. The absolute ethanol was discarded, and the cells were resuspended in staining buffer. Both cell suspensions, viable and dead cells, were further diluted in staining buffer to a final concentration of 1×10^6 CFU/mL and served together with unstained cells as single-stained compensation controls. The tested QAC candidates were diluted in the staining buffer to the final concentration of 2×MIC and MIC. Treated bacteria were labelled according to the manufacturer's instructions with a mixture of two fluorescent dyes, thiazole orange (TO) and propidium iodide (PI), both of which are components of the commercially available BD™ Cell Viability Kit (BD Biosciences, Promega). The viability of the cells during the treatment with the QAC candidates was measured using the NovoCyte Advanteon flow cytometer (Agilent Technologies) and compared with the untreated cells labelled in the same way.

Atomic force microscopy and optical fluorescence microscopy measurements

Adhesive Petri dishes (WPI, Sarasota, FL, USA) coated with Cell-Tak were prepared as previously described⁵⁶. An overnight culture of *Escherichia coli* DH5 α cells was diluted in fresh Mueller-Hinton broth and propagated for one hour. An aliquot of exponentially grown *E. coli* DH5 α cells was incubated in the coated Petri dish for ten minutes. Unbound cells were thoroughly rinsed with culture medium, making sure that the sample did not desiccate. The remaining immobilized cells were incubated for one hour in culture medium at 37 °C. Once the viability (cell division) of the immobilized cells was confirmed, the dish contents were rinsed again with culture medium and the untreated control cells were immediately measured or treated with a 4×MIC concentration of the candidate compounds for three hours. All atomic force microscopy measurements were performed using the Nano-wizard IV system (Bruker, Billerica, MA, USA) operating in quantitative imaging (QI) mode utilizing the MLCT-BIO-DC (E) probe (Bruker, Billerica, MA, USA). All data was acquired at a 500 pN setpoint with the extend/retract speed up to 150 μ m/s while the Z length was up to 3000 nm at 128×128 pixels resolution. The collected AFM data were plane and line fitted and low-pass filtered using the JPK data processing software.

To obtain images of fluorescently stained cells after treatment, the culture medium was replaced with sterile physiological saline solution. Treated cells were stained in the dark with the nucleic fluorophores from the LIVE/DEAD™ BacLight™ Bacterial Viability Kit (ThermoFischer Scientific) according to the manufacturer's instructions. Fluorescence images were taken half an hour after staining using the IX73 inverted fluorescence optical microscope (Olympus, Tokyo, Japan).

Scanning electron microscopy measurements

Each side of a microscopy coverglass was subjected to ultraviolet (UV) radiation for 30 min in a laminar flow hood. The sterile coverglass was then coated with a Cell-Tak solution in 0.1 M NaHCO₃, rinsed with deionized water (mQ water), and air-dried within the sterile environment of the laminar flow hood. An overnight culture of *Escherichia coli* DH5 α was diluted 1:10 in fresh Mueller-Hinton broth (MHB) and incubated for an additional hour at 37 °C with shaking at 170 revolutions per minute (rpm) in an orbital shaker incubator.

Aliquots (1 mL) of the propagated cell culture were transferred into sterile microtubes for the following treatments: untreated control, treatment with 16x minimum inhibitory concentration (MIC) of quaternary ammonium compound QApCl, and treatment with 8x MIC of QApBr. Both untreated and treated cells were incubated at 37 °C with shaking at 600 rpm for one hour.

Subsequently, 50 μ L of each prepared cell sample was transferred onto the previously coated sterile coverglasses and incubated in a closed sterile Petri dish within the laminar flow hood to ensure optimal cell adhesion without

desiccation. Each coverglass was then rinsed three times with sterile phosphate-buffered saline (PBS) and the cells were fixed with 1 mL of 2.5% glutaraldehyde solution. After fixation, the coverglasses were rinsed three times with PBS followed by three additional rinses with mQ water. The coverglasses were then air-dried in the sterile laminar flow hood and subsequently mounted onto round specimen stubs covered with conductive carbon adhesive tape. Finally, to improve conductivity of the prepared samples, the samples were coated using the direct current coater Q150T ES Plus manufactured by Quorum Technologies (Quorum Technologies, UK). All samples were sputtered with a 3 nm layer of platinum using argon while the sputter current was 15 mA. The SEM imaging was done using the SM-74190UEC microscope produced by JEOL (Tokyo, Japan). The measurements were done in Gentle Beam mode with a 2 kV accelerating voltage using the SEI detector. The working distance was kept between 4 mm and 6 mm.

Detection of reactive oxygen species

Overnight culture of *Escherichia coli* ATCC25922 cells was diluted in fresh Mueller Hinton Broth and propagated for one hour. The cell suspension was centrifuged at 4500 g for 10 min at room temperature. The supernatant was discarded and the remaining cell pellet was resuspended (1:10) in sterile phosphate buffer saline (PBS). Aliquot of diluted cells was added to the Eppendorf tube containing PBS solution of compound to be tested. 2 μ L of 2,7-dichlorodihydrofluorescein diacetate (DCFH₂-DA) stock solution (1 mg/mL) was added to each reaction mix tube. Samples were incubated for 30 min in the thermal shaker at 37 °C. Fluorescence signal intensity was measured in 3 min time intervals using Tecan Infinite Pro200 plate reader at the 492 nm excitation and 523 nm emission wavelengths. Hydrogen peroxide was used as positive control. Blank samples were prepared correspondingly to each concentration of compounds tested with PBS buffer containing no cells.

Cytotoxicity

Healthy human cell lines, namely human embryonic kidney cells (HEK293) and retinal pigment epithelial cells (RPE1) were cultured in Dulbecco's Modified Eagle Medium (DMEM, Capricorn Scientific) at 37 °C in a humidified atmosphere with 5% CO₂. The culture medium was supplemented with 10% heat-inactivated fetal bovine serum (FBS, Capricorn Scientific) and a 1% mixture of penicillin and streptomycin (Pen/Strep, Capricorn Scientific). Prior to the experiment, the fully confluent cells were detached with trypsin-EDTA (0.05%) solution (Capricorn Scientific) and gently resuspended in DMEM medium. The concentration of cells in the solution was determined using a cell counter (Scepter, Merck) and the cells were further diluted in DMEM to a final concentration of 1×10^5 cells/mL. Duplicate serial dilutions of the compounds to be tested (250 μ M to 0.25 μ M) were prepared in DMEM in 96-well plates. The cells diluted to the desired concentration were added to the prepared plate containing the compounds and incubated for 48 h at 37 °C in a humidified atmosphere with 5% CO₂. Upon the treatment, 20 μ L of the reagent MTS (CellTiter 96[®] Aqueous One Solution Cell Proliferation Assay, Promega) was added to each well and cells were further incubated with the reagent for additional three hours. Absorbance was measured at 490 nm in ELx808 optical reader (Bio-Tek). The IC₅₀ values were calculated using GraFit 6.0 software and are given as the mean of three independent experiments performed in duplicates.

Conclusion

Quaternary ammonium compounds (QACs) represent a potent class of antimicrobial agents with widespread use and application possibilities. However, fast pace in resistance development demands new QACs design with elucidation of resistance mechanism(s). Here, a new class of QACs based on rationally designed 3-substituted quinuclidine have been synthesized and biologically tested revealing potent broad-spectrum bactericidal candidates with low potential to induce bacterial resistance. Namely, two candidates, QApCl and QApBr were selected for further investigation of their mode of action mechanism. Our results point out membranolytic activities accompanied by high levels of reactive oxygen species (ROS) that together with QACs treatment contribute to potent bactericidal activities. Both candidate compounds can disrupt bacterial membrane in just 15 min of exposure resulting in almost complete annihilation of bacterial population. Taken together, our results contribute to QACs field indicating that careful design choices might lead to structures of potent biological activity and strong membranolytic mode of action accompanied by production of ROS.

Data availability

All data generated or analysed during this study are included in this published article and its supplementary information files.

Received: 7 September 2024; Accepted: 24 October 2024

Published online: 31 October 2024

References

- Dan, W., Gao, J., Qi, X., Wang, J. & Dai, J. Antibacterial quaternary ammonium agents: chemical diversity and biological mechanism. *Eur. J. Med. Chem.* **243**. <https://doi.org/10.1016/j.ejmech.2022.114765> (2022) Elsevier Masson s.r.l.
- Allen, R. A. et al. Ester- and amide-containing multiQACs: exploring multicationic soft antimicrobial agents. *Bioorg. Med. Chem. Lett.* **27**(10), 2107–2112. <https://doi.org/10.1016/j.bmcl.2017.03.077> (2017).
- SkyQuest Technology Consulting Pvt. Ltd. *Quaternary ammonium compounds market* (SkyQuest). <https://www.skyquestt.com/report/quaternary-ammonium-compoundsmarket>
- Vereshchagin, A. N., Frolov, N. A., Egorova, K. S., Seitkalieva, M. M. & Ananikov, V. P. Quaternary ammonium compounds (Qacs) and ionic liquids (ils) as biocides: from simple antiseptics to tunable antimicrobials. *Int. J. Mol. Sci.* **22**(13). <https://doi.org/10.3390/ijms22136793> (2021).
- Fedorowicz, J. & Sączewski, J. Advances in the Synthesis of biologically active quaternary ammonium compounds. *Int. J. Mol. Sci.* **25**(9), 4649. <https://doi.org/10.3390/ijms25094649> (2024).

6. Jennings, M. C., Minbiole, K. P. C. & Wuest, W. M. Quaternary ammonium compounds: an antimicrobial mainstay and platform for innovation to address bacterial resistance. *ACS Infect. Dis.* **1**(7), 288–303. <https://doi.org/10.1021/acinfecdis.5b00047> (2016) Am. Chem. Soc.
7. Alkhalifa, S. et al. Analysis of the destabilization of bacterial membranes by quaternary ammonium compounds: a combined experimental and computational study. *ChemBioChem* **21**(10), 1510–1516. <https://doi.org/10.1002/cbic.201900698> (2020).
8. Gilbert, P. & Moore, L. E. Cationic antiseptics: diversity of action under a common epithet. *J. Appl. Microbiol.* **99**(4), 703–715. <https://doi.org/10.1111/j.1365-2672.2005.02664.x> (2005) Blackwell Publishing Ltd.
9. Maillard, J. Y. Bacterial target sites for biocide action. *J. Appl. Microbiol.* **92**(S1), 16S–27S (2002).
10. Kwaśniewska, D., Chen, Y. L. & Wieczorek, D. Biological activity of quaternary ammonium salts and their derivatives. *Pathogens* **9**(6), 1–12. <https://doi.org/10.3390/pathogens9060459> (2020) MDPI AG.
11. Ferreira, C., Pereira, A. M., Pereira, M. C., Melo, L. F. & Simões, M. Physiological changes induced by the quaternary ammonium compound benzyltrimethylammonium chloride on *Pseudomonas fluorescens*. *J. Antimicrob. Chemother.* **66**(5), 1036–1043. <https://doi.org/10.1093/jac/dkr028> (2011).
12. Inácio, Á. S. et al. Quaternary ammonium surfactant structure determines selective toxicity towards bacteria: Mechanisms of action and clinical implications in antibacterial prophylaxis. *J. Antimicrob. Chemother.* **71**(3), 641–654. <https://doi.org/10.1093/jac/dkv405> (2016).
13. Zhang, C. et al. Quaternary ammonium compounds (QACs): a review on occurrence, fate and toxicity in the environment. *Sci. Total Environ.* **518–519**, 352–362. <https://doi.org/10.1016/j.scitotenv.2015.03.007> (2015) Elsevier.
14. Mohapatra, S. et al. Quaternary ammonium compounds of emerging concern: classification, occurrence, fate, toxicity and antimicrobial resistance. *J. Hazard. Mater.* **445**. <https://doi.org/10.1016/j.jhazmat.2022.130393> (2023) Elsevier B.V.
15. Liao, M., Wei, S., Zhao, J., Wang, J. & Fan, G. Risks of benzalkonium chlorides as emerging contaminants in the environment and possible control strategies from the perspective of ecopharmacovigilance. *Ecotoxicol Environ Saf.* **266**. <https://doi.org/10.1016/j.ecoenv.2023.115613>. (2023). Academic Press.
16. Buffet-Bataillon, S., Tattevin, P., Bonnaure-Mallet, M. & Jolivet-Gougeon, A. Emergence of resistance to antibacterial agents: the role of quaternary ammonium compounds - a critical review. *Int. J. Antimicrob. Agents.* **39**(5), 381–389. <https://doi.org/10.1016/j.ijantimicag.2012.01.011> (2012) (Elsevier B.V.).
17. Jennings, M. C., Forman, M. E., Duggan, S. M., Minbiole, K. P. C. & Wuest, W. M. Efflux pumps might not be the major drivers of QAC resistance in methicillin-resistant staphylococcus aureus. *ChemBioChem* **18**(16), 1573–1577. <https://doi.org/10.1002/cbic.201700233> (2017).
18. Morrison, K. R., Allen, R. A., Minbiole, K. P. C. & Wuest, W. M. More QACs, more questions: Recent advances in structure activity relationships and hurdles in understanding resistance mechanisms. *Tetrahedron Lett.* **60**(3). <https://doi.org/10.1016/j.tetlet.2019.07.026> (2019) Elsevier Ltd.
19. Schallenhammer, S. A. et al. Hybrid BisQACs: potent bicationic quaternary ammonium compounds merging the structures of two commercial antiseptics. *ChemMedChem* **12**(23), 1931–1934. <https://doi.org/10.1002/cmdc.201700597> (2017).
20. Kontos, R. C. et al. An Investigation into rigidity–activity relationships in BisQAC amphiphilic antiseptics. *ChemMedChem* **14**(1), 83–87. <https://doi.org/10.1002/cmdc.201800622> (2019).
21. Leitgeb, A. J. et al. Further investigations into rigidity–activity relationships in BisQAC amphiphilic antiseptics. *ChemMedChem* **15**(8), 667–670. <https://doi.org/10.1002/cmdc.201900662> (2020).
22. B. Belter, S. J. McCarlie, C. E. Boucher-van Jaarsveld, and R. R. Bragg. Investigation into the metabolism of quaternary ammonium compound disinfectants by bacteria. *Microb Drug Resist.* <https://doi.org/10.1089/mdr.2022.0039> (2022).
23. Hoque, J. et al. Cleavable cationic antibacterial amphiphiles: synthesis, mechanism of action, and cytotoxicities. *Langmuir* **28**(33), 12225–12234. <https://doi.org/10.1021/la302303d> (2012).
24. Radman Kastelic, A. et al. New and potent quinuclidine-based antimicrobial agents. *Molecules*. **24**, 1–17. <https://doi.org/10.3390/molecules24142675> (2019).
25. Odžak, R. et al. Quaternary salts derived from 3-substituted quinuclidine as potential antioxidative and antimicrobial agents. *Open. Chem.* **15**(1), 320–331 (2017).
26. Odžak, R. et al. Further Study of the Polar Group's influence on the antibacterial activity of the 3-substituted quinuclidine salts with long alkyl chains. *Antibiotics* **12**(8). <https://doi.org/10.3390/antibiotics12081231> (2023).
27. Bazina, L. et al. Discovery of novel quaternary ammonium compounds based on quinuclidine-3-ol as new potential antimicrobial candidates. *Eur. J. Med. Chem.* **163**, 626–635. <https://doi.org/10.1016/j.ejmech.2018.12.023> (2019).
28. Odžak, R., Crnčević, D., Sabljčić, A., Primožič, I. & Šprung, M. Synthesis and biological evaluation of 3-amidoquinuclidine quaternary ammonium compounds as new soft antibacterial agents. *Pharmaceuticals* **16**(2). <https://doi.org/10.3390/ph16020187> (2023).
29. Odžak, R., Primožič, I. & Tomić, S. 3-Amidoquinuclidine derivatives: synthesis and interaction with butyrylcholinesterase. *Croat Chem. Acta* **80**(1), 101–107 (2007).
30. Paniak, T. J. et al. The antimicrobial activity of mono-, bis-, tris-, and tetracationic amphiphiles derived from simple polyamine platforms. *Bioorg. Med. Chem. Lett.* **24**, 5824–5828. <https://doi.org/10.1016/j.bmcl.2014.10.018> (2014).
31. Black, J. W. et al. TMEDA-derived bicationic amphiphiles: an economical preparation of potent antibacterial agents. *Bioorg. Med. Chem. Lett.* **24**(1), 99–102. <https://doi.org/10.1016/j.bmcl.2013.11.070> (2014).
32. Joondan, N., Caumul, P., Jackson, G. & Jhaumeer Lalloo, S. Novel quaternary ammonium compounds derived from aromatic and cyclic amino acids: Synthesis, physicochemical studies and biological evaluation. *Chem. Phys. Lipids.* **235** <https://doi.org/10.1016/j.chemphyslip.2021.105051> (2021).
33. Takechi-Haraya, Y. et al. Effect of hydrophobic moment on membrane interaction and cell penetration of apolipoprotein E-derived arginine-rich amphiphilic α -helical peptides. *Sci. Rep.* **12**(1). <https://doi.org/10.1038/s41598-022-08876-9> (2022).
34. Joyce, M. et al. Natural product-derived quaternary ammonium compounds with potent antimicrobial activity. *J Antibiot (Tokyo)* **1–4**. <https://doi.org/10.1038/ja.2015.107> (2015).
35. Ali, I. et al. Synthesis and characterization of pyridine-based organic salts: their antibacterial, antibiofilm and wound healing activities. *Bioorg. Chem.* **100** <https://doi.org/10.1016/j.bioorg.2020.103937> (2020).
36. Jennings, M. C., Buttaro, B. A., Minbiole, K. P. C. & Wuest, W. M. Bioorganic investigation of multicationic antimicrobials to combat QAC-resistant staphylococcus aureus. *ACS Infect. Dis.* **1**(7), 304–309. <https://doi.org/10.1021/acinfecdis.5b00032> (2016).
37. Sommers, K. J. et al. Quaternary phosphonium compounds: an examination of non-nitrogenous cationic amphiphiles that evade disinfectant resistance. *ACS Infect. Dis.* **8**(2). <https://doi.org/10.1021/acinfecdis.1c00611> (2022).
38. Bridier, A., Briandet, R., Thomas, V. & Dubois-Brissonnet, F. Resistance of bacterial biofilms to disinfectants: a review. *Biofouling* **27**(9), 1017–1032. <https://doi.org/10.1080/08927014.2011.626899> (2011).
39. Hoque, J. et al. Selective and broad spectrum amphiphilic small molecules to combat bacterial resistance and eradicate biofilms. *Chem. Comm.* **51**(71), 13670–13673. <https://doi.org/10.1039/c5cc05159b> (2015).
40. Saverina, E. A. et al. From antibacterial to antibiofilm targeting: an emerging paradigm shift in the development of Quaternary Ammonium Compounds (QACs). *A ACS Infect. Dis.* **9**(3), 394–422. <https://doi.org/10.1021/acinfecdis.2c00469> (2023) American Chemical Society.
41. Tuon, F. F. et al. Antimicrobial treatment of staphylococcus aureus biofilms. *Antibiotics* **12**(1). <https://doi.org/10.3390/antibiotics12010087> (2023) MDPI.

42. Garrison, M. A., Mahoney, A. R. & Wuest, W. M. Tricypyridinium-inspired QACs yield potent antimicrobials and provide insight into QAC resistance. *ChemMedChem* **16**(3) 463–466. <https://doi.org/10.1002/cmdc.202000604> (2021).
43. Lemos, J. A. et al. The biology of streptococcus mutans. *Microbiol. Spectr.* **7**(1). <https://doi.org/10.1128/microbiolspec.gpp3-0051-2018> (2019).
44. Theophel, K. et al. The importance of growth kinetic analysis in determining bacterial susceptibility against antibiotics and silver nanoparticles. *Front. Microbiol.* **5**(11), 544. <https://doi.org/10.3389/fmicb.2014.00544> (2014).
45. Yates, G. T. & Smotzer, T. On the lag phase and initial decline of microbial growth curves. *J. Theor. Biol.* **244**(3), 511–517. <https://doi.org/10.1016/j.jtbi.2006.08.017> (2007).
46. Brayton, S. R. et al. Soft QPCs: biscationic quaternary phosphonium compounds as soft antimicrobial agents. *ACS Infect. Dis.* <https://doi.org/10.1021/acsinfecdis.2c00624> (2023).
47. Loftsson, T. et al. Soft Antimicrobial Agents: Synthesis and Activity of Labile Environmentally Friendly Long Chain Quaternary Ammonium Compounds. *J. Med. Chem.* **46**, 4173–4181. <https://doi.org/10.1021/jm030829z> (2003).
48. Tischer, M., Pradel, G., Ohlsen, K. & Holzgrabe, U. Quaternary ammonium salts and their antimicrobial potential: targets or nonspecific interactions?. *ChemMedChem* **7**(1), 22–31. <https://doi.org/10.1002/cmdc.201100404> (2012).
49. Kiernan, J. A. Formaldehyde, formalin, paraformaldehyde and glutaraldehyde: what they are and what they do. *Micros Today* **8**(1), 8–13. <https://doi.org/10.1017/s1551929500057060> (2000).
50. Dapson, R. W. Macromolecular changes caused by formalin fixation and antigen retrieval. *Biotech. Histochem.* **82**, 133–140. <https://doi.org/10.1080/10520290701567916> (2007). no. 3.
51. Boulos, L. et al. *LIVE / DEAD BacLightE: application of a new rapid staining method for direct enumeration of viable and total bacteria in drinking water* (1999).
52. Stocks, S. M. Mechanism and use of the commercially available viability stain, BacLight. *Cytometry. Part A* **61**(2), 189–195. <https://doi.org/10.1002/cyto.a.20069> (2004).
53. Kim, T. et al. Design, synthesis, and evaluation of N1,N3-dialkyldioxonaphthoimidazoliums as antibacterial agents against methicillin-resistant *Staphylococcus aureus*. *Eur. J. Med. Chem.* **272** <https://doi.org/10.1016/j.ejmech.2024.116454> (2024).
54. Zhang, X., Ma, J., Chen, M., Wu, Z. & Wang, Z. Microbial responses to transient shock loads of quaternary ammonium compounds with different length of alkyl chain in a membrane bioreactor. *AMB Express.* **8**(1). <https://doi.org/10.1186/s13568-018-0649-5> (2018).
55. Ceragioli, M. et al. Comparative transcriptomic and phenotypic analysis of the responses of *Bacillus cereus* to various disinfectant treatments. *Appl. Environ. Microbiol.* **76**(10), 3352–3360. <https://doi.org/10.1128/AEM.03003-09> (2010).
56. Rončević, T. et al. Antibacterial activity affected by the conformational flexibility in glycine-lysine based α -helical antimicrobial peptides. *J. Med. Chem.* **61**, 2924–2936. <https://doi.org/10.1021/acs.jmedchem.7b01831> (2018).

Acknowledgements

This work was financially supported by the the Croatian Science Foundation grant numbers UIP-2020-02-2356 (M.Š.), IP-2016-06-3775 (I.P.), STIM-REL, Contract Number: KK.01.1.1.01.0003, a project funded by the European Union through the European Regional Development Fund – the Operational Programme Competitiveness and Cohesion 2014–2020 (KK.01.1.1.01) and institutional projects 641-01/23-02/0008 (M.Š.), 641-01/23-02/0010 (R.O.) funded by the Faculty of Science, University of Split.

Author contributions

I.P. designed the new compounds; A.R., and A.R.K. were responsible for the preparation, characterization and purity analysis of the compounds; D.C. determined the antibacterial activity and cytotoxicity; D.C. performed fluorescence measurements, D.C. and M.Š. analyzed and interpreted biological data; L.K. and D.C. collected and analyzed AFM and fluorescence microscopy data; L.K., D.C. and I.W. determined and analyzed SEM data; R.O., I.P. and M.Š. designed and directed the study, I.P. and M.Š. secured funding, M.Š. wrote the manuscript. All authors contributed to and approved the final version of the manuscript.

Declarations

Declaration of generative AI and AI-assisted technologies in the writing process

During the preparation of this work the author(s) used ChatGPT in order to improve language and readability. After using this tool/service, the author(s) reviewed and edited the content as needed and take(s) full responsibility for the content of the publication.

Competing interests

The authors declare no competing interests.

Additional information

Supplementary Information The online version contains supplementary material available at <https://doi.org/10.1038/s41598-024-77647-5>.

Correspondence and requests for materials should be addressed to I.P. or M.Š.

Reprints and permissions information is available at www.nature.com/reprints.

Publisher's note Springer Nature remains neutral with regard to jurisdictional claims in published maps and institutional affiliations.

Open Access This article is licensed under a Creative Commons Attribution-NonCommercial-NoDerivatives 4.0 International License, which permits any non-commercial use, sharing, distribution and reproduction in any medium or format, as long as you give appropriate credit to the original author(s) and the source, provide a link to the Creative Commons licence, and indicate if you modified the licensed material. You do not have permission under this licence to share adapted material derived from this article or parts of it. The images or other third party material in this article are included in the article's Creative Commons licence, unless indicated otherwise in a credit line to the material. If material is not included in the article's Creative Commons licence and your intended use is not permitted by statutory regulation or exceeds the permitted use, you will need to obtain permission directly from the copyright holder. To view a copy of this licence, visit <http://creativecommons.org/licenses/by-nc-nd/4.0/>.

© The Author(s) 2024

4. CONCLUSIONS AND FUTURE PERSPECTIVE

This dissertation presents a comprehensive exploration of the antibacterial potential and mode of action of novel quaternary ammonium compounds (QACs), with the aim of developing QACs with enhanced antibacterial profiles while minimizing environmental and toxicity concerns. The antibacterial potential of three distinct series of QAC led to a progressive strategy in structure optimization derived from findings related to mechanisms of action and of resistance related to structure.

The first series of QACs was derived from the heterocyclic backbone of pyridinium-4-aldoxime, yielding analogues of the commercially available cetylpyridinium chloride (CPC). Unlike CPC, these derivatives contain a polar oxime functional group at the aromatic backbone, which was further modified with long-chain alkyl and aryl substituents. Compounds with alkyl chains containing 14 and 16 carbon atoms exhibited the strongest antimicrobial potential, particularly against Gram-positive bacteria, including methicillin-resistant *Staphylococcus aureus* (MRSA). Atomic force microscopy revealed membranolytic effect against Gram-negative *Escherichia coli*, while cytotoxicity studies showed reduced toxicity toward mammalian cells compared to CPC. However, their overall antibacterial potential was lower than that of CPC, suggesting that the introduction of the polar functional group at the backbone might hinder initial electrostatic interactions with the bacterial membrane by introducing a dipole moment. In addition to reduced ability to interact with the bacterial membrane, the selected compound displayed high potential to activate bacterial resistance by disrupting the QacR dimer responsible for regulation of efflux pump expression. These findings underscored the need for further structural optimization to mitigate the negative impact of increased backbone polarity on antibacterial efficacy.

To address environmental concerns arising from the high chemical stability of commercially available QAC variants, we next focused on synthesizing "soft" QACs with reduced environmental impact. These derivatives were synthesized from the bicyclic quinuclidine scaffold, functionalized with a hydrolysable amide group at the third carbon atom. Building on prior findings, we aimed to reduce the negative effects of increased polarity by introducing long alkyl chains adjacent to the amide functionality. Additionally, the nitrogen atom of the quinuclidine core was substituted with short-chained methyl and allyl groups to minimize steric hindrance. The resulting compounds demonstrated

improved antibacterial activity and potent biofilm inhibition compared to the pyridinium-4-aldoxime derivatives. However, the most potent candidates exhibited a bacteriostatic mode of action, maintaining treated bacterial population in a stationary phase. Membrane integrity was largely preserved, indicating a lower membranolytic potential. Molecular dynamics simulations suggested reduced interaction with a realistic *Staphylococcus aureus* model membrane, likely due to a "hook-like" conformation that diminished penetration through the lipid bilayer. *In vitro* studies indicated that these compounds may act on intracellular targets to inhibit protein synthesis, suggesting a dual mode of antibacterial action. Additionally, docking studies supported the possibility of decomposition by serine proteases like trypsin, highlighting the potential of these derivatives as environmentally safer alternatives with a reduced likelihood of inducing bacterial resistance. This degradation potential is particularly noteworthy given their lower *in vitro* and *in vivo* toxicity rates compared to the conventional commercial analogue, CPC. These findings underscore their potential use as safer ingredients of disinfectant and antiseptic formulations.

Structural optimization in QACs derived from 3-dodecylaminoquinuclidine, featuring non-polar aromatic substituents at the quaternary center, resulted in the most potent antibacterial activity toward both Gram-positive and Gram-negative strains. These compounds exhibited low single-digit micromolar minimum inhibitory concentrations (MICs) and were more effective than CPC in inhibiting biofilm formation. Moreover, these QACs demonstrated potent bactericidal activity, eliminating bacterial populations within fifteen minutes of treatment. Atomic force and scanning electron microscopy revealed extensive membrane damage following exposure to low micromolar concentrations of the selected compounds. Mechanistic analyses indicated that the membranolytic effect was followed by the generation of reactive oxygen species, leading to rapid bacterial death. This strong membranolytic potential led us to hypothesize that the protonation state of the amine functionality under physiological conditions mimics the double-positive charge of bis-QACs, indicating that the amino group is a favorable addition to monoquaternary derivatives. In addition to their strong antibacterial properties, these compounds demonstrated reduced toxicity toward healthy human epidermal cell lines. Moreover, their lower propensity to activate bacterial resistance mechanisms compared to CPC further underscores their potential for therapeutic use.

In summary, this dissertation highlights the importance of rational design in developing next-generation QACs. By exploring structure-activity relationships, it

demonstrates how molecular modifications can enhance antibacterial performance. The structural optimization process showed that fine-tuning hydrophilic and hydrophobic ratio is critical for improvement of antibacterial efficacy while minimizing environmental impact (Figure 5). These findings provide a foundation for the design of structurally optimized QAC derivatives with broad application.

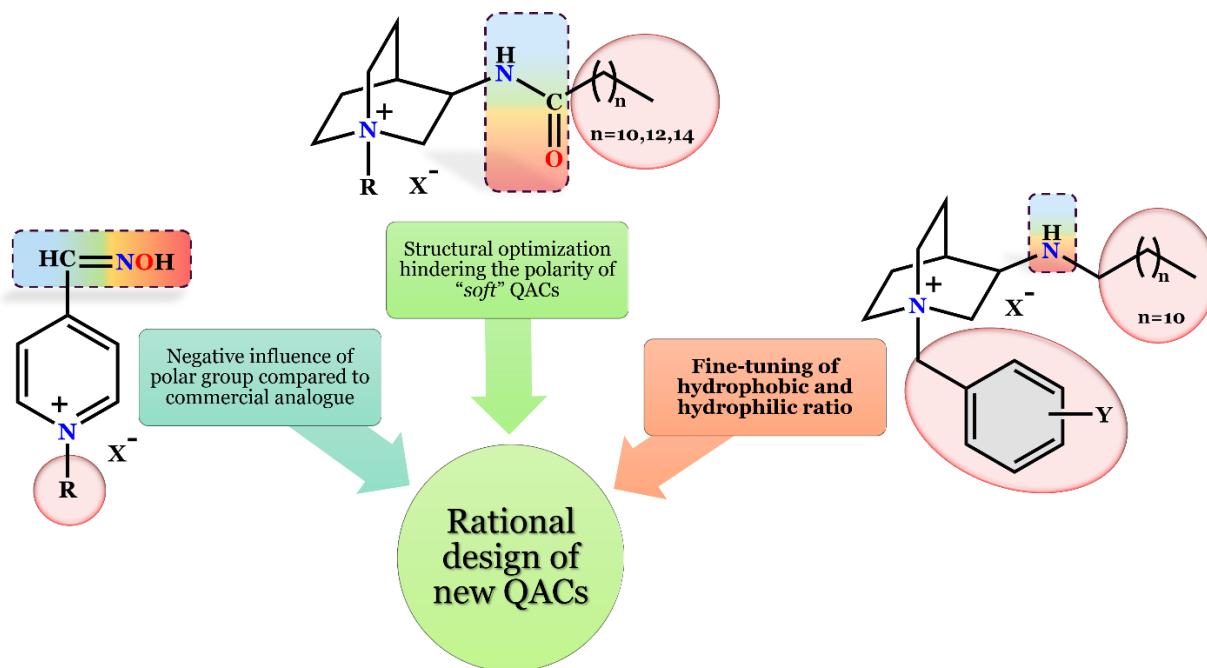


Figure 5. Schematic representation of the structural optimization process to yield QACs as potent antibacterial agents. Polar groups are highlighted in a dashed rectangle with red color indicating high electron density and dipole moment. In contrast, increased hydrophobicity is represented by pink circles/ellipses.

Building on these findings, future research should refine the structure-activity relationships of QAC derivatives by exploring additional functional groups and substituents to enhance antibacterial potency while maintaining low toxicity. A deeper investigation into alternative modes of action, such as intracellular targets, could shed light on the bacteriostatic effects and other mechanisms underlying the activity of this class of compounds. Broadening the evaluation of these derivatives to include a wider range of clinically relevant pathogens, particularly multidrug-resistant strains, and assessing their antifungal and antiviral potential, offers promising avenues for application. Environmental safety remains a critical consideration, necessitating long-term biodegradation studies to ensure the development of sustainable antimicrobial agents. By addressing these research priorities, the field can advance toward creating multifunctional, eco-friendly antimicrobials capable of effectively combating bacterial resistance while ensuring safety for human health and the environment.

5. APPENDIX

5.1. Supplementary material to chapter 3.2.

A dual antibacterial action of soft quaternary ammonium compounds: bacteriostatic effects, membrane integrity, and reduced *in vitro* and *in vivo* toxicity

Supporting Information

Table S1. Phospholipid constituents of the model *Staphylococcus Aureus* (left column) together with their assigned 4-letter codes (right column).¹

Lipids	Lipid code
PG (a15:0/a15:0)	FFPG
PG (i15:0/a15:0)	IFPG
PG (16:0/a15:0)	PFPG
PG (i17:0/a15:0)	JFPG
PG (a17:0/a15:0)	ZFPG
PG (i17:0/i15:0)	JIPG
PG (a17:0/i15:0)	ZIPG
PG (18:0/a15:0)	SFPG
PG (i19:0/a15:0)	VFPG
PG (a19:0/a15:0)	TFPG
PG (a19:0/i15:0)	TIPG
PG (20:0/a15:0)	XFPG
PG (18:1/i15:0)	OIPG
PG (18:1/a15:0)	OFPG
LPG (i17:0/a15:0)	JFGK
LPG (a17:0/a15:0)	ZFGK
LPG (18:0/a15:0)	SFGK
LPG (a19:0/a15:0)	TFGK
CL (a17:0/a15:0)	ZFCL

Table S2. Letter Codes representing Fatty Acyl Tails which are not present in CHARMM-GUI Membrane Builder module.¹

Lipid tail	Code	Explanation
a15:0	F	anteisopentadecanoyl, F ifteen for pentadecane
i15:0	I	I sopentadecanoyl
a17:0	Z	anteisomargaroyl, Z for g
i17:0	J	isomargaroyl, J for g
a19:0	T	an T eisononadecanoyl
i19:0	V	isononadecanoyl, V is after T and resembles an iso branch
20:0	X	arachidoyl, X for ch

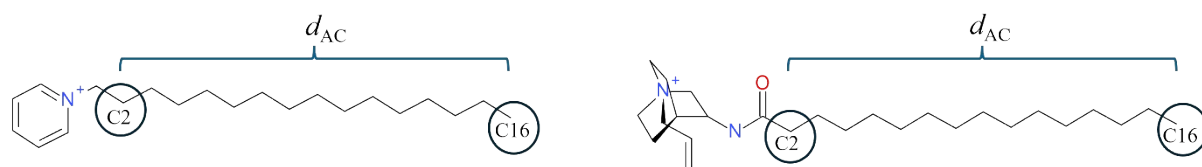
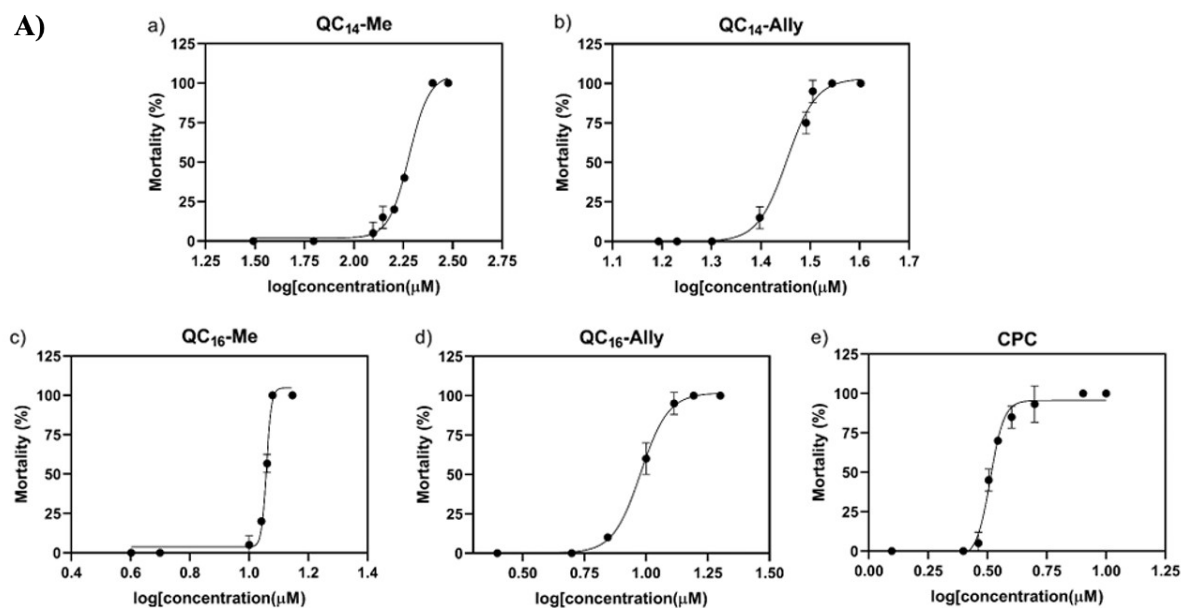


Figure S1. CPC (left) and QC₁₆-Allyl molecules. Atoms used to define the distance d_{AC} (distance between the C2 and C16 atoms in the aliphatic chain) are denoted with the blue ellipses.



B)

Sample	LC ₅₀ , μM	Confidence interval, CI (95%)	Hill Slope
QC ₁₄ -Me	190.1	183.0-200.1	8.481
QC ₁₄ -Allyl	28.37	27.46-29.30	14.75
QC ₁₆ -Me	11.45	11.38-11.52	51.81
QC ₁₆ -Allyl	9.516	9.082-9.895	7.756
CPC	3.250	3.150-3.360	14.97

Figure S2. **A)** Concentration-response curves used for the calculation of the *Danio rerio* mortality after 120 hours of exposure to: a) QC₁₄-Me, b) QC₁₄-Allyl, c) QC₁₆-Me, d) QC₁₆-Allyl and e) CPC. **B)** Dose-inhibition results obtained after 120 hours of *Danio rerio* exposure to tested samples.

5.2. Supplementary material to chapter 3.3.

Naturally derived 3-aminoquinuclidine salts as new promising therapeutic agents

SUPPORTING INFORMATION

Naturally derived 3-aminoquinuclidine salts as new promising therapeutic agents

Doris Crnčević^{1,2}, Alma Ramić³, Andrea Radman Kastelić³, Renata Odžak¹, Lucija Krce⁴, Ines Primožić³ and Matilda Šprung^{1*}

¹ University of Split, Faculty of Science, Department of Chemistry, R. Bošković 33, Split, Croatia

² University of Split, Faculty of Science, Doctoral Study in Biophysics, R. Bošković 33, Split, Croatia

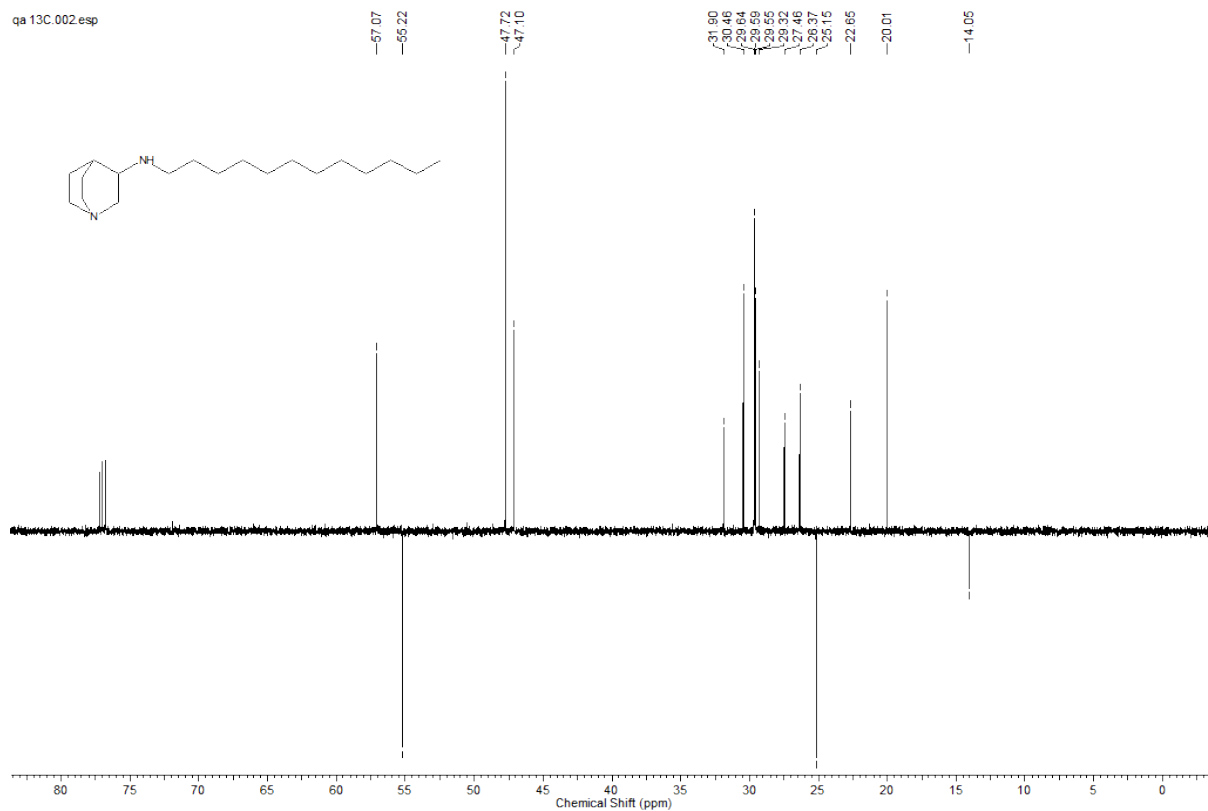
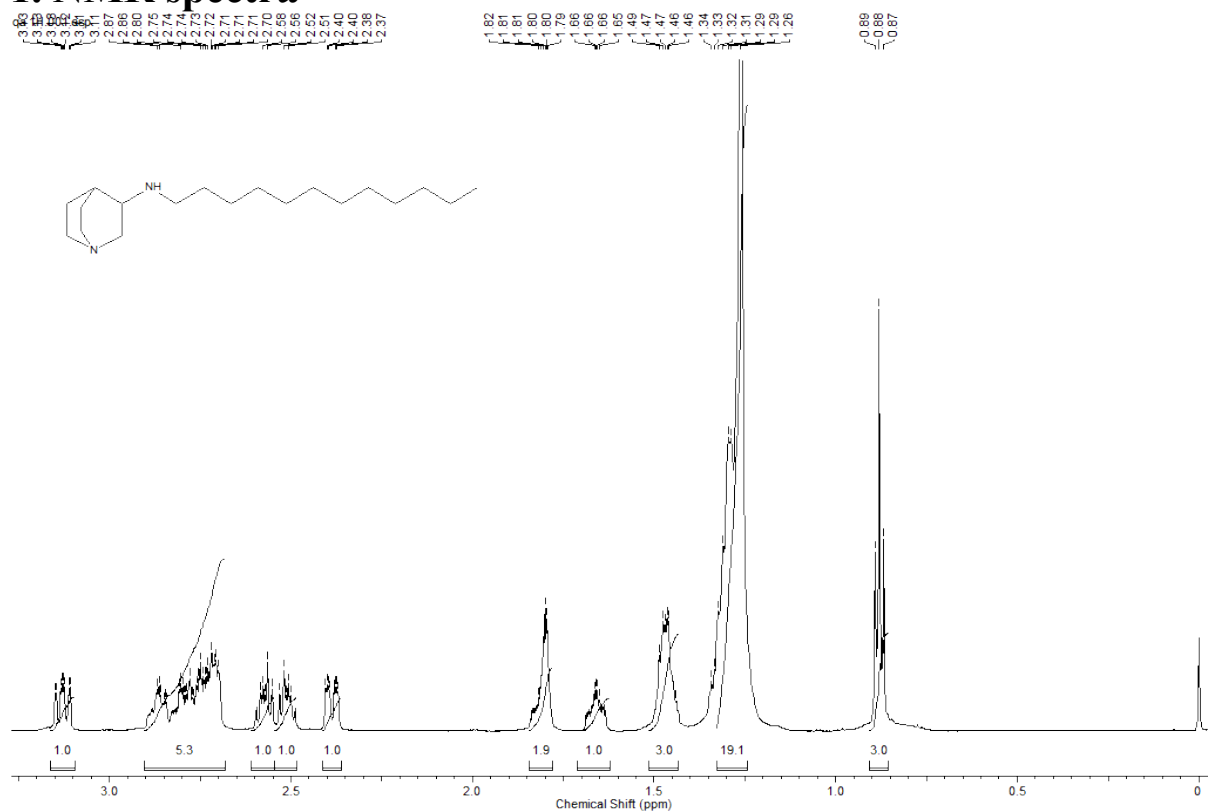
³ University of Zagreb, Faculty of Science, Department of Chemistry, Horvatovac 102a, Zagreb, Croatia

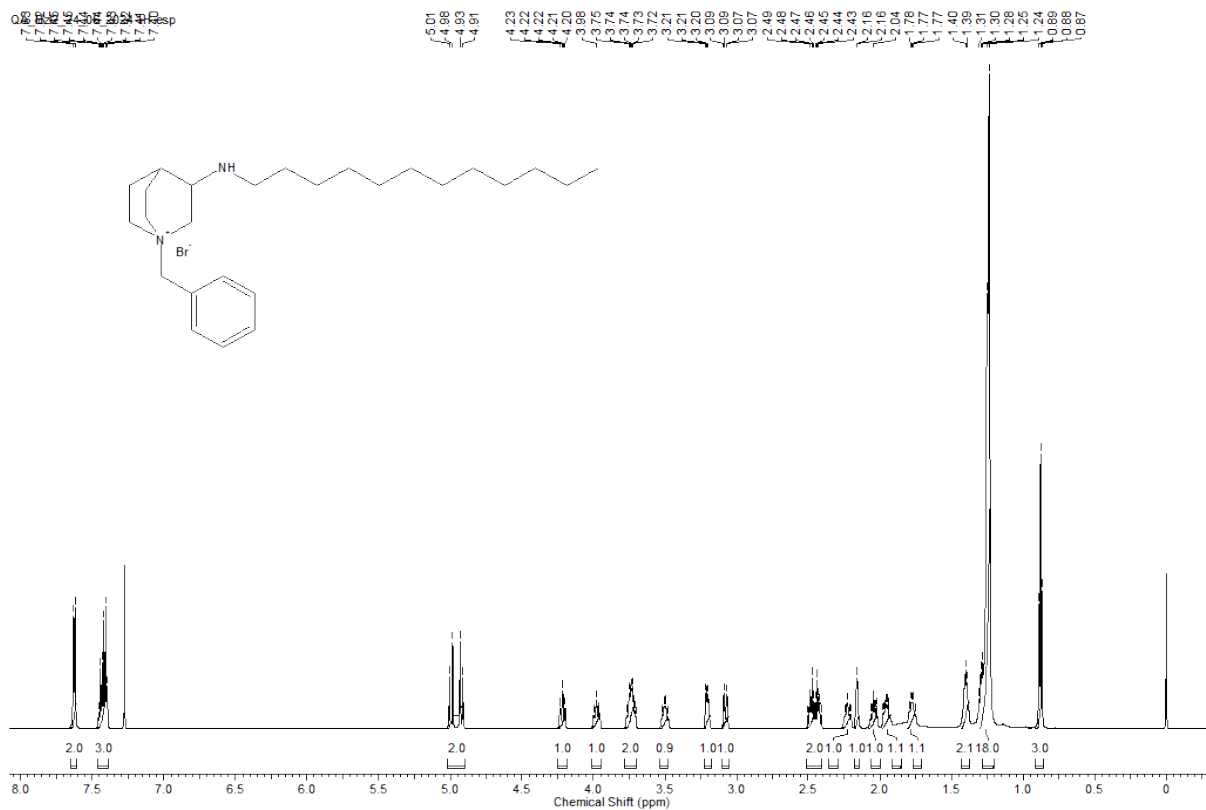
⁴ University of Split, Faculty of Science, Department of Physics, R. Bošković 33, Split, Croatia

Contents

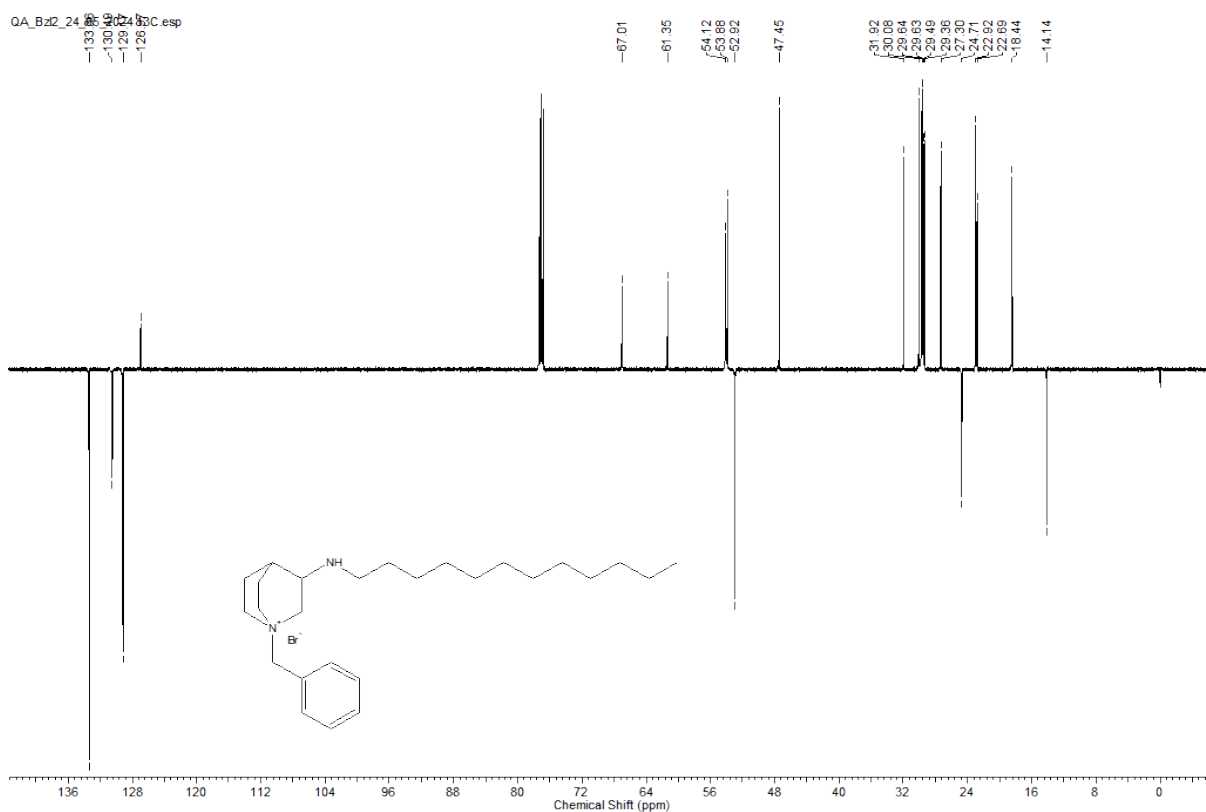
1. NMR spectra	2
2. HRMS spectra.....	11
3. HPLC chromatograms	14

1. NMR spectra

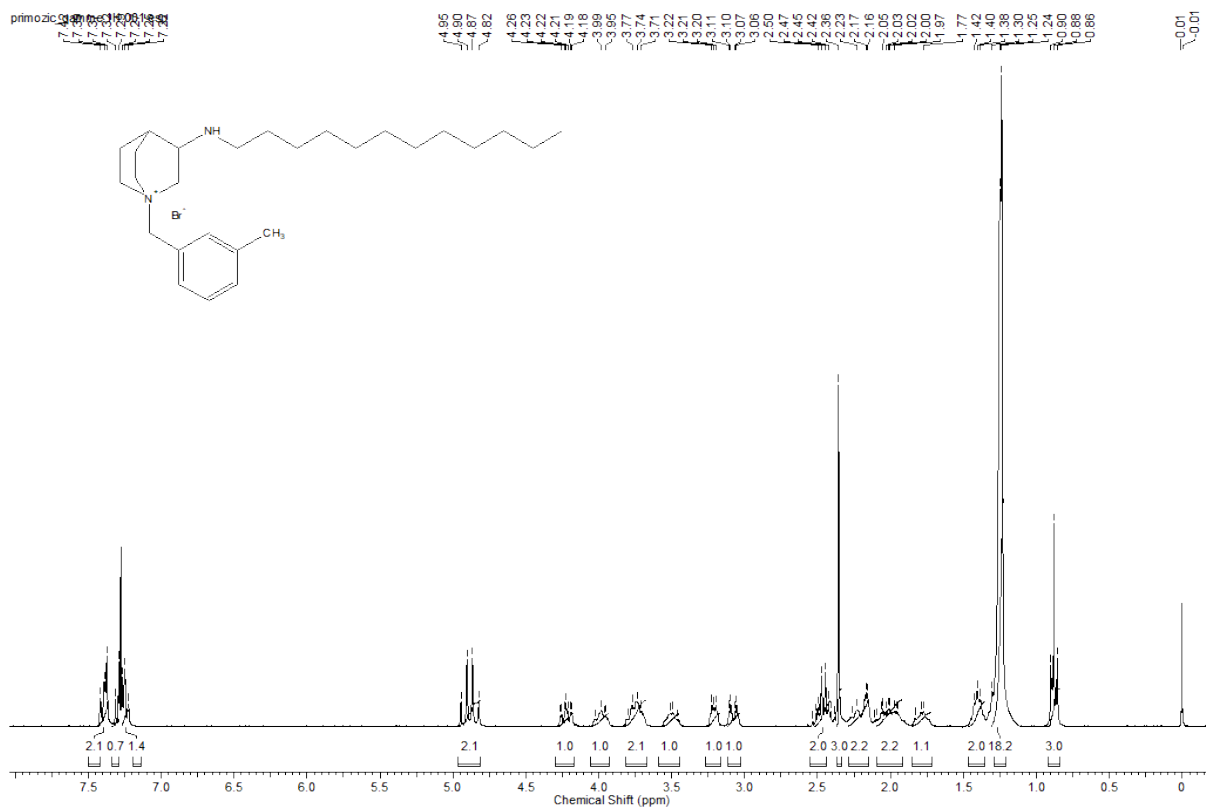




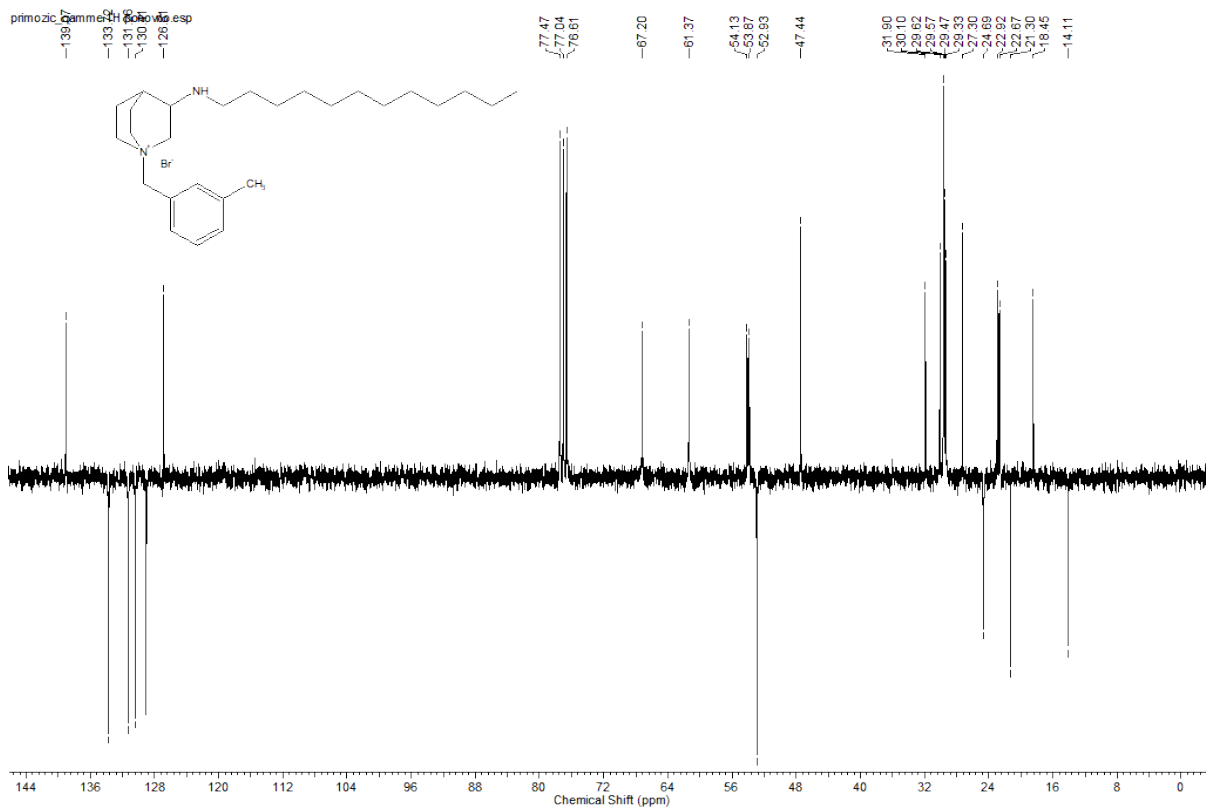
S5. ^1H NMR spectra of QABn



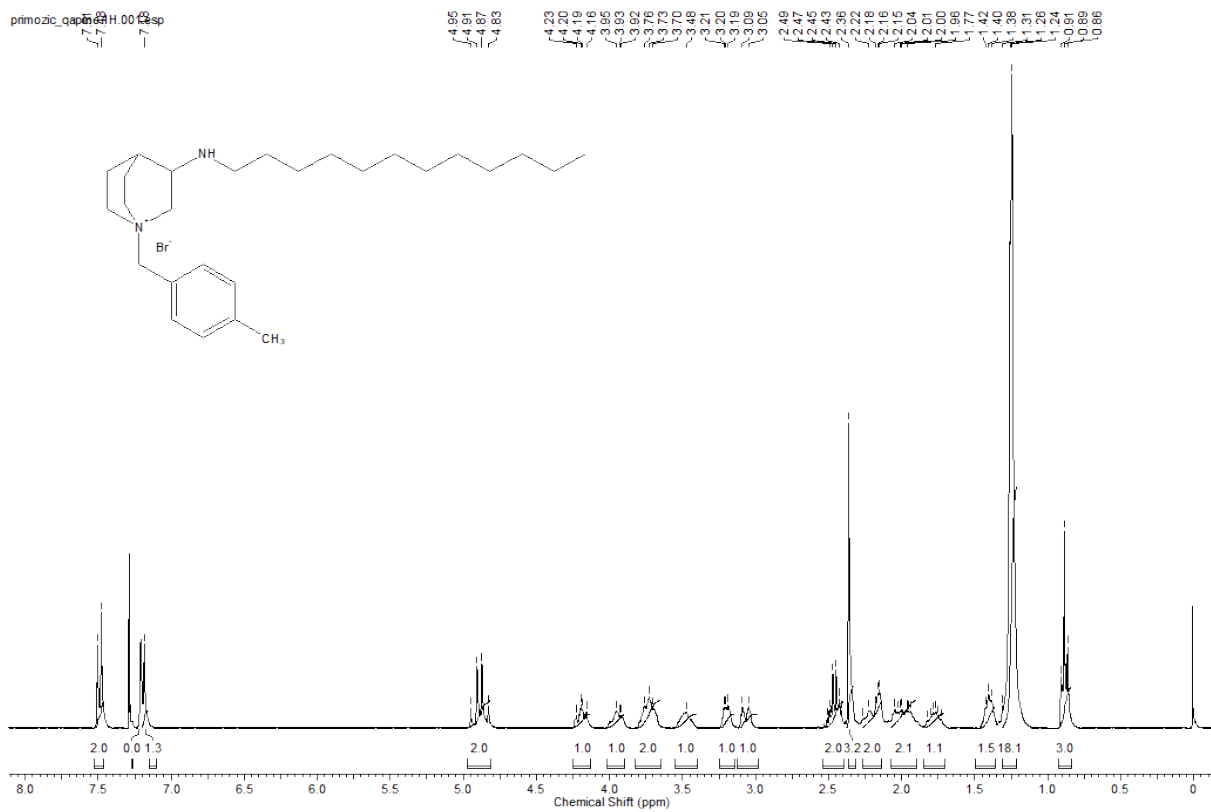
S6. ^{13}C NMR spectra of QABn



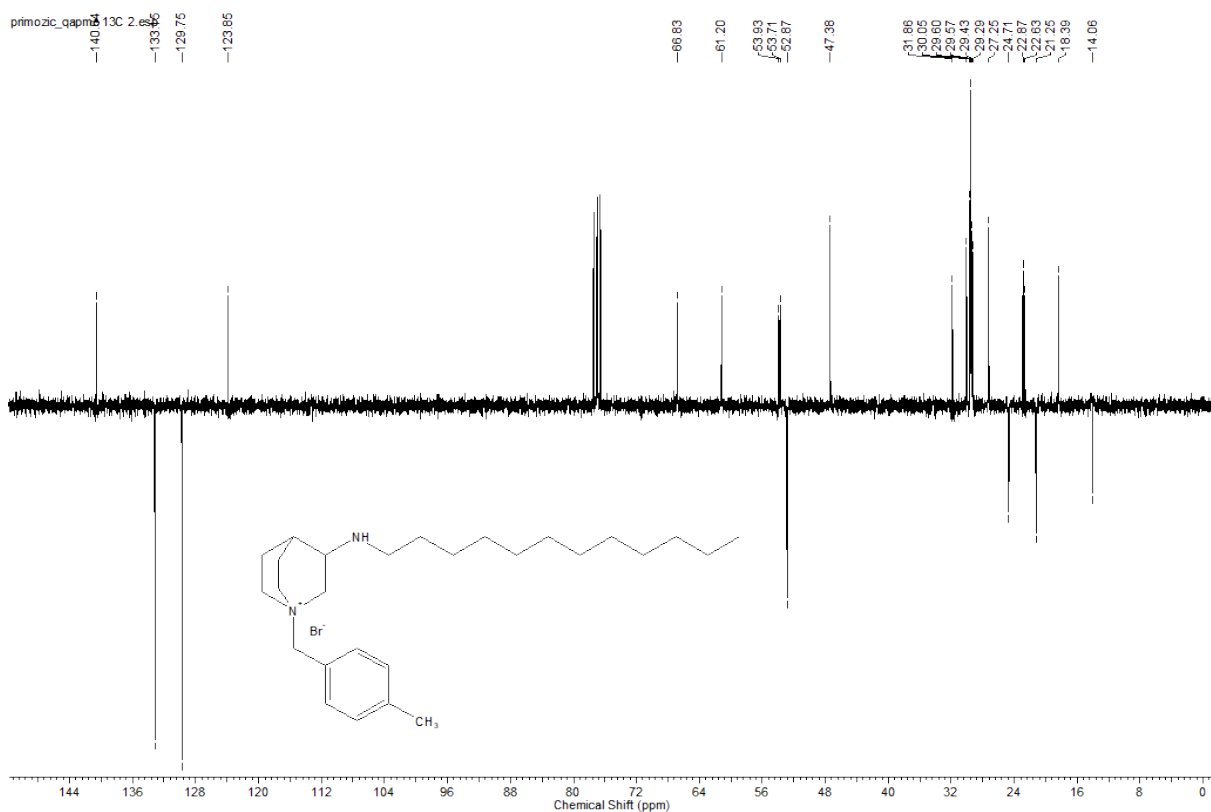
S7. ^1H NMR spectra of QAmMe



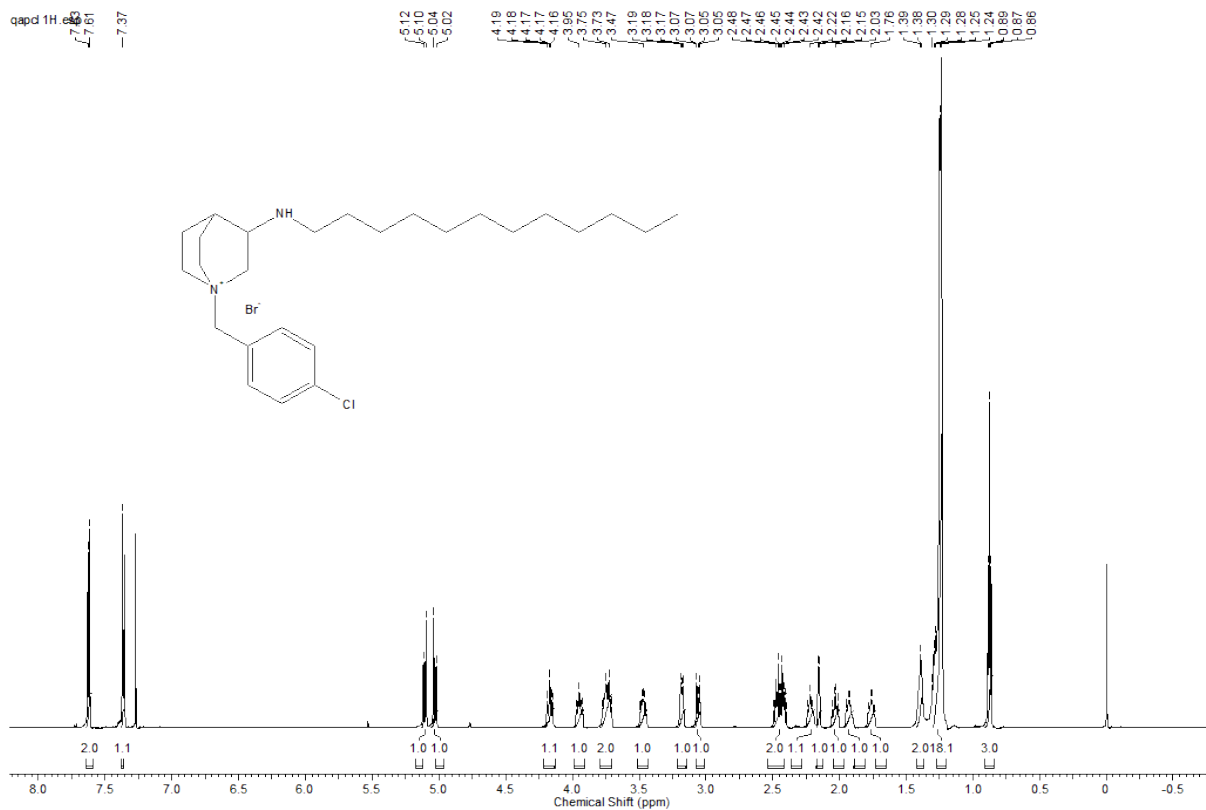
S8. ^{13}C NMR spectra of QAmMe



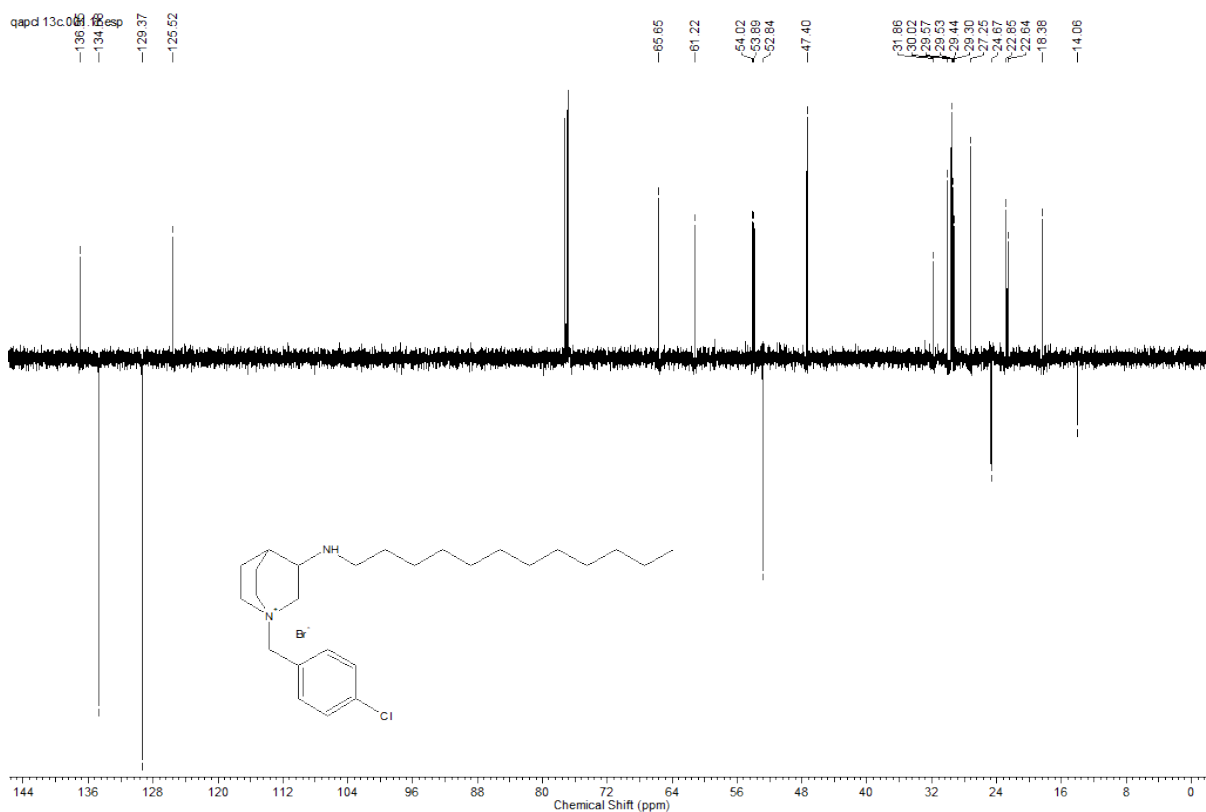
S9. ^1H NMR spectra of QApMe



S10. ^{13}C NMR spectra of QApMe

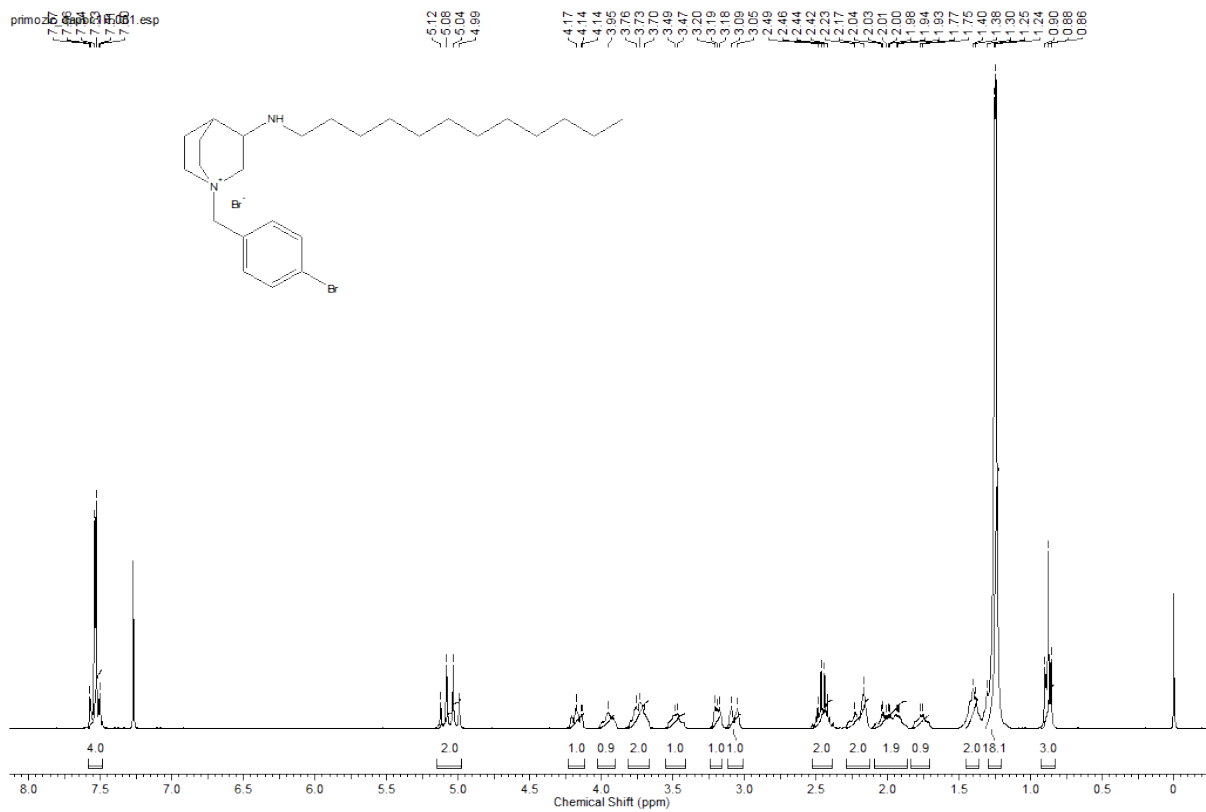


S13. ¹H NMR spectra of QApCl

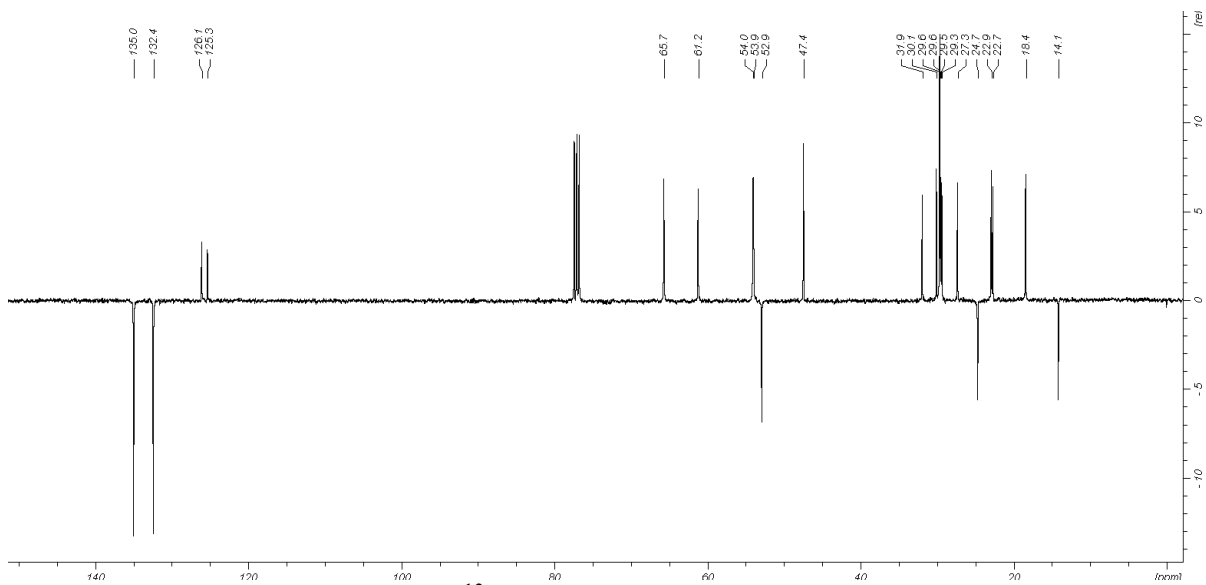


S14. ¹³C NMR spectra of QApCl

primo26_0apb1f001.esp



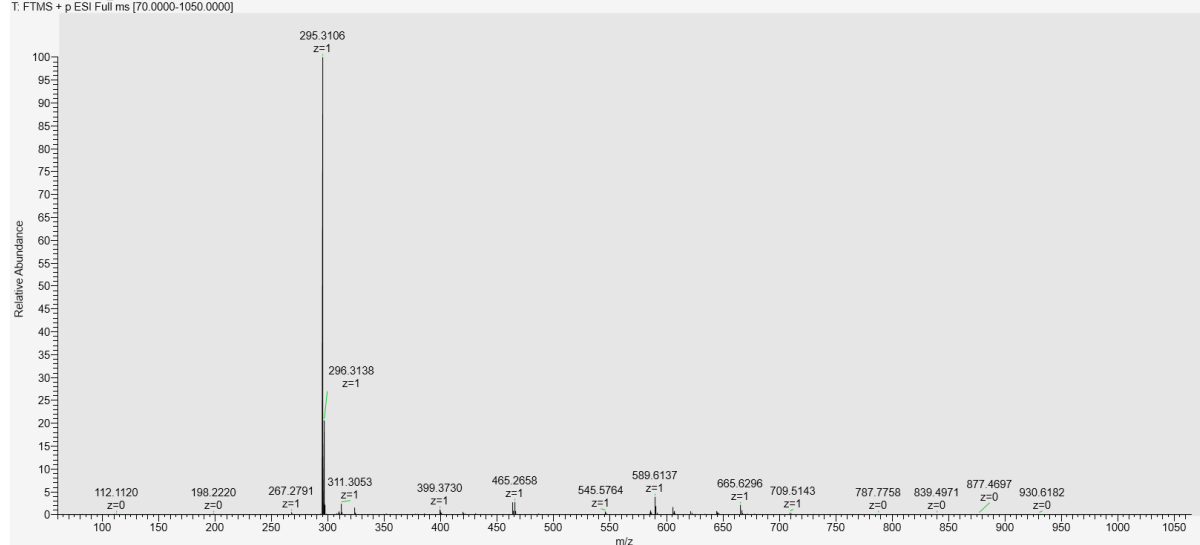
S17. ^1H NMR spectra of QApBr



S18. ^{13}C NMR spectra of QApBr

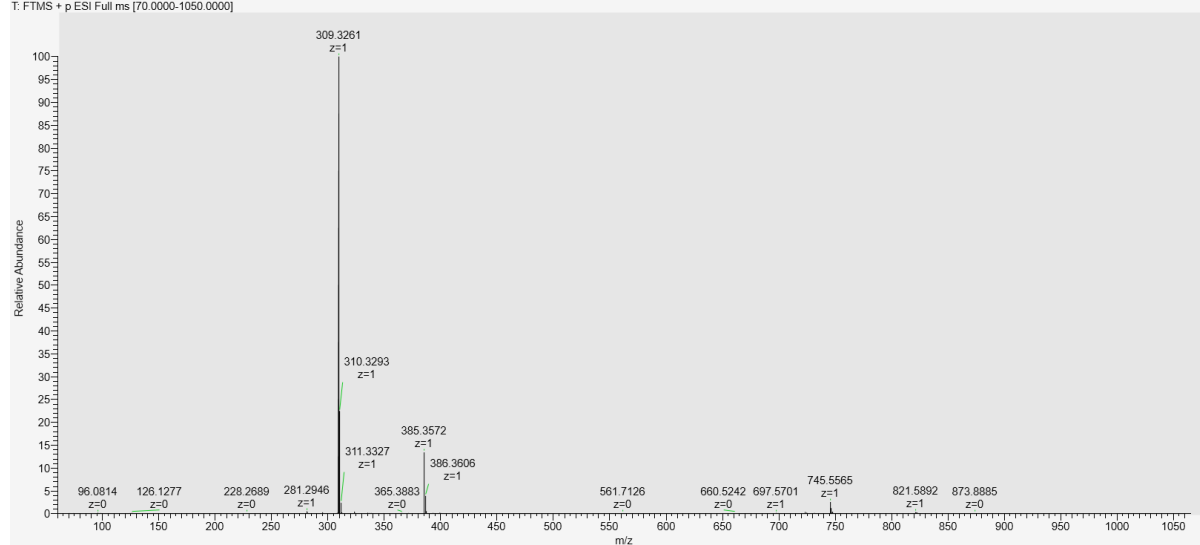
2. HRMS spectra

T: FTMS + p ESI Full ms [70.0000-1050.0000]

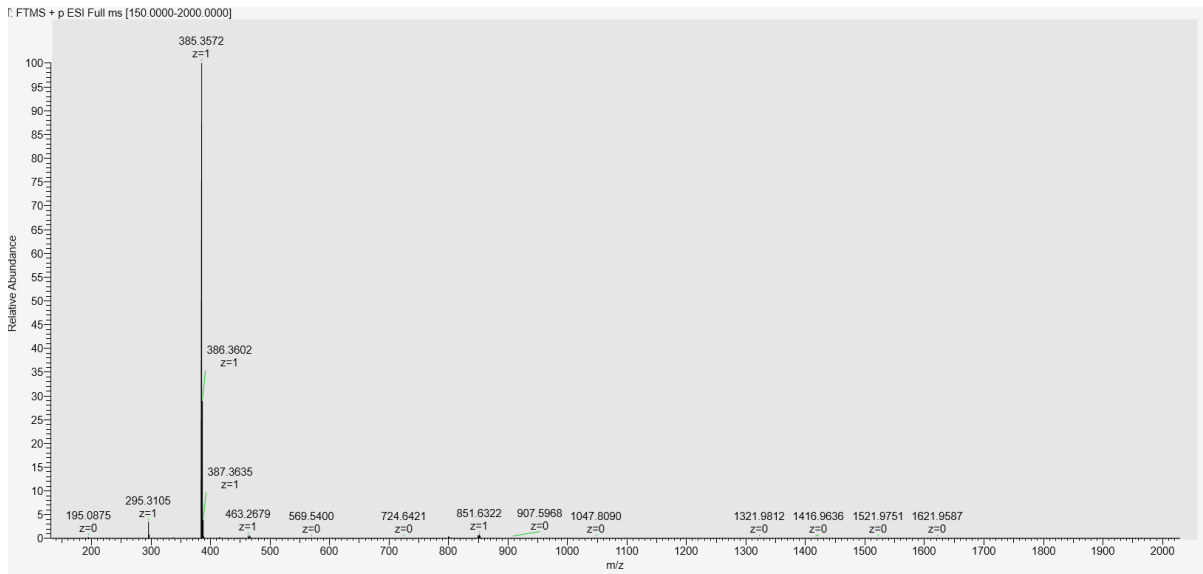


S19. HRMS of QA

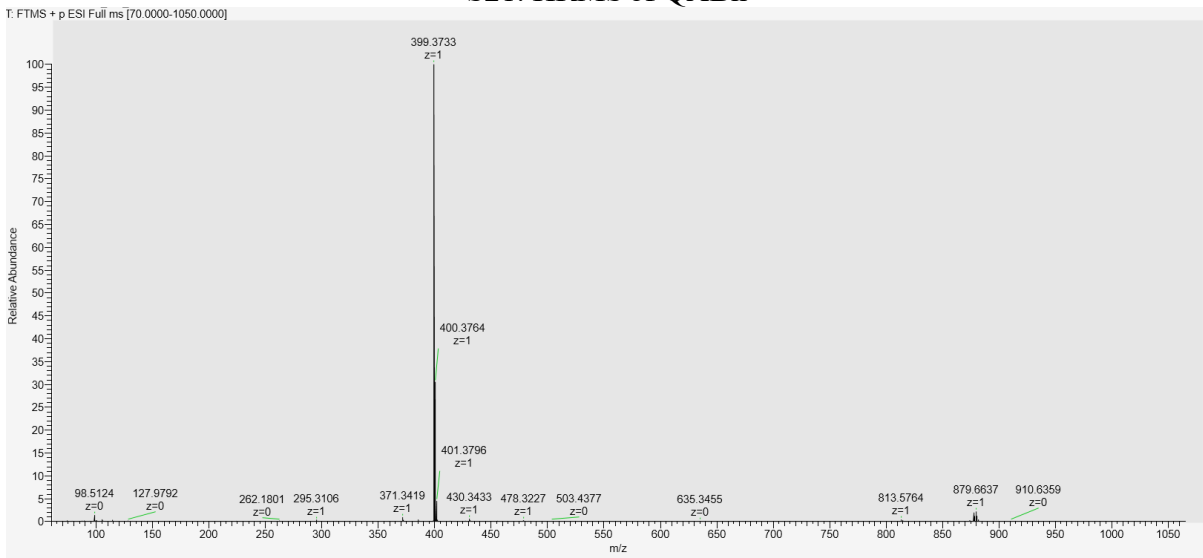
T: FTMS + p ESI Full ms [70.0000-1050.0000]



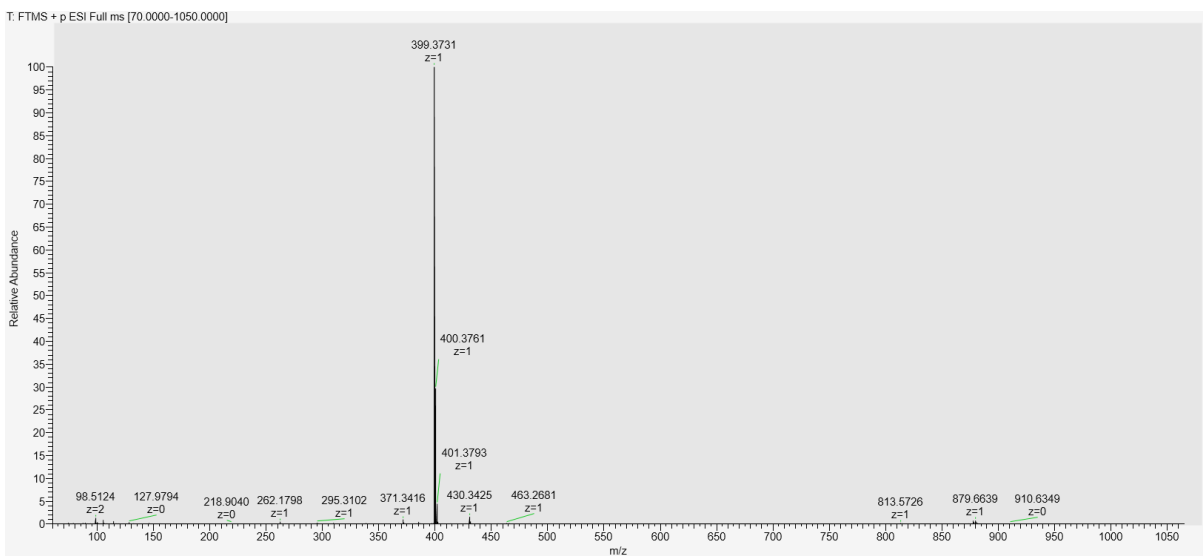
S20. HRMS of QAMe



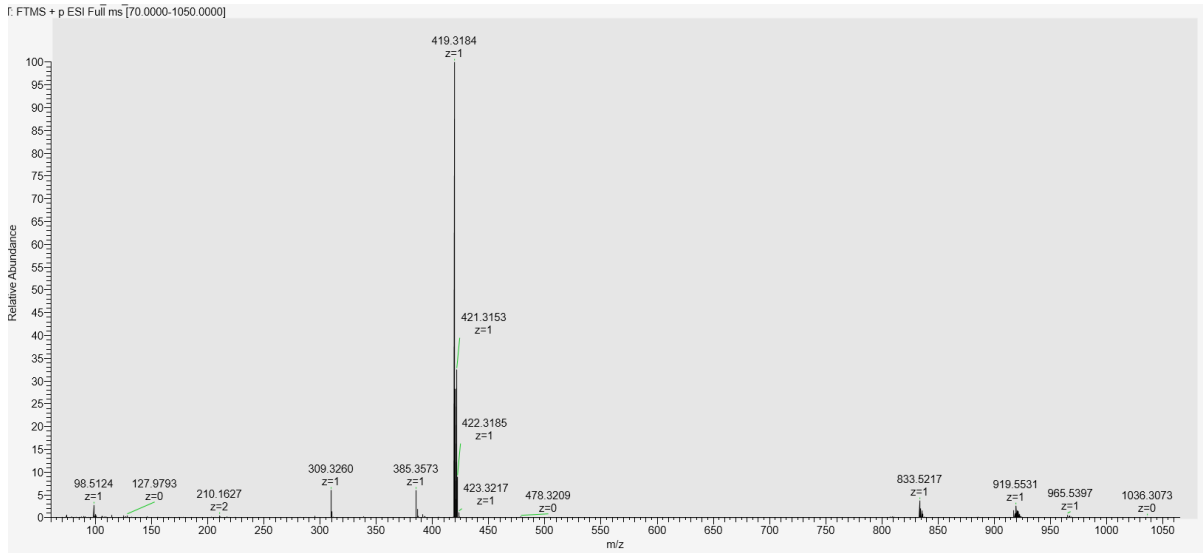
S21. HRMS of QABn



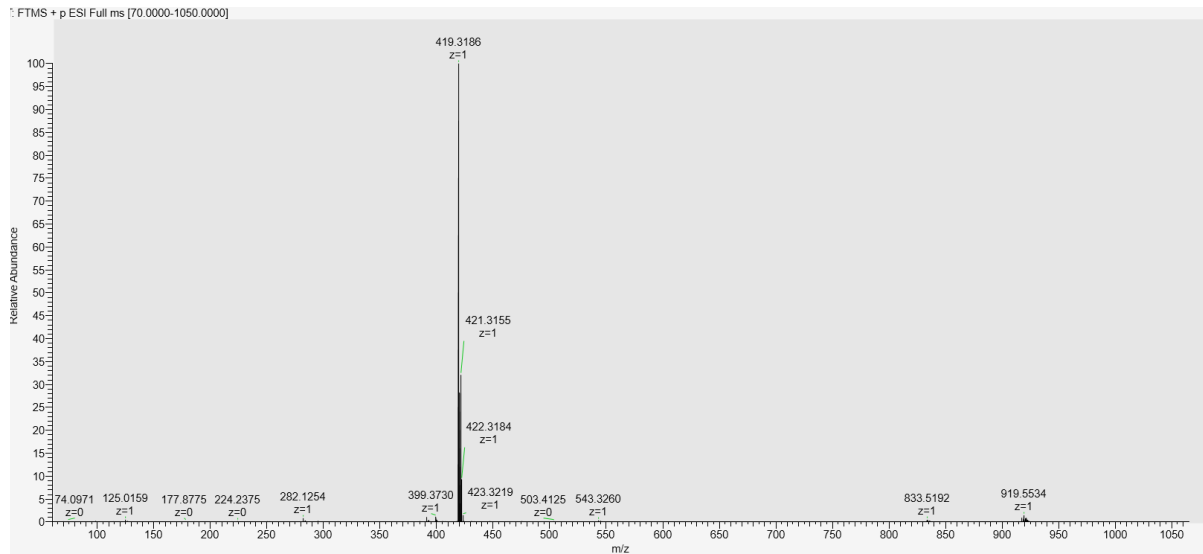
S22. HRMS of QAmMe



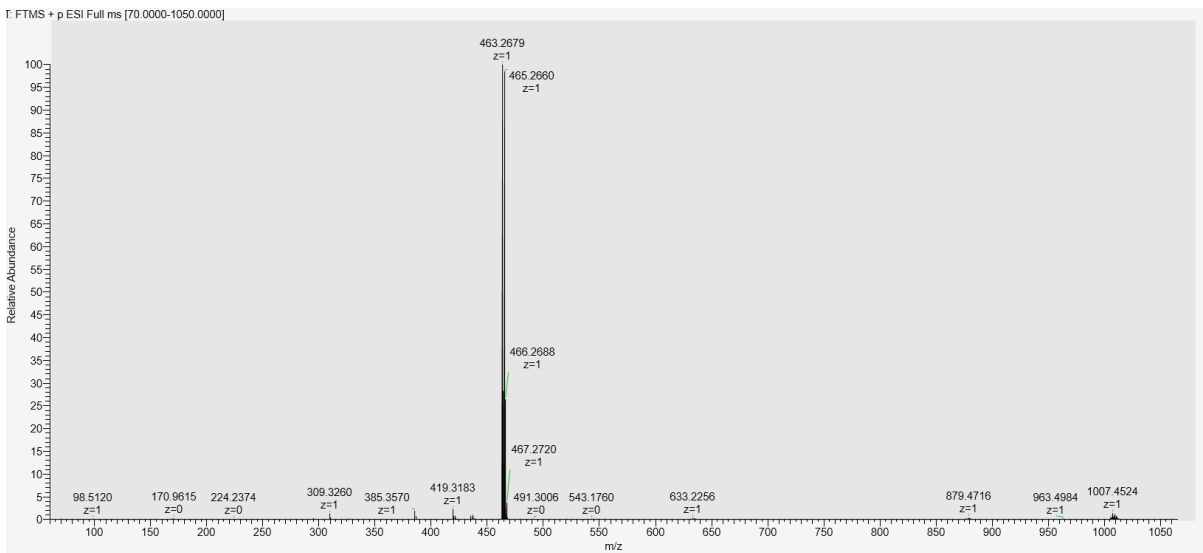
S23. HRMS of QApMe



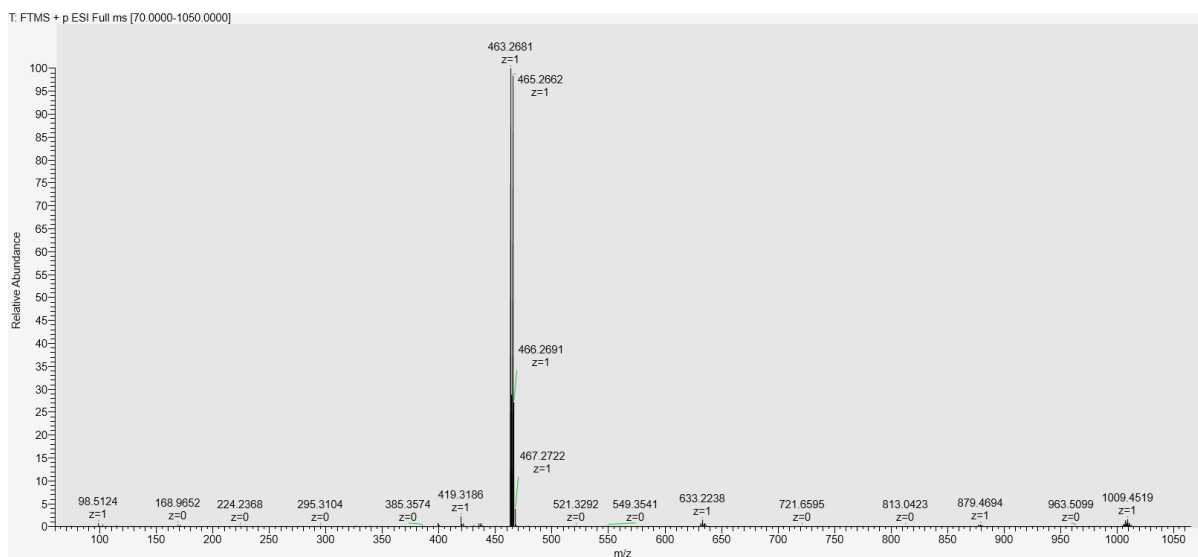
S24. HRMS of QAmCl



S25. HRMS of QApCl

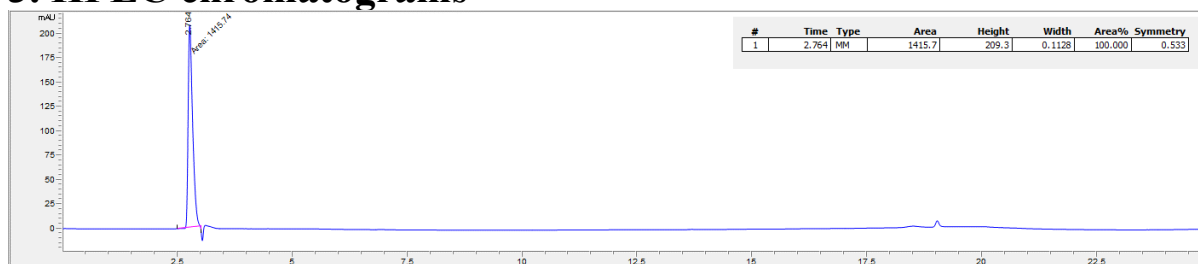


S26. HRMS of QAmBr

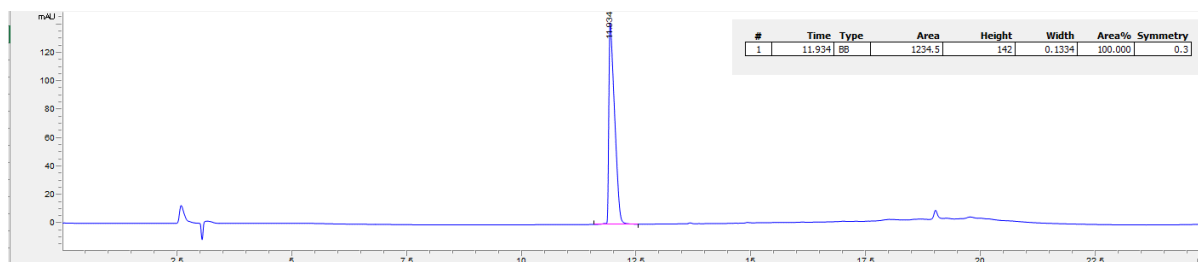


S27. HRMS of QApBr

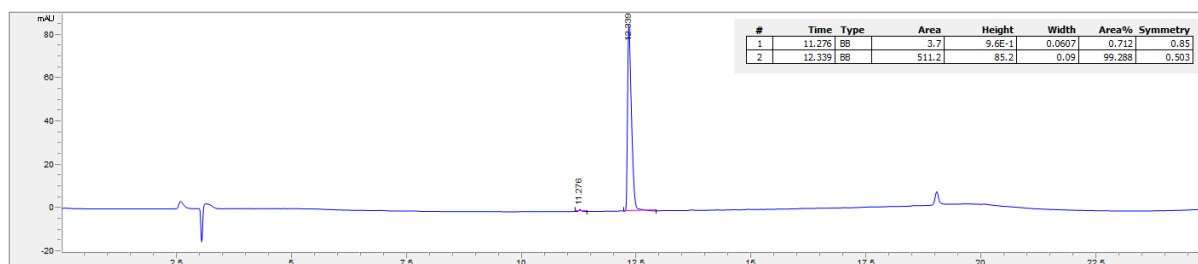
3. HPLC chromatograms



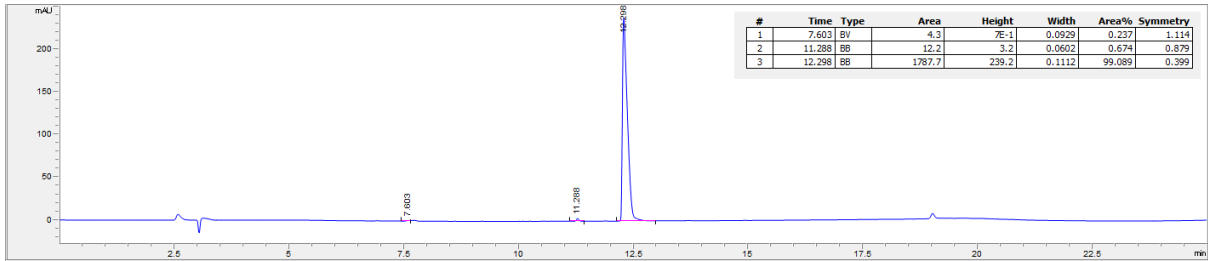
S28. HPLC chromatogram of QAMe



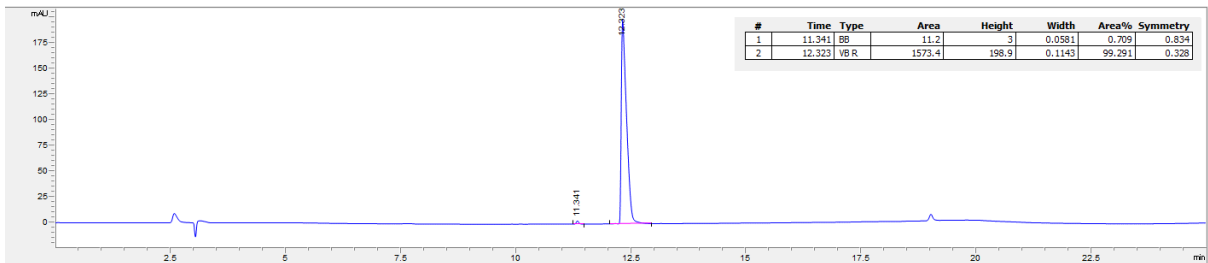
S29. HPLC chromatogram of QABn



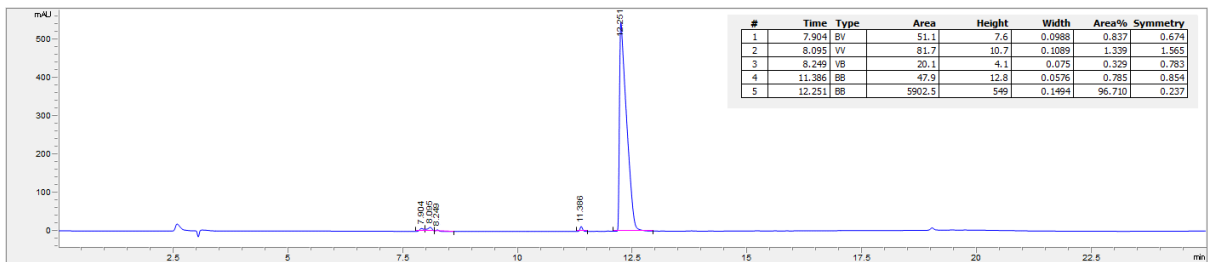
S30. HPLC chromatogram of QAmMe



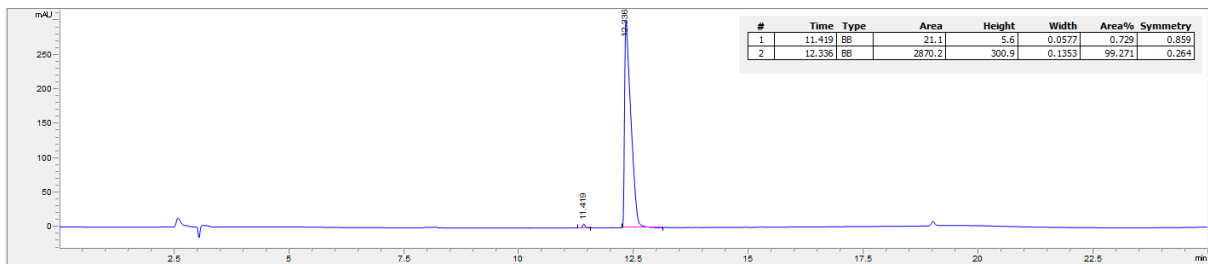
S31. HPLC chromatogram of QApMe



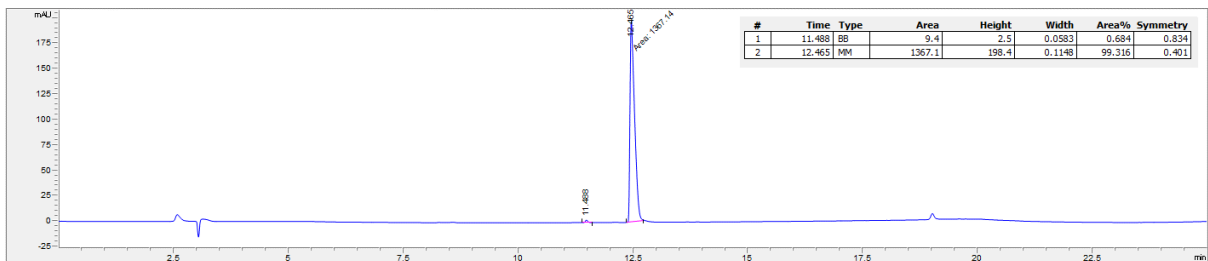
S32. HPLC chromatogram of QAmCl



S33. HPLC chromatogram of QApCl



S34. HPLC chromatogram of QAmBr



S35. HPLC chromatogram of QApBr

6. REFERENCES

- [1] F. Bureš, “Quaternary Ammonium Compounds: Simple in Structure, Complex in Application,” Jun. 01, 2019, *Springer International Publishing*. doi: 10.1007/s41061-019-0239-2.
- [2] C. P. Gerba, “Quaternary ammonium biocides: Efficacy in application,” 2015, *American Society for Microbiology*. doi: 10.1128/AEM.02633-14.
- [3] M. Ramanathan, L. K. Shrestha, T. Mori, Q. Ji, J. P. Hill, and K. Ariga, “Amphiphile nanoarchitectonics: From basic physical chemistry to advanced applications,” Jul. 14, 2013. doi: 10.1039/c3cp50620g.
- [4] W. A. Arnold *et al.*, “Quaternary Ammonium Compounds: A Chemical Class of Emerging Concern,” May 23, 2023, *American Chemical Society*. doi: 10.1021/acs.est.2c08244.
- [5] I. Johansson, P. Somasundaran, and J. Steber, “Handbook for Cleaning/Decontamination of Surfaces The Ecotoxicity of Cleaning Product Ingredients.” doi: 10.1016/B978-0-444-51664-0.50022-X.
- [6] M. Eddleston, “Bipyridyl Herbicides,” in *Critical Care Toxicology*, Springer International Publishing, 2016, pp. 1–20. doi: 10.1007/978-3-319-20790-2_100-1.
- [7] “Calderbank A. The bipyridylium herbicides. *Adv Pest Control Res.* 1968;8:127-235. PMID: 4884782.”.
- [8] C. Zhang *et al.*, “Quaternary ammonium compounds (QACs): A review on occurrence, fate and toxicity in the environment,” Jun. 05, 2015, *Elsevier*. doi: 10.1016/j.scitotenv.2015.03.007.
- [9] T. G. Osimitz and W. Droege, “Quaternary ammonium compounds: perspectives on benefits, hazards, and risk,” *Toxicology Research and Application*, vol. 5, p. 239784732110490, Jan. 2021, doi: 10.1177/23978473211049085.
- [10] Z. Lu, A. K. Mahony, W. A. Arnold, C. W. Marshall, and P. J. McNamara, “Quaternary ammonia compounds in disinfectant products: evaluating the potential for promoting antibiotic resistance and disrupting wastewater treatment plant performance,” *Environmental Science: Advances*, vol. 3, no. 2, pp. 208–226, Nov. 2023, doi: 10.1039/d3va00063j.
- [11] K. P. C. Minbiole *et al.*, “From antimicrobial activity to mechanism of resistance: the multifaceted role of simple quaternary ammonium compounds in bacterial eradication,” *Tetrahedron*, vol. 72, no. 25, pp. 3559–3566, 2016, doi: 10.1016/j.tet.2016.01.014.
- [12] J. M. Boyce, “Quaternary ammonium disinfectants and antiseptics: tolerance, resistance and potential impact on antibiotic resistance,” Dec. 01, 2023, *BioMed Central Ltd*. doi: 10.1186/s13756-023-01241-z.
- [13] G. McDonnell, A. D. Russell, L. Operations, and S. Louis, “Antiseptics and Disinfectants: Activity, Action, and Resistance,” 1999. [Online]. Available: <http://cmr.asm.org/>
- [14] I. Mulder, J. Siemens, V. Sentek, W. Amelung, K. Smalla, and S. Jechalke, “Quaternary ammonium compounds in soil: implications for antibiotic resistance development,” Mar. 01, 2018, *Springer Netherlands*. doi: 10.1007/s11157-017-9457-7.
- [15] X. Wen *et al.*, “Comparative study of two methods of enteric virus detection and enteric virus relationship with bacterial indicator in poyang lake, Jiangxi, China,” *Int J Environ Res Public Health*, vol. 16, no. 18, Sep. 2019, doi: 10.3390/ijerph16183384.
- [16] M. J. M. Vaerewijck, K. Sabbe, J. Baré, H. P. Spengler, H. W. Favoreel, and K. Houf, “Assessment of the efficacy of benzalkonium chloride and sodium hypochlorite against

- Acanthamoeba polyphaga and Tetrahymena spp.," *J Food Prot*, vol. 75, no. 3, pp. 541–546, Mar. 2012, doi: 10.4315/0362-028X.JFP-11-359.
- [17] J. N. Mbithi, V. S. Springthorpe, and S. A. Sattar, "Chemical Disinfection of Hepatitis A Virus on Environmental Surfaces." [Online]. Available: <https://journals.asm.org/journal/aem>
- [18] L. E. Moore, R. G. Ledder, P. Gilbert, and A. J. McBain, "In vitro study of the effect of cationic biocides on bacterial population dynamics and susceptibility," *Appl Environ Microbiol*, vol. 74, no. 15, pp. 4825–4834, Aug. 2008, doi: 10.1128/AEM.00573-08.
- [19] W. A. Jacobs, "THE BACTERICIDAL PROPERTIES OF THE QUATERNARY SALTS OF HEXAMETHYLENETETRAMINE. I. THE PROBLEM OF THE CHEMOTHERAPY OF EXPERIMENTAL BACTERIAL INFECTIONS."
- [20] G. Domagk, "Domagk, G. (1935). Eine neue Klasse von Desinfektionsmitteln. Deutsche Medizinische Wochenschrift, 61, 829-832."
- [21] B. Direktor Geh-Rat Uhienhuth and V. H. Stabsarzt HORNUNG, "Zephirol, ein neues Desinfektionsmittel."
- [22] P. B. Price, "PRICE, P. B. (1950). PRESENT DAY METHODS OF DISINFECTING THE SKIN. Archives of Surgery, 61(3), 583. doi:10.1001/archsurg.1950.01250020588017." [Online]. Available: <http://archsurg.jamanetwork.com/>
- [23] P. B. Price, "BENZALKONIUM CHLORIDE (ZEPHIRAN CHLORIDE®) AS A SKIN DISINFECTANT. Archives of Surgery, 61(1), 23. doi:10.1001/archsurg.1950.01250020026004," 1950. [Online]. Available: <http://archsurg.jamanetwork.com/>
- [24] R.; Quisno and M. J. Foter2, "CETYL PYRIDINIUM CHLORIDE' I. GERMICIDAL PROPERTIES." [Online]. Available: <https://journals.asm.org/journal/jb>
- [25] W. Krzyściak, A. Jurczak, D. Kościelniak, B. Bystrowska, and A. Skalniak, "The virulence of Streptococcus mutans and the ability to form biofilms," 2014, *Springer Verlag*. doi: 10.1007/s10096-013-1993-7.
- [26] F. Cieplik *et al.*, "Antimicrobial efficacy of alternative compounds for use in oral care toward biofilms from caries-associated bacteria in vitro," *Microbiologyopen*, vol. 8, no. 4, Apr. 2019, doi: 10.1002/mb03.695.
- [27] A. Ohnuma *et al.*, "Didecyldimethylammonium chloride induces pulmonary inflammation and fibrosis in mice," *Experimental and Toxicologic Pathology*, vol. 62, no. 6, pp. 643–651, Nov. 2010, doi: 10.1016/j.etp.2009.08.007.
- [28] T. T. M. K. E. H. Kumiko Jono, "Effect of Alkyl Chain Length of Benzalkonium Chloride on the Bactericidal Activity and Binding to Organic Materials," Apr. 1986.
- [29] C. Ho Kim, J. Won Choi, H. Jae Chun, and K. Suk Choi, "Synthesis of chitosan derivatives with quaternary ammonium salt and their antibacterial activity," 1997.
- [30] "Quaternary Ammonium Compounds (QACs)."
- [31] C. J. Ioannou, G. W. Hanlon, and S. P. Denyer, "Action of disinfectant quaternary ammonium compounds against Staphylococcus aureus," *Antimicrob Agents Chemother*, vol. 51, no. 1, pp. 296–306, Jan. 2007, doi: 10.1128/AAC.00375-06.
- [32] M. C. Jennings, K. P. C. Minbiole, and W. M. Wuest, "Quaternary Ammonium Compounds: An Antimicrobial Mainstay and Platform for Innovation to Address Bacterial Resistance," Jan. 08, 2016, *American Chemical Society*. doi: 10.1021/acsinfecdis.5b00047.
- [33] M. R. J. Salton, "Lytic Agents, Cell Permeability, and Monolayer Penetrability The Journal of General Physiology."
- [34] T. J. Silhavy, D. Kahne, and S. Walker, "The bacterial cell envelope.," 2010. doi: 10.1101/cshperspect.a000414.

- [35] D. E. Kruyt, Y. Kamio, and H. Nikaido, "971)," Muller, A, 1972.
- [36] W. Vollmer, D. Blanot, and M. A. De Pedro, "Peptidoglycan structure and architecture," Mar. 2008. doi: 10.1111/j.1574-6976.2007.00094.x.
- [37] L. Pasquina-Lemonche *et al.*, "The architecture of the Gram-positive bacterial cell wall," *Nature*, vol. 582, no. 7811, pp. 294–297, Jun. 2020, doi: 10.1038/s41586-020-2236-6.
- [38] F. C. Neuhaus and J. Baddiley, "A Continuum of Anionic Charge: Structures and Functions of d-Alanyl-Teichoic Acids in Gram-Positive Bacteria," *Microbiology and Molecular Biology Reviews*, vol. 67, no. 4, pp. 686–723, Dec. 2003, doi: 10.1128/mubr.67.4.686-723.2003.
- [39] M. Rajagopal and S. Walker, "Envelope structures of gram-positive bacteria," in *Current Topics in Microbiology and Immunology*, vol. 404, Springer Verlag, 2017. doi: 10.1007/82_2015_5021.
- [40] P. A. Lambert and S. M. Hammond, "BIOCHEMICAL AND BIOPHYSICAL RESEARCH COMMUNICATIONS POTASSIUM FLUKES, FIRST INDICATIONS OF MEMBRANE DAMAGE IN MICRO-ORGANISMS," 1973.
- [41] J. Fedorowicz and J. Sączewski, "Advances in the Synthesis of Biologically Active Quaternary Ammonium Compounds," May 01, 2024, *Multidisciplinary Digital Publishing Institute (MDPI)*. doi: 10.3390/ijms25094649.
- [42] T. T. Yu *et al.*, "Design, synthesis and biological evaluation of biphenylglyoxamide-based small molecular antimicrobial peptide mimics as antibacterial agents," *Int J Mol Sci*, vol. 21, no. 18, pp. 1–38, Sep. 2020, doi: 10.3390/ijms21186789.
- [43] S. V. Sapozhnikov *et al.*, "Design, synthesis, antibacterial activity and toxicity of novel quaternary ammonium compounds based on pyridoxine and fatty acids," *Eur J Med Chem*, vol. 211, Feb. 2021, doi: 10.1016/j.ejmech.2020.113100.
- [44] R. Dey, K. De, R. Mukherjee, S. Ghosh, and J. Haldar, "Small antibacterial molecules highly active against drug-resistant: *Staphylococcus aureus*," *Medchemcomm*, vol. 10, no. 11, pp. 1907–1915, 2019, doi: 10.1039/c9md00329k.
- [45] S. Alkhalifa *et al.*, "Analysis of the Destabilization of Bacterial Membranes by Quaternary Ammonium Compounds: A Combined Experimental and Computational Study," *ChemBioChem*, vol. 21, no. 10, pp. 1510–1516, May 2020, doi: 10.1002/cbic.201900698.
- [46] S. J. Mccarlie, E. Coetsee, H. Grobler, and R. R. Bragg, "Microscopy techniques unveil the effect of QAC-disinfectants on biofilm formation, cell morphology, and localisation of QAC compounds," 2013. [Online]. Available: <https://ssrn.com/abstract=4915151>
- [47] L. Bazina *et al.*, "Discovery of novel quaternary ammonium compounds based on quinuclidine-3-ol as new potential antimicrobial candidates," *Eur J Med Chem*, vol. 163, pp. 626–635, Feb. 2019, doi: 10.1016/j.ejmech.2018.12.023.
- [48] M. Crismaru *et al.*, "Survival of adhering staphylococci during exposure to a quaternary ammonium compound evaluated by using atomic force microscopy imaging," *Antimicrob Agents Chemother*, vol. 55, no. 11, pp. 5010–5017, Nov. 2011, doi: 10.1128/AAC.05062-11.
- [49] D. Crnčević *et al.*, "The mode of antibacterial action of quaternary N-benzylimidazole salts against emerging opportunistic pathogens," *Bioorg Chem*, vol. 112, Jul. 2021, doi: 10.1016/j.bioorg.2021.104938.
- [50] W. B. Hugo and A. M. Frier, "Mode of Action of the Antibacterial Compound Dequalinium Acetate," 1969.
- [51] M. Tischer, G. Pradel, K. Ohlsen, and U. Holzgrabe, "Quaternary ammonium salts and their antimicrobial potential: Targets or nonspecific interactions?," Jan. 02, 2012. doi: 10.1002/cmcd.201100404.

- [52] S. V. Sapozhnikov *et al.*, “Design, synthesis, antibacterial activity and toxicity of novel quaternary ammonium compounds based on pyridoxine and fatty acids,” *Eur J Med Chem*, vol. 211, Feb. 2021, doi: 10.1016/j.ejmech.2020.113100.
- [53] J. Fedorowicz *et al.*, “Synthesis and biological evaluation of hybrid quinolone-based quaternary ammonium antibacterial agents,” *Eur J Med Chem*, vol. 179, pp. 576–590, Oct. 2019, doi: 10.1016/j.ejmech.2019.06.071.
- [54] U. Tezel and S. G. Pavlostathis, “Quaternary ammonium disinfectants: Microbial adaptation, Degradation and ecology,” Jun. 01, 2015, *Elsevier Ltd.* doi: 10.1016/j.copbio.2015.03.018.
- [55] U. Tezel and S. G. Pavlostathis, “ROLE OF QUATERNARY AMMONIUM COMPOUNDS ON ANTIMICROBIAL RESISTANCE IN THE ENVIRONMENT.”
- [56] H. M. Dewey, J. M. Jones, M. R. Keating, and J. Budhathoki-Uprety, “Increased Use of Disinfectants during the COVID-19 Pandemic and Its Potential Impacts on Health and Safety,” Jan. 24, 2022, *American Chemical Society*. doi: 10.1021/acs.chas.1c00026.
- [57] C. Zhang *et al.*, “Quaternary ammonium compounds (QACs): A review on occurrence, fate and toxicity in the environment,” Jun. 05, 2015, *Elsevier*. doi: 10.1016/j.scitotenv.2015.03.007.
- [58] M. Clara, S. Scharf, C. Scheffknecht, and O. Gans, “Occurrence of selected surfactants in untreated and treated sewage,” *Water Res*, vol. 41, no. 19, pp. 4339–4348, 2007, doi: 10.1016/j.watres.2007.06.027.
- [59] G. G. Ying, “Fate, behavior and effects of surfactants and their degradation products in the environment,” 2006, *Elsevier Ltd.* doi: 10.1016/j.envint.2005.07.004.
- [60] U. Tezel and S. G. Pavlostathis, “Quaternary ammonium disinfectants: Microbial adaptation, Degradation and ecology,” Jun. 01, 2015, *Elsevier Ltd.* doi: 10.1016/j.copbio.2015.03.018.
- [61] K. Kümmerer, “The presence of pharmaceuticals in the environment due to human use - present knowledge and future challenges,” 2009, *Academic Press*. doi: 10.1016/j.jenvman.2009.01.023.
- [62] L. H. Johnston and K. G. H. Dyke, “Ethidium Bromide Resistance, a New Marker on the Staphylococcal Penicillinase Plasmid,” 1969. [Online]. Available: <https://journals.asm.org/journal/jb>
- [63] Z. Jaglic and D. Cervinkova, “Genetic basis of resistance to quaternary ammonium compounds-the qac genes and their role: a review.”
- [64] B. A. Mitchell, M. H. Brown, and R. A. Skurray, “QacA Multidrug Efflux Pump from *Staphylococcus aureus*: Comparative Analysis of Resistance to Diamidines, Biguanidines, and Guanylhydrazones,” 1998. [Online]. Available: <https://journals.asm.org/journal/aac>
- [65] I. T. Paulsen, M. H. Brown, T. G. Littlejohn, B. A. Mitchell, and R. A. Skurray, “Multidrug resistance proteins QacA and QacB from *Staphylococcus aureus*: Membrane topology and identification of residues involved in substrate specificity (drug efflux pumps/protein topology/major facilitator superfamily),” 1996.
- [66] D. A. Rouch, ^ D S Cram, D. Diberardino, T. G. Littlejohn, and R. A. Skurray, “Efflux-mediated antiseptic resistance gene qacA from *Staphylococcus aureus*: common ancestry with tetracycline- and sugar-transport proteins,” 1990.
- [67] S. Grkovic, M. H. Brown, N. J. Roberts, I. T. Paulsen, and R. A. Skurray, “QacR Is a Repressor Protein That Regulates Expression of the *Staphylococcus aureus* Multidrug Efflux Pump QacA*,” 1998. [Online]. Available: <http://www.jbc.org/>

- [68] B. A. Mitchell, M. H. Brown, and R. A. Skurray, "QacA Multidrug Efflux Pump from *Staphylococcus aureus*: Comparative Analysis of Resistance to Diamidines, Biguanidines, and Guanylhydrazones," 1998. [Online]. Available: <https://journals.asm.org/journal/aac>
- [69] M. C. Jennings, M. E. Forman, S. M. Duggan, K. P. C. Minbiole, and W. M. Wuest, "Efflux Pumps Might Not Be the Major Drivers of QAC Resistance in Methicillin-Resistant *Staphylococcus aureus*," *ChemBioChem*, vol. 18, no. 16, pp. 1573–1577, Aug. 2017, doi: 10.1002/cbic.201700233.
- [70] S. S. Costa *et al.*, "Identification of the plasmid-encoded qacA efflux pump gene in methicillin-resistant *Staphylococcus aureus* (MRSA) strain HPV107, a representative of the MRSA Iberian clone," *Int J Antimicrob Agents*, vol. 36, no. 6, pp. 557–561, Dec. 2010, doi: 10.1016/j.ijantimicag.2010.08.006.
- [71] S. Grkovic, M. H. Brown, M. A. Schumacher, R. G. Brennan, and R. A. Skurray, "The staphylococcal QacR multidrug regulator binds a correctly spaced operator as a pair of dimers," *J Bacteriol*, vol. 183, no. 24, pp. 7102–7109, 2001, doi: 10.1128/JB.183.24.7102-7109.2001.
- [72] I. T. Paulsen, M. H. Brown, T. G. Litrlejohn, B. A. Mitchell, and R. A. Skurray, "Multidrug resistance proteins QacA and QacB from *Staphylococcus aureus*: Membrane topology and identification of residues involved in substrate specificity (drug efflux pumps/protein topology/major facilitator superfamily)," 1996.
- [73] R. A. Allen, M. C. Jennings, M. A. Mitchell, S. E. Al-Khalifa, W. M. Wuest, and K. P. C. Minbiole, "Ester-and Amide-containing MultiQACs: Exploring Multicationic Soft Antimicrobial Agents," 2017. [Online]. Available: <http://www.elsevier.com/open-access/userlicense/1.0/>
- [74] K. M. Peters, J. T. Schuman, R. A. Skurray, M. H. Brown, R. G. Brennan, and M. A. Schumacher, "QacR-cation recognition is mediated by a redundancy of residues capable of charge neutralization," *Biochemistry*, vol. 47, no. 31, pp. 8122–8129, Aug. 2008, doi: 10.1021/bi8008246.
- [75] M. A. Schumacher, M. C. Miller, S. Grkovic, M. H. Brown, R. A. Skurray, and R. G. Brennan, "Structural mechanisms of QacR induction and multidrug recognition," *Science (1979)*, vol. 294, no. 5549, pp. 2158–2163, Dec. 2001, doi: 10.1126/science.1066020.
- [76] J. M. Boyce, "Quaternary ammonium disinfectants and antiseptics: tolerance, resistance and potential impact on antibiotic resistance," Dec. 01, 2023, *BioMed Central Ltd.* doi: 10.1186/s13756-023-01241-z.
- [77] L. Mé Chin, F. Dubois-Brissonnet, B. Heyd, and J. Y. Leveau, "Adaptation of *Pseudomonas aeruginosa* ATCC 15442 to didecyldimethylammonium bromide induces changes in membrane fatty acid composition and in resistance of cells," 1999.
- [78] L. Gué rin-Mé chin, F. Dubois-Brissonnet, B. Heyd, and J. Leveau, "Specific variations of fatty acid composition of *Pseudomonas aeruginosa* ATCC 15442 induced by Quaternary Ammonium Compounds and relation with resistance to bactericidal activity," 1999.
- [79] M. S. To, S. Favrin, N. Romanova, and M. W. Griffiths, "Postadaptational Resistance to Benzalkonium Chloride and Subsequent Physicochemical Modifications of *Listeria monocytogenes*," *Appl Environ Microbiol*, vol. 68, no. 11, pp. 5258–5264, 2002, doi: 10.1128/AM.68.11.5258-5264.2002.
- [80] Katsuhiko Nagai, Takahiro Murata, Shin Ohta, Hiroshi Zenda, Makoto Ohnishi, and Tetsuya Hayashi, "nagai2003," *Microbiol Immunol*, vol. 10, no. 47, pp. 709–715, 2003.
- [81] "Microbial community degradation of widely used quaternary ammonium disinfectants," *Appl Environ Microbiol*, vol. 80, no. 19, pp. 5892–5900, 2014, doi: 10.1128/AEM.01255-14.

- [82] P. I. Hora and W. A. Arnold, "Photochemical fate of quaternary ammonium compounds in river water," *Environ Sci Process Impacts*, vol. 22, no. 6, pp. 1368–1381, Jun. 2020, doi: 10.1039/d0em00086h.
- [83] X. Li and B. J. Brownawell, "Quaternary ammonium compounds in urban estuarine sediment environments - A class of contaminants in need of increased attention?," *Environ Sci Technol*, vol. 44, no. 19, pp. 7561–7568, Oct. 2010, doi: 10.1021/es1011669.
- [84] N. Kreuzinger, M. Fuerhacker, S. Scharf, M. Uhl, O. Gans, and B. Grillitsch, "Methodological approach towards the environmental significance of uncharacterized substances - quaternary ammonium compounds as an example," *Desalination*, vol. 215, no. 1–3, pp. 209–222, Sep. 2007, doi: 10.1016/j.desal.2006.10.036.
- [85] A. Utsunomiya, "TOXIC EFFECTS OF LINEAR ALKYL BENZENE SULFONATE, QUATERNARY ALKYLAMMONIUM CHLORIDE AND THEIR COMPLEXES ON DUNALIELLA SP. AND CHLORELLA PYRENOIDOSA," 1997.
- [86] K. Jardak, P. Drogui, and R. Daghrir, "Surfactants in aquatic and terrestrial environment: occurrence, behavior, and treatment processes," *Environmental Science and Pollution Research*, vol. 23, no. 4, pp. 3195–3216, Feb. 2016, doi: 10.1007/s11356-015-5803-x.
- [87] G. Jing, Z. Zhou, and J. Zhuo, "Quantitative structure-activity relationship (QSAR) study of toxicity of quaternary ammonium compounds on *Chlorella pyrenoidosa* and *Scenedesmus quadricauda*," *Chemosphere*, vol. 86, no. 1, pp. 76–82, 2012, doi: 10.1016/j.chemosphere.2011.09.021.
- [88] M. T. Garcõ A, I. Ribosa, T. Guindulain, J. Saâ Nchez-Leal, and J. Vives-Rego, "Fate and effect of monoalkyl quaternary ammonium surfactants in the aquatic environment." [Online]. Available: www.elsevier.com/locate/envpol
- [89] A. Van De Voorde, C. Lorgeoux, M. C. Gromaire, and G. Chebbo, "Analysis of quaternary ammonium compounds in urban stormwater samples," *Environmental Pollution*, vol. 164, pp. 150–157, May 2012, doi: 10.1016/j.envpol.2012.01.037.
- [90] T. Ivanković and J. Hrenović, "Surfactants in the environment," Mar. 01, 2010. doi: 10.2478/10004-1254-61-2010-1943.
- [91] W. A. Arnold *et al.*, "Quaternary Ammonium Compounds: A Chemical Class of Emerging Concern," May 23, 2023, *American Chemical Society*. doi: 10.1021/acs.est.2c08244.
- [92] D. M. Mercer Mb, "Cetrimide burn in an infant," 1983.
- [93] P. J. August, "MEDICAL MEMORANDA Cutaneous Necrosis Due to Cetrimide Application," 1975.
- [94] S. T. Larsen, H. Verder, and G. D. Nielsen, "Airway Effects of Inhaled Quaternary Ammonium Compounds in Mice," *Basic Clin Pharmacol Toxicol*, vol. 110, no. 6, pp. 537–543, Jun. 2012, doi: 10.1111/j.1742-7843.2011.00851.x.
- [95] N. Miguères *et al.*, "Occupational Asthma Caused by Quaternary Ammonium Compounds: A Multicenter Cohort Study," *Journal of Allergy and Clinical Immunology: In Practice*, vol. 9, no. 9, pp. 3387–3395, Sep. 2021, doi: 10.1016/j.jaip.2021.04.041.
- [96] M. Gonzalez *et al.*, "Asthma among workers in healthcare settings: Role of disinfection with quaternary ammonium compounds," *Clinical and Experimental Allergy*, vol. 44, no. 3, pp. 393–406, Mar. 2014, doi: 10.1111/cea.12215.
- [97] A. L. Frantz, "Chronic quaternary ammonium compound exposure during the COVID-19 pandemic and the impact on human health," Sep. 01, 2023, *Korean Society of Environmental Risk Assessment and Health Science*. doi: 10.1007/s13530-023-00173-w.
- [98] T. C. Hrubec *et al.*, "Altered toxicological endpoints in humans from common quaternary ammonium compound disinfectant exposure," *Toxicol Rep*, vol. 8, pp. 646–656, Jan. 2021, doi: 10.1016/j.toxrep.2021.03.006.

- [99] G. Zheng, E. Schreder, S. Sathyanarayana, and A. Salamova, "The first detection of quaternary ammonium compounds in breast milk: Implications for early-life exposure," *J Expo Sci Environ Epidemiol*, vol. 32, no. 5, pp. 682–688, Sep. 2022, doi: 10.1038/s41370-022-00439-4.
- [100] Z. A. Kirkpatrick, V. E. Melin, and T. C. Hrubec, "Quaternary ammonium compound exposure causes infertility by altering endocrine signaling and gametogenesis," *Reproductive Toxicology*, vol. 132, p. 108817, Mar. 2025, doi: 10.1016/J.REPROTOX.2024.108817.
- [101] J. Pernak, I. Mirska, R. Kmiecik, and K. Marcinkowski, "Antimicrobial activities of new analogues of benzalkonium chloride," 1999.
- [102] B. Brycki, I. Małecka, A. Koziróg, and A. Otlewska, "Synthesis, structure and antimicrobial properties of novel benzalkonium chloride analogues with pyridine rings," *Molecules*, vol. 22, no. 1, Jan. 2017, doi: 10.3390/molecules22010130.
- [103] B. Brycki, A. Koziróg, I. Kowalczyk, T. Pospieszny, P. Materna, and J. Marciniak, "Synthesis, structure, surface and antimicrobial properties of new oligomeric quaternary ammonium salts with aromatic spacers," *Molecules*, vol. 22, no. 11, Nov. 2017, doi: 10.3390/molecules22111810.
- [104] Z. E. A. Toles *et al.*, "Double BAC and Triple BAC: A Systematic Analysis of the Disinfectant Properties of Multicationic Derivatives of Benzalkonium Chloride (BAC)," *ChemMedChem*, vol. 18, no. 10, May 2023, doi: 10.1002/cmde.202300018.
- [105] J. Fedorowicz and J. Sączewski, "Advances in the Synthesis of Biologically Active Quaternary Ammonium Compounds," May 01, 2024, *Multidisciplinary Digital Publishing Institute (MDPI)*. doi: 10.3390/ijms25094649.
- [106] M. C. Jennings, L. E. Ator, T. J. Paniak, K. P. C. Minbiole, and W. M. Wuest, "Biofilm-eradicating properties of quaternary ammonium amphiphiles: simple mimics of antimicrobial peptides," *Chembiochem*, vol. 15, no. 15, pp. 2211–2215, Oct. 2014, doi: 10.1002/cbic.201402254.
- [107] T. T. Yu *et al.*, "Design, synthesis and biological evaluation of biphenylglyoxamide-based small molecular antimicrobial peptide mimics as antibacterial agents," *Int J Mol Sci*, vol. 21, no. 18, pp. 1–38, Sep. 2020, doi: 10.3390/ijms21186789.
- [108] T. T. Yu *et al.*, "Design, Synthesis and Biological Evaluation of N-Sulfonylphenyl glyoxamide-Based Antimicrobial Peptide Mimics as Novel Antimicrobial Agents," *ChemistrySelect*, vol. 2, no. 12, pp. 3452–3461, Apr. 2017, doi: 10.1002/slct.201700336.
- [109] R. G. Carden *et al.*, "Advancements in the Development of Non-Nitrogen-Based Amphiphilic Antiseptics to Overcome Pathogenic Bacterial Resistance," Nov. 04, 2020, *John Wiley and Sons Ltd*. doi: 10.1002/cmde.202000612.
- [110] Y.- Kggdo, "ORGANIC AND BIOLOGICAL ASPECTS OF BERBERINE ALKALOIDS*," 1976.
- [111] F. E. Hahn and J. Ciak, "Berberine."
- [112] A. Hoshi *et al.*, "ANTITUMOR ACTIVITY OF BERBERINE DERIVATIVES," 1976.
- [113] K. Iwasal, M. Kamigauchil, M. Uek, and M. Taniguch, "Antibacterial activity and structure-activity relationships of berberine analogs," 1996.
- [114] M. D. Joyce, M. C. Jennings, C. N. Santiago, M. H. Fletcher, W. M. Wuest, and K. P. Minbiole, "Natural product-derived quaternary ammonium compounds with potent antimicrobial activity," *Journal of Antibiotics*, vol. 69, no. 4, pp. 344–347, Apr. 2016, doi: 10.1038/ja.2015.107.
- [115] E. A. Burilova *et al.*, "Synthesis, biological evaluation and structure-activity relationships of self-assembled and solubilization properties of amphiphilic quaternary ammonium

- derivatives of quinuclidine,” *J Mol Liq*, vol. 272, pp. 722–730, Dec. 2018, doi: 10.1016/j.molliq.2018.10.008.
- [116] L. Bazina *et al.*, “Discovery of novel quaternary ammonium compounds based on quinuclidine-3-ol as new potential antimicrobial candidates,” *Eur J Med Chem*, vol. 163, pp. 626–635, Feb. 2019, doi: 10.1016/j.ejmech.2018.12.023.
- [117] R. C. Kontos *et al.*, “An Investigation into Rigidity–Activity Relationships in BisQAC Amphiphilic Antiseptics,” *ChemMedChem*, vol. 14, no. 1, pp. 83–87, Jan. 2019, doi: 10.1002/cmde.201800622.
- [118] R. A. Allen, C. E. M. McCormack, and W. M. Wuest, “Deriving Novel Quaternary Ammonium Compound Disinfectant Scaffolds from a Natural Product: Mechanistic Insights of the Quaternization of Ianthelliformisamine C,” *ChemMedChem*, vol. 18, no. 22, Nov. 2023, doi: 10.1002/cmde.202300253.
- [119] M. Lindstedt, S. Allenmark, R. A. Thompson, and L. Edebo, “Antimicrobial Activity of Betaine Esters, Quaternary Ammonium Amphiphiles Which Spontaneously Hydrolyze into Nontoxic Components,” 1990. [Online]. Available: <https://journals.asm.org/journal/aac>
- [120] A. J. Leitgeb *et al.*, “Further Investigations into Rigidity-Activity Relationships in BisQAC Amphiphilic Antiseptics,” *ChemMedChem*, vol. 15, no. 8, pp. 667–670, Apr. 2020, doi: 10.1002/cmde.201900662.

7. CURRICULUM VITAE

Date of birth: 4th January 1994

Place of birth: Split, Croatia

Nationality: Croatian

EDUCATION

2021. – present Doctoral Study of Biophysics, Faculty of Science, University of Split

2015. – 2017. Graduate study programme Biology and Chemistry, Faculty of Science, University of Split

2012. – 2015. Undergraduate study programme Biology and Chemistry, Faculty of Science, University of Split

EMPLOYMENT

2020 – present Research Assistant at Croatian Science Foundation installation research project “Discovery and Development of New Bioactive Quaternary Ammonium Compounds Derived from Quinuclidine”, Faculty of Science, University of Split

2019 – 2021 Teaching/research assistant, Faculty of Science, University of Split (temporary position).

2019 – 2019 Senior laboratory assistant, Faculty of Science, University of Split (temporary position).

AWARDS

Dean award, Faculty of Science, University of Split, 2015

Dean award, Faculty of Science, University of Split, 2017

8. LIST OF PUBLICATIONS

1. Crnčević D, Krce L, Brkljača Z, Cvitković M, Babić Brčić S, Čož-Rakovac R, Odžak R, Šprung M. A dual antibacterial action of soft quaternary ammonium compounds: bacteriostatic effects, membrane integrity, and reduced *in vitro* and *in vivo* toxicity. RSC Advances, 15 (2025), doi: 10.1039/D4RA07975B
2. Paut A, Guć L, Vrankić M, Crnčević D, Šenjug P, Pajić D, Odžak R, Šprung M, Nakić K, Marciuš M *et al.* Plant-Mediated Synthesis of Magnetite Nanoparticles with Matricaria chamomilla Aqueous Extract. Nanomaterials, 14 (2024), 8; 729, 22. doi: 10.3390/nano14080729
3. Crnčević D, Ramić A, Radman Kastelic A, Odžak R, Krce L, Weber I, Primožič I, Šprung M. Naturally derived 3-aminoquinuclidine salts as new promising therapeutic agents. Scientific reports, 14 (2024), 26211, 18. doi: 10.1038/s41598-024-77647-5
4. Odžak R, Crnčević D, Sabljic A, Krce L, Paladin A, Primožič I, Šprung M. Further study of the polar group's influence on the antibacterial activity of the 3-substituted quinuclidine salts with long alkyl chains. Antibiotics, 12 (2023), 8; 1231, 21. doi: 10.3390/antibiotics12081231
5. Odžak R, Crnčević D, Sabljic A, Primožič I, Šprung M. Synthesis and Biological Evaluation of 3-Amidoquinuclidine Quaternary Ammonium Compounds as New Soft Antibacterial Agents. Pharmaceuticals, 16 (2023), 2; 187, 20. doi: 10.3390/ph16020187
6. Crnčević D, Krce L, Cvitković M, Brkljača Z, Sabljic A, Vuko E, Primožič I, Odžak R, Šprung M. New Membrane Active Antibacterial and Antiviral Amphiphiles Derived from Heterocyclic Backbone of Pyridinium-4-Aldoxime. Pharmaceuticals, 15 (2022), 7; 775, 21. doi: 10.3390/ph15070775
7. Crnčević D, Krce L, Mastelić L, Maravić A, Soldo B, Aviani I, Primožič I, Odžak R, Šprung M. The mode of antibacterial action of quaternary N-benzylimidazole salts against emerging opportunistic pathogens. Bioorganic chemistry, 112 (2021), 104938, 8. doi: 10.1016/j.bioorg.2021.104938
8. Crnčević D, Odžak R. Synthesis of quaternary ammonium salts based on quinuclidin-3-ol and pyridine-4-aldoxime with alkyl chains. St open, 1 (2020), e2020.2006.3., 8. doi:10.48188/so.1.8

